



National Library  
of Canada

Acquisitions and  
Bibliographic Services Branch

395 Wellington Street  
Ottawa, Ontario  
K1A 0N4

Bibliothèque nationale  
du Canada

Direction des acquisitions et  
des services bibliographiques

395, rue Wellington  
Ottawa (Ontario)  
K1A 0N4

Your file    *Votre référence*

Our file    *Notre référence*

## NOTICE

The quality of this microform is heavily dependent upon the quality of the original thesis submitted for microfilming. Every effort has been made to ensure the highest quality of reproduction possible.

If pages are missing, contact the university which granted the degree.

Some pages may have indistinct print especially if the original pages were typed with a poor typewriter ribbon or if the university sent us an inferior photocopy.

Reproduction in full or in part of this microform is governed by the Canadian Copyright Act, R.S.C. 1970, c. C-30, and subsequent amendments.

## AVIS

La qualité de cette microforme dépend grandement de la qualité de la thèse soumise au microfilmage. Nous avons tout fait pour assurer une qualité supérieure de reproduction.

S'il manque des pages, veuillez communiquer avec l'université qui a conféré le grade.

La qualité d'impression de certaines pages peut laisser à désirer, surtout si les pages originales ont été dactylographiées à l'aide d'un ruban usé ou si l'université nous a fait parvenir une photocopie de qualité inférieure.

La reproduction, même partielle, de cette microforme est soumise à la Loi canadienne sur le droit d'auteur, SRC 1970, c. C-30, et ses amendements subséquents.

Canada

**University of Alberta**

**A Study of Acid Mine Drainage Formation and Prevention Methods**

By



**Kafui Nyavor**

A thesis submitted to the Faculty of Graduate Studies and Research in partial fulfillment of  
the requirement for the degree of Doctor of Philosophy

in

**Mineral Engineering**

**Department of Mining, Metallurgical and Petroleum Engineering**

Edmonton, Alberta

Spring 1996



National Library  
of Canada

Acquisitions and  
Bibliographic Services Branch

395 Wellington Street  
Ottawa, Ontario  
K1A 0N4

Bibliothèque nationale  
du Canada

Direction des acquisitions et  
des services bibliographiques

395, rue Wellington  
Ottawa (Ontario)  
K1A 0N4

Your file / Votre référence

Our file / Notre référence

**The author has granted an irrevocable non-exclusive licence allowing the National Library of Canada to reproduce, loan, distribute or sell copies of his/her thesis by any means and in any form or format, making this thesis available to interested persons.**

**L'auteur a accordé une licence irrévocable et non exclusive permettant à la Bibliothèque nationale du Canada de reproduire, prêter, distribuer ou vendre des copies de sa thèse de quelque manière et sous quelque forme que ce soit pour mettre des exemplaires de cette thèse à la disposition des personnes intéressées.**

**The author retains ownership of the copyright in his/her thesis. Neither the thesis nor substantial extracts from it may be printed or otherwise reproduced without his/her permission.**

**L'auteur conserve la propriété du droit d'auteur qui protège sa thèse. Ni la thèse ni des extraits substantiels de celle-ci ne doivent être imprimés ou autrement reproduits sans son autorisation.**

ISBN 0-612-10618-7

**Canada**

**University of Alberta**

**Library Release Form**

**Name of Author: Kafui Nyavor**

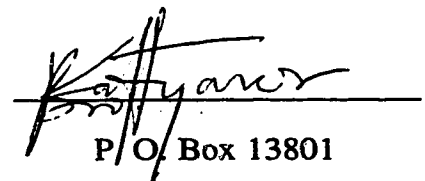
**Title of Thesis: A Study of Acid Mine Drainage Formation and  
Prevention Methods**

**Degree: Doctor of Philosophy**

**Year this Degree Granted: 1996**

Permission is hereby granted to the University of Alberta Library to reproduce single copies of this thesis and to lend or sell such copies for private, scholarly, or scientific research purposes only.

The author reserves all other publication and other rights in association with the copyright in the thesis, and except as hereinbefore provided, neither the thesis nor any substantial portion thereof may be printed or otherwise reproduced in any material form whatever without the author's prior written permission.



P/O. Box 13801

Accra, Ghana

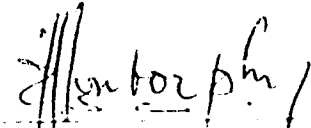
West Africa.


4<sup>TH</sup> MARCH, 1996

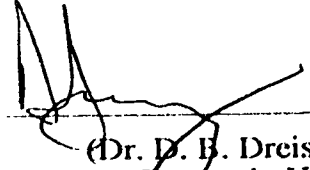
University of Alberta

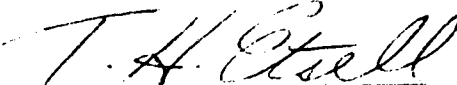
Faculty of Graduate Studies and Research


The undersigned certify that they have read, and recommend to the Faculty of Graduate Studies and Research for acceptance, a thesis entitled **A Study of Acid Mine Drainage Formation and Prevention Methods** submitted by **Kafui Nyavor** in partial fulfillment of the requirements for the degree of **Doctor of Philosophy in Mineral Engineering**.

  
\_\_\_\_\_  
(Dr. N. O. Egiebor)  
Supervisor

  
\_\_\_\_\_  
(Prof. L. R. Plitt)

  
\_\_\_\_\_  
(Dr. D. B. Dreisinger)  
External - UBC

  
\_\_\_\_\_  
(Dr. T. H. Etsell)

  
\_\_\_\_\_  
(Dr. P. M. Fedorak)  
Co-supervisor

2nd March, 1996

*"The important thing is not to stop questioning."*

**Albert Einstein**

*"If you have no confidence in self, you are twice defeated in the race of life. With confidence, you have won even before you have started."*

**Marcus Garvey**

## **DEDICATION**

**Dedicated to my affectionate mother (Nanna) and father (Uncle Nelson) for their great help and inspiration.**

**To Uncle Nelson I say, I wish you waited to see me as an adult, however, "*Man proposes, but HE disposes.*" May you rest in peace.**

## ABSTRACT

Acid mine drainage (AMD) is presently the biggest single environmental problem facing the mining industry. New and expanding metal mines in most parts of the world have to demonstrate their ability to contain this problem to obtain operating permits. The need to control or prevent AMD formation has led to the study of various techniques. While some of these techniques are directed towards the treatment of the resulting drainage, others are directed towards prevention of AMD at-source. Conventional methods of controlling AMD have primarily been limited to collecting the drainage and neutralizing with alkaline materials which do not provide a permanent solution to the AMD problem.

In this study, the two mechanisms of bacteria oxidation of pyrite and AMD formation, bacteria ferrous ion oxidation kinetics, and ferric ion product effect on bacterial ferrous oxidation kinetics were investigated. The results showed that the direct contact mechanism of pyrite oxidation by *Thiobacillus ferrooxidans* is insignificant. The predominant, and possibly the only, pathway involves the indirect bacteria oxidation of available ferrous to ferric ion, which in turn oxidizes pyrite to generate additional ferrous ion and acidity in a cyclic process. The kinetics of oxidation of ferrous to ferric ions by *T. ferrooxidans* was observed to change from the standard Michaelis-Menten type to first order kinetics as the concentration of cells was increased above a certain level in relation to ferrous concentration. At very low cell concentration relative to ferrous ion concentration, the Michaelis-Menten kinetics approached a zero order kinetics.

Ferric ions generated by the bacteria competitively inhibited ferrous ion oxidation by the bacteria. The inhibitory effects of ferric ion was however reduced by increasing cell concentration. The apparent ferric ion inhibition constant did not change with increasing cell concentration.

Since AMD results from the oxidation of sulfides in the presence of oxygen, water and iron-oxidizing bacteria, controlling any of these three factors contributing to pyrite oxidation provides a potential at-source remedy for reducing or preventing AMD formation.



Physical properties such as hydrophobicity also play an important role in the attachment of bacteria, and the adsorption of oxygen, water, and other ions that subsequently lead to the oxidation of pyrite. Also, since the oxidation of sulfide in acid medium is initiated by preferential release of iron ion into solution, the mechanism of sulfide oxidation can be likened to the corrosion of metals, and therefore could potentially be protected by metal phosphating techniques.

This project also investigated the suppression of pyrite oxidation by treatment with fatty acid amine, which makes the pyrite highly hydrophobic, and the formation of phosphate coating on the pyrite surface. The fatty acid amine treatment significantly suppressed the oxidation of pyrite in the absence and presence of bacteria. The phosphate coating also reduced the rate of pyrite oxidation significantly in the absence of bacteria under near-neutral pH. However, in the presence of bacteria under acidic conditions, the rate of oxidation of phosphate coated pyrite was only slightly reduced.

## **ACKNOWLEDGEMENT**

The author would like to thank Dr. N. O. Egiebor, supervisor, for his encouragement, guidance, support and supervision during this program. The author also wishes to express his sincere gratitude and appreciation to Dr. P. M. Fedorak (co-supervisor, Biological Sciences Department) for fostering the author's interest in microbiology and making his knowledge and laboratory available for the microbiological aspects of the project. The comments made by anonymous reviewers for the published parts of the thesis project helped improve the project and is greatly appreciated.

The author thanks Messrs. Roy Ifill and Bashir Mohamedhai for their great support and companionship. He also wish to acknowledge the tremendous support shown by the Department of Mining, Metallurgical and Petroleum Engineering technical staff (Ms. Tina Barker, Messrs. Shiraz Merali, Doug Booth, Jacques Gibeau, Bob Konzuk and John Czuroski), administrative staff (Mesdames Key Whiting, Nancy Evans, and Erika Auton), and academic staff, especially Dr. J. M. Whiting, Dr. H. Henein, and Prof. W. H. Griffin.

His sincere thanks to the members of Dr. P. M. Fedorak's research team (Room M437, Biological Sciences), especially Mrs. Neili Sifeldeen, Ms. Sara Ebert, Ms. Lisa Gieg, and Debbie for their technical assistance and companionship. The author thanks his external examiner, Dr. D. Driesinger, and other members of his examining committee, Prof. L. R. Plitt and Dr. T. Etseil, for their contribution to the thesis.

The study was made possible in part by the financial assistance provided by the Natural Sciences and Engineering Council (NSERC) of Canada and Luscar Graduate Scholarship in Environmental Engineering (Luscar Limited), to which the author is greatly indebted.

Above all, the author wishes to thank his wife, Pat Mayo, Billie and Jake Troughton, Sean Mayo, Ellen Mayo, and Clayton, Cassie and Cathy Molloy, for their moral support, companionship and tolerance during this program.

## TABLE OF CONTENTS

	<b>Page</b>
<b>CHAPTER 1 - INTRODUCTION</b> .....	1
1.1 INTRODUCTION.....	1
1.2 MAGNITUDE OF ACID ROCK DRAINAGE PROBLEM.....	4
1.3 MONITORING OF LIQUID EFFLUENT.....	5
1.4 LITERATURE REVIEW.....	7
1.4.1 Mechanism of Pyrite Oxidation.....	7
1.4.1.1 Chemical Reaction Theory.....	8
1.4.1.2 Electrochemical Theory.....	10
1.4.1.3 Semiconductor Theory.....	12
1.4.1.4 Preferential Oxidation of Pyrite.....	15
1.4.2 Mechanism of Acid Rock Drainage Formation.....	16
1.4.3 The Role of Bacteria in Acid Rock Drainage Formation.....	18
1.4.3.1 Mechanism of Bacteria Oxidation of Pyrite.....	20
1.4.3.2 Attachment of Bacteria onto Pyrite.....	21
1.4.4 Treatment of Acid Rock Drainage.....	22
1.4.4.1 Chemical Treatment of Acid Rock Drainage.....	22
1.4.4.2 Passive Treatment of Acid Rock Drainage.....	25
1.4.5 At-Source Control and Prevention of Acid Rock Drainage.....	27
1.4.5.1 Control of Bacteria Activity.....	28
1.4.5.2 Control of Oxygen.....	29
1.4.5.3 Chemical Pretreatment of Pyrite.....	30
1.5 SUMMARY OF REVIEW.....	32
1.6. PROJECT OBJECTIVES.....	33
1.7 ORGANIZATION OF THESIS.....	35

1.7.1 Summary of Chapters.....	35
1.8 REFERENCES.....	36

**CHAPTER 2 - CONTROL OF PYRITE OXIDATION BY PHOSPHATE COATING..... 45**

2.1 INTRODUCTION.....	45
2.2 THEORY AND BACKGROUND.....	45
2.2.1 Metal Phosphating.....	45
2.2.2 Phosphate Coating Formation.....	48
2.2.3 Sulfide Oxidation.....	50
2.3 EXPERIMENTAL.....	51
2.3.1 Materials.....	51
2.3.2 Phosphating.....	51
2.3.3 Accelerated Oxidation Column Tests.....	52
2.3.4 Pressure Oxidation Tests.....	53
2.3.5 Chemical Analysis.....	54
2.3.6 Scanning Electron Microscopy.....	55
2.4 RESULTS AND DISCUSSION.....	55
2.5 SUMMARY OF CHAPTER.....	69
2.6 REFERENCES.....	70

**CHAPTER 3 - SUPPRESSION OF PYRITE OXIDATION BY FATTY ACID AMINE TREATMENT..... 73**

3.1 INTRODUCTION.....	73
3.2 THEORY AND BACKGROUND.....	73
3.3 EXPERIMENTAL.....	76
3.3.1 Materials.....	76

3.3.2	Pyrite Treatment.....	76
3.3.3	Accelerated Column Oxidation Tests.....	77
3.3.4	Pressure Oxidation Tests.....	78
3.3.5	Contact Angle Hydrophobicity.....	78
3.3.6	Zeta Potential Determination.....	79
3.3.7	Chemical Analysis.....	80
3.3.8	Scanning Election Microscopy.....	81
3.4	RESULTS AND DISCUSSION.....	81
3.5	SUMMARY OF CHAPTER.....	95
3.6	REFERENCES.....	96

**CHAPTER 4 - RELATIONSHIP BETWEEN GROWTH PARAMETERS AND FERRIC CONCENTRATION EFFECT ON VIABILITY OF *THIOBACILLUS FERROOXIDANS*** 100

4.1	INTRODUCTION.....	100
4.2	EXPERIMENTAL METHODS.....	102
4.2.1	Culture and Medium.....	102
4.2.2	Activity and Growth of Strains.....	103
4.2.3	Agar-growth Medium.....	103
4.2.4	Most Probable Number Method.....	103
4.2.5	Turbidity and pH.....	104
4.2.6	Total and Ferrous iron.....	104
4.2.7	Protein Analysis.....	104
4.2.8	Effect of Initial Ferric Iron.....	105
4.3	RESULTS AND DISCUSSION.....	106
4.3.1	Changes in MPN and Fe <sup>2+</sup> Concentration in Batch Cultures.....	106
4.3.2	Changes in MPN and Turbidity (OD <sub>600</sub> ) in Batch Cultures.....	109

4.3.3	Changes in MPN and Protein Concentration in Batch Cultures.....	111
4.3.4	Changes in Turbidity and Protein Concentration in Batch Cultures.....	113
4.3.5	Changes in Fe <sup>3+</sup> and Protein Concentration in Batch Cultures.....	114
4.3.6	Changes in MPN and pH in Batch Cultures.....	116
4.3.7	Effect of Initial Fe <sup>3+</sup> on Number of Viable Cells.....	117
4.4	SUMMARY OF CHAPTER.....	120
4.5	REFERENCES.....	121

**CHAPTER 5 - KINETICS OF FERROUS IRON OXIDATION BY  
*THIOBACILLUS FERROOXIDANS* ..... 127**

5.1	INTRODUCTION.....	127
5.2	THEORY AND BACKGROUND.....	129
5.3	MATERIALS AND METHODS.....	132
5.3.1	Culture and Medium.....	132
5.3.2	Determination of Growth Phases of Strains.....	132
5.3.3	Most Probable Number Method.....	132
5.3.4	Preparation of Cell Suspension.....	133
5.3.5	Determination of Time for Initial Linear Drop in Fe <sup>2+</sup> concentration.....	133
5.3.6	Determination of Initial Oxidation Rates and pH.....	134
5.3.7	Total and Ferrous Iron.....	134
5.4	RESULTS AND DISCUSSION.....	135
5.4.1	Change in the Number of Viable Cells During Growth of Cultures.....	135
5.4.2	Determination of Kinetic Parameters.....	136
5.4.2.1	Low Initial Fe <sup>2+</sup> Concentration and Low Cell Concentration.....	137
5.4.2.2	Low Initial Fe <sup>2+</sup> Concentration and High Cell Concentration.....	139
5.4.2.3	High Initial Fe <sup>2+</sup> Concentration.....	141
5.5	CHAPTER SUMMARY.....	143

5.6 REFERENCES.....	144
---------------------	-----

**CHAPTER 6 - THE EFFECT OF FERRIC ION ON THE RATE OF FERROUS OXIDATION BY *THIOBACILLUS FERROOXIDANS* ... 147**

6.1 INTRODUCTION.....	147
6.2 MATERIALS AND METHODS.....	149
6.2.1 Culture and Medium.....	149
6.2.2 Most Probable Number (MPN) Method.....	149
6.2.3 Preparation of Cell Suspension.....	149
6.2.4 Determination of Initial Oxidation Rates and pH.....	149
6.2.5 Total, Ferrous and Ferric Iron Determination.....	150
6.2.6 Theory and Background.....	150
6.3 RESULTS AND DISCUSSION.....	153
6.4 CHAPTER SUMMARY.....	160
6.5 REFERENCES.....	161

**CHAPTER 7 - MECHANISM OF MICROBIAL OXIDATION OF PYRITE DURING ACID ROCK DRAINAGE FORMATION..... 164**

7.1 INTRODUCTION.....	164
7.2 THEORY AND BACKGROUND.....	166
7.3 EXPERIMENTAL.....	169
7.3.1 Materials.....	169
7.3.2 Culture and Medium.....	169
7.3.3 Most Probable Number (MPN) Method.....	169
7.3.4 Fe <sup>2+</sup> -oxidizing Activity of Fe <sup>2+</sup> - and FeS <sub>2</sub> -grown and Colonized Cells...	170
7.3.5 Pyrite Oxidation by FeS <sub>2</sub> -Colonized and Fe <sup>2+</sup> -grown Cells.....	170
7.3.6 Solid and Liquid Phase Relative Activities.....	171

7.3.7	Effect of pH on Fe <sup>2+</sup> -oxidizing Activity of Fe <sup>2+</sup> -grown Cells.....	171
7.3.8	Effect of pH on Chemical and Microbial Oxidation of FeS <sub>2</sub> .....	171
7.3.9	Total and Ferrous Iron Analysis.....	172
7.3.10	Surface Area and Density.....	172
7.3.11	Scanning Election Microscopy.....	172
7.4	RESULTS AND DISCUSSION.....	173
7.4.1	Pyrite Oxidation by Fe <sup>2+</sup> - and FeS <sub>2</sub> -grown Cells.....	173
7.4.2	Ferrous Oxidation by Fe <sup>2+</sup> - and FeS <sub>2</sub> -grown Cells.....	174
7.4.3	Oxidation of FeS by FeS <sub>2</sub> -colonized Cells.....	176
7.4.4	Effect of Initial Cell Concentration on FeS <sub>2</sub> and Fe <sup>2+</sup> Oxidation.....	177
7.4.5	Comparison of Activity of Attached and Suspended Cells.....	179
7.4.6	Effect of pH on Fe <sup>2+</sup> -oxidizing Activity.....	181
7.4.7	Effect of pH on Biotic and Abiotic FeS <sub>2</sub> Oxidation.....	182
7.4.8	Scanning Electron Microscopy (SEM).....	185
7.5	CHAPTER SUMMARY.....	188
7.6	REFERENCES.....	189

**CHAPTER 8 - SUPPRESSION OF MICROBIAL PYRITE OXIDATION BY FATTY ACID AMINE TREATMENT..... 193**

8.1	INTRODUCTION.....	193
8.2	EXPERIMENTAL METHODS.....	194
8.2.1	Culture and Medium.....	194
8.2.2	Pyrite and Surfactants.....	194
8.2.3	Pyrite Treatment.....	195
8.2.4	Most Probable Number (MPN) Method.....	195
8.2.5	Preparation of Cell Suspension.....	195
8.2.6	Stability Tests.....	195



8.2.7 Chemical Analysis and pH.....	196
8.2.8 Theory and Background.....	196
8.3 RESULTS AND DISCUSSION.....	197
8.4 SUMMARY OF CHAPTER.....	205
8.5 REFERENCES.....	206

**CHAPTER 9 - STABILITY OF PHOSPHATE COATED PYRITE IN THE PRESENCE OF *THIOBACILLUS FERROOXIDANS*... 209**

9.1 INTRODUCTION.....	209
9.2 THEORY AND BACKGROUND.....	210
9.3 EXPERIMENTAL METHODS.....	210
9.3.1 Culture and Medium.....	210
9.3.2 Pyrite and Phosphate Coating.....	210
9.3.3 Most Probable Number (MPN) Method.....	210
9.3.4 Preparation of Cell Suspension.....	211
9.3.5 Stability Tests.....	211
9.3.6 Chemical Analysis and pH.....	211
9.4 RESULTS AND DISCUSSION.....	211
9.5 SUMMARY OF CHAPTER.....	220
9.6 REFERENCES.....	221

**CHAPTER 10 - GENERAL DISCUSSION AND CONCLUSIONS..... 223**

10.1 Bacteria Growth Parameters.....	223
10.2 Phosphating of Pyrite.....	224
10.3 Fatty Acid Amine Treatment.....	225
10.4 Comparison of Phosphate and Fatty Acid Amine Treatment.....	225
10.5 Microbial Ferrous Oxidation Kinetics.....	226

10.6	Effect of Ferric Ion on Ferrous Oxidation Kinetics.....	226
10.7	Mechanism of Acid Rock Drainage.....	226
<b>CHAPTER 11 - RECOMMENDATIONS FOR FURTHER STUDIES....</b>		<b>230</b>
<b>APPENDIX.....</b>		<b>232</b>

## LIST OF TABLES

<b>Table</b>	<b>Page</b>
1-1. Authorized levels of deleterious substances prescribed in the Metal Mining Liquid Effluent Regulation (Part 1 and Part 2).....	6
1-2 Comparative cost of limestone and alkaline chemicals commonly used in the treatment of acid rock drainage.....	23
2-1 Elemental analysis of pyrite use for experiments.....	55
5-1 Michaelis constants for Fe <sup>2+</sup> oxidation by <i>T. ferrooxidans</i> .....	139
5-2 First order rate constants (K <sub>n</sub> ) for Fe <sup>2+</sup> oxidation by <i>T. ferrooxidans</i> .....	140

## LIST OF FIGURES

Figure	Page
1-1 Schematic representation of pyrite oxidation reactions by molecular oxygen.....	8
1-2 Schematic representation of pyrite oxidation by Fe(III).....	9
1-3 Idealized molecular orbital diagrams for the linear combination of 6p orbitals (from 2 sulfur atoms) to form 6 molecular orbitals.....	13
1-4 Reaction scheme visualizing the electroadsorption of OH <sup>-</sup> on iron site and subsequent transfer of OH group onto S <sub>2</sub> <sup>2-</sup> site.....	14
1-5 Cross section of anoxic limestone drain (ALD).....	24
1-6 Compost wetland.....	27
2-1 Diagrammatic representation of metal phosphating reactions.....	47
2-2 Model of the formation of an embryo prior to precipitation of ionic crystals.....	49
2-3 Representation of layered growth of phosphate coating on a pyrite surface.....	49
2-4 Accelerated oxidation column test setup.....	53
2-5 pH and Fe in solution during coating of pyrite at 40°C in 0.1 M KH <sub>2</sub> PO <sub>4</sub> and 2.0% H <sub>2</sub> O <sub>2</sub> .....	56
2-6 Scanning electron micrograph and EDS spectrum of untreated pyrite particles.....	58
2-7 Scanning electron micrograph and EDS spectrum of phosphate-treated pyrite particle. Tested at 25°C with 2.0% H <sub>2</sub> O <sub>2</sub> and 0.1 M K <sub>2</sub> HPO <sub>4</sub> .....	59
2-8 Scanning electron micrograph and EDS spectrum of phosphate-treated pyrite particle. Tested at 40°C with 2.0% H <sub>2</sub> O <sub>2</sub> and 0.1 M K <sub>2</sub> HPO <sub>4</sub> .....	60
2-9 Scanning Electron Micrograph and EDS spectrum of phosphate-treated pyrite particle. Tested at 80°C with 2.0% H <sub>2</sub> O <sub>2</sub> and 0.1 M K <sub>2</sub> HPO <sub>4</sub> .....	61

2-10 Accelerated Oxidation Columns after 30 days. Col. 1 (left) = untreated, Cols. 2 & 3 (center and right) = phosphate-treated.....	62
2-11 Accelerated oxidation column test of untreated and phosphate- treated pyrite.....	63
2-12 Cumulative acidity of solution from accelerated oxidation columns.....	64
2-13 Oxidation of untreated pyrite tested at 25°C, 40°C and 60°C and 1000 psi of pure oxygen.....	66
2-14 Oxidation of untreated pyrite tested at 100 psi, 200 psi, 500 psi, and 1000 psi of pure oxygen, and 60°C.....	67
2-15 Oxidation of untreated and phosphate-treated pyrite tested at 200 psi of pure oxygen and 60°C.....	68
2-16 Oxidation of untreated and phosphate-treated pyrite tested at 1000 psi of pure oxygen and 60°C.....	69
3-1 Concentration of iron in solution during deactivation of pyrite with fatty acid amines.....	82
3-2 Amine value of solution during deactivation of pyrite with fatty acid amine.....	83
3-3 Contact angle of untreated and fatty acid amine-treated pyrite particles.....	84
3-4 Zeta potential of pyrite as a function of pH in the absence and presence of fatty acid amines.....	85
3-5 Scanning electron micrographs of (a) untreated and (b) Armac T- treated pyrite samples.....	87
3-6 Oxidation of untreated pyrite tested at 25°C, 40°C, and 60°C and 1000 psi of pure oxygen.....	88
3-7 Oxidation of untreated pyrite tested at 100 psi, 200 psi, 500 psi, and 1000 psi of pure oxygen, and 60°C.....	89
3-8 Oxidation of untreated and fatty acid amine-treated pyrite tested at 200 psi of pure oxygen and 60°C.....	91

3-9	Schematic representation of the chemisorption of fatty acid amine onto pyrite surface.....	92
3-10	Oxidation of Armac T-treated pyrite tested at 100 psi, 200 psi, 500 psi, and 1000 psi of pure oxygen, and 60°C.....	93
3-11	Accelerated column oxidation test of untreated and fatty acid amine-treated pyrite.....	94
4-1	Change in number of viable cells and ferrous concentration during growth of strain 13598.....	107
4-2	Plot of change in viable cells versus ferric ion concentration, strain 13598.....	109
4-3	Change in number of viable cells and turbidity during growth of strain 13598.....	110
4-4	Change in number of viable cells and protein concentration during growth of strain 13598.....	112
4-5	Plot of change in viable cells versus protein concentration strain 13598.....	113
4-6	Change in turbidity and protein concentration during growth of strain 13598.....	114
4-7	Plot of change in protein versus ferric ion concentration in batch culture of strains 13598, 13661, and 14119.....	115
4-8	Change in number of viable cells and pH during growth of strain 13598.....	116
4-9	Effect of initial Fe <sup>3+</sup> concentration on the number of viable cells in batch cultures of strain 13598.....	118
4-10	Plot of maximum number of viable cells versus initial Fe <sup>3+</sup> concentration.....	119
5-1	Change in the number of viable cells during incubation of <i>T. ferrooxidans</i> strains 13598, 13661, and 14119.....	135

5-2	Change in Fe <sup>2+</sup> concentration with time. (Initial Fe <sup>2+</sup> and cell concentrations of 12 mg/L and 4.3 x 10 <sup>5</sup> /mL respectively).....	137
5-3	The effect of low initial Fe <sup>2+</sup> and low cell concentrations on the rate of Fe <sup>2+</sup> oxidation with strain 13598.....	138
5-4	The effect of low initial Fe <sup>2+</sup> and high cell concentrations on the rate of Fe <sup>2+</sup> oxidation with strain 13598.....	140
5-5	The effect of high initial Fe <sup>2+</sup> and various cell concentrations on the rate of Fe <sup>2+</sup> oxidation with strain 13598.....	141
6-1	The effect of Fe <sup>3+</sup> concentration on the initial rate of Fe <sup>2+</sup> oxidation using cell concentration of 4.3x10 <sup>5</sup> /mL, strain 13598.....	154
6-2	The effect of Fe <sup>3+</sup> concentration on the initial rate of Fe <sup>2+</sup> oxidation using cell concentration of 2.3x10 <sup>6</sup> /mL, strain 13598.....	155
6-3	The effect of Fe <sup>3+</sup> concentration on the initial rate of Fe <sup>2+</sup> oxidation using cell concentration of 9.3x10 <sup>7</sup> /mL, strain 13598.....	156
6-4	Plot of slopes from double reciprocal graphs at various cell concentrations versus Fe <sup>3+</sup> concentration, strain 13598.....	157
6-5	Plot of secondary slopes from Figure 6-4 versus reciprocal of cell concentration, strain 13598.....	158
7-1	E <sub>h</sub> -pH diagram for Fe-S-H <sub>2</sub> O system at 25°C and 1 atmosphere.....	167
7-2	The pH and E <sub>h</sub> tolerance contours of thiobacilli.....	168
7-3	Pyrite oxidation of Fe <sup>2+</sup> - and FeS <sub>2</sub> -grown cells at initial of pH 2.5.....	173
7-4	Change in MPN, ferrous and total Fe concentration during colonization of pyrite, initial pH of 2.4.....	175
7-5	Ferrous oxidation by Fe <sup>2+</sup> -grown, FeS <sub>2</sub> -grown, and FeS <sub>2</sub> -colonized cells. (Initial MPN of 2.4x10 <sup>9</sup> /mL, 1.2x10 <sup>9</sup> /mL, and 8.2x10 <sup>8</sup> /mL).....	176
7-6	Pyrite oxidation by FeS <sub>2</sub> -colonized cells. (Initial MPN of 1.7x10 <sup>8</sup> /mL, 8.2x10 <sup>8</sup> /mL, 1.6x10 <sup>9</sup> /mL, and 3.3x10 <sup>10</sup> /mL respectively).....	177
7-7	The effect of initial cell concentration on pyrite oxidation.....	178

7-8	The effect of initial cell concentration on ferrous oxidation.....	179
7-9	Ferrous-oxidizing activity of suspended and attached cells.....	180
7-10	Effect of pH on ferrous-oxidizing activity of cells.....	181
7-11	Effect of pH on abiotic and biotic oxidation of H <sub>2</sub> SO <sub>4</sub> -washed pyrite.....	182
7-12	Viability of cells tested at pH 4.5 during biotic oxidation of H <sub>2</sub> SO <sub>4</sub> -washed pyrite.....	183
7-13	Change in E <sub>h</sub> during biotic and abiotic oxidation of H <sub>2</sub> SO <sub>4</sub> -washed pyrite.....	184
7-14	Change in pH during biotic and abiotic oxidation of H <sub>2</sub> SO <sub>4</sub> -washed pyrite.....	185
7-15	Scanning Electron Micrographs of (a) pyrite in control medium for 6 months and (b) pyrite in inoculated medium for 1 month.....	186
7-15	Scanning Electron Micrographs of (c) pyrite in inoculated medium for 2 months and (d) pyrite in inoculated medium for 6 months.....	187
8-1	Change in total Fe concentration during oxidation of untreated pyrite (initial pH = 2.4).....	198
8-2	Change in total Fe concentration during leaching of untreated treated pyrite (no cells added).....	200
8-3	Percentage of total Fe as ferrous during leaching of untreated and treated pyrite (no cells added).....	201
8-4	Change in total Fe concentration during bioleaching of untreated and treated pyrite (strain 13661).....	202
8-5	Percentage of total iron as ferrous during bioleaching of untreated and treated pyrite (strain 13661).....	203
9-1	Change in total Fe (Fe <sup>T</sup> ) and ferrous (Fe <sup>2+</sup> ) concentration during oxidation of untreated pyrite (initial pH = 2.4).....	212
9-2	Effect of phosphate coating at 25°C and 40°C on the oxidation of pyrite (no cells added, initial pH of 2.5).....	214



9-3	Percentage of total Fe as ferrous during leaching of untreated, 25°C and 40°C phosphate-treated pyrite (no cells added).....	216
9-4	Change in total Fe concentration during bioleaching of untreated, 25°C and 40°C phosphate-treated pyrite, initial pH of 2.5.....	217
9-5	Percentage of total iron as ferrous during bioleaching of untreated, 25°C and 40°C phosphate-treated pyrite, initial pH of 2.5.....	218
10.1	Representation of the indirect contact mechanism.....	227
10.2	Representation of the direct contact mechanism.....	228

# CHAPTER 1

## 1.1 INTRODUCTION

Pyrite, as well as being the most important member of the disulfide group, is the most abundant sulfide in the earth's crust and has been extensively studied (Vaughan and Craig, 1978). An aspect of pyrite that has come under extensive investigation of late is its oxidation chemistry. The oxidation of pyrite is important to a wide variety of disciplines, including hydrometallurgy, coal science, electrochemistry, condensed matter physics, mining engineering, mineral processing, soil science and geology (Moses and Herman, 1991; Ahlberg et al., 1990; Buckley and Woods, 1987; Tributsch, 1986).

The mining and mineral industry has recently been adversely affected by the oxidation of pyrite which leads to acid mine drainage (AMD) formation, also known as acid rock drainage (ARD) formation. ARD/AMD is defined as a low pH leachate formed by the oxidation of sulfide minerals contained in a waste usually produced by a mining and mineral processing operation (Bell et al., 1987). This ARD problem stems from the fact that most base metal, precious metal, uranium, and coal deposits contain sulfide minerals, either in the ore or the surrounding waste rock (Jensen and Bateman, 1979). After mining and processing of these ores, the sulfide minerals are exposed to oxygen and water, and they begin to oxidize almost immediately. The oxidation may also be catalyzed by bacteria such as, *Thiobacillus ferrooxidans* (Colmer et al., 1950; Temple and Colmer, 1951).

The origin of contaminated wastewater at many mine sites is attributed to the ease of oxidation of the sulfide minerals with the consequent generation of acid. In the absence of calcareous materials, the acid produced leaches heavy metals associated with the waste deposit. Rainfall and snowmelt may then flush the toxic solutions from the waste sites into the downstream environment. ARD may contain very high concentrations of sulfate, iron, and base metals such as lead, copper, nickel, zinc, or silver depending on the constituent of

the waste, and exhibit pH values below 7. Whereas the quality of ARD may vary from mine to mine, the contaminated mine effluents often exceed regulatory standards for metals and acidity by several orders of magnitude. If the ARD is left uncollected and untreated, the drainage could contaminate groundwater and local watercourses, damaging the health of plants, wildlife, and fish (Filion et al., 1990).

ARD may arise as mine water from open pits and underground mine workings, or as surface drainage and seepage from tailings disposal facilities and waste rock dumps, and has been identified as the biggest single environmental problem facing the mining industry today. As a result of this problem, in order to obtain operating permits new and expanding mines have to demonstrate the ability to contain ARD (Lawrence, 1990). Many major mining projects cannot start because permits have been refused due to fears that this problem may not be addressed adequately.

Several techniques have been considered in the past for the treatment and abatement of ARD. While some of these methods are directed towards the treatment of the resulting drainage, others are directed towards prevention of ARD at-source. Presently, at active mine sites and some inactive mine sites, where responsibility has reverted to the crown, mining companies and governments operate comprehensive systems to collect and treat effluents and seepage from all sources. Although these facilities, when well operated and maintained, may be sufficient to prevent downstream environmental impact, acid generation may persist for hundreds of years following mine closure (Filion et al., 1990). Besides the obvious problems associated with maintaining an effective treatment system for very long periods of time after mining activities have ceased, the disposal of chemical treatment plant sludge produced from the neutralization of ARD is an additional major operational problem (Halbert et al., 1989).

Other methods investigated for treating ARD are deep-well injection, constructed wetlands, and dilution and precipitation of effluents (Hedin et al. 1989; Ziemkiewicz et al. 1990). All these traditional treatment methods allow pyrite oxidation to run its course, thus

producing contaminated effluents which is then treated. Some other proposed methods for the abatement of ARD include the oxidation of pyritic materials prior to disposal and alkaline material capping (Meek, 1991). A common method used for controlling ARD formation is the blending of the pyritic waste with alkaline materials such as limestone, lime, sodium carbonate, phosphate rock, basic slag and fly ash (Stiller et al., 1989; Harshberger and Bowders, 1991; Spotts and Dollhopf, 1992). Apart from being very expensive, this approach has been found to be ineffective in the long term. Problems also arise with the use of limestone and other alkaline materials because of the formation of ferric oxyhydroxides, which armor these materials in oxidizing environments and eliminate any further buffering capability (Wentzler and Aplan, 1992).

Research have been conducted on establishing sustainable vegetative growth on tailings and waste rock by the mining industry and the Department of Energy, Mines and Resources, Canada. The vegetative growth was to alleviate ARD from these sites, thus allowing companies to meet environmental requirements upon closure. However, the vegetation of these sites have also failed to improve drainage quality (Filion et al., 1990).

Methods directed towards prevention of ARD at-source have been found to be more promising since these are permanent solutions to the ARD problem and will not require treatment facilities after mine closure. These at-source prevention methods depend on the creation of conditions which chemically, biochemically or physically retard the rate of oxidation of pyrite. Based on this, many approaches have been investigated, including: (1) complexation of ferric ions in solution or at the surface of the pyrite so that they are not available for oxidation (Nebgen et al., 1981; Chander and Zhou, 1992); (2) the use of bactericides to reduce bacteria population and thereby reduce the catalytic effect of the bacteria (Dugan, 1987); (3) creation of fully anoxic environments by using clay liners, plastic liners, and asphalt (Healey and Robertson, 1989); (4) coating of the surface of pyrite with ferric-phosphate in an effort to stop electron transfer between the pyrite and oxidizing agents (Evangelou and Huang, 1992); and (5) electrochemical passivation by

addition of copper and silver ions to form sulfur layers on the surface of pyrite particles (Lalvani and Shami, 1989).

Most of these techniques have not been very successful because they are directed at eliminating only one of the reaction paths available for ARD formation. The application of limestone and bactericides have been found to have short life span due to repopulation of bacteria and abiotic oxidation of pyrite (Dugan, 1987). The creation of fully anoxic environment by liner technologies are said to be cost prohibitive as well as ineffective over time due to liner deterioration and biotic oxidation of pyrite. While several additives are still under evaluation and development, there is presently no widely accepted technology which controls ARD production at-source without indefinite maintenance.

A factor contributing to the lack of success in the at-source control of ARD formation is the lack of a detailed understanding of the mechanisms and kinetics of pyrite oxidation. The exact mechanisms of strictly chemical oxidation of pyrite is a subject of controversy, while in the case of ARD formation, the mechanism is further complicated by the presence of bacteria.

## **1.2 MAGNITUDE OF ACID ROCK DRAINAGE PROBLEM**

Recent studies (1984-1987) conducted by CANMET (Natural Resources, Canada) and industry have shown that British Columbia, Saskatchewan, Manitoba, Ontario, Quebec, New Brunswick, Newfoundland, Yukon and Northwest Territories currently have operating and/or abandoned acid generating waste sites, with a total area of 15,000 hectares (37,000 acres). These wastes are the accumulation of 40 years of mining since World War II. As for the future, it seems reasonable to assume that the mining of lower grade ores together with the likelihood of increasing annual mineral production could lead to the accumulation of an equal quantity of acidic tailings and waste rock over the next 20 years (Filion et al., 1990).

The above surveys do not include gold mines, coal mines, uranium mines and abandoned mine sites in which responsibility has reverted to the crown. In Ontario, 100 abandoned mines sites were identified and 20 of these were found to pose acidic drainage problem. The 20 sites were found to contain about 55,000,000 tonnes (60,000,000 tons) of reactive sulfide tailings over a surface area of 830 hectares (2030 acres). In Quebec, about 107 abandoned mines sites were identified, with 21 of these covering 4,500 hectares (11,110 acres) been classified as hazardous waste sites due to acidic drainage (Filion et al., 1990).

The cost of stabilizing ARD waste is highly site specific. Stabilization cost also depends on the method employed. Under the most difficult conditions and applying existing, but unproven technology, the cost of stabilizing some sites have been estimated to be as high as CDN \$41,000 per hectare. Applying an average cost of CDN \$125,000 per hectare to existing and future accumulation of acid generating waste in Canada, the cost of reclamation of non-ferrous mines sites will be CDN \$3 billion over the next twenty years. Funds required to deal with abandoned sites, where liability have reverted to the crown, are estimated to be about CDN \$1 billion (Filion et al., 1990). In response to the need to conduct research on ARD in Canada, two groups, the National Mine Environment Neutral Drainage (MEND) and the British Columbia Acid Mine Drainage (BC AMD) task force were assembled in 1986.

### **1.3 MONITORING OF LIQUID EFFLUENT**

In the province of Alberta, statutes and regulations relating to industrial development are contained in the Environmental Protection and Enhancement Act which became law on June 26, 1992 and came into force on September 1, 1993. The Acts regulate industrial activities from exploration through developments to abandonment in relation to environmental impacts. For all regulated industries (which includes mining), development requires an application to Alberta Environmental and/or Energy Resources

Conservation Board (ERCB). The application must be supported by Environmental Impact Assessment (EIA) Report.

Federal standards for the mineral industry are contained in the Metal Mining Liquid Effluent Regulations and Guidelines under section 33 of the Fisheries Act. The authorized levels of deleterious substances and pH prescribed in the Metal Liquid Effluent Regulations is shown in Table 1-1 (Part 1 and 2 respectively).

**Table 1-1**

**Authorized levels of deleterious substances  
prescribed in the Metal Mining Liquid Effluent Regulation**

**Part 1**

Substance	Maximum authorized monthly arithmetic mean concentration	Maximum authorized concentration in a composite sample	Maximum authorized concentration in a grab sample
Arsenic	0.5 mg/L	0.75 mg/L	1.0 mg/L
Copper	0.3 mg/L	0.45 mg/L	0.6 mg/L
Lead	0.2 mg/L	0.30 mg/L	0.4 mg/L
Nickel	0.5 mg/L	0.75 mg/L	1.0 mg/L
Zinc	0.5 mg/L	0.75 mg/L	1.0 mg/L
Total suspended matter (TSM)	25.0 mg/L	37.5 mg/L	50 mg/L
Radium-226	10.0 pCi/L	20.0 pCi/L	30.0 pCi/L

**Part 2**

**Authorized levels of pH**

Parameter	Minimum authorized monthly arithmetic mean pH	Minimum authorized pH of a composite sample	Minimum authorized pH of grab sample
pH	6.0	5.5	5.0

The provincial Clean Water Act allows Alberta Environment to impose additional standards on mining and processing facilities, as well as, all other industrial operations that may contribute to water pollution within its jurisdiction. Guidelines are provided for various industrial operations, and considerations are given to individual projects. The provincial guidelines specify standards and acceptable discharge limits for traditional parameters. These parameters include chemical oxygen demand (COD), total suspended solids, sulfide, pH, and acute toxicity (LC<sub>50</sub>). A monthly bioassay fish toxicity test is required. If the bioassay indicate acute toxicity of the liquid effluent, then surveys of chromium (Cr), cyanide (CN<sup>-</sup>), mercury (Hg), lead (Pb), zinc (Zn), and nickel (Ni) may be required.

## **1.4 LITERATURE REVIEW**

In order to successfully control and prevent ARD formation, a clear and thorough understanding of the chemistry, mechanisms, and all reactants involved in ARD formation is important.

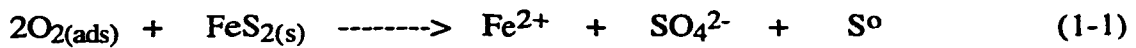
### **1.4.1 Mechanism of Pyrite Oxidation**

The mechanism of pyrite oxidation is complex and theories to explain this oxidation process differ considerably. While the chemical reaction theories consider the adsorption and reaction of molecular oxygen directly on the surface of pyrite, the electrochemical theories take into account the anodic dissolution of pyrite and cathodic reduction of oxygen (Hamilton and Woods, 1981). Another theory which has been used to explain the oxidation of pyrite is the semiconductor theory. Based on these theories, many reaction paths and mechanisms of pyrite oxidation have been proposed. In addition, the products of pyrite oxidation have been found to vary considerably, depending upon the conditions of oxidation (Pugh et al., 1984).



### 1.4.1.1 Chemical Reaction Theory

Smith and Shumate (1970), using the chemical reaction theory, outlined a mechanism where oxygen is adsorbed on "reactive sites" of the pyrite, the oxygen then dissociates and forms an activated complex which decomposes to form an oxidation product. The oxidation product then desorbs and another reactive site is formed. McKay and Halpern (1958) suggested that the adsorbed oxygen reacts only in a fully molecular path, designated as an atom transfer reaction as illustrated in Equation 1-1.



Goldhaber (1983) later suggested that the initiation of pyrite oxidation is by the direct attachment of a dissolved oxygen molecule to a partially protonated pyrite surface, as shown in Figure 1-1. The molecular oxygen sequence is initiated by the attachment of  $\text{O}_2$

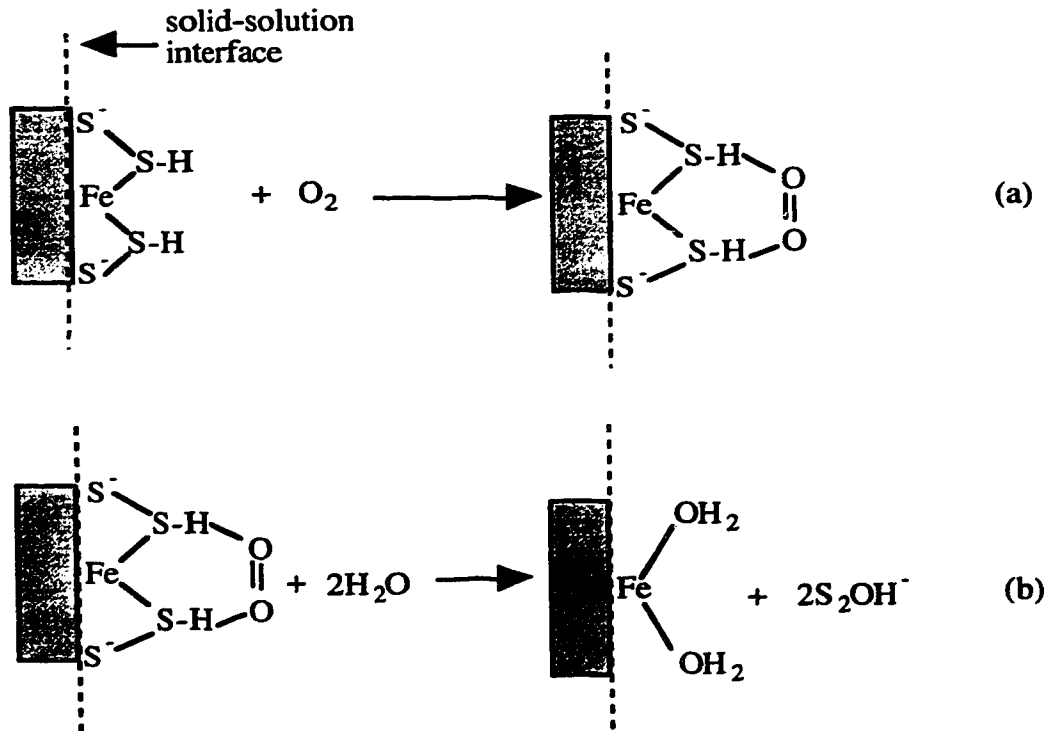


**Figure 1-1. Schematic representation of pyrite oxidation reactions by molecular oxygen.**

as shown in Figure 1-1a. The second step, considered as the rate-limiting step, requires breaking of the double bond in the  $O_2$  and displacement by  $H_2O$  of an  $S_2OH^-$  molecule (Figure 1-1b).

Moses and Herman (1991), however, found that although dissolved oxygen can directly oxidize pyrite, it can effectively do so only in the absence of Fe(II) adsorbed to the pyrite surface, as illustrated in Figure 1-2. They proposed that the transfer of electrons from pyrite to dissolved oxygen occurs through adsorbed Fe(II), which is cyclically oxidized to Fe(III). The sequence is initiated by the transfer of a hydroxyl group (OH) to a pyrite sulfur atom from the hydration sphere of the aquo-Fe(III) complex in exchange for an electron from the pyrite sulfur atom (Figure 1-2a). As more hydroxyl ions are added to the pyrite sulfur and electrons transferred to Fe(III), the Fe-S bond weakens until a sulfoxy species is formed that is stable enough in solution to dissociate from the surface (Figure 1-2b).

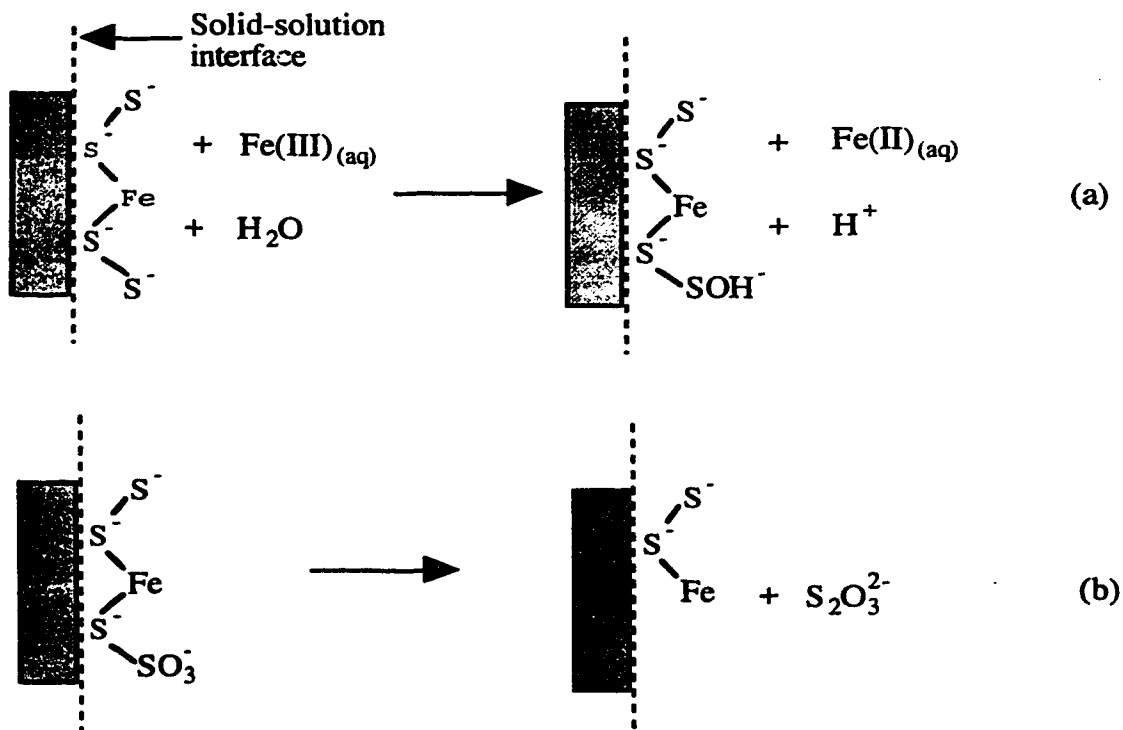
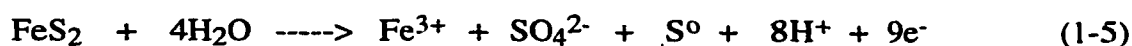
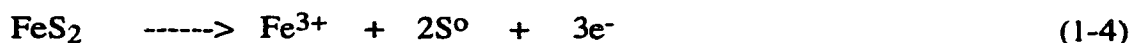
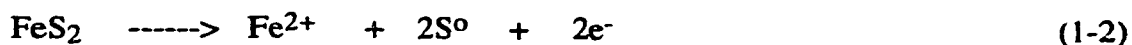


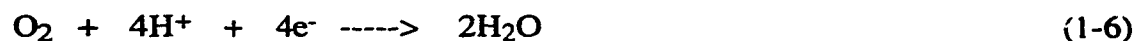
**Figure 1-2. Schematic representation of pyrite oxidation by Fe(III).**

### 1.4.1.2 Electrochemical Theory

Electrochemically, pyrite dissolution is generally believed to occur according to one of the following anodic reactions (Bailey and Peters, 1976);



The principal cathodic reaction is a four-electron oxygen reduction process and is represented by Equation 1-6;



In the presence of dissolved Fe(III) ions, the following cathodic reaction is also suggested;

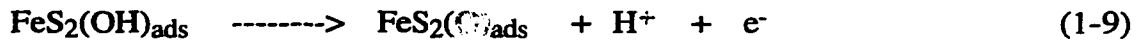
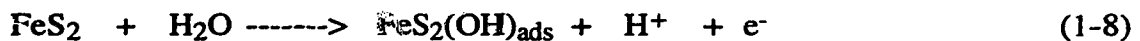


The overall process is the summation of cathodic and anodic reactions that occurs at the pyrite surface. Nagai and Kiuchi (1975), suggested that pyrite reacts electrochemically to produce ferrous ions and elemental sulfur (Equation 1-2). Peters and Majima (1968) reported that pyrite oxidation follows the sulfate route, and apparently leads to only ferric and sulfate ions in solution (Equation 1-3). Bailey and Peters (1976) observed that lowering the leaching potential correspondingly lowers the sulfate yield, and therefore concluded that the partitioning of pyrite sulfur between sulfate and elemental sulfur is a result of two competing reactions shown by Equations 1-2 and 1-3, the rates of which are in turn controlled by the pyrite potential. They suggested that at lower anodic potentials,

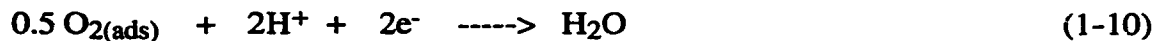
dissolution takes place predominantly according to Equation 1-2, while dissolution via Equation 1-3 predominates at higher potentials.

Springer (1970), and Hamilton and Wood (1981) proposed that elemental sulfur is an intermediate in the formation of sulfate, whereas Biegler and Swift (1979) reported that the elemental sulfur and sulfate routes are independent. Mishra and Osseo-Asare (1988) also reported that sulfur is not an intermediate product but rather the end product from the decomposition of thiosulfate formed on the surface of pyrite by the oxidation of  $S_2^{2-}$ .

A mechanism which involves the direct transfer of oxygen from water to sulfur atoms in the pyrite lattice, with oxygen addition occurring through adsorption and deprotonation of water molecules according to a series of reactions to form sulfate was proposed by Biegler and Swift (1979). The slowest steps in the sulfate formation is given by Equations 1-8 and 1-9.



Using  $O^{18}$  tracer tests, Bailey and Peters (1976) had shown earlier that the sulfate formed from pyritic sulfur contains oxygen taken from water rather than from the gas phase. They suggested that the adsorbed oxygen reacts only with electrons supplied from the anodic decomposition of pyrite in a cathodic reaction:



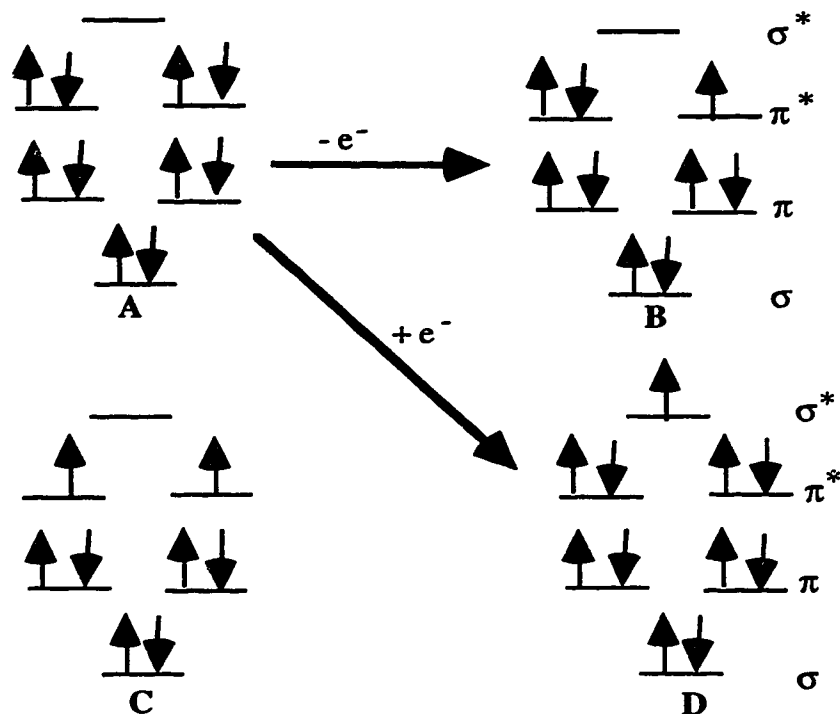
and not by a fully molecular path as suggested by McKay and Halpern (1958).

### 1.4.1.3 Semiconductor Theory

The semiconductor theory considers electrons in discrete energy levels, and is based on the molecular orbital and band theories derived from the principles of quantum mechanics and has been used by some investigators to explain the oxidation of pyrite (Vaughan and Craig, 1978; Luther, 1987). Whereas some investigators (Springer, 1970) have observed that the electronic conduction properties of minerals do not normally play a significant role in hydrometallurgical oxidation and dissolution reactions in which electrochemical corrosion processes are important, and also found no obvious correlation between kinetic parameters for oxygen reduction and the nature of semiconduction of pyrite (Biegler, 1976), others have reported a significant role for semiconductor electrochemistry in the oxidation of pyrite (Mishra and Osseo-Asare, 1988).

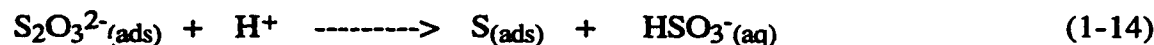
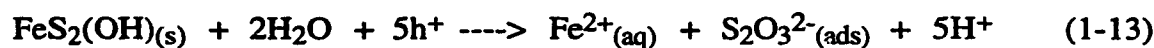
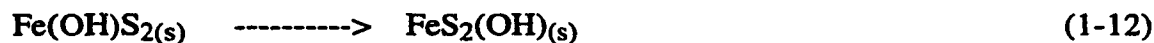
Using the molecular orbital theory, Luther (1987) proposed that the mechanism of pyrite oxidation by  $\text{Fe}^{3+}$  occurs as the result of three important criteria: (1) a suitable oxidant having a vacant orbital or site to bind to the  $\text{FeS}_2$  surface via a sulfur, (2) the initial formation of a persulfido bridge between  $\text{FeS}_2$  and the oxidant, and (3) the electron transfer from a  $\pi^*$  orbital (highest occupied molecular orbital) in  $\text{S}_2^{2-}$  and a  $\pi$  or  $\pi^*$  orbital (lowest unoccupied molecular orbital) of the oxidant, as illustrated in Figure 1-3. The slow rate of oxidation of pyrite by oxygen was attributed to oxygen having no vacant  $\sigma$  orbital of low energy and similar symmetry to accept a pair of electrons from  $\text{S}_2^{2-}$ .

On the basis of the semiconduction theory, Mishra and Osseo-Asare (1988) suggested that the initial process of aqueous oxidation of pyrite involves the electroadsorption of  $\text{OH}^-$ , which undergoes reversible and irreversible electroadsorption and electrodesorption at the surface. They concluded that the Fe d-electrons play a catalytic role in capturing OH radical and transferring it to  $\text{S}_2^{2-}$ . Osseo-Asare (1992) proposed a mechanism in which the first step in the decomposition of pyrite is the strong interaction of  $\text{H}_2\text{O}$  (or  $\text{OH}^-$ ) with the holes ( $h^+$ ) in the iron 3-d band (Equation 1-11). In the next step the



**Figure 1-3. Idealized molecular orbital diagrams for the linear combination of 6p orbitals (from 2 sulfur atoms) to form 6 molecular orbitals. A)  $S_2^{2-}$  or  $O_2^{2-}$  (bond order 1); B)  $S_2^-$  or  $O_2^-$  (bond order 1.5); C)  $O_2$  (bond order 2); D)  $S_2^{3-}$  (bond order 0.5).**

OH radical moves to an anionic site (Equation 1-12) where it participates in the oxidation of  $S_2^{2-}$  (Equation 1-13). The surface thiosulfate can decompose to give elemental sulfur and a bisulfite ion (Equation 1-14). The schematic of the proposed mechanism is illustrated in Figure 1-4.



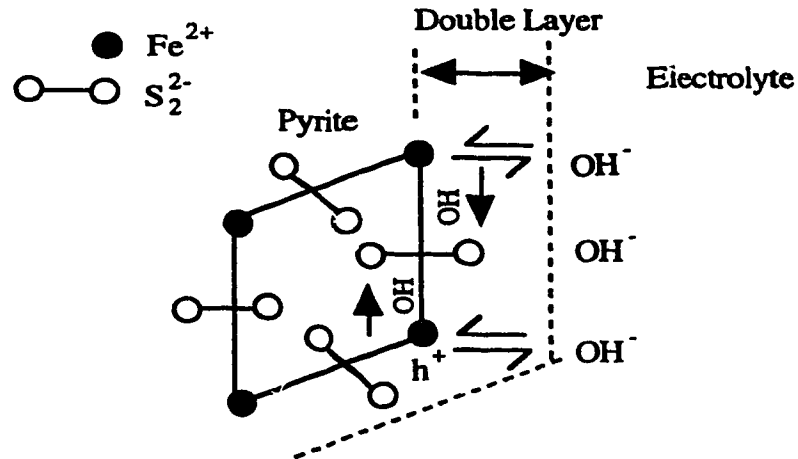


**Figure 1-4. Reaction scheme visualizing the electroadsorption of OH<sup>-</sup> on iron site and subsequent transfer of OH group onto S<sub>2</sub><sup>2-</sup> site.**

However, Springer (1970) and Biegler (1976), after studying p- and n-type pyrite specimens, concluded that the conduction type of a mineral does not normally play a significant role in oxidation and dissolution reactions. Biegler (1976) also found that there is no obvious correlation between kinetic parameters for oxygen reduction and the nature of semiconduction of pyrite. Doyle and Mirza (1990) reported that the electrochemical behaviour is correlated to some extent with the composition and electrical properties of pyrite. However, they question the use of electrochemical studies to predict the rate of acid and heavy metal release from pyrite wastes. It is suggested that under real weathering conditions, where external redox couples such as O<sub>2</sub>/H<sub>2</sub>O, Fe<sup>3+</sup>/Fe<sup>2+</sup> and bacterial processes are responsible for charge transfer, the effect of semiconducting layers and junctions is likely to be different (Doyle and Mirza, 1990).

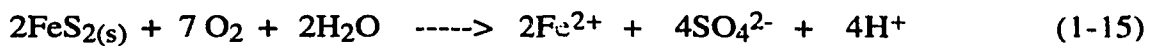
#### **1.4.1.4 Preferential Oxidation of Pyrite**

Another controversial aspect of pyrite oxidation is regarding the oxidation process of the sulfur and iron components of the mineral. Two different mechanisms have been proposed, the preferential release of sulfur atoms and the preferential release of iron from the pyrite. Goldhaber (1983) proposed that the sulfur component in pyrite is first released and oxidized to sulfate and then hydroxide ions go to the surface to react with iron sites to form an iron hydroxide layer. However, Sato (1960) and Peters (1986) proposed that the oxidation of pyrite occurs first at the iron sites. They suggested that iron is released into solution or precipitated on the surface as hydroxide, leaving a reacted layer of elemental sulfur. Hamilton and Woods (1981), using potential sweep voltammetry, reported that the formation of sulfur is restricted to the order of a monolayer at pH 9.2 and 13 but significant yield occurs at a pH of 4.6. This claim was subsequently supported by Buckley (1987) who carried out pyrite oxidation studies by electrochemical and X-ray photoelectron spectroscopy techniques. They observed that in acetic acid at pH 4.6, oxidation of pyrite results in the formation of a sulfur-rich surface layer, while in alkaline media, sulfate was the only sulfur oxidation product formed. Palencia et al. (1991) reported that the S/Fe atomic ratio of pyrite increased after a pyrite electrode had been oxidized electrochemically, and concluded that sulfur remains on the pyrite surface as a product layer while iron goes into solution. Ogunsola and Osseo-Asare (1986) also reported an increase in the S:Fe atomic ratio, obtained by X-ray energy dispersive spectrometry after pyrite had been leached electrochemically. Other investigators have also postulated the formation of a sulfur-rich surface as the initial oxidation phase during pyrite oxidation (Chander and Briceno, 1987). In spite of the large volume of literature on pyrite aqueous chemistry, there is little agreement on the mechanism of the dissolution process.

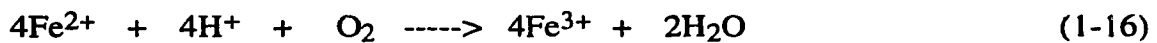


### 1.4.2 Mechanism of Acid Rock Drainage Formation

Acid rock drainage formation is recognized as a complicated process that includes several oxidation-reduction reactions, complexation and hydrolysis reactions, and solid-solution equilibria. Furthermore, the reactions are not only chemical but are also biological which adds to the complexity of the process. There have been various studies on the mechanism of ARD formation. Kleinmann et al. (1981) described three stages in the generation of ARD. Stage 1 involves the relatively slow chemical or biological oxidation of pyrite and other sulfide minerals near neutral pH by Equation 1-15.



They suggested that this initial step may be catalyzed by the bacterium *T. ferrooxidans* through direct contact with sulfide minerals. As acid begins to accumulate around the minerals, the process enters stage 2. In stage 2, ferrous iron is oxidized to ferric iron (Equation 1-16) which precipitates as ferric hydroxide (Equation 1-17) and releases more acidity.

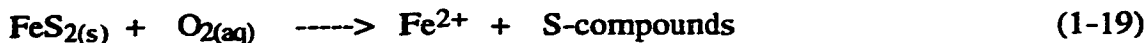


As the pH falls even further, below about 3.5, ferric iron remains in solution and oxidizes the pyrite directly (Equation 1-18).

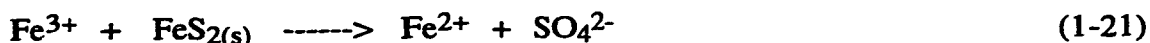


In stage 3, the bacteria rapidly catalyze the process by oxidizing ferrous iron to ferric iron and the overall rate of acid production is increased by several orders of magnitude. Equation 1-16 and 1-18 combine to form a rapid cyclic process which produces large quantities of acid associated with the release of heavy metals into solution.

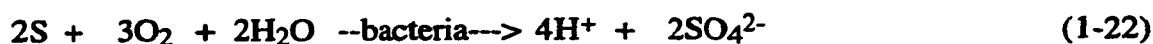
Singer and Stumm (1970) represented the oxidation of pyrite and the release of acidity by an initiator reaction,



and propagation cycle,



Ferrous ion is released in the initiator reaction (Equation 1-19) either by simple dissociation of pyrite or by the oxidation of pyrite by oxygen. After the sequence has been initiated, a cycle is established in which  $\text{Fe}^{2+}$  is oxidized by oxygen to  $\text{Fe}^{3+}$  (Equation 1-20) which is subsequently reduced by pyrite thereby generating additional  $\text{Fe}^{2+}$  and acidity (Equation 1-21). The major oxidant of pyrite was observed to be ferric iron and the oxidation of  $\text{Fe}^{2+}$  to  $\text{Fe}^{3+}$  was suggested to be the rate-determining step in abiotic systems. In the presence of microorganisms, the rate of oxidation of  $\text{Fe}^{2+}$  to  $\text{Fe}^{3+}$  was found to be accelerated. Temple and Delchamps (1953) had earlier proposed a model similar to the above, however they also proposed that the elemental sulfur liberated is also oxidized by bacteria, *Thiobacillus thiooxidans* by the reaction,



Other investigators suggest that the direct oxygen oxidation of pyrite, and Fe(III) oxidation of pyrite are independent processes and that the Fe(III) oxidation of pyrite is a chemical analogy of the microbially-enhanced pyrite oxidation process (Smith and Shumate, 1970).

### **1.4.3 The Role of Bacteria in Acid Rock Drainage Formation**

The specific role of acidophilic chemoautotrophic bacteria in pyrite oxidation to ARD formation has been a matter of considerable debate. Since its isolation in 1947, *T. ferrooxidans* has been regarded as a possible agent in the problem of ARD formation, although it was first thought that it merely accelerated the precipitation of  $\text{Fe}(\text{OH})_3$  (Colmer and Hinkle, 1947; Colmer et al., 1950; Temple and Colmer, 1951). Later experiments suggested that *T. ferrooxidans* also increased the rate of pyrite oxidation (Leathen, 1953). Singer and Stumm (1970) reported that the rate of oxidation of  $\text{Fe}^{2+}$  to  $\text{Fe}^{3+}$  was accelerated by a factor of more than  $10^6$  in the presence of microorganisms when compared to their absence. Colmer et al. (1950) also observed that the oxidation of  $\text{FeSO}_4$  to  $\text{Fe}_2(\text{SO}_4)_3$  was prevented when the growth of the organism was prevented.

Since oxidation of  $\text{FeS}_2$  may proceed solely by chemical routes, as in electrochemical oxidation of pyrite, it has been suggested that microorganisms are not essential to ARD formation. Their role has been suggested to be as a direct catalyst which alters the overall chemical reaction rates or as specific catalytic agents which alter the rate of intermediate reactions and the nature of the resulting byproducts but not the overall rate (Baker and Wilshire, 1970). It is suggested that the microorganisms remove electrons from surface pyritic iron to start a reaction chain and/or catalyze sulfur oxidation or they simply increase  $\text{Fe}(\text{III})$  concentration and hence the  $\text{Fe}(\text{III})$  to  $\text{Fe}(\text{II})$  ionic ratio.  $\text{Fe}(\text{III})$  is then reduced by pyrite and releases  $\text{Fe}(\text{II})$  which is oxidized by the bacteria (Silverman, 1967; Baker and Wilshire, 1970). Dugan and Lundgren (1965) reported that in the presence of bacteria, the ferrous ion forms a complex in the medium or at the cell surface. The complexed ferrous ion is then oxygenated and oxidized by iron oxidase which causes the release of an electron from ferrous ion. The energy evolved in this process is used as a reducing power for carbon dioxide fixation by the bacteria.

Some investigators have argued that in underground and waste heap environments, low water-pyrite ratios necessary for oxidation would rapidly lead to pH levels below the

0.8 tolerance of *T. ferrooxidans*. Strains of the bacteria, however, have been found to survive at pH as low as 0. Brock (1975) has also cited the buildup of dissolved solids as a factor that eliminates *T. ferrooxidans* as a significant factor in pyrite oxidation. Using laboratory simulations, Kleinmann and Crerar (1979) reported that *T. ferrooxidans* is not important in saturated environments. They however found that it significantly increased acid formation near the land surface, and that it is significant in the intermediate belt of the zone of aeration.

Silverman (1967) found that *T. ferrooxidans* and *Ferrobacillus ferrooxidans* are strict aerobes and oxygen is the only electron acceptor which will support the bacterial oxidation of ferrous to ferric. This claim was later supported by Baker and Wilshire (1970) who found that nonaerated reactor environments did not support the aerobic chemoautotrophs. Hence, the ferrous iron and acidity released from seeded and nonseeded reactors under nonaerated conditions were comparable. However, Omura et al. (1991) reported that ferrous iron oxidation by *T. ferrooxidans* was independent of oxygen concentration above 2 mg/L. Pugh et al. (1984) had earlier suggested that oxygen level of between 0 to 2% by volume inhibited microbial oxidation of pyrite.

Since it is reported that the bacteria derive their energy through electron transfer, it has been suggested that a redox reaction plays a vital role in biochemical oxidation of pyrite. However, Palencia et al. (1991) studied the electrochemical oxidation of pyrite in sterile and inoculated solutions using both linear-scan voltammetric and chronoamperometric techniques and found that electrochemical experiments did not distinguish any significant effect of the bacteria on the electrochemical oxidation of pyrite electrode. They suggested that electrochemical techniques were not sufficiently sensitive to the slow surface activity of bacteria and the resulting complex chemical changes at the pyrite surface.

### **1.4.3.1 Mechanism of Bacteria Oxidation of Pyrite**

Silverman and Ehrlich (1964) proposed two different mechanisms of bacterial oxidation, the indirect and direct contact mechanisms. According to the indirect contact mechanism, ferric ions are the primary oxidant, oxidizing metal sulfides while being reduced in turn to the ferrous state. The bacteria then enter the reaction by oxidizing ferrous ions to the ferric state, thereby regenerating the primary oxidant. The direct contact mechanism is independent of the action of ferric ions, requiring only intimate physical contact between the bacteria and sulfide mineral under aerobic conditions.

Silverman (1967) suggested that the indirect and direct mechanisms operate concurrently. They reported that ferric ions oxidize pyrite in the absence of oxygen and bacteria. However, in contrast to the indirect mechanism, Schaeffer et al. (1963) had earlier presented evidence that the bacteria exert their catalytic effect only while attached to the pyrite surface. They suggested that the nature of the attachment was chemical rather than physical. Omura et al. (1991) reported that the iron-oxidizing bacteria could not grow in the liquid phase, but could multiply only on a support medium, and therefore suggested that the oxidation of ferrous iron is carried out by attached cells.

Palencia et al. (1991), and Vitaya and Toda (1991) observed deep crevices and pits after bacteria oxidation of pyrite and attributed it to the attachment of bacteria onto pyrite. The rod-shaped organisms were also found attached to the pyrite surface. Since no pits were observed after pyrite oxidation by ferric ions in the absence of bacteria, Vitaya and Toda (1991) concluded that the cell adsorbed onto pyrite and catalyzed the dissolution of the mineral from the surface. Murthy and Natarajan (1992) studied the effect of surface attachment of *T. ferrooxidans* on the oxidation of pyrite and reported that increasing bacterial attachment on pyrite surface resulted in an increased iron dissolution. Scanning electron microscopy (SEM) and cyclic voltammetry techniques have been used to show that the pyrite surface undergoes dramatic changes in the presence of bacteria. It was observed

that the pyrite surface became completely covered with a layer of active bacteria after 2 days of bioleaching (Pesic and Kim, 1993).

From a practical standpoint, the important difference between these two conceptual models lies in the fact that in the indirect case the total number of bacteria in a given system is potentially a rate-determining factor, while in the direct model, only those bacteria absorbed on the pyrite surface will directly affect oxidation rates.

On the basis of an SEM examination of bacteria cells, and X-ray and chemical characterization of reaction products, Pesic and Kim (1993) proposed a mechanism by which bacteria cells serve as nucleation sites for the formation of jarosite. According to this mechanism, jarosite formation begins on a cell, and with time, the initial nuclei of jarosite  $\{KFe_3(SO_4)_2(OH)_6, (H_3O)Fe_3(SO_4)_2(OH)_6\}$  grow and new nucleation sites are initiated.

#### **1.4.3.2. Attachment of Bacteria onto Pyrite**

Bagdigian and Myerson (1986) demonstrated that *T. ferrooxidans* do not adsorb randomly onto pyrite but congregate selectively at sites where dislocations, grain boundaries and the nonuniformities in the pyrite crystal structure emerge at the surface. The grain boundaries and cracks are said to be energetically unstable regions which facilitate easier attachment (Vitaya and Toda, 1991). It is suggested that the bacteria possess chemotacticity to locate such preferential (active) sites (Murthy and Natarajan, 1992). Andrew (1988) supported the selective adsorption model and suggested a survival advantage as the reason for bacteria adsorbing at a dislocation site. They hypothesized molecular diffusion of sulfur through pyrite to dislocations and grain boundaries where bacteria are attached.

Extracellular adhesive polymers are reported to be involved in the adhesion of bacteria onto surfaces (Marshall and Mitchell, 1971; Fletcher and Floodgate, 1973; Murthy and Natarajan, 1992). Vitaya and Toda (1991) reported that when ATPase functions of the bacteria were blocked by the use of an inhibitor, NaF, the cells could not hydrolyze ATP

and therefore lost the ability of adsorption or synthesis of extracellular slimes needed for adsorption. Hydrophobicity was also found to play an important role in cell adsorption. A surfactant, Tween 80, resulted in the prevention of adsorption of cells onto coal pyrite. The electrical properties of coal and cell surfaces such as zeta potential, however, were found to have no effects upon the adsorption of bacteria onto coal pyrite surfaces.

#### **1.4.4 Treatment of Acid Rock Drainage**

Several techniques have been investigated in the past for the treatment and abatement of ARD. These techniques can be divided into two general groups, the first group are those directed towards the treatment of the resulting drainage and the second group comprises techniques directed towards controlling of ARD at source. The former treatment approach allows pyrite oxidation to run its course, then, after the acid-forming salts and metals are leached, the discharged acidic drainage is collected and treated.

##### **1.4.4.1 Chemical Treatment of Acid Rock Drainage**

The collection and treatment of acid water drainage is well established, the common treatment method being neutralization with alkaline materials and precipitation of metals as hydroxides. The current ARD control technology for active mine sites involves the collection of the drainage from all sources and continual addition of hydrated lime in an effort to neutralize their acidity and precipitate dissolved metals (Ziemkiewicz et al., 1990). Other nonconventional materials like fly ash, bentonite, kaolinite, spent lime and cement have also been used for this purpose (Harshberger and Bowders, 1991).

Limestone, being the most inexpensive of the common neutralizing agents, has been used for many years for treating acidic waters. The comparative cost of limestone and alkaline chemicals commonly used in the treatment of ARD is shown in Table 1-2.

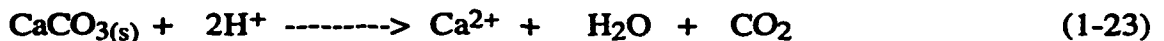
**Table 1-2**

**Comparative cost of limestone and alkaline chemicals commonly used in the treatment of acid rock drainage.**

Material	Chemical composition	Cost per Kmole of OH <sup>-</sup> equivalent* (1990 US \$)
Limestone	CaCO <sub>3</sub>	0.69
Hydrated lime	Ca(OH) <sub>2</sub>	2.64
Ammonia	NH <sub>3</sub>	5.61
Soda ash	Na <sub>2</sub> CO <sub>3</sub>	15.16
Caustic soda	NaOH	21.56

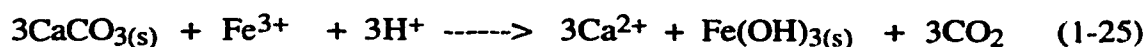
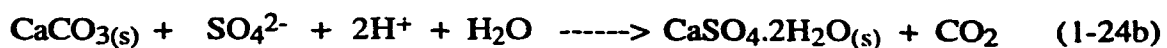
\* Chemical cost from Skousen et al. (1990). Limestone cost is based on a 95% content at US \$13 Mg<sup>-1</sup>.

On contact with ARD, the limestone dissolves producing carbonate alkalinity and increases pH. The use of limestone, however, has been abandoned in most chemical treatment systems because of the formation of ferric oxyhydroxides which coat limestone in oxidizing environments and eliminate any further neutralizing capability (Nairn et al., 1989). Wentzler and Aplan (1992) have also reported that iron hydroxide and gypsum coatings build up on the limestone surface inhibiting further neutralization reactions. Furthermore, the rate of the neutralization reaction was observed to decrease dramatically with increasing pH, so that limestone is not very useful above pH of 5. They concluded that, though attractive economically, a fresh limestone surface must continually be presented to the acidic drainage for neutralization to occur. The typical reactions involved in limestone neutralization of acid mine effluent are (Wentzler and Aplan,1992):





or more likely:



To prevent the formation of oxyhydroxides which armor limestone in oxidizing environments, anoxic limestone drains have been proposed. Nairn et al. (1989) used an anoxic limestone drain as an alkalinity generator prior to a passive treatment system. In the anoxic system, the limestone drain is covered with plastic and clay or soil to inhibit oxygen penetration and prevent the oxidation of ferrous iron in the effluent as illustrated in Figure 1-5. It is reported that limestone under this condition does not become armored.

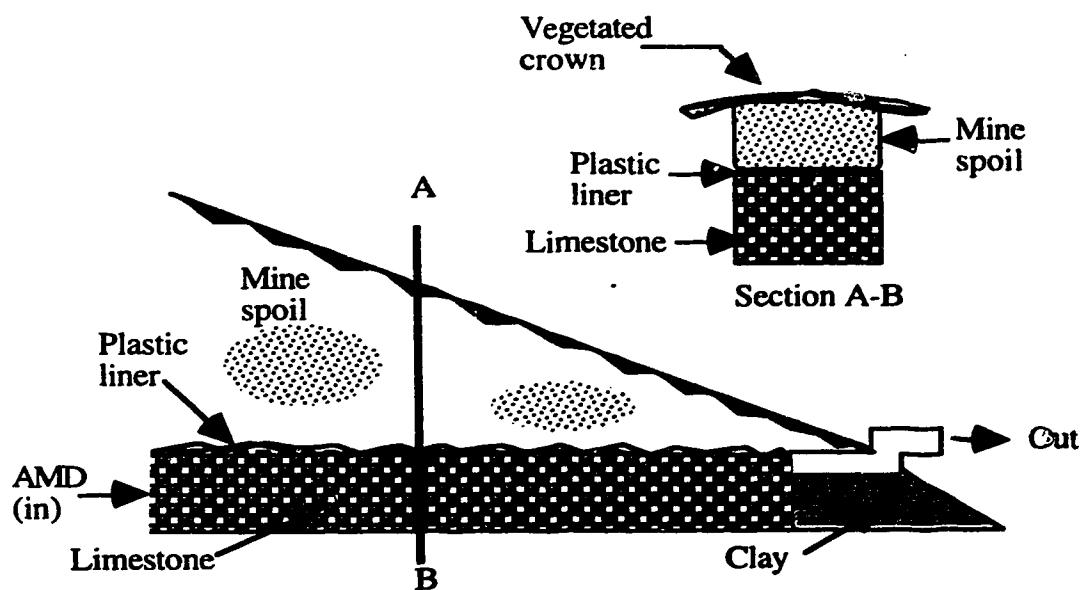


**Figure 1-5. Cross section of anoxic limestone drain (ALD).**

The precipitation of metals as insoluble sulfides by the use of limestone and gaseous hydrogen sulfide have also been reported (Hammack and Edenborn, 1991). However, a sulfide precipitation plant is considered expensive to operate because of high cost of H<sub>2</sub>S or Na<sub>2</sub>S. There are also safety concerns when transporting or applying toxic H<sub>2</sub>S gas or caustic Na<sub>2</sub>S.

While alkaline effluent treatment is acceptable during active mining and processing operation, it is not an efficient solution to the problem at inactive sites. Another drawback to effluent treatment is incomplete removal of contaminants already leached into solution and the requirement of an appropriate disposal method for the treatment plant sludges.

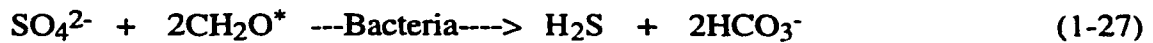
#### **1.4.4.2 Passive Treatment of Acid Rock Drainage**

Alternatives to the chemical methods (or processes) used to treat ARD are the passive systems, which include natural and constructed wetland. Wetlands is a general term, encompassing swamps, marshes, bogs, wet meadows, and fens. The wetlands are normally dominated by plants that prefer slightly to moderately acidic environments. These plants also tolerate levels of sulfate and various metals that would eliminate most plant forms (Hedin and Nairn, 1992).

The most common passive treatment systems are the constructed wetlands in which *Sphagnum*, spent mushroom compost or especially cattails (*Typha*) are used (Hedin et al., 1989). In most of the constructed wetland systems, the principal processes that take place include: adsorption and ion exchange, bioaccumulation, bacterial and abiotic oxidation, sedimentation, neutralization, sulfate reduction and possibly formation of carbonate minerals. The most important metal removing mechanisms in wetlands are bacterially-catalyzed oxidation and hydrolysis reactions that cause dissolved iron to precipitate (Hedin and Nairn, 1992). The processes involved in sulfate reduction are the reverse of pyrite oxidation; acidity is consumed by the sulfate reduction processes. Unlike bacterial oxidation processes which leach heavy metals, hydrogen sulfide produced by bacterial

sulfate reduction reacts with many metals to form virtually insoluble sulfide compounds (Kleinmann and Hedin, 1989).

The dissimilatory sulfate reduction is accomplished by heterotrophic anaerobic bacteria that, in the absence of oxygen, decompose simple organic compounds using sulfate as a terminal electron acceptor. The sulfate reduction is represented by the reaction (Hedin et al., 1989);



where  $\text{CH}_2\text{O}^*$  represents a simple organic molecule such as lactate or acetate. The dissimilatory sulfate-reducing bacteria is inhibited by low pH and the most well-known bacterial genus, *Desulfovibrio*, is not active at pH of less than 5, and therefore neutralization of the ARD is required (Hedin et al., 1989). Neutralization is achieved by the use of anoxic limestone drains (Figure 1-5) or compost wetland. The common substrate in compost wetland is spent mushroom compost, which is an ideal organic material because it is an excellent microbial substrate, and it also contains limestone. Cattails or other emergent vegetation are planted in the substrate to stabilize it and provide organic matter to "fuel" the sulfate reduction process as illustrated in Figure 1-6 (Hedin and Nairn, 1992).

Sulfate esterification has also been reported to occur in the presence of plant residues such as humic and fulvic acids, lignin, and cellulose, and appears to be mediated by microbes. This mechanism is reported to be responsible for the neutralization effects when acid drainage passes through decomposing materials (Tuttle et al., 1969).

Most of the wetlands treatment systems are constructed to treat acidic coal mine drainage, as opposed to effluent from metal mines. In the coal effluents the principal contaminants of concern are excessive acidity, iron, manganese and aluminum. These processes have been reported to be quite effective in removing iron, but inconsistent with respect to other water quality parameters. The removal of most of the iron eliminates much

of the need for chemical treatment, but does not, by itself, eliminate its necessity. At most sites supplemental chemical treatment is necessary (Nairn et al., 1991). Bioaccumulation of toxic metal also causes problems, for it could result in the chronic poisoning of foraging animals (Kleinmann and Hedin, 1989).

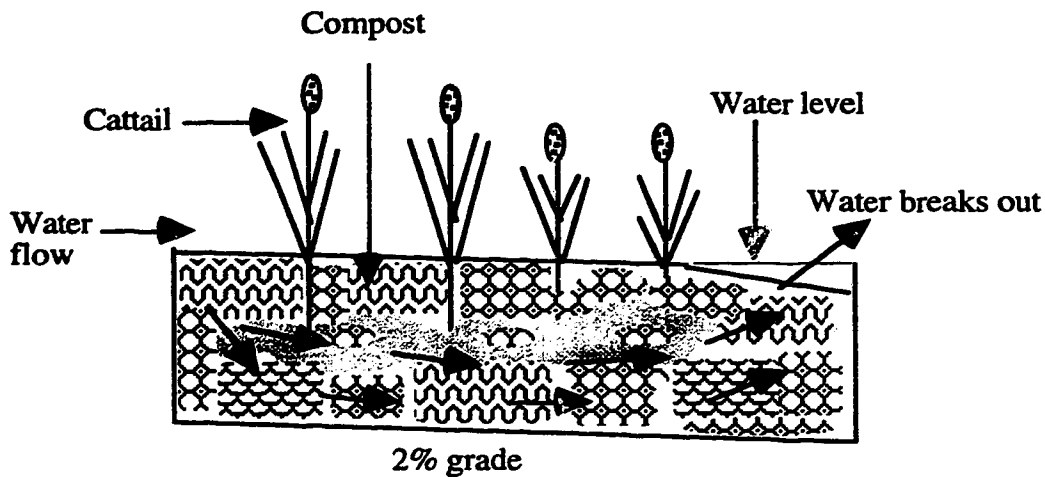


**Figure 1-6. Compost wetland.**

The fundamental problem with the treatment methods, which allow pyrite oxidation to run its course, is that, while pyrite oxidation may be fairly rapid, its weathering products leach out of the waste tailings or rock over a period of many decades. This imposes long-term commitments on mining companies and governments.

#### **1.4.5 At-source Control and Prevention of Acid Rock Drainage**

Since ARD results from the oxidation of pyrite in the presence of oxygen, water, and/or iron-oxidizing bacteria, any of these three components acting on the pyrite may provide a potential at-source control point for reducing or preventing ARD formation. All the at-source methods are therefore directed towards controlling one or more of these components. Although the concept is simple, the application of this concept is difficult to

achieve. Various control schemes have been proposed, including: removal of sulfide minerals prior to disposal, coating of sulfide surfaces, control of bacterial activity, temperature control, limiting gaseous oxygen infiltration and blending of acid and base materials.

#### **1.4.5.1 Control of Bacteria Activity**

Control of ARD formation through killing or inhibition of bacteria (*T. ferrooxidans*) activity by the use of bactericides have been studied by several investigators. The possibility of reducing acid drainage by bacterial inhibition was first considered in 1953 but was rejected as impractical due to rapid repopulation (Temple and Delchamps, 1953). However, Klienmann and Erickson (1983) studied the inhibitory effects of anionic surfactants, sodium lauryl sulfate (SLS), alkyl benzene sulfonate and alpha olefin sulfonate on *T. ferrooxidans* and concluded that SLS was the most effective in limiting bacterial population. They observed that by inhibiting bacteria activity, the biotic oxidation of pyrite and ferrous iron and therefore ARD were significantly reduced. However, the SLS did not affect direct (air) oxidation or abiotic ferric oxidation of pyrite. Erickson et al. (1984) reported that by using SLS concentrations of 2 to 5mg/L, *T. ferrooxidans* were killed and water quality from an active mine site improved. The elimination of iron-oxidizing bacteria after treatment with SLS and benzoic acid have also been reported by Dugan (1987). However, it was observed that the microorganisms and acid formation reappeared within 2 to 5 weeks after treatment was terminated.

Many other bactericides have been investigated for the use as inhibitors of microorganisms in ARD, including sodium benzoate, potassium sorbate, sodium chloride, thymol, etc (Siwik et al., 1989; Silver and Ritcey, 1985). They concluded that it cannot be regarded as a long-term control measure because of the repopulation problem which arises, necessitating continuous application of the bactericides (Siwik et al., 1989; Erickson et al., 1984). Furthermore, the bactericides only controlled the biotic aspect of pyrite oxidation.

To prevent repopulation of the bacteria, other methods of application have been reported in which SLS is added to various elastomers to obtain controlled release of the inhibitor in the waste for extended periods of time (Kleinmann and Crerar, 1979; Kleinmann et al., 1981). The mechanism for this inhibition is not clear, but it is proposed that semipermeable properties of the cytoplasmic membrane are altered so that  $H^+$  is allowed to seep into the normally neutral interior of the cell. Thus, the bacteria are attacked by the acid they helped produce (Olem et al., 1983).

Studies of chronic and acute effects of SLS surfactant on fish and aquatic invertebrates indicate that kidney damage occurs in fish after long exposure at low levels of concentrations, and acute toxicity occurs in some species at concentrations as varied as 0.6 to 40 mg/L (Abel, 1976; Bromage and Fuchs, 1976).

#### **1.4.5.2 Control of Oxygen**

It is reported that the role of oxygen in the formation of ARD is the direct oxidation of pyrite, and ferrous iron oxidation to ferric iron which in turn oxidizes pyrite (Singer and Stumm 1970). The exact dependence of the pyrite oxidation rate on gas phase oxygen concentration however, is not well understood. Laboratory and pilot-scale studies reported in the literature show conflicting results. Studies conducted in a small underground test mine found that acid production increased consistently as oxygen in the gas phase increased from 0.02 to 20% by volume (U.S. Environment, 1971). Pugh et al. (1984) also reported that in the absence of bacteria the rate of pyrite oxidation increased significantly with increasing oxygen concentration from 0 to 20% by volume. However, various laboratory studies indicate that acid production rate is independent of oxygen concentration at values ranging from 1.6% to 10% by volume (Erickson et al., 1984). The variation in the oxygen concentration was attributed to the differences in the materials and experimental conditions used.

In the presence of bacteria, Baker and Wilshire (1970) observed that oxygen exclusion did not prevent pyrite oxidation whereas Pugh et al. (1984) reported that the rate of oxidation of pyrite was dependent on oxygen concentrations between 0 to 8% by volume. In spite of this controversy, the control of ARD formation through the prevention of oxygen and water contact with the pyrite waste has been investigated. These techniques use low permeability materials such as polyethylene, asphalt, or clay covers to cover the waste material, or vegetation of waste surface, so as to reduce access to water and oxygen.

Silver and Ritcey (1985) reported that sulfuric acid generation in pyrite-containing uranium tailings was greatly decreased when the influx of oxygen into the tailings is impeded by submersion under water, or by the deposition of a sufficiently thick layer of organic material that acts as an effective oxygen barrier on the tailings surface. Healey and Robertson (1989) investigated the use of a till cover over an abandoned copper mine and reported that the cover did not exclude water and oxygen to the extent of preventing acid generation, but migration of ARD was significantly reduced. The establishment of vegetation directly on the tailings surfaces has also been investigated by several investigators and was found to decrease but not eliminate acid generation (Silver and Ritcey, 1985; Filion et al., 1990).

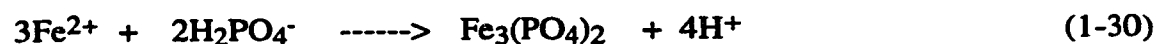
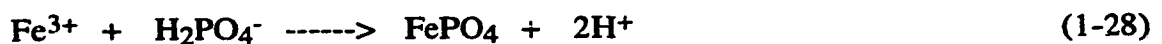
Attempts to prevent water and oxygen from contacting the pyritic materials in wastes have only been partially successful. The partial success has been attributed to the extremely low (of the order of  $10^{-30}$ ) partial pressure of oxygen required to prevent pyrite oxidation and the extreme difficulty of completely preventing water flow in the waste, especially into rock that has been disturbed, such as overburden and refuse, due to its higher porosity (Chander and Zhou, 1992).

#### **1.4.5.3 Chemical Pretreatment of Pyrite**

Chemical pretreatment methods for reduction and abatement of ARD depend upon the creation of conditions which chemically or physically retard the oxidation of pyrite.

Chander and Zhou (1992) studied the effect of organic reagents on acid generation from pyrite waste and reported that coal pyrite pretreated with reagents containing carboxylic functional groups attached to aromatic hydrocarbon groups show a high rate of oxidation whereas the rate of oxidation decreased when samples were pretreated with complexing agents containing hydroxyl functional groups. It was suggested that the carboxyl groups react with iron to form complexes in the bulk solution, exposing pyrite to further attack, while reagents containing hydroxyl functional groups form surface compounds with iron species and coat the particle surface thus preventing the pyrite from further oxidation.

Stiller et al. (1989), by assuming that the  $\text{Fe}^{3+}/\text{FeS}_2$  reaction is the major step in the oxidation of pyrite and production of acid from toxic mine waste materials reported that the average equilibrium voltage for the  $\text{Fe}^{3+}/\text{FeS}_2$  system is 0.42 volts, and corresponds to  $\text{Fe}^{3+}:\text{Fe}^{2+}$  ratio of  $10^{-6}:1$ . They proposed that if the  $\text{Fe}^{3+}:\text{Fe}^{2+}$  ratio could be reduced to less than  $10^{-6}:1$ , the  $\text{Fe}^{3+}$  oxidation of  $\text{FeS}_2$  could not take place. Phosphate was used to precipitate  $\text{Fe}^{2+}$  and  $\text{Fe}^{3+}$  under ideal conditions at near-neutral pH to a  $\text{Fe}^{3+}:\text{Fe}^{2+}$  ratio of  $10^{-11}:1$ , thus reducing pyrite oxidation by  $\text{Fe}^{3+}$ . Spotts and Dollhopf (1992) also investigated the use of phosphate to precipitate  $\text{Fe}^{3+}$  into relatively insoluble forms,  $\text{FePO}_4$  (Equation 1-28) or  $\text{FePO}_4 \cdot 2\text{H}_2\text{O}$  (Equation 1-29). It was suggested that the phosphate may also be able to precipitate  $\text{Fe}^{2+}$  as  $\text{Fe}_3(\text{PO}_4)_2$  (Equation 1-30), reducing the amount of  $\text{Fe}^{2+}$  available in solution for oxidation to  $\text{Fe}^{3+}$ , either by  $\text{O}_2$  or bacteria.



They reported that by pretreating an acid-producing coal overburden with phosphate, the cumulative Fe, acidity, and  $\text{SO}_4^{2-}$  levels were reduced when tested in a soxhlet humidity cell. The reduction in the rate of oxidation of pyrite after pretreatment with phosphate was



also reported by Evangelou and Huang (1992) who attributed this to the formation of a ferric phosphate coating on pyrite surface.

The corrosion current of pyrite was reported to decrease after oxalic acid treatment. The decrease was attributed to the formation of a  $\beta\text{-FeC}_2\text{O}_4\cdot 2\text{H}_2\text{O}$  protective layer formed on the pyrite after oxalic acid treatment. Acetyl acetone and humic acid were also found to lower the corrosion current, while methyl triacetoxyl silane treatment increased the corrosion current (Lalvani et al., 1990).

## 1.5 SUMMARY OF REVIEW

In spite of the numerous studies on the mechanisms and kinetics of ARD formation, ARD still remains a serious environmental problem facing the mining and mineral industry today. Current ARD control technology involves the continual collection and treatment of the resulting acidic effluent. Apart from being expensive and ineffective, this technology require an indefinite period of maintenance of treatment facilities and disposal of treatment sludges, since acid generation may persist for hundreds of years following mine closure.

Most of the studies on ARD control have been directed towards improving the effluent treatment systems rather than towards controlling the ARD formation at-source. The treatment of pyritic waste such as to permanently reduce or eliminate pyrite oxidation would be the most desirable solution to the ARD problem. Only a few studies have been directed towards preventing or controlling ARD at-source, and none have been very successful. Presently, there is no widely accepted technology that controls or prevents ARD formation at-source without indefinite maintenance. The strategy adopted in this project will be to investigate the effectiveness of potentially promising at-source control and prevention techniques in order to avoid the oxidation of pyrite.

While it is known that ARD is produced by the oxidation of metallic sulfides, often found in conjunction with coal and metal deposits, the oxidation of these metallic sulfides is a complex process and is not fully understood. The exact mechanism of strictly chemical

oxidation of pyrite in a closely defined environment is also a subject of controversy. Although many theories have been used to explain the mechanism of pyrite oxidation, there is only little agreement, and only a general picture of the oxidation processes can be visualized. In the formation of ARD, the mechanism is further complicated by the presence of bacteria, which results in not only a chemical oxidation route, but also a biological oxidation route for sulfide.

The review of the relevant literature on ARD formation show that there is a general agreement on the main reactants of the reaction. Most investigators agree that the main reactants are pyrite, water, ferric ions, oxygen and/or oxidizing bacteria. However, the role of each reactant is not clear. The role of bacteria have sometimes been assumed to be limited to catalyzing the reaction, while at other times, it has been considered as a reactant. The increase in the rate of ARD formation in the presence of bacteria has also been a subject of controversy, although most studies agree that its presence increases the rate of formation of ARD. In the presence of bacteria, the role of oxygen has been considered as unimportant by some investigators, while other investigators have reported its importance in the presence and absence of bacteria.

In order to successfully control or prevent ARD at-source, a detailed understanding of the fundamental chemistry, mechanisms and kinetics involved in its formation is important. Only when these fundamentals are known, can effective and promising methods be formulated and improved upon.

## **1.6 PROJECT OBJECTIVES**

The preceding review of the literature on pyrite oxidation and ARD formation clearly suggest that a significant amount of fundamental studies is needed before effective techniques are found for preventing the onset of pyrite oxidation, and the subsequent formation of ARD. Although there is controversy over the exact chemical mechanism of pyrite oxidation, a basic phenomenon common to the various proposed mechanisms is the

initial adsorption of oxidizing agents, oxygen, aqueous ferric ions, water and bacteria, onto an active pyrite surface before the commencement of oxidation.

Consequently, a control and prevention strategy aimed at rendering the pyrite surface inactive or incapable of adsorbing the primary oxidation reactants should show some promise for preventing ARD formation. Such an at-source control and prevention method would reduce or eliminate the surface adsorption of oxygen, water, ferric ions, and bacteria, thus preventing the onset of pyrite oxidation.

The primary aim of this project therefore, was to investigate methods for the prevention of ARD formation by the deactivation of pyrite surface. The objectives were to investigate:

- (1) the formation and precipitation of an inorganic iron-phosphate complex coating on the pyrite surface to prevent or reduce the ingress of oxidizing agents.
- (2) chemical treatment with organic cationic surfactants which are capable of strong chemisorption onto the pyrite surface to impart a high surface hydrophobicity. Such a treatment should prevent the adsorption of oxidizing agents, e.g.  $\text{Fe}^{3+}$ ,  $\text{H}_2\text{O}$ ,  $\text{O}_2$ , and bacteria, thus eliminating the onset of oxidation.

These at-source control methods were tested using a laboratory column and an autoclave in the absence and presence of bacteria to evaluate their effectiveness.

Since understanding the chemistry, mechanisms and kinetics of formation of acid rock drainage is the key to developing and improving effective at-source control and prevention methods, the secondary objectives of this research were:

- (3) to study the mechanisms and kinetics of ARD formation and to evaluate the effect of the major reactants; oxygen, water and bacteria on the rate of pyrite oxidation.
- (4) to study the effect of pertinent parameters such as: pressure, temperature and other ions in solution on pyrite oxidation.

The results of the kinetics and mechanistic studies should provide further insight into the effectiveness or non-effectiveness of the at-source control methods outlined in the primary objectives.

## **1.7 ORGANIZATION OF THESIS**

The mixed format (A Manual of Regulations and Guidelines for Thesis Preparation, University of Alberta, 1995) was adopted for the preparation of this thesis. The first chapter is a general introduction to the entire thesis. It covers a general literature review of the subject, the objectives of the project, and a synopsis of material in each chapter of the thesis.

Chapters 2 through 9, deal with independent, but related topics. Each chapter starts with a short introduction to the subject addressed in that chapter, followed by theory and background, experimental, results and discussion, summary of the chapter, and references cited. To reduce repetition of some experimental procedures, references are made to previous chapters as much as possible.

### **1.7.1 Summary of Chapters**

Chapter 2 summarizes the use of low and elevated temperature phosphate coatings techniques to suppress chemical oxidation of pyrite, and hence control ARD formation at-source. The pyrite coated particles were tested at ambient and elevated temperatures and pressures in the absence of bacteria. Chapter 3 explores the use of a fatty acid amine to produce a highly hydrophobic pyrite surface as a means of suppressing pyrite oxidation and controlling ARD. The chemical oxidation of the treated pyrite were tested at ambient and elevated temperatures and pressures.

The growth of *T. ferrooxidans* and the relationship between some of the commonly used parameters in bioleaching, oxidation kinetics and ARD studies were investigated and

reported in Chapter 4. The results of this chapter were used to design experiments for Chapters 5 to 9, in which the bacteria were employed.

Chapter 5 summarizes the kinetics of ferrous oxidation in the absence and presence of *T. ferrooxidans*. The effect of ferric iron and cell concentrations on the oxidation kinetics of ferrous iron by bacteria is reported in Chapter 6.

Chapter 7 investigates the mechanism of pyrite oxidation and ARD formation. The effect of *T. ferrooxidans* on the stability of the fatty acid treated and phosphate-coated pyrite particles are given in Chapters 8 and 9, respectively. General discussion and conclusions from the separate chapters are given in Chapter 10.

## 1.8 REFERENCES

- Abel, P. D. 1976. Toxic action of several lethal concentrations of an anionic detergent on the gills of the brown trout. *J. Fish Biology*. 9: 441-446.
- Ahlberg, E., K. S. E. Forssberg, and X. Wang. 1990. The surface oxidation of pyrite in alkaline solution. *J. Appl. Electrochem*. 2C: 1033-1039.
- Andrews, G. F. 1988. The selective adsorption of *Thiobacilli* to dislocation sites on pyrite surfaces. *Biotechnol. Bioeng*. 31: 378-381.
- Bagdigian, R. M., and A. S. Myerson. 1986. The adsorption of *Thiobacillus ferrooxidans* on coal surfaces. *Biotechnol. Bioeng*. 28: 467-479.
- Bailey, L. K., and E. Peters. 1976. Decomposition of pyrite in acids by pressure leaching and anodization: the case for an electrochemical mechanism. *Can. Metallurg. Quart.* 15: 333-344.
- Baker, R. A., and A. G. Wilshire. 1970a. Microbiological factor in acid mine drainage formation: A pilot plant study. *Environ. Sci. Technol.* 4: 401-407.
- Baker, R. A., and A. G. Wilshire. 1970b. Microbiological factor in acid mine drainage formation. *Wat. Pollut. Control Res. Series no. 14010 DKN 11/70*. pp. 6-8.

- Bell, A., K. D. Phinney, K. Ferguson, A. Gosselin, J. Ingles, and J. S. Scott. 1987. Mine and mill wastewater treatment. Mining, Mineral and Metallurgical Process Division, Environ. Protect., Environment Canada. Report EPS 3/HA. pp. 3.
- Biegler, T. 1976. Oxygen reduction on sulphide minerals. Part II. Relation between activity and semiconducting properties of pyrite electrodes. *J. Electroanal. Chem.* 70: 265-275.
- Biegler, T., and D. A. Swift. 1979. Anodic behaviour of pyrite in acid solutions. *Electrochim. Acta.* 24: 415-420.
- Bistline, R. G. Jr., and W. N. Linfield. 1984. Modification by surfactants of soil water absorption. *Structure / Performance Relationships in Surfactants*, M. J. Rosen (ed.). ACS symposium series 253. pp. 209-223.
- Brock, T. D. 1975. Effect of water potential on growth and iron oxidation by *Thiobacillus ferrooxidans*. *Appl. Microbiol.* 29: 495-501.
- Bromage, N. R., and A. Fuchs. 1976. A histological study of the response of the interrenal cells of the goldfish (*Carassius auratus*) to treatment with sodium lauryl sulphate. *J. Fish Biology.* 9: 529-535.
- Buckley, A. N., and R. Woods. 1987. The surface oxidation of pyrite. *Appl. Surf. Sci.* 27: 437-452.
- Chander, S., and A. Briceno. 1987. Kinetics of pyrite oxidation, *Miner. Metallurg. Process.* 4: 171-176.
- Chander, S., and R. Zhou. 1992. Effect of organic additives on acid generation from pyrite waste. *Proceedings of the symposium on emerging process technologies for a cleaner environment*, S. Chander, P. E. Richardson, and H. El-Shall (eds.). SME, Phoenix, Arizona. pp. 131-139.
- Colmer, A. R., and M. E. Hinkle. 1947. The role of microorganisms in acid mine drainage: A preliminary report. *Sci.* 106: 253-256.

- Colmer, A. R., K. L. Temple, and M. E. Hinkle. 1950. An iron-oxidizing bacterium from the acid drainage of some bituminous coal mines. *J. Bacteriol.* 59: 317-328.
- Doyle, F. M., and A. H. Mirza. 1990. Understanding the mechanisms and kinetics of acid and heavy metals release from pyritic wastes. Proceedings of the western regional symposium on mining and mineral processing wastes. Berkeley, CA. pp. 43-51.
- Dugan, P. R. 1987. Prevention of formation of acid drainage from high-sulfur coal refuse by inhibition of iron- and sulfur-oxidizing microorganisms. II. Inhibition in "run of mine" refuse under simulated field conditions. *Biotechnol. Bioeng.* 29: 49-54.
- Dugan, P. R., and D. G. Lundgren. 1965. Energy supply for the chemoautotroph *Ferrobacillus ferrooxidans*. *J. Bacteriol.* 89: 825-834.
- Erickson, P. M. R. L. P. Kleinmann, W. R. Homeister, and R. C. Briggs. 1984. Reclamation and the control of acid mine drainage. Proceedings of the symposium on the reclamation, treatment and utilization of coal mining wastes, A.K.M. Rainbow (ed.), Durham, England.
- Evangelou, V. P., and X. Huang. 1992. A new technology for armoring and deactivating pyrite. Environmental issues and waste management in energy and minerals production, R. K. Singhal, A. K. Mehrotra, K. Fytas, and J-L. Collins (eds.). Calgary, Alberta. Balkema, Rotterdam. pp. 413-417.
- Filion, M. P., L. L. Sirois, and K. Ferguson. 1990. Acid mine drainage research in Canada. *CIM Bull.* 83: 33-40.
- Fletcher, M., and G. D. Floodgate. 1973. An electronmicroscopic demonstration of an acidic polysaccharide involved in the adhesion of a marine bacteria to solid surfaces. *J. Gen. Microbiol.* 74: 325-334.
- Goldhaber, M. B. 1983. Experimental study of metastable sulfur oxyanion formation during pyrite oxidation at pH 6-9 and 30°C. *Am. J. Sci.* 283: 193-217.
- Halbert, B.E., R. A. Knapp, J. W. Maltby, and A. J. Vivyurka. 1989. Application of the reactive acid tailings assessment program to pyritic mine tailings. *Tailings and effluent*

- management, Proceedings of the international symposium on tailings and effluent management, M. E. Chalkley, B. R. Conard, V. I. Lakshmanan, and K. G. Wheeland (eds.). CIM, Halifax. Pergamon, New York. pp. 83-90.
- Hamilton, I. C., and R. Woods. 1981. An investigation of surface oxidation of pyrite and pyrrhotite by linear potential sweep voltametry. *J. Electroanal. Chem.* 118: 327-343.
- Hammack, R. W., and H. M. Edenborn. 1991. The removal of nickel from mine waters using bacterial sulfate reduction. American society for surface mining and reclamation, Durango, CO.
- Harshberger, K. L., and J. J. Bowders Jr. 1991. Acid mine drainage control utilizing fly ash. *Energy in The 90's. Proceedings of a Specialty conference, sponsored by the Energy Division of the American Society of Civil Engineers, B. F. Hobbs (ed.). pp. 300-305.*
- Healey, P. M., and A. M. Robertson. 1989. A case history of an acid generation abatement program for an abandoned copper mine. *Geotechnical aspects of tailings disposal and acid mine drainage. The Vancouver Geotechnical Society, Vancouver, B. C.*
- Hedin, R. S., R. W. Hammack, and D. M. Hyman. 1989. Potential importance of sulfate reduction processes in wetlands constructed to treat mine drainage. *Constructed wetlands for wastewater treatment. Lewis publishers, Michigan. pp. 508-514.*
- Hedin, R. S., and R. W. Nairn. 1992. *Passive treatment of coal mine drainage. Pennsylvania DER Workshop Course Notes. Edensburg, PA.*
- Jensen, M. L., and A. M. Bateman. 1979. *Economic Mineral Deposits. John Wiley & Sons. New York, NY. pp. 41-59.*
- Kleinmann, R. L. P., and D. A. Crerar. 1979. *Thiobacillus ferrooxidans* and the formation of acidity in simulated coal mine environments. *J. Geomicrobiol.* 1: 373-388.
- Kleinmann, R. L. P., D. A. Crerar, and R. P. Pacelli. 1981. Biogeochemistry of acid mine drainage and a method to control acid formation. *Min. Eng.* 33: 300-305.



- Kleinmann, R. L. P., and P. M. Erickson. 1983. Control of acid drainage from coal refuse using anionic surfactants. U. S. Bureau of Mines, RI8847.
- Kleinmann, R. L. P., and R. Hedin. 1989. Biological treatment of mine water: An update. Tailings and effluent Management, Proceedings of the international symposium on tailings and effluent management, M. E. Chalkley, B. R. Conard, V. I. Lakshmanan, and K. G. Wheeland (eds.). CIM, Halifax. Pergamon, New York. pp. 173-179.
- Lalvani, S. B., B. A. Deneve, and A. Weston. 1990. Passivation of pyrite due to surface treatment. Fuel. 69: 1567-1569.
- Lalvani, S. B., and M. Shami. 1989. Passivation of pyrite oxidation with metal cations. J. Mater. Sci. 22: 3503-3507.
- Lawrence, R. W. 1990. Prediction of the behaviour of mining and processing wastes in the environment. Proceedings of the western regional symposium on mining and mineral processing wastes. Berkeley, CA. pp. 115-121.
- Leathen, W., S. Braley Sr., and L. D. McIntyre. 1953. The role of bacteria in the formation of acid from certain surfuritic constituents associated with bituminous coal; Part 2. Ferrous iron oxidizing bacteria. Appl. Microbiol. 1: 65-68.
- Luther, G. W. III. 1987. Pyrite oxidation and reduction: Molecular orbital theory considerations. Geochim. Cosmochim. Acta. 51: 3193-3199.
- Marshall, K. C. R. and R. Mitchell. 1971. Mechanisms of the initial events in the sorption of marine bacteria to surfaces. J. Gen. Microbiol. 68: 337-348.
- Meek, F. A. Jr. 1991. Evaluation of acid preventative techniques used in surface mining. Proceedings of the symposium on environmental management for the 1990's, Denver, CO. pp. 167-172.
- McKay, D. R., and J. Halpern. 1958. A kinetic study of the oxidation of pyrite in aqueous suspension. Trans. Metallurg. Soc. AIME. 212: 301-309.
- Mishra, K. K., and K. Osseo-Asare. 1988. Aspects of the electrochemistry of semiconductor pyrite (FeS<sub>2</sub>). J. Electrochem. Soc. 135: 2502-2509.

- Moses, O. C., and J. S. Herman. 1991. Pyrite oxidation at circumneutral pH. *Geochim. Cosmochim. Acta.* 55: 471-482.
- Murthy, K. S. N., and K. A. Natarajan. 1992. The role of surface attachment of *Thiobacillus ferrooxidans* on the biooxidation of pyrite. *Miner. Metallurg. Process.* 9: 20-24.
- Nagai, T., and H. Kiuchi. 1975. Electrochemical studies on the pressure leaching. Part 3. Studies on the pressure leaching of pyrite. *J. Instit. Min. Metall. Japan.* 91: 547.
- Nairn, R. W., R. S. Hedin, and G. R. Watzlaf. 1991. A preliminary review of the use of anoxic limestone drains in the passive treatment of acid mine drainage. Proceedings, 12th annual West Virginia surface mine drainage task force symposium. Morgantown, West Virginia.
- Nebgen, J. W., W. H. Engelmann, and D. F. Weatherman. 1981. Inhibition of acid mine drainage formation: The role of insoluble iron compounds. *J. Environ. Sci.* 24: 23-27.
- Ogunsola, O. M., and K. Osseo-Asare. 1986. The electrochemical behaviour of coal pyrite, 1. Effect of mineral source and composition. *Fuel.* 56: 811-815.
- Olem, H., T. L. Bell, and J. J. Longaker. Prevention of acid drainage from stored coal, *J. Energy Eng.* 109: 103-112.
- Omura, T., T. Umita, V. Nenov, J. Aizawa, and M. Onuma. 1991. Biological oxidation of ferrous iron in high acid mine drainage by fluidized bed reactor. *Wat. Sci. Technol.* 23: 1447-1456.
- Osseo-Asare, K. 1992. Semiconductor electrochemistry and hydrometallurgical dissolution processes. *Hydrometallurgy.* 29: 61-90.
- Palencia, I., R. Y. Wan, and J. D. Miller. 1991. Electrochemical behavior of a semiconducting natural pyrite in the presence of bacteria. *Metallurg. Trans. B.* 22: 765-774.
- Pesic, B., and I. Kim. 1993. Electrochemistry of *Thiobacillus ferrooxidans* interactions with pyrite. *Metallurg. Trans. B.* 24: 717-727.

- Peters, E. 1986. Leaching of sulfides. Advances in mineral processing, Arbiter symposium, P. Somasundaran (ed.). New Orleans, Louisiana. pp. 445-462.
- Peters, E., and H. Majima. 1968. Electrochemical reactions of pyrite in acid perchlorate solutions. *Can. Metallurg. Quart.* 7: 111-117.
- Pugh, C. E., L. R. Hossner, and J. B. Dixon. 1984. Oxidation rate of iron sulfides as affected by surface area, morphology, oxygen concentration, and autotrophic bacteria. *Soil Sci.* 137: 309-314.
- Sato, M. 1960. Oxidation of sulfide ore bodies, II. Oxidation mechanisms of sulfide minerals at 25°C. *Econ. Geology.* 55: 1202-1231.
- Schaeffer, W. I., P. E. Holbert, and W. W. Umbreit. 1963. Attachment of *Thiobacillus thiooxidans* to sulfur crystals. *J. Bacteriol.* 85: 137-140.
- Silver, M., and G. M. Ritcey. 1985. Effects of iron-oxidizing bacteria and vegetation on acid generation in laboratory lysimeter tests on pyrite-containing uranium tailings. *Hydrometallurgy.* 15: 255-264.
- Silverman, M. P. 1967. Mechanism of bacterial pyrite oxidation. *J. Bacteriol.* 94: 1046-1051.
- Silverman, M. P., and H. L. Ehrlich. 1964. Microbial formation and degradation of minerals. *Adv. Appl. Microbiol.* 6: 153-206.
- Singer, P. C., and W. Stumm. 1970. Acid mine drainage: The rate-determining step. *Science.* 167: 1121-1123.
- Siwik, R., S. Payant, and K. Wheeland. 1989. Control of acid generation from reactive waste rock with the use of chemicals. Tailings and effluent management, Proceedings of the international symposium on tailings and effluent management, M. E. Chalkley, B. R. Conard, V. I. Lakshmanan, and K. G. Wheeland (eds.). CIM, Halifax. Pergamon, New York. pp. 181-193.
- Skousen, J., K. Politan, T. Hilton, and A. Meek. 1990. Acid mine drainage treatment systems: chemicals and costs. *Green Lands.* 20: 31-37.

- Smith, E. E., and R. S. Shumate. 1970. The sulfide to sulfate reaction mechanism. Fed. Wat. Pollut. Control Admin., no. 14010 FPS. pp. 20.
- Spotts, E., and D. J. Dollhopf. 1992. Evaluation of phosphate materials for control of acid production in pyritic mine overburden. J. Environ. Qual. 21: 627-634.
- Springer, G. 1970. Observations on the electrochemical reactivity of semiconducting minerals. Trans. Institut. Min. Metallurgy, Sect. C. 79: 11-14.
- Stiller, A. H., J. J. Renton, and T. E. Rymer. 1989. An experimental evaluation of the use of rock phosphate (apatite) for the amelioration of acid-producing coal mine waste. Min. Sci. Technol. 9: 283-287.
- Temple, K. L., and A. R. Colmer. 1951. The autotrophic oxidation of iron by a new bacterium: *Thiobacillus ferrooxidans*. J. Bacteriol. 62: 605-611.
- Temple, K. L., and E. W. Delchamps. 1953. Autotrophic bacteria and the formation of acid in bituminous coal mines. Appl. Microbiol. 1: 255-258.
- Tributsch, H. 1986. Photoelectrolysis and photoelectrochemical catalysis. Mod. Aspects Electrochem. 17: 303-355.
- Tuttle, J. H., P. R. Dugan, and C. I. Randles. 1969. Microbial sulfate reduction and its potential utility as an acid mine water pollution abatement procedure. Appl. Microbiol. 17: 279-302.
- U.S. Environmental Protection Agency. 1970. The effects of various gas atmospheres on the oxidation of coal mine pyrites. Wat. Pollut. Control Res. Series no. 14010 ECC. pp. 140.
- Vitaya, V. B., and K. Toda. 1991. Kinetics and mechanism of the adsorption of *Sulfolobus acidocaldarius* on coal surfaces. Biotechnol. Prog. 7: 427-433.
- Vaughan, D. J., and J. R. Craig. 1978. Mineral chemistry of metal sulfides. Cambridge University Press. New York, NY. pp. 36-38.
- Wentzler, T. H., and F. F. Aplan. 1992. Neutralization reactions between acid mine waters and limestone. Proceedings of the symposium on emerging process technologies for a

cleaner environment, S. Chander, P. E. Richardson, and H. El-Shall (eds.). SME, Phoenix, Arizona. pp. 149-160.

Ziemkiewicz, P. F., A. H. Stiller, T. E. Rymer, and W. M. Hart. 1990. Advances in the prediction and control of acid mine drainage. Proceedings of the western regional symposium on mining and mineral processing wastes. Berkeley, CA. pp. 93-101.

## **CHAPTER 2**

### **CONTROL OF PYRITE OXIDATION BY PHOSPHATE COATING\***

#### **2.1 INTRODUCTION**

While several additives are still under evaluation and development, there is presently no widely accepted technology which controls acid rock drainage production at-source without indefinite maintenance. Since the oxidation of pyrite in acidic medium has been reported to occur by the preferential release of iron into solution (Hamilton and Woods, 1981; Buckley, 1987), the mechanism of pyrite oxidation can be likened to the corrosion of metals and therefore can potentially be prevented by phosphating techniques.

Although physical phosphate rock addition to sulfide wastes have been investigated as a means of controlling pyrite oxidation (Watkin and Watkin, 1983; Stiller et al., 1989, Siwik et al., 1989; Spotts and Dollhopf, 1992), only limited studies have been done on the effectiveness of pyrite phosphating (Reimers and Franke, 1991; Evangelou and Huang, 1992). In this chapter, the use of low and elevated temperature metal phosphating techniques to suppress pyrite oxidation rates, and hence control ARD formation at-source is reported.

#### **2.2 THEORY AND BACKGROUND**

##### **2.2.1 Metal Phosphating**

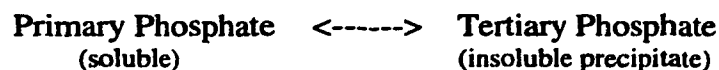
Chemical surface conversion treatment of metals to modify their intrinsic properties and to provide new physical or physico-chemical characteristics is well-known (Lorin,

---

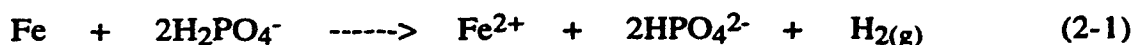
\* A version of this chapter, co-authored with N. O. Egiebor has been published in *Science of the Total Environment*. 162: 225-237, 1995.

1974; Freeman, 1986). Phosphating or phosphate coating is the most widely used form of metal pre-treatment, and has been used to modify the properties of iron for various purposes including corrosion protection, improving paint adhesion, improved lubricity and modification of electrical properties (Kiselev, 1990; Losch et al., 1991). The first reliable record of a phosphate coating being applied as a means of corrosion protection was by Ross (1869). However, iron articles with apparent phosphate coatings have been found in archaeological excavations and it has been conjectured that the ancient Egyptians were familiar with the use of phosphoric acid to form phosphate coatings. Other investigators have found no reliable evidence that such coatings were formed deliberately and have suggested that the phosphate coatings were formed in the earth over an extended period, with the phosphate having been leached from bones by carbonated water (Van Wazer, 1958).

Phosphating is essentially an electrochemical phenomenon in which dissolution of the metal occurs in the presence of phosphate ions at the micro-anodes and discharge of hydrogen, followed by hydrolysis and precipitation of insoluble phosphates, takes place at the micro-cathodes as illustrated in Figure 2-1 (Freeman, 1986). The mechanism involved in the formation of phosphate coatings is quite complex, but, for all processes based on metal phosphate solutions, it depends on the basic equilibrium;



The first step in the metal phosphating process is the dissolution of iron into the phosphating solution. This reaction puts ferrous into solution, as described by Equation 2-1:



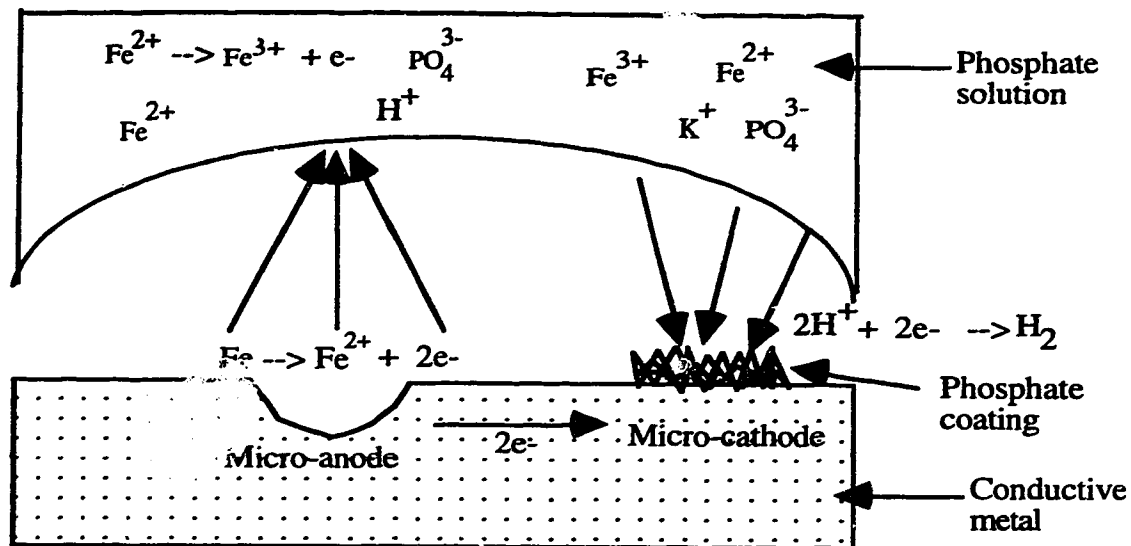


**Figure 2-1. Diagrammatic representation of metal phosphating reactions.**

Ferrous iron in solution then reacts with secondary and tertiary phosphate ions (Equations 2-2 and 2-3).



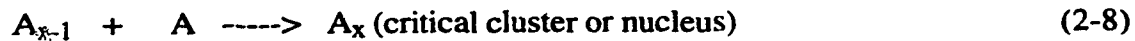
The phosphate compounds formed are highly insoluble and form the coating material. In the presence of accelerators (hydrogen peroxide, sodium molybdate or sodium nitrite) in the phosphating solution, some of the ferrous iron reacts with the accelerators to form ferric iron which in turn reacts with phosphate ions (Equations 2-4 and 2-5).





## 2.2.2 Phosphate Coating Formation

The first detailed theoretical consideration of crystal growth in supersaturated solution was by Kossel (1934). The initial step in the crystal growth process, in terms of this model, is the formation of a two-dimensional nucleus, from which layered growth proceeds. The interaction between ions and molecules which leads to cluster formation and eventually to the evolution of crystals has been likened to a chemical reaction. The largest cluster which may exist before spontaneous crystallization is referred to as the critical cluster, or nucleus, so that in terms of molecular aggregation, the process may be represented as follows (where A is a molecule):



The precipitation of ionic crystals is treated by the "embryo in a cavity" model (Figure 2-2) which corresponds to tight binding for strong interaction or weak binding for strong solvation.

The theories of stepwise growth recognized the non-equivalence of sites on a surface and proposed the formation of mono-molecular layers in a layer-by-layer growth mechanism. In the process of adsorption onto a crystal surface, molecules or ions may be attached to the smooth surface, an edge or step, or a kink site (positions c, d, and e respectively in Figure 2-3). The layered growth has been shown to have a particularly unfavorable energy requirement and the model predicts a stepwise energy barrier as each layer is completed and new surface nucleation is required.

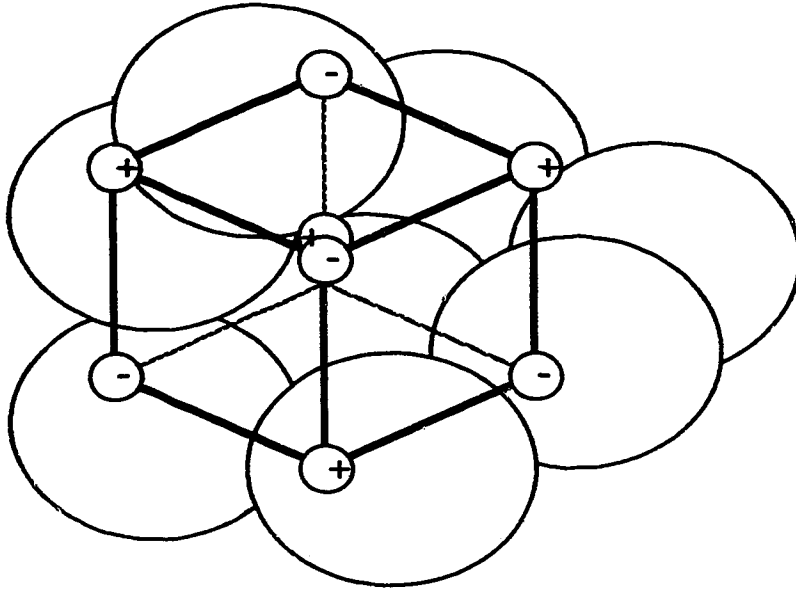


**Figure 2-2. Model of the formation of an embryo prior to precipitation of ionic crystals.**

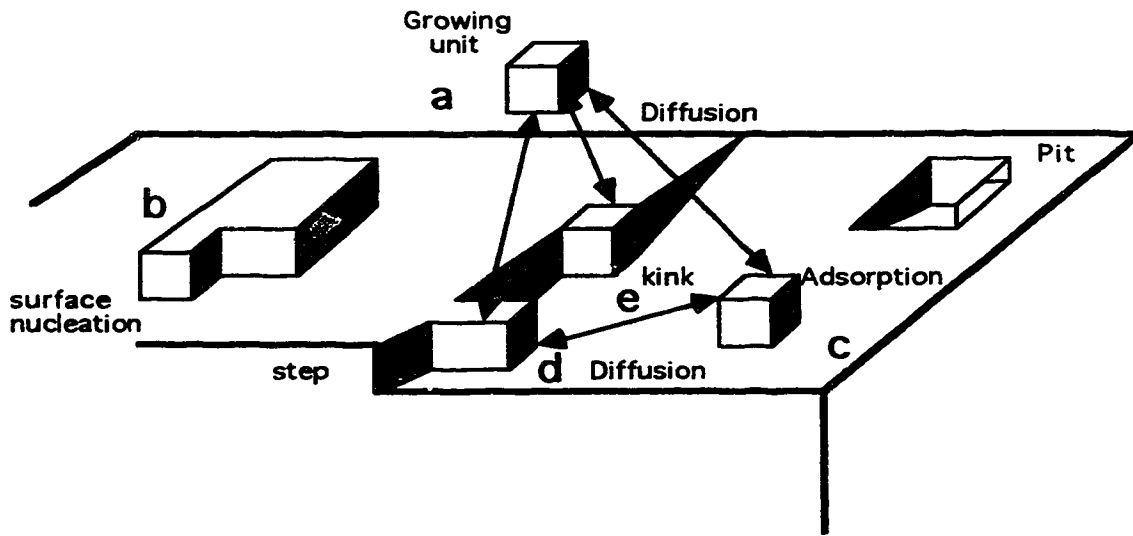


**Figure 2-3. Representation of layered growth of phosphate coating on a pyrite surface.**

### **2.2.3 Sulfide Oxidation**

Two mechanisms regarding the oxidation of sulfur and iron components in pyrite have been proposed: the preferential release of sulfur and the preferential release of iron. Goldhaber (1983) proposed that the sulfur component in pyrite is first released and oxidized to sulfate. However, Sato (1960), and Peters (1986), proposed that the oxidation of pyrite occurs first at the iron sites. They suggested that iron is released into solution leaving a reacted layer of elemental sulfur. Hamilton and Woods (1981), using potential sweep voltammetry, reported that the formation of sulfur is restricted to the order of a monolayer at pH between 9.2 and 13 but significant yield occurs at pH of 4.6. This claim was subsequently supported by Buckley (1987) using X-ray photoelectron spectroscopy techniques. They observed that in acetic acid at pH 4.6, oxidation of pyrite results in the formation of a sulfur-rich surface layer, whereas in alkaline media, sulfate was the only sulfur oxidation product formed. Ogunsola and Osseo-Asare (1986) and Palencia et al. (1991) reported that the S/Fe atomic ratio of pyrite increased after a pyrite electrode had been oxidized electrochemically, and concluded that sulfur remains on the pyrite surface as a product layer while iron goes into solution. Chander and Briceno (1987) have also postulated the formation of a sulfur-rich surface as the initial oxidation phase during pyrite oxidation.

If the mechanism of pyrite oxidation in acidic media involves the preferential release of iron into solution, then metal phosphating techniques which employ acidic phosphate solutions could be used to prevent or suppress pyrite oxidation by forming a complex phosphate coating on the pyrite surface. Based on this premise, the study reported here was aimed at investigating the suppression of pyrite oxidation by low and elevated temperature phosphating. A typical iron-phosphate precipitate formed in the presence of potassium ions will have a chemical formula of  $\text{Fe}_3(\text{PO}_4)_2 \cdot 8\text{H}_2\text{O}$  (hydrated iron(II) phosphate) which occurs naturally as vivianite and is the most stable Fe(II) phase (Nriagu, 1972a). Besides, several acid phosphate precipitates are also known to form,

$\text{FeHPO}_4 \cdot \text{H}_2\text{O}$ ,  $\text{FeHPO}_4 \cdot 2\text{H}_2\text{O}$ ,  $\text{Fe}(\text{H}_2\text{PO}_4)_2 \cdot 2\text{H}_2\text{O}$  and  $\text{KFePO}_4 \cdot 6\text{H}_2\text{O}$ . The hydrated iron (III) phosphate,  $\text{FePO}_4 \cdot 2\text{H}_2\text{O}$ , is also found as the mineral strengite (Nriagu, 1972b).

## **2.3 EXPERIMENTAL**

### **2.3.1 Materials**

The natural pyrite used in this study was obtained from Inuvik, Yukon, Canada. Potassium dihydrogen orthophosphate ( $\text{KH}_2\text{PO}_4$ ) was obtained from BDH chemicals. All other reagents were analar grade obtained from Fisher Scientific, Edmonton, Canada and used without further purification. The natural pyrite was ground in a jaw crusher and separated into +850, +710, +600, +300, +150, +75 and -75  $\mu\text{m}$  size fractions by dry sieving. These fractions were then stored under nitrogen gas and used for the experiments.

### **2.3.2. Phosphating**

The phosphate treatment of pyrite samples was carried out in a cylindrical glass reactor with four inlet ports at the top. The desired concentration of the phosphate solution was prepared in the reactor and a desired weight of pyrite added. An oxidizing accelerator,  $\text{H}_2\text{O}_2$ , was also added to the phosphating solution. For treatments done at temperatures above ambient, the reactor and its contents were raised to the desired temperature before the pyrite samples were added. Agitation of the mixture was achieved by passing compressed air into the solution via a tube through one of the inlet ports. Compressed air was used for agitation so as to minimize abrasion of the particles during the reaction. Two other inlet ports were used for pH and temperature probes to monitor these parameters in the solution during the reaction. The fourth inlet port was used for collecting samples by means of a syringe. For a typical treatment, 50 g of pyrite was treated with 200 mL of 0.1 M phosphate and 1.0% or 2.0% hydrogen peroxide solution. After the reaction, the resulting suspension was filtered to remove the solid, which was washed with distilled water and

dried in air. These solid samples were characterized and used for evaluating the rate of oxidation in the accelerated oxidation column, and in autoclave pressure oxidation tests. The liquid was analyzed for total dissolved Fe. Although equilibrium was attained in about 40 min, each sample was agitated for 60 min. For the phosphating kinetic studies, samples were taken periodically and analyzed for total dissolved Fe.

### **2.3.3. Accelerated Oxidation Column Tests**

Accelerated oxidation column tests of the untreated and the various phosphate treated pyrite samples was carried out in a glass column at ambient conditions. To improve mass transfer and prevent clogging of the column during the oxidation test, 50 g of 600  $\mu\text{m}$  of untreated or phosphate-treated pyrite was mixed with 100 g of +850  $\mu\text{m}$  glass beads and fed into the glass column. The column was made of a Pyrex glass tube with an upper section diameter of 5 cm and height of 14 cm, while the lower section had a diameter of 1.8 cm and height of 12 cm (see Figure 2-4). The lower portion was packed with indicating glass beads which enables one to tell by visual observation if there is significant precipitation of ferric hydroxide. When there is any significant precipitation, the color of the glass beads turns reddish-yellow. The packed column was filled with 50 mL of distilled water and compressed air was fed into the bed through a fine glass tube with a diameter of 0.5 cm. The column was drained and refilled every 3 to 7 days depending on the results of the preceding analysis and the coloring of the indicating beads. The drainage volume was measured and analyzed for total Fe,  $\text{Fe}^{2+}$ , pH and titratable acidity. The accelerated oxidation columns were run for 81 days.

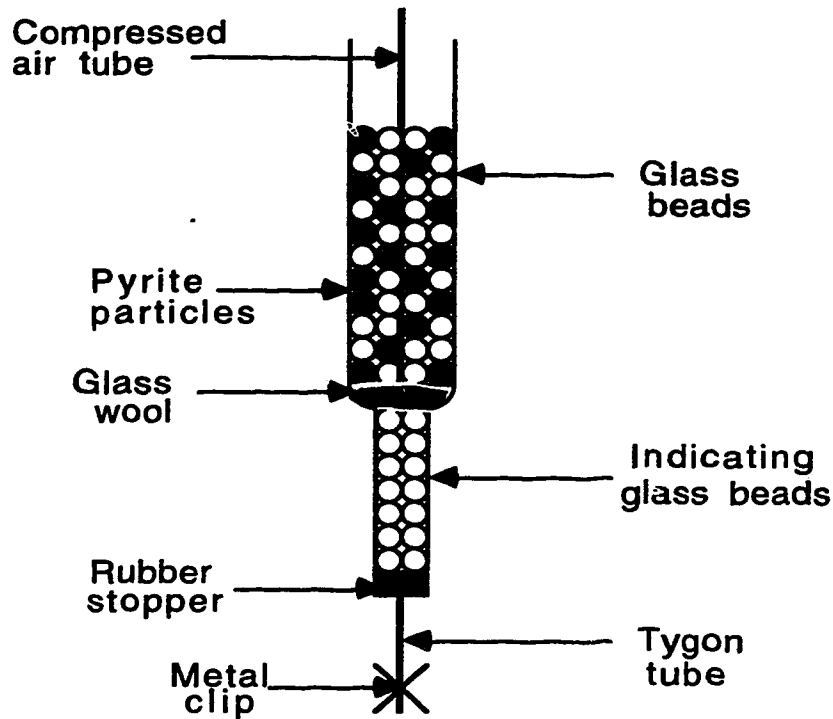


**Figure 2-4. Accelerated oxidation column test setup.**

#### **2.3.4. Pressure Oxidation Tests**

Since the oxidation rates of the pyrite in the accelerated oxidation columns were generally very low and required long periods for testing samples, pressure oxidation experiments in an autoclave were designed as a faster means of evaluating the effect of the various phosphating treatments on the rate of pyrite oxidation. The pressure oxidation tests were conducted in a stainless steel jacketed 300 mL Parr autoclave equipped with Teflon internals, a magnetic stirrer, a temperature controller and a pressure gauge. The temperature was maintained within  $\pm 1.0^{\circ}\text{C}$  of the desired temperature and 99.9% pure oxygen was supplied to the autoclave via a dip tube. Samples were taken at intervals through a sampling spout. For the pressure oxidation tests, a 1 g sample of the pyrite, treated or untreated was mixed with 150 mL of distilled water in the autoclave, sealed, pressurized with oxygen to the chosen reaction pressure, and heated to the desired temperature. Once

the reaction temperature was reached, aliquots were taken through the sampling spout. Samples were also taken at regular intervals during the 600 min of reaction. The samples taken during the reaction were analyzed for pH and total Fe content.

### **2.3.5. Chemical Analysis**

Total sulfur content of the pyrite samples was determined on a Leco total sulfur analyzer (ASTM D3177, 1982) and total Fe by Atomic Absorption Spectrophotometry (AAS) after aqua regia digestion. Total Fe and  $\text{Fe}^{2+}$  in solution during the accelerated column and pressure oxidation tests were determined by colorimetric method (DR/2000 Spectrophotometer) and the total Fe present was verified by AAS. Total Fe analysis by colorimetric method (American Public Health Association, 1985) required addition of hydroxylamine hydrochloride, o-phenanthroline and sodium acetate, however hydroxylamine hydrochloride (a reducing agent which keeps iron in the +2 state) was not added for  $\text{Fe}^{2+}$  determination (Kenkel, 1988). The o-phenanthroline is a ligand which reacts with  $\text{Fe}^{2+}$  to form an orange-colored complex ion which is the absorbing species. Since the reaction is pH-dependent, sodium acetate is added for buffer at the optimum pH. Absorbance readings were taken at 510 nm. Ferric ion concentration was obtained by the difference between total Fe and  $\text{Fe}^{2+}$ . The total Fe content of the solutions was taken as a measure of the amount of pyrite oxidized, except where there is precipitation of iron hydroxide.

The pH of the solutions was determined by a Cole-Parmer Chemcadet pH/mV meter equipped with a temperature compensation probe. Titratable acidity of solutions from the columns were determined by titration with NaOH (which had been standardized against HCl) using phenolphthalein as an indicator.

### 2.3.6. Scanning Electron Microscopy

The phosphate-treated and untreated pyrite samples were viewed and analyzed with a Hitachi S-2700 scanning electron microscope (SEM) equipped with a Link analytical EXL energy-dispersive X-ray spectrometer (EDS). The EDS is equipped with a Si(Li) solid state x-ray detector and a Be and ultra-thin windows for detecting light elements. Secondary electron images of the samples were constructed. Since at high magnifications, the size of the area sampled represented a tiny fraction of the sample, an adequate number of areas were studied to gain a valid description of the sample.

## 2.4. RESULTS AND DISCUSSION

Table 2-1 presents the chemical composition of the natural pyrite determined by SEM-EDS, AAS and Leco total sulfur analyzer. The iron and sulfur analysis, and S/Fe mole ratio from both methods are comparable. Although the natural pyrite is fairly pure (S/Fe mole ratio of 1.96) it contains small amounts of Si, Ca, Al, and K impurities. The variation in the composition of pyrite has been reported to be within limits of  $\text{FeS}_{2.0}$  to  $\text{FeS}_{1.94}$  (Smith, 1942).

**Table 2-1. Elemental analysis of pyrite use for experiments.**

Elements	SEM-EDS (%)	AAS and Leco (%)
Fe	46.11	46.85
S	50.46	52.40
Ca	0.15	nd
Al	0.90	nd
K	0.25	nd
Si	2.10	nd
S/Fe mole ratio	1.92	1.96

nd = not determined



Figure 2-5 presents a typical plot of the change in concentration of Fe and pH of the phosphating solution during treatment of pyrite with 0.1M  $\text{KH}_2\text{PO}_4$ , 2.0%  $\text{H}_2\text{O}_2$  at 40°C. The pH of the phosphating solution dropped rapidly to about 1.8 in the first 40 min and then remained constant. The most rapid decrease was observed within the first 5 min of the

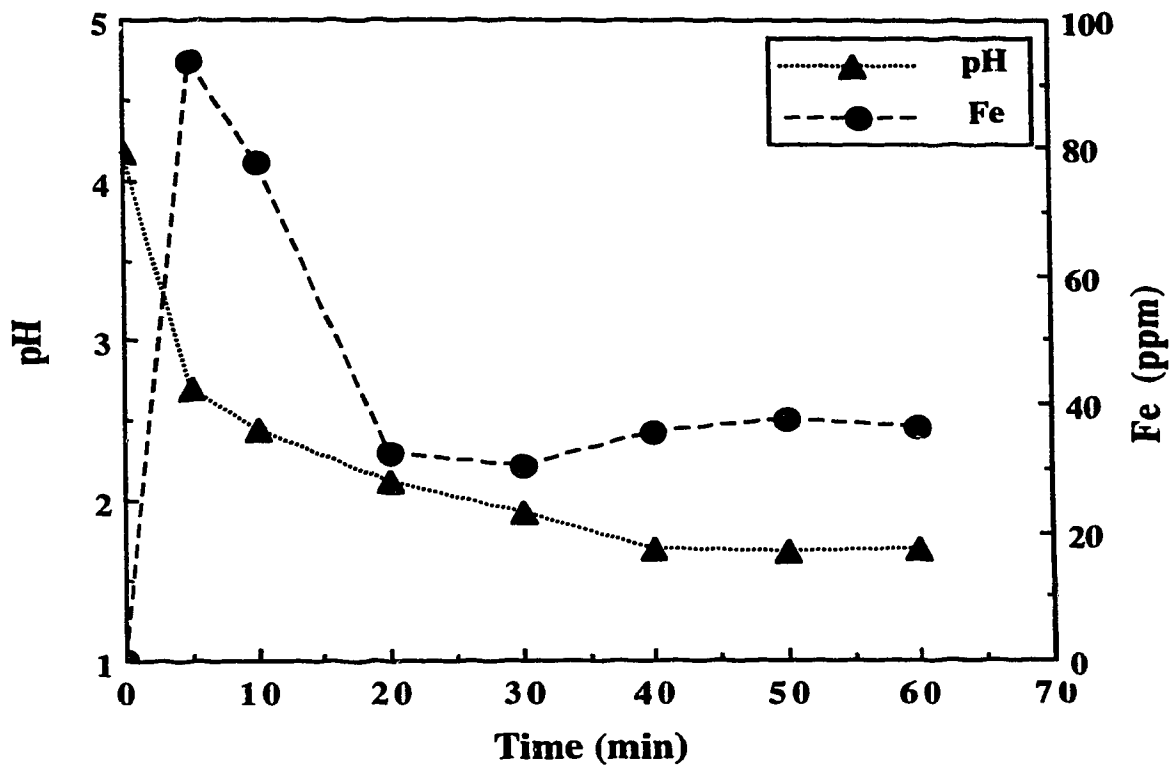


Figure 2-5. pH and Fe in solution during coating of pyrite at 40°C, in 0.1 M  $\text{KH}_2\text{PO}_4$  and 2.0%  $\text{H}_2\text{O}_2$ .

reaction, where the pH was observed to drop from 4.3 to 2.8. The decrease in the pH of phosphating solutions during the precipitation of ferric phosphate on cellulose and collagen have also been reported by other investigators (Dalas, 1990; Dalas and Koutsoukos, 1990; Dalas, 1991) and it is attributable to the release of hydrogen ions in the potassium hydrogen orthophosphate precursor into solution. The Fe concentration in solution was observed to increase rapidly in the first 5 min resulting in a concentration of 90 mg/L. The

concentration then dropped over the next 35 min before remaining relatively constant at about 35 mg/L. Three stages of the coating formation can be distinguished. The first stage occurs within the first 5 min, in which Fe is rapidly leached into the phosphate solution. In the second stage, the solubility product of iron phosphate is exceeded and its precipitate starts to form on the surface of the pyrite particles. The precipitation of iron phosphates on the pyrite results in the observed rapid decrease in the concentration of Fe in solution. The third stage involves the levelling off of the concentration of Fe in solution, which indicates a cessation in further iron dissolution due to phosphate coating. A similar trend was observed when the phosphating reaction was carried out at 25°C and 80°C with the same initial concentration of phosphate and H<sub>2</sub>O<sub>2</sub>.

After phosphate coating, the untreated and phosphated pyrite particles were viewed under the SEM-EDS to determine the reaction products formed on the surface of the pyrite particles. The surface morphology and EDS spectrum obtained from the untreated pyrite particle surface is shown in Figure 2-6. The spectrum shows some impurities, mainly silicon. The SEM surface morphology also shows a clean, relatively homogeneous surface.

Figure 2-7 shows the SEM micrograph and EDS spectra of a pyrite particle which had been phosphate treated with 0.1 M phosphate and 2.0% H<sub>2</sub>O<sub>2</sub>, at 25°C. A significant change in the morphology of the treated pyrite due to the formation of a coating can be seen. The EDS spectra shows the presence of phosphorus and potassium on the surface which indicate the formation of an iron-potassium phosphate complex coating.

The SEM micrographs and EDS spectra of pyrite particles phosphated at 40°C and 80°C are shown in Figures 2-8 and 2-9. The surface morphology suggest an amorphous phosphate deposit. The observed cracks on the deposit indicate that a thicker layer of coating is formed at 40°C and 80°C as compared to the coating formed at 25°C in Figure 2-7. The thicker coating formed at 40°C and 80°C is attributable to the lower solubility product of iron phosphate at higher temperatures. Dalas and Koutsoukos (1990) also

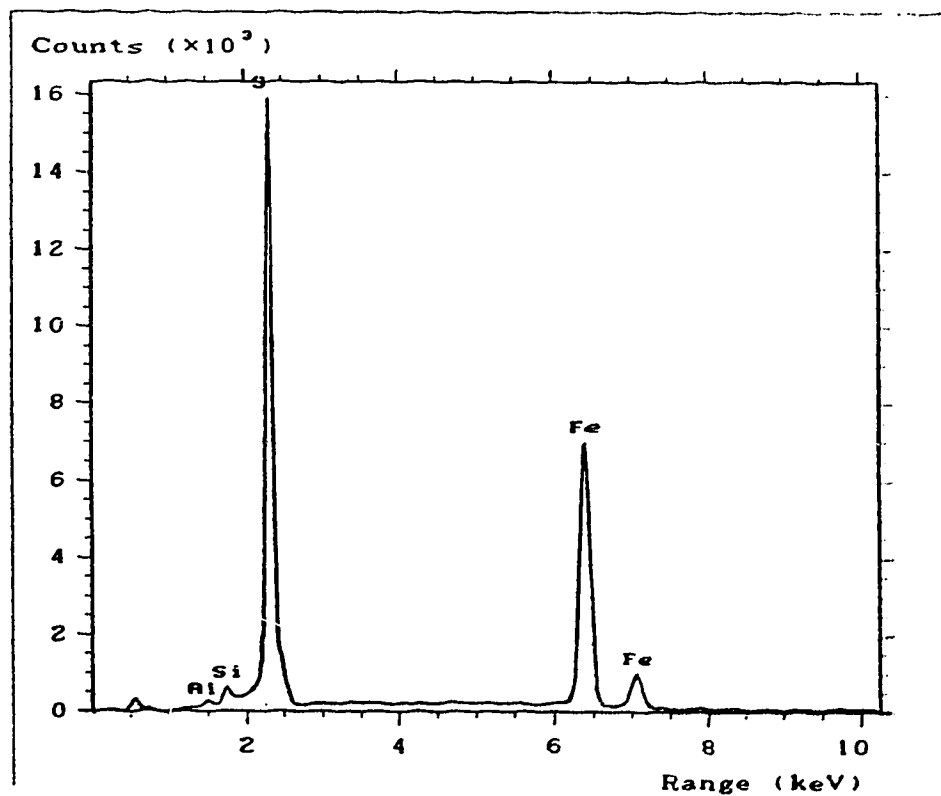
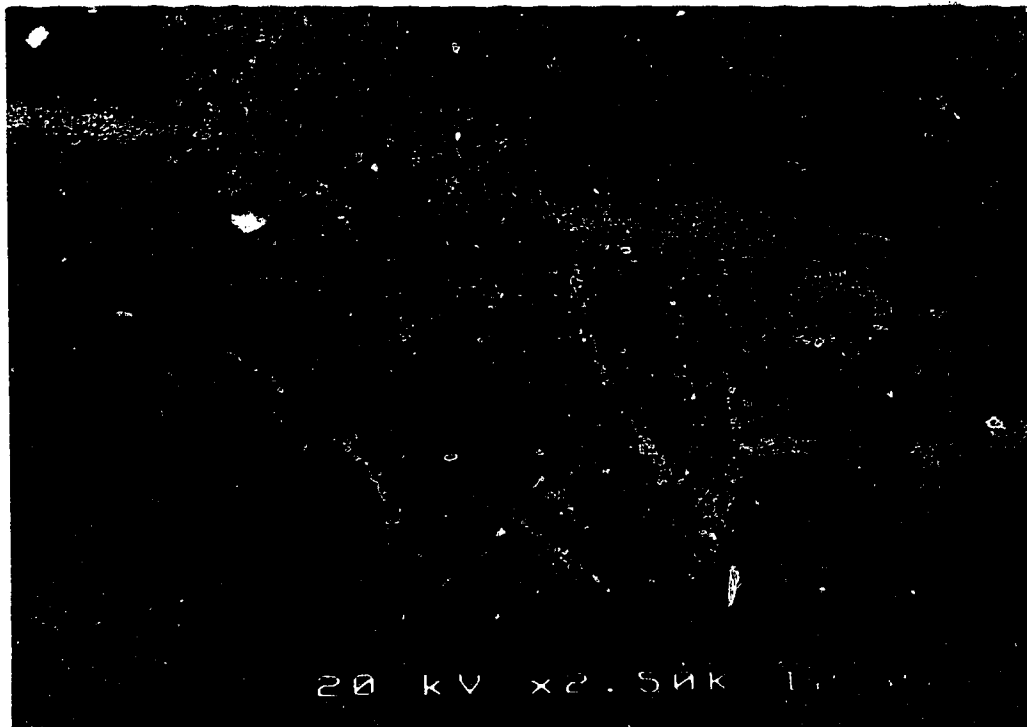
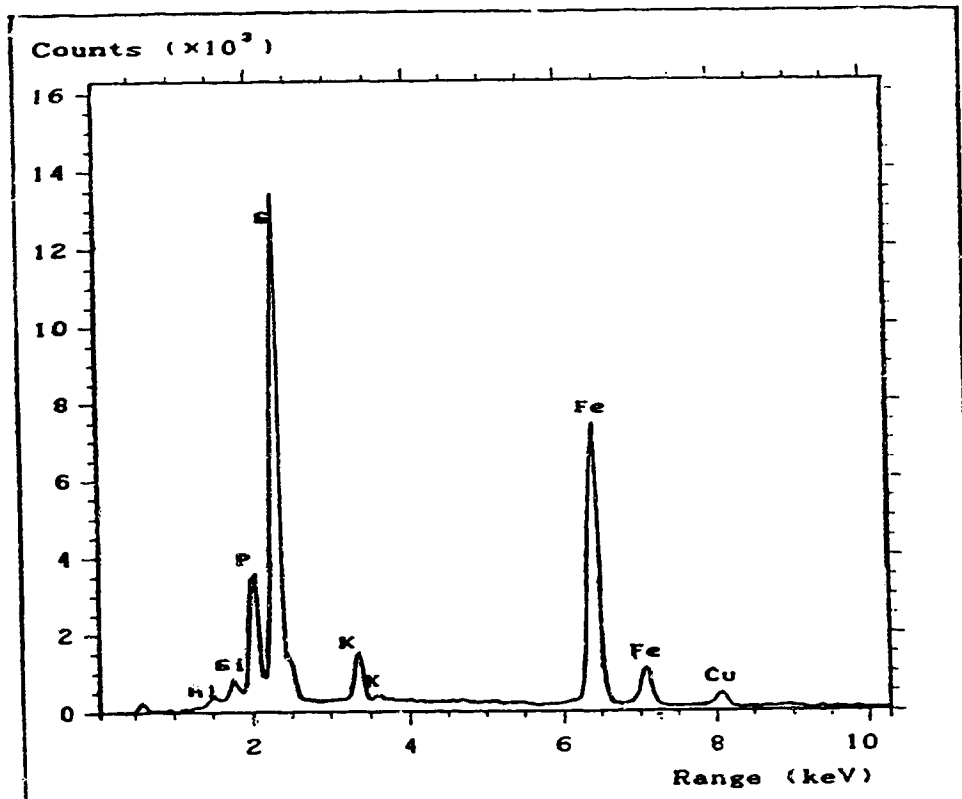
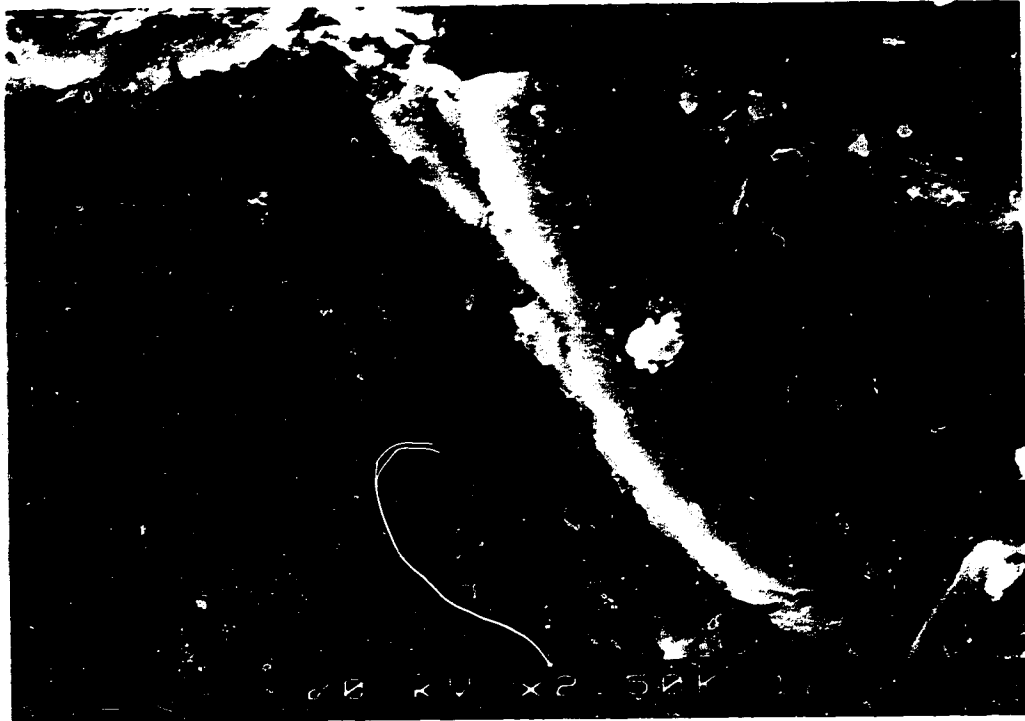
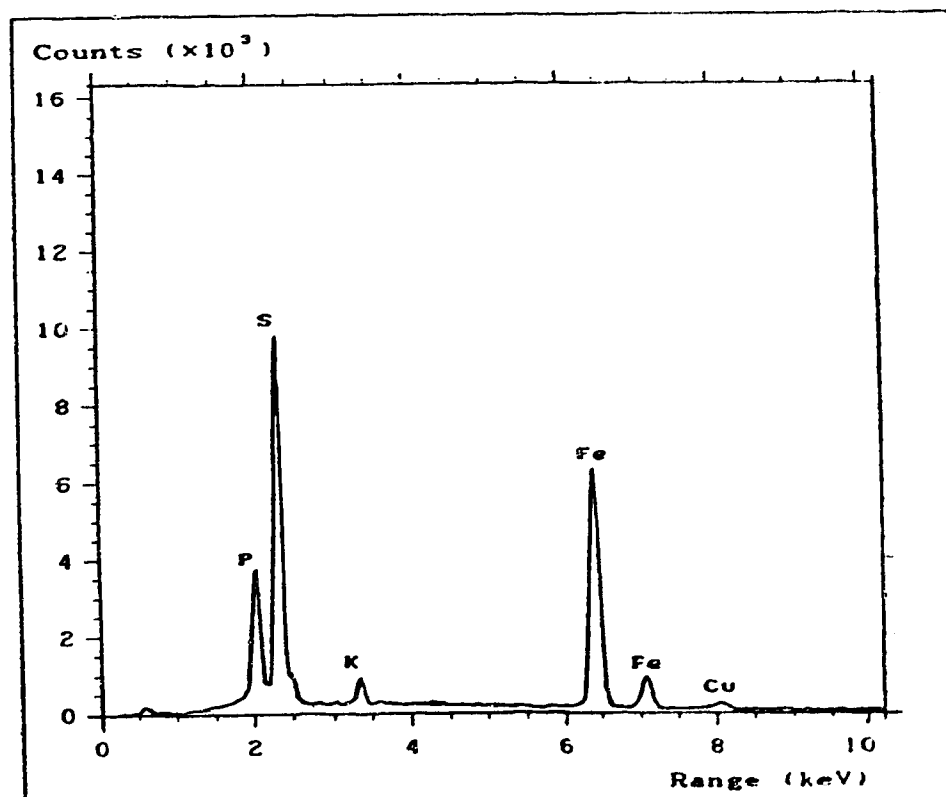
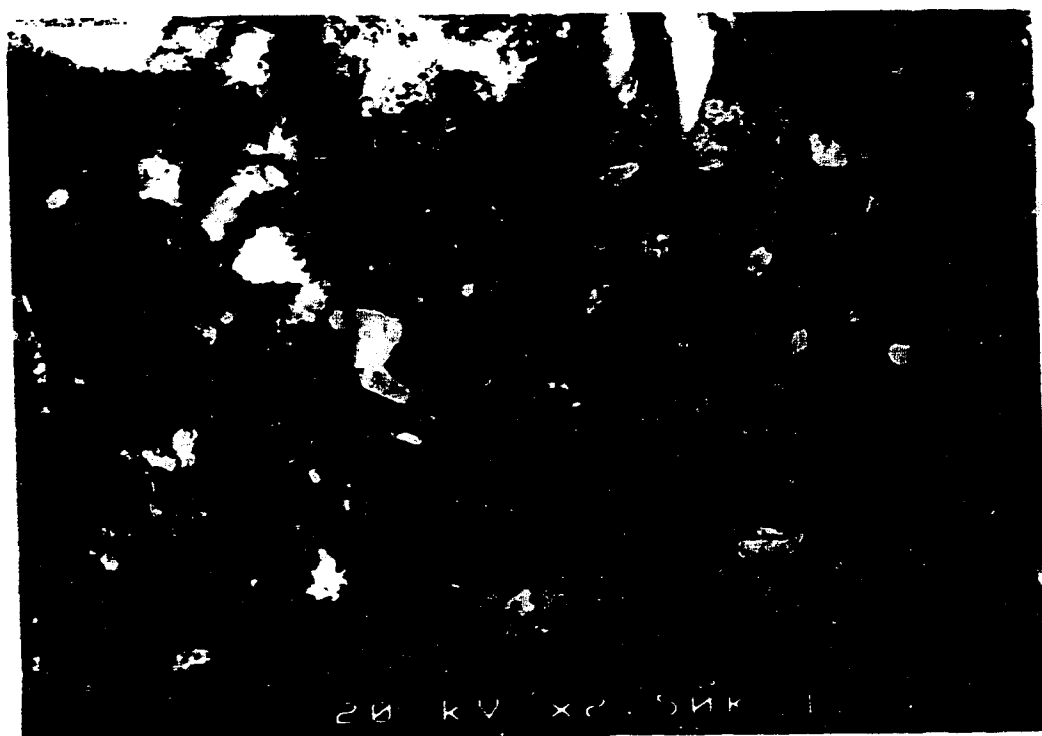


Figure 2-6. Scanning electron micrograph and EDS spectrum of untreated pyrite particle.



**Figure 2-7. Scanning electron micrograph and EDS spectrum of phosphate-treated pyrite particle. Tested at 25°C with 2.0%  $H_2O_2$  and 0.1 M  $KH_2PO_4$ .**



**Figure 2-8. Scanning electron micrograph and EDS spectrum of phosphate-treated pyrite particle. Tested at 40°C with 2.0% H<sub>2</sub>O<sub>2</sub> and 0.1 M KH<sub>2</sub>PO<sub>4</sub>.**

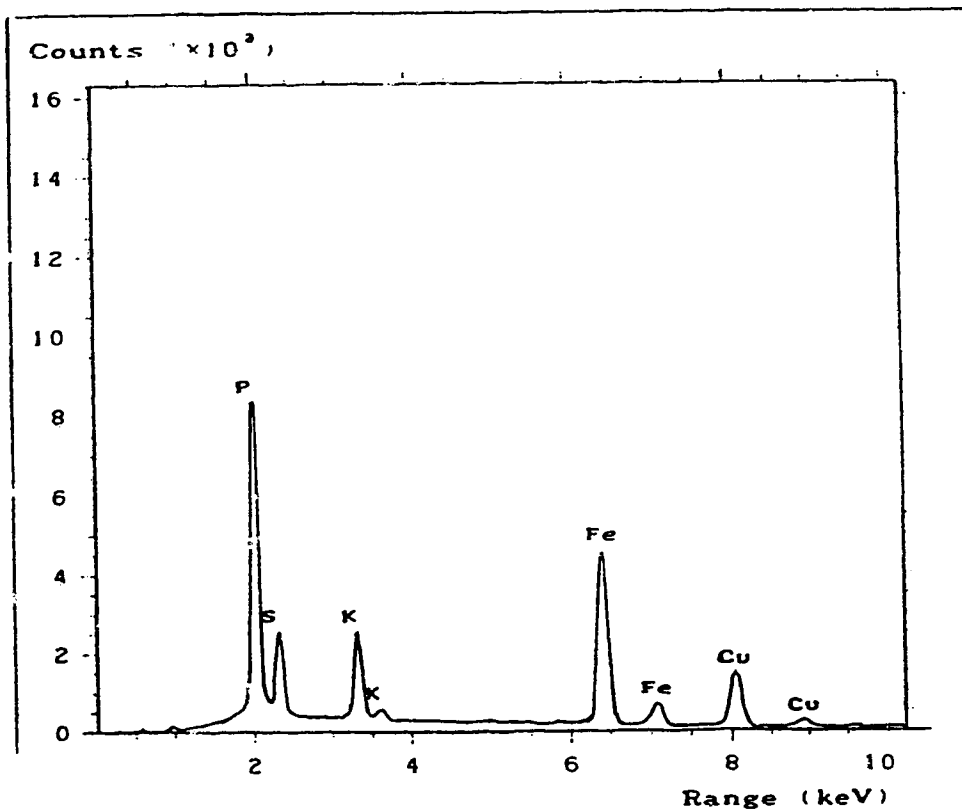
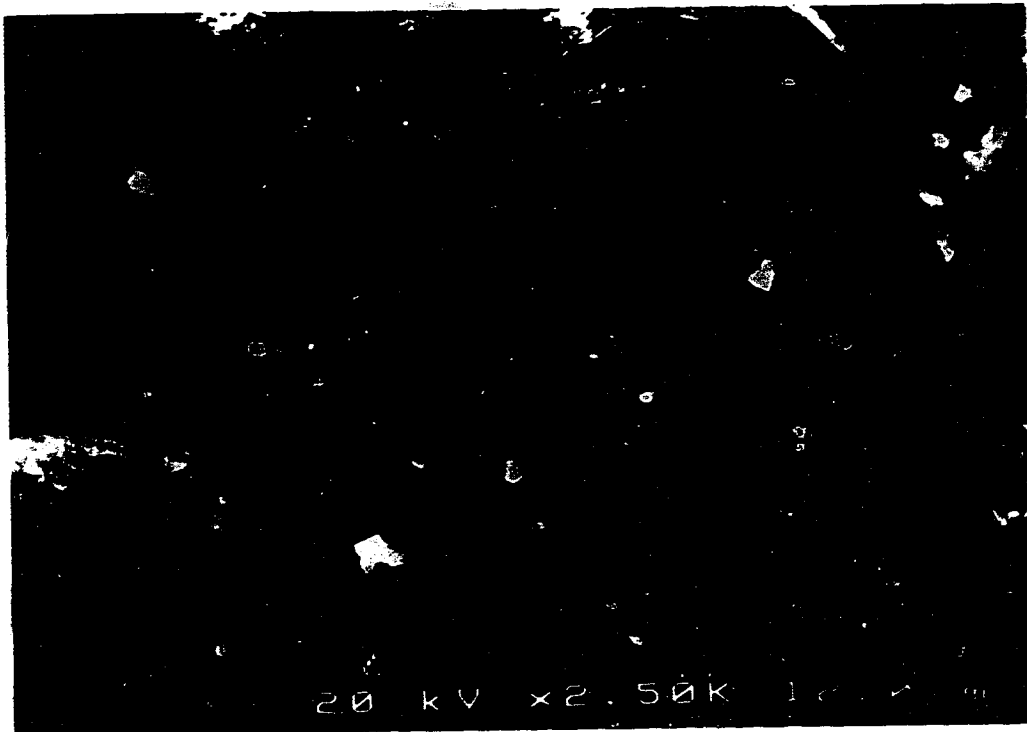


**Figure 2-9. Scanning electron micrograph and EDS spectrum of phosphate-treated pyrite particle. Tested at 80°C with 2.0% H<sub>2</sub>O<sub>2</sub> and 0.1 M KH<sub>2</sub>PO<sub>4</sub>.**

reported an increase in the amount of phosphate deposited on porous glass when the temperature was increased from 25°C to 40°C. The EDS spectra of the phosphated pyrite indicate the presence of P and K.

The stability of the phosphate-treated and the untreated pyrite particles in terms of their oxidation rates were tested in the accelerated oxidation columns (Section 2.3.3). Precipitation of ferric hydroxide was observed to occur in the untreated pyrite column, which resulted in the change in color of the indicating beads from colorless to reddish-yellow. This was indicative of a rapid oxidation of the untreated pyrite during the column test. No color changes were observed in the phosphate-treated pyrite columns during the experiment. Figure 2-10 shows a photograph of the untreated and phosphate-treated pyrite columns after 30 days of testing in the accelerated oxidation column.

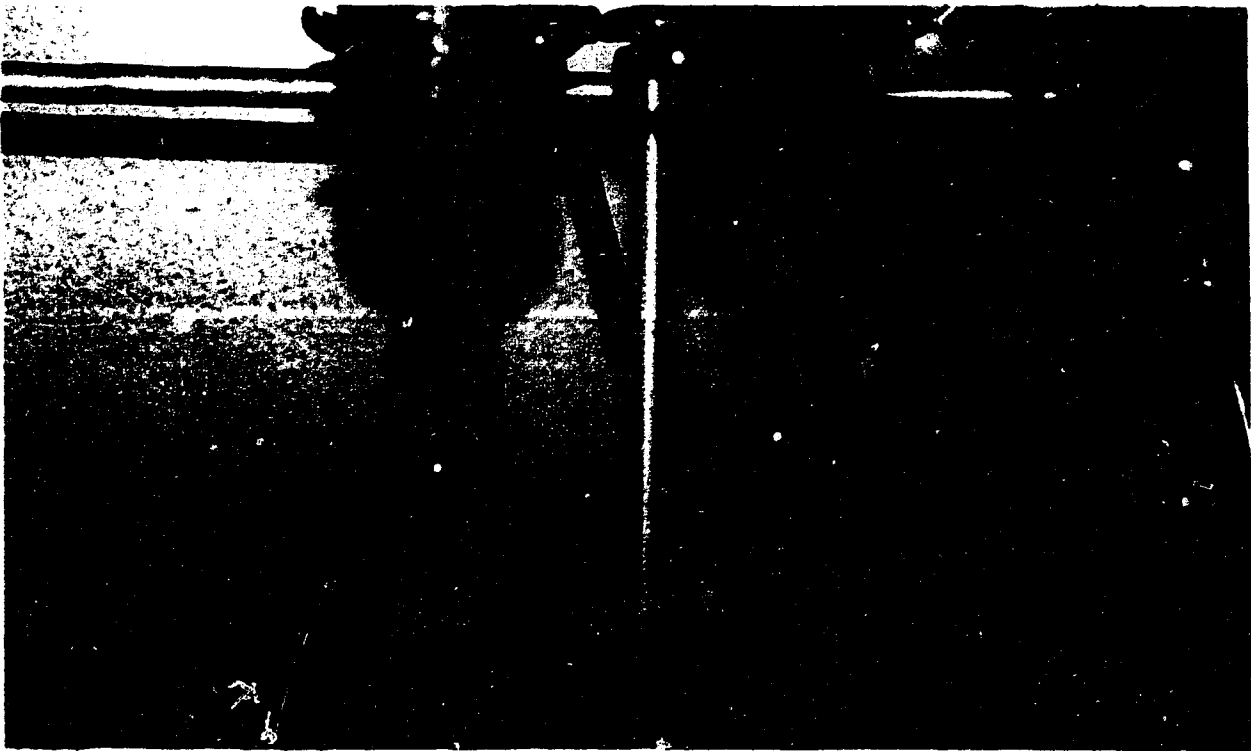


**Figure 2-10. Accelerated oxidation columns after 30 days. Col. 1 (left) = untreated, Cols. 2 & 3 (center and right) = phosphate-treated.**

The results of the stability of the untreated pyrite and phosphated-pyrite samples at 25°C, 40°C and 80°C in the columns are illustrated in Figure 2-11. The cumulative percent oxidation of the untreated pyrite sample was observed to increase rapidly throughout the testing period. After 81 days of testing 0.45% oxidation was obtained for the untreated pyrite. The cumulative percent oxidation of the phosphate-treated pyrite samples were also observed to increase gradually throughout the testing period but at a much lower rate. After

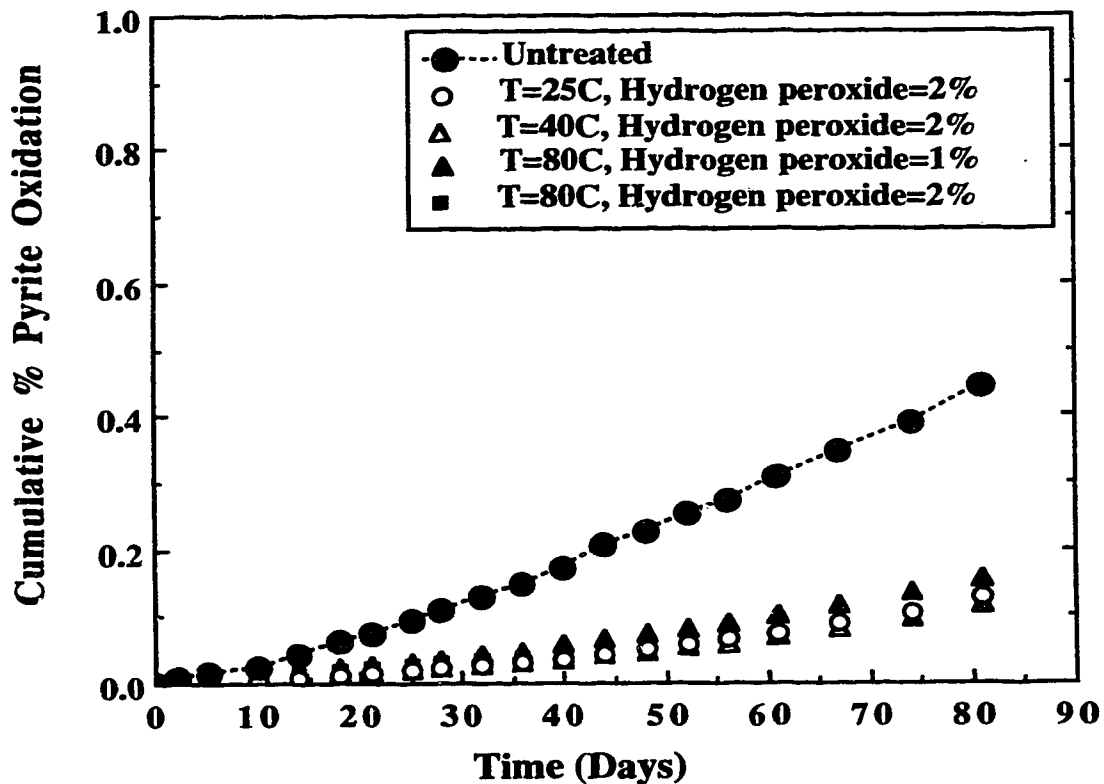


**Figure 2-11. Accelerated oxidation column test of untreated and phosphate-treated pyrite.**

81 days, 0.13%, 0.12% and 0.11% oxidation was obtained for the 25°C, 40°C and 80°C phosphate treated pyrite particles, respectively. Reducing the concentration of the oxidizing accelerator, H<sub>2</sub>O<sub>2</sub>, from 2% to 1% at 80°C resulted in an insignificant increase in percent



oxidation from 0.11 to 0.14%. Compared with the untreated pyrite, the phosphate treatment resulted in the suppression of the rate of pyrite oxidation from  $5.45 \times 10^{-3}\%/day$  to  $1.40 \times 10^{-3}\%/day$ . This translates to about 75% reduction in the rate of pyrite oxidation after 81 days. Increasing the phosphating reaction temperature above 25°C did not result in any significant improvement in the stability of the pyrite particles in terms of oxidation.

The cumulative acidity from the accelerated oxidation columns is shown in Figure 2-12. The phosphating of the pyrite also reduced the rate of acid generation from the columns. Pyrite samples phosphated at 25°C showed slightly lower acid generation rates than those treated at 40°C and 80°C. While about 120 mg of acidity was obtained after

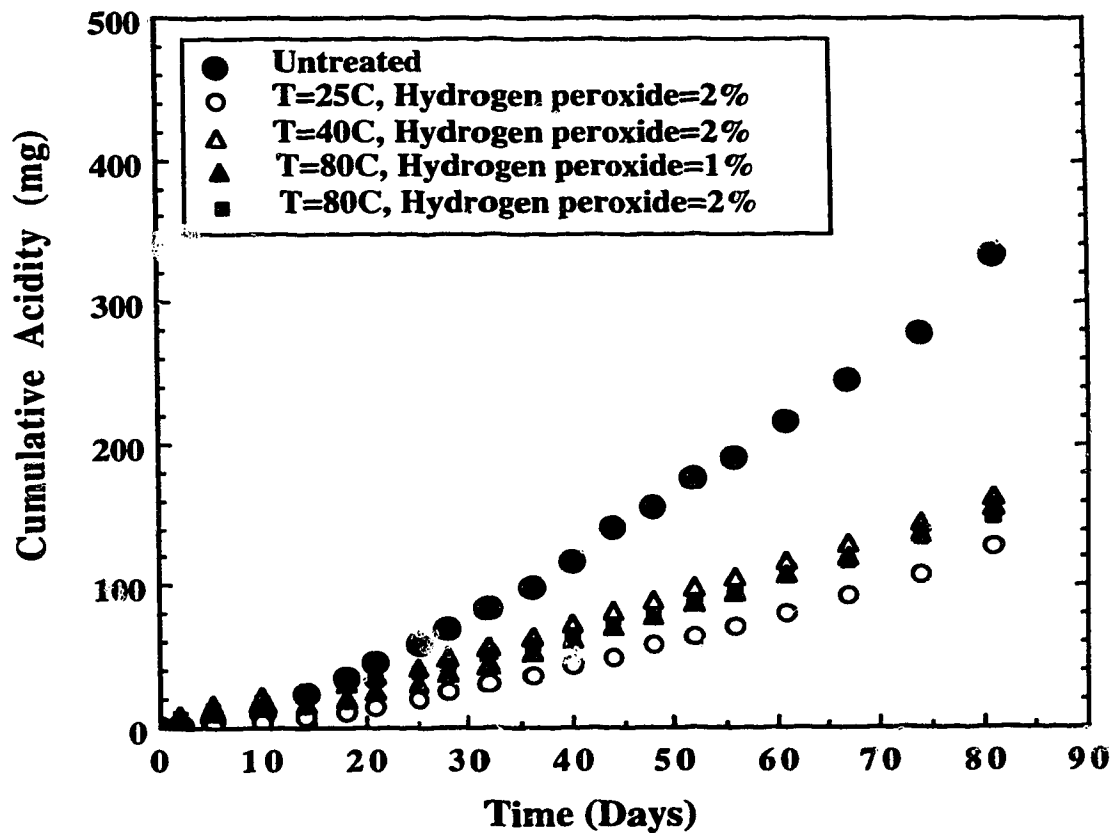


**Figure 2-12. Cumulative acidity of solution from accelerated oxidation columns.**

81 days for the 25°C treated pyrite, 160 mg and 140 mg were obtained for the 40°C and 80°C phosphated pyrite samples, respectively. The untreated pyrite resulted in about 350 mg of acidity after 81 days. It appears that the cracks formed on the surface deposits at high phosphating temperatures reduces the effectiveness of the phosphate coating in preventing the ingress of oxidants into the pyrite matrix, although higher temperatures resulted in thicker coatings. This would explain the lower cumulative acidity generated with the pyrite sample treated at 25°C.

Since very long periods of time, 81 days, were required to evaluate the stability of the treated pyrite particles, pressure oxidation experiments were designed and investigated as a faster means of testing the oxidative stability of samples. Conditions were chosen such that the coating was not destroyed during the pressure oxidation testing. Also, precipitation of Fe during the reaction was to be avoided, since Fe in solution was to be used as a measure of pyrite oxidation. The untreated pyrite particles were first used to obtain appropriate test conditions.

Figure 2-13 illustrates the percent oxidation of the untreated pyrite samples at 24°C, 40°C and 60°C using an oxygen pressure of 1000 psi. The figure shows that at 24°C, an insignificant oxidation of pyrite occurs within 600 min. When the temperature is increased to 40°C, only 0.2% oxidation was obtained after 600 min of reaction time. Increasing the reaction temperature to 60°C resulted in about 1.2% oxidation of pyrite. Precipitation of Fe was not observed at these temperatures with an initial pH of 6 (pH of distilled water).

Figure 2-14 illustrates the effect of pressure on the oxidation of untreated pyrite at 60°C. As expected, the oxidation of the untreated pyrite is observed to increase with oxygen pressure. At 100 psi, the oxidation of pyrite increases steadily throughout the testing period and 0.5% oxidation was obtained after 600 min of reaction time. A similar trend was observed for 200 psi resulting in 0.6% oxidation after 600 min. This trend changes for 500 and 1000 psi, where a steady increase in oxidation is obtained until after 400 min, when a higher oxidation rate is observed. Testing at temperatures above 60°C

resulted in the re-precipitation of some dissolved Fe. Base on these results, 60°C (data not shown) was chosen as an appropriate temperature for testing the stability of the phosphated pyrite particles in the autoclave.

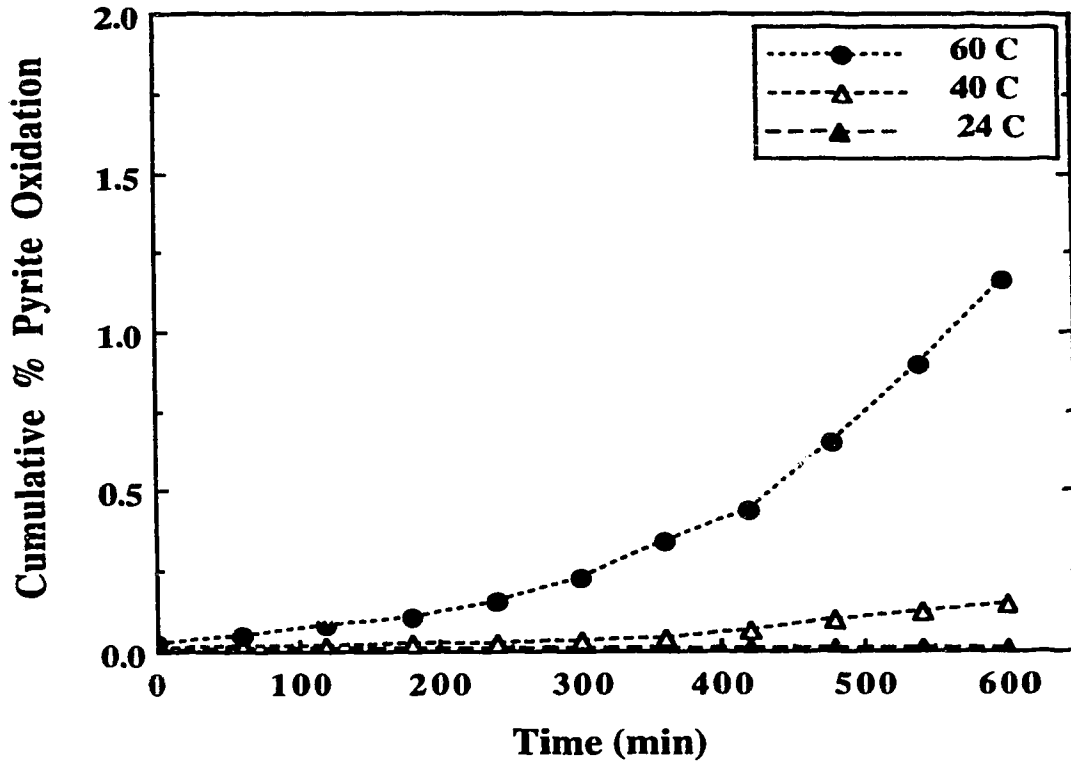


**Figure 2-13. Oxidation of untreated pyrite tested at 24°C, 40°C and 60°C, and 1000 psi of pure oxygen.**

Figure 2-15 illustrates the percent pyrite oxidation of untreated and phosphate-treated pyrite tested in the autoclave at 60°C and 200 psi of oxygen pressure. Under these conditions, about 480 min of reaction time in the autoclave corresponds to about 81 days in the accelerated oxidation column in terms of the degree of pyrite oxidation. After 480 min in the autoclave, 0.43% oxidation was obtained for the untreated pyrite, while 0.23%, 0.19% and 0.16% oxidation was obtained for the 25°C, 40°C and 80°C phosphated-pyrite samples respectively. These percent oxidation results for the phosphated-pyrite samples

are slightly higher than those obtained after 81 days of testing in the accelerated oxidation column. After 600 min reaction in the autoclave, 0.62% oxidation was obtained for the

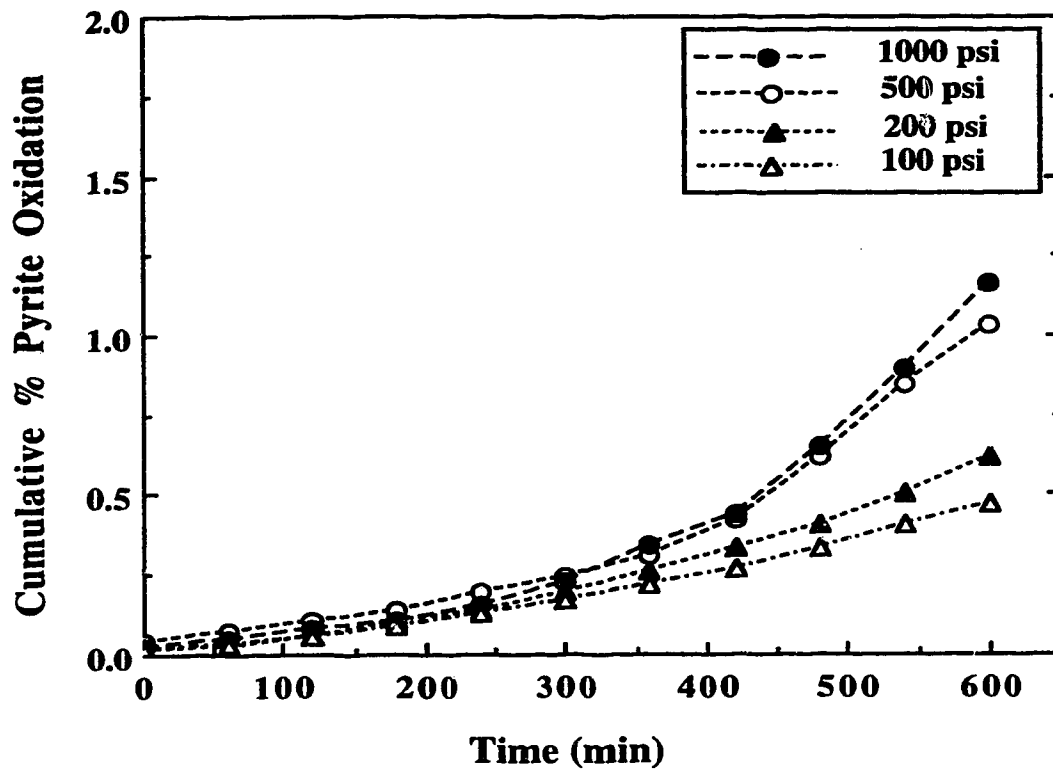


**Figure 2-14. Oxidation of untreated pyrite tested at 100 psi, 200 psi, 500 psi and 1000 psi of pure oxygen, and 60°C.**

untreated pyrite, while 0.36%, 0.30% and 0.25% was obtained for the 24°C, 40°C and 80°C phosphate-coated pyrite samples, respectively. As observed in the accelerated oxidation column tests, the phosphate treatment significantly lowered the rate of oxidation of the pyrite. No significant difference in the stability of the pyrite particles phosphated at 25°C, 40°C and 80°C was observed, in agreement with the accelerated oxidation column tests under ambient conditions.

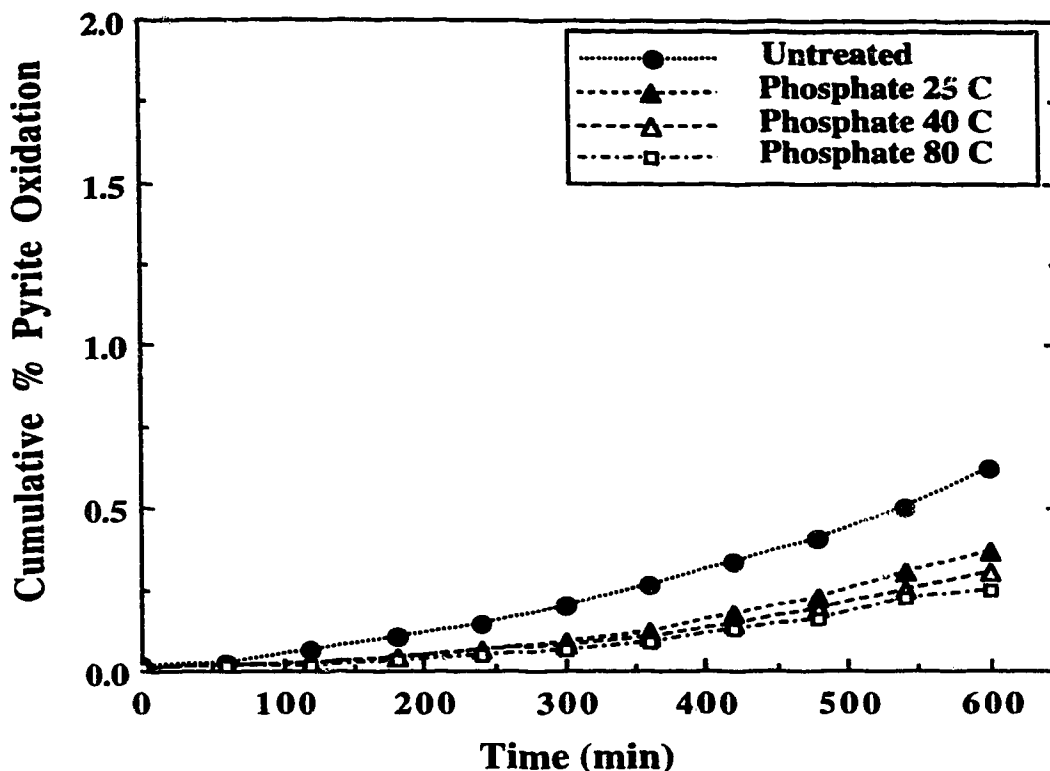


**Figure 2-15. Oxidation of untreated and phosphate-treated pyrite tested at 200 psi of pure oxygen and 60°C.**

Figure 2-16 shows the untreated and phosphate-treated pyrite tested at 1000 psi and 60°C. Under these conditions, about 360 min of autoclave reaction time corresponds to about 81 days in the accelerated oxidation column in terms of the degree of pyrite oxidation. After 360 min of oxidation in the autoclave, about 0.44% oxidation was obtained for the untreated pyrite and 0.22%, 0.25% and 0.22% was obtained for pyrite particles phosphated at 25°C, 40°C and 80°C respectively. These percent oxidation values for the phosphate-coated pyrite samples in the autoclave are higher than those obtained after 81 days in the accelerated oxidation columns. Ten hours of reaction in the autoclave under this condition resulted in 1.2% oxidation for the untreated pyrite, and 0.66%, 0.68% and 0.60% oxidation for the pyrite samples phosphated at 25°C, 40°C, and 80°C, respectively.

Under these conditions, the phosphate treatment was again observed to lower the rate of pyrite oxidation. Also, no significant differences in the stability of phosphate coating formed at higher temperatures was observed.

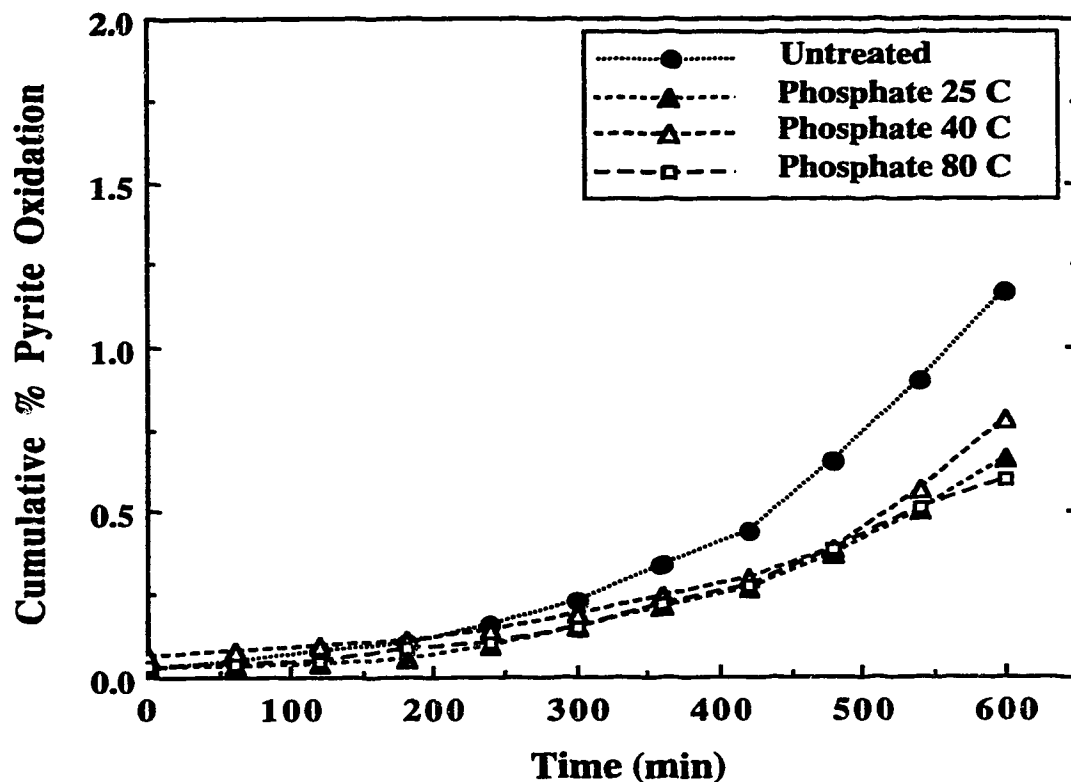


Figure 2-16. Oxidation of untreated and phosphate-treated pyrite tested at 1000 psi of pure oxygen and 60°C.

## 2.5. SUMMARY OF CHAPTER

The results of this study have shown that chemical oxidation of pyrite and ARD formation can be reduced significantly by phosphating. The phosphate treatment has been shown to form an iron phosphate coating on pyrite particles, thereby preventing the ingress of oxidants into the pyrite matrix, which in turn reduces the rate of pyrite oxidation and

ARD formation. Although thicker coatings are formed using high phosphating temperatures, these thicker coatings do not significantly improve the protection of the pyrite over thinner coatings formed under ambient conditions. The use of an autoclave for testing the stability of phosphate treated particles, in terms of oxidation, has been shown to be reliable and a faster alternative to the conventional column oxidation test. Using 60°C and 200 psi oxygen pressure, about 480 min of reaction time in the autoclave corresponded to about 81 days in the accelerated oxidation column. Results obtained for the phosphated pyrite samples under these conditions in the autoclave agree well with those obtained in the accelerated oxidation column test.

## 2.6 REFERENCES

- American Public Health Association. 1985. Standard methods for the examination of water and wastewater. APHA, Washington, DC.
- American Society for Testing and Materials. 1982. Annual book of ASTM standards. Part 26. Philadelphia, Pa. pp. 408-414.
- Buckley, A. N., and R. Woods. 1987. The surface oxidation of pyrite. *Appl. Surf. Sci.* 27: 437-452.
- Chander, S., and A. Briceno. 1987. Kinetics of pyrite oxidation. *Miner. Metallurg. Process.* 4: 171-184.
- Dalas, E. 1990. Overgrowth of iron(III) phosphate on collagen. *J. Chem. Soc. Faraday Trans.* 86: 2967-2970.
- Dalas, E., and P. G. Koutsoukos. 1990. Phosphate adsorption at the porous glass/water and SiO<sub>2</sub>/water interfaces. *J. Colloid Interface Sci.* 134: 299-304.
- Dalas, E. 1991. The crystallization of ferric phosphate on cellulose. *J. Crystal Growth.* 113: 140-146.
- Evangelou, V. P., and X. Huang. 1992. A new technology for armoring and deactivating pyrite. *Environmental issues and waste management in energy and minerals*

- production, R. K. Singhal, A. K. Mehrotra, K. Fytas, and J-L. Collins (eds.). Calgary, Alberta. Balkema, Rotterdam. pp. 413-417.
- Freeman, D. B. 1986. Phosphating and metal pre-treatment. Industrial Press Inc., New York, NY. pp. 3-49.
- Goldhaber, M. B. 1983. Experimental study of metastable sulfur oxyanion formation during pyrite oxidation at pH 6-9 and 30°C. *Am. J. Sci.* 283: 193-217.
- Hamilton, I.C., and R. Woods. 1981. An investigation of surface oxidation of pyrite and pyrrhotite by linear potential sweep voltametry. *J. Electroanal. Chem.* 118: 327-343.
- Kenkel, J. 1988. Analytical chemistry for technicians. Lewis Publishers, Inc., Chelsea, Michigan. pp. 236.
- Kiselev, I. Y. 1990. Protection of metals. English translation of *Zaschita Metallov*. 26: 215-218.
- Kossel, W. 1934. Theory of crystal growth. *Ann. Phys.* 21: 455-458.
- Lorin, G. 1974. Phosphating of metals. Finishing Publications Ltd., Hampton Hill, Middlesex. pp. 7-20.
- Losch, A., J. W. Schultze, and H. D. Speckmann. 1991. A new electrochemical method for the determination of the free surface of phosphate layers. *Appl. Surf. Sci.* 52: 29-38.
- Nriagu, J. O. 1972a. Stability of vivianite and ion-pair formation in the system  $\text{Fe}_3(\text{PO}_4)_2\text{-H}_3\text{PO}_4\text{-H}_2\text{O}$ . *Geochim. Cosmochim. Acta.* 36: 459-470.
- Nriagu, J. O. 1972b. Solubility equilibrium constant of strengite. *Am. J. Sci.* 272: 476-484.
- Ogunsola, O. M., and K. Osseo-Asare. 1986. The electrochemical behaviour of coal pyrite. 1. Effect of mineral source and composition. *Fuel.* 56: 811-815.
- Palencia, I., R. Y. Wan, and J. D. Miller. 1991. Electrochemical behavior of a semiconducting natural pyrite in the presence of bacteria. *Metallurg. Trans. B.* 22: 765-774.



- Peters, E. 1986. Leaching of Sulfides. *Advances in Mineral Processing*, Arbiter symposium, P. Somasundaran (ed.). New Orleans, Louisiana. SME-AIME. pp. 445-462.
- Reimers, G. M. and D. F. Franke. 1991. Effect of additives on pyrite oxidation. U. S. Bureau of Mines, RI 9353.
- Ross, W. A. 1869. Preserving metals from oxidation. British Patent No. 3119.
- Sato, M. 1960. Oxidation of sulfide ore bodies, II. Oxidation mechanisms of sulfide minerals at 25°C. *Econ. Geol.* 55: 1202-1231.
- Siwik, R., S. Payant, and K. Wheeland. 1989. Control of acid generation from reactive waste rock with the use of chemicals. *Tailings and effluent management, Proceedings of the international symposium on tailings and effluent management*, M. E. Chalkley, B. R. Conard, V. I. Lakshmanan, and K. G. Wheeland (eds.). CIM, Halifax. Pergamon, New York. pp. 181-193.
- Smith, G. F. 1942. Variation in the properties of pyrite. *Am. Mineralogist.* 27: 1-18.
- Spotts, E., and D. J. Dollhopf. 1982. Evaluation of phosphate materials for control of acid production in pyritic mine overburden. *J. Environ. Qual.* 21: 627-634.
- Stiller, A. H., J. J. Renton, and T. E. Rymer. 1989. An experimental evaluation of the use of rock phosphate (apatite) for the amelioration of acid-producing coal mine waste. *Min. Sci. Technol.* 9: 283-287.
- Van Wazer, J. R. 1958. Phosphorus and its compounds. Vol. 1. Interscience Publishers, New York, NY.
- Watkin, E. W., and J. Watkin. 1983. Inhibiting pyrite oxidation can lower reclamation costs. *Can. Min. J.* 104: 29-31.

## CHAPTER 3

### SUPPRESSION OF PYRITE OXIDATION BY FATTY ACID AMINE TREATMENT\*

#### 3.1 INTRODUCTION

Methods for the control and prevention of acid rock drainage (ARD) at-source depend on the creation of conditions which chemically, biochemically or physically retard the rate of oxidation of sulfide minerals. Since ARD results from the oxidation of sulfides in the presence of an oxidizing agent, water and/or iron-oxidizing bacteria, all the at-source methods are directed towards controlling one or more of these components.

Although physical waterproofing of waste heaps by the use of physical barriers has been investigated as a means of preventing water and oxygen ingress into the waste (Healey and Robertson, 1989; Nicholson et al., 1989), only limited studies have been done on the effectiveness of chemical waterproofing of sulfide particles. This study explores the use of a fatty acid amine to produce a highly hydrophobic pyrite surface as a means of suppressing pyrite oxidation and hence controlling ARD formation at-source.

#### 3.2 THEORY AND BACKGROUND

In order to successfully control pyrite oxidation, a clear understanding of its mechanism of oxidation is important. The mechanism of pyrite oxidation is complex and theories to explain this oxidation process differ considerably. Although the chemical reaction theories consider the adsorption and reaction of molecular oxygen directly on the

---

\* Part of this chapter, co-authored with N. O. Egiebor has been published in the proceedings of an international symposium sponsored by TMS. Extraction and processing for the treatment and minimization of wastes, J. P. Hager et al. San Francisco, Feb. 27-March 3, pp. 773-790, 1994.

surface of pyrite, the electrochemical theories take into account the anodic dissolution of pyrite and cathodic reduction of oxygen (Hamilton and Woods, 1981). Although a number of reviews have been published on the electrochemistry of pyrite (Lowson, 1982; Hiskey and Schlitt, 1982; Osseo-Asare, 1992), the detailed mechanism of pyrite oxidation is still not well established. Another electrochemical theory which has been used to explain the oxidation of pyrite is the semiconductor theory. This theory considers electrons in discrete energy levels, and is based on the molecular orbital and band theories (Vaughan and Craig, 1978; Luther, 1987). Some investigators (Springer, 1970; Biegler, 1976) have observed that the electronic conduction properties of minerals do not normally play a significant role in hydrometallurgical oxidation and dissolution reactions in which electrochemical corrosion processes are important, and also found no obvious correlation between kinetic parameters for oxygen reduction and nature of semiconduction of pyrite. Other investigators have reported a significant role for semiconductor electrochemistry in the oxidation of pyrite (Mishra and Osseo-Asare, 1988; Crundwell, 1988; Osseo-Asare, 1993).

Based on these theories, many reaction mechanisms of pyrite oxidation have been proposed. A detailed study of these theories and mechanisms revealed that they have some aspects in common. One fundamental aspect all these mechanisms have in common is the initiation step of pyrite oxidation. All the mechanisms agree on the initial adsorption of ions or molecules on the surface of the pyrite. Biegler and Swift (1979) concluded that the first step involves the electroadsorption of  $\text{OH}^-$  on an  $\text{S}_2^{2-}$  (lattice) site which rapidly oxidizes to  $\text{SO}_4^{2-}$ . Moses and Herman (1991) observed that the oxidation is accompanied by adsorption of  $\text{Fe(II)}$  from solution. They concluded that although dissolved oxygen can directly oxidize pyrite, it can effectively do so only in the absence of  $\text{Fe(II)}$  adsorbed to the pyrite surface. Garrels and Thompson (1960) found that the rate of oxidation of pyrite was proportional to the fraction of pyrite surface occupied by ferric ion.

It is therefore not surprising that the passivation behavior of pyrite during acidic leaching had been attributed to the formation of elemental sulfur on the pyrite surface. It is

well established that the presence of elemental sulfur renders a surface strongly hydrophobic. This hydrophobic property is utilized in collectorless flotation of pyrite by using an amine such as ethylene diamine tetraacetic acid (EDTA) (Ahlberg et al., 1990). EDTA has been studied for reducing ARD formation, but the mechanism is attributed to complexation of ferric ion in solution or at the surface of the pyrite so that they are not available for oxidation (Chander and Zhou, 1992).

The specific role of acidophilic chemoautotrophic bacteria in ARD formation has been a matter of considerable debate. When bacteria is involved in the oxidation of pyrite, two major mechanisms, direct and indirect have been proposed. In the direct mechanism, the bacteria act as the primary oxidant, necessitating a direct contact between the bacteria and the pyrite surface. The indirect mechanism involves the leaching of the pyrite by ferric ions generated by bacteria (Palencia et al., 1991). Although controversy exists over the relative significance of the two mechanisms (Omura et al., 1991), the latter mechanism also requires adsorption of the ferric ions on to the surface of pyrite for oxidation to occur. Murthy and Natarajan (1992) observed that, by improving bacterial attachment to pyrite surface, its oxidation increased.

If the initial step in pyrite oxidation involves the adsorption of ions and molecules from solution onto the surface, it should be expected that an increase in the surface hydrophobicity of pyrite would lead to an effective suppression of oxidation. Based on this premise, the study reported in this chapter was aimed to investigate the suppression of pyrite oxidation by treatment with surfactants which are capable of significantly increasing the hydrophobicity of pyrite by chemisorption.

A survey of the relevant chemical literature suggests that surfactants containing amine functional groups impart water repellent properties on soils. One type of cationic surfactant which impacts hydrophobic properties to soil is the fatty acid derivatives of polyamines. Hydrophobicity has been shown to intensify with increasing molecular weight of saturated fatty acids (Bistline and Linfield, 1984). Although 2-alkyl-2-

imidazoline were found not to impart sufficient hydrophobicity to soils, the fatty acid derivatives of higher molecular weight polyamines (hydrogenated tallow fatty acid-diethylenetriamine reaction product) were found to impart high hydrophobicity to soils. Amines have been reported to protonate in soil and replace inorganic cations from clay complexes by ion exchange (Bistline et al., 1983).

### **3.3 EXPERIMENTAL**

#### **3.3.1 Materials**

The pyrite used for the experiments is the same as that described in Section 2.3.1. The fatty acid amines, Armac T and Armac HR were obtained from Akzo Chemicals Ltd, Toronto, Canada, and Armac C was obtained from Akzo Chemical Inc., Chicago, U.S.A. These surfactants are primary amines with a general chemical formula of  $\text{RNH}_3^+\text{CH}_3\text{COO}^-$ , where R represents tallow, hydrogenated rapeseed and coconut oil derivatives in Armac T, Armac HR and Armac C, respectively. All other chemical reagents were analar grade obtained from Fisher Scientific, Edmonton, Canada and used without further purification. Silica sand was obtained from Fisher Scientific, Ottawa, Canada. The pyrite was ground in a jaw crusher and separated into +850, +710, +600, +300, +150, +75 and -75  $\mu\text{m}$  size fractions by dry sieving. These various fractions were then stored under nitrogen gas and used for the experiments.

#### **3.3.2 Pyrite Treatment**

The treatment of pyrite samples with various reagents was carried out in a cylindrical glass reactor with four inlet ports at the top. The desired concentration of the reagent was prepared in the reactor and a desired weight of pyrite added. Agitation of the mixture was achieved by passing compressed air into the solution via a tube through one of the inlet ports. Compressed air was used for agitation to minimize breaking up of the

particles during the reaction. Two other inlet ports were used for pH and temperature probes to monitor these parameters in the solution during the reaction. The fourth inlet port was used for collecting samples by means of a syringe. For a typical treatment, 50 g of pyrite was treated with 200 mL of a 1.23 g/L surfactant solution. After the reaction, the resulting suspension was filtered to remove the solid, which was washed with distilled water and dried in air. These solid samples were used for evaluating the rate of oxidation in the accelerated column, and pressure oxidation tests. The liquid was analyzed for total dissolved Fe. Although equilibrium surfactant uptake was attained in about 15 min, each sample was agitated for 1 h. For the adsorption kinetic studies, samples were taken periodically and analyzed for total dissolved Fe and surfactant concentration in terms of amine value.

### **3.3.3 Accelerated Column Oxidation Tests**

Accelerated column oxidation tests of the untreated and the various treated pyrite samples was carried out in a glass column at ambient conditions. Details of the accelerated column oxidation test procedure was reported in Section 2.3.3. The column was made of a Pyrex glass tube with an upper section diameter of 5 cm and height of 14 cm. The lower section of the column had a diameter of 1.8 cm and height of 12 cm. The column was packed with a mixture of 50 g of 600  $\mu\text{m}$  of untreated or treated pyrite and 100 g of +850  $\mu\text{m}$  glass beads. The packed column was filled with 50 mL of distilled water and compressed air was fed into the bed through a fine glass tube with a diameter of 0.5 cm. The column was drained and refilled every 3 to 7 days depending on the results of the preceding analysis and the coloring of the indicating beads. The drainage volume was measured and analyzed for total Fe,  $\text{Fe}^{2+}$ , pH and titratable acidity.

### 3.3.4 Pressure Oxidation Tests

Since the oxidation rates of the pyrite in accelerated columns are generally very low and required long periods for testing samples, pressure oxidation experiments were designed as a faster means of evaluating the effect of the various reagents on the suppression of pyrite oxidation. Details of the pressure oxidation test procedure has been reported in Section 2.3.4. Samples taken during the experiment were analyzed for pH, total Fe and Fe<sup>2+</sup> content.

### 3.3.5 Contact Angle and Hydrophobicity

The degree of hydrophobicity of the treated and untreated pyrite particles were determined through contact angle measurements. Contact angles were determined on 300 µm pyrite and silica sand particles by penetration test. The silica sand was cleaned in 30% hydrogen peroxide, washed with distilled water, and dried at 80°C. Contact angle measurements on silica sand treated by this method was shown to be zero (McCaffery and Mungan, 1970). In the penetration test, 2 g of indicating drierite was packed into a glass tube of 1.2 cm diameter and 28 cm high. The pyrite or silica particles were then placed on the drierite and compacted by tapping the side of the glass tube with a rubber hose. Five milliliters of distilled water was then placed on the surface of the packed pyrite or silica sand. The time required to change the indicating drierite from blue to pink was recorded as the penetration time. The distance of penetration (L) in time (t) of water with surface tension ( $\lambda_w$ ) and viscosity ( $\eta$ ) is given by the modified Washburn equation (Rosen, 1978):

$$L^2 = \frac{(kr) t \lambda_w \text{Cos}\theta}{2\eta} \quad (3-1)$$

where r is the mean equivalent radius of the capillary passages through the fine particles and k a constant to allow for the tortuous path through them. The (kr) product depends on the packing of the powder. When the fine particles are packed to the same bulk density,

(kr) is assumed to be constant. The (kr) product was evaluated by passing distilled water through silica sand particles whose contact angle is  $0^\circ$ . The penetration tests were repeated a number of times and the average of five timings was taken as the penetration time. The contact angle was obtained from the expression:

$$\theta = \text{Cos}^{-1} \left( \frac{t_s}{t_x} \right) \quad (3-2)$$

where  $\theta$  is the contact angle,  $t_s$  is the penetration time for silica particles and  $t_x$  is the penetration time for pyrite particles for which the contact angle is required.

### 3.3.6 Zeta Potential Determination

Electrophoretic mobility of the  $-45 \mu\text{m}$  pyrite particles (untreated and treated with various concentrations of surfactant) were determined by using Rank Brothers Mark II Electrophoretic apparatus equipped with a timer handset, and a flat rectangular cell with an electrode at each end. The electrophoretic method has the advantage over the streaming potential technique in that it gives an indication of the distribution of charges among the particles rather than a net value of the charge of the particles in the system (Shaw, 1980). Electrophoretic velocity was found by timing 20 individual particles over a fixed distance ( $250 \mu\text{m}$ ) on a calibrated eyepiece scale. The field strength was adjusted to give timings of about 10 s; faster times introduce timing errors, and slower times increase the unavoidable error due to Brownian motion. Timings were made at the stationary level, and by alternating the direction of the current, errors due to drift were largely eliminated. The electrophoretic velocities were calculated from the average of the reciprocals of 20 timings. In estimating the double layer repulsive forces between particles, it is assumed that the stern potential and the zeta potential calculated from electrophoretic mobilities are identical (Shaw, 1980). The pH of the solutions were adjusted with NaOH and HCl to the experimental pH where necessary.



The zeta potential was calculated using Smoluchowski's formula (Shaw, 1969; Shaw, 1980), Equation (3-3):

$$E\epsilon\zeta = \eta V_E \quad (3-3)$$

where  $V_E$  is the electrophoretic velocity, i.e. the velocity of the surface relative to stationary liquid,  $E$  is the electric field strength,  $\eta$  is the viscosity of the water,  $\epsilon$  is the permittivity, and  $\zeta$  is the zeta potential.

### 3.3.7 Chemical Analysis

Methods used for the analysis of total sulfur and iron content of the pyrite samples, and total iron and ferrous iron in solution during the accelerated column and pressure oxidation experiments has been outlined in Section 2.3.5.

The pH of the solutions was determined by a Cole-Parmer Chemcadet pH/mV meter equipped with a temperature compensation probe. Titratable acidity of solutions from the columns were determined by titration with NaOH (which had been standardized against HCl) using phenolphthalein.

Amine concentration was determined according to American Oil Chemist Society test method (1979). A solution of the amine was titrated with 0.2 N HCl in isopropyl alcohol using bromocresol green as an indicator. The total amine value (number of milligrams of potassium hydroxide equivalent to the basicity in 1 g of sample) was used as the concentration of amine present and calculated by the equation:

$$\text{Total amine value} = \frac{\text{mL} \times \text{N} \times 56.1}{\text{sample weight (g)}} \quad (3-4)$$

where mL is the volume of HCl required to reach the end point, and N is the normality of the HCl used.

### 3.3.8 Scanning Electron Microscopy

The untreated and treated pyrite samples were viewed and analyzed with a Hitachi S-2700 scanning electron microscope (SEM) equipped with a Link analytical EXL energy-dispersive X-ray spectrometer (EDS). The EDS is equipped with a Si(Li) solid state x-ray detector and a Be and ultra-thin windows for detecting light elements. Both backscattered and secondary electron images of the samples were constructed. At high magnifications, the size of the area sampled represented a tiny fraction of the sample, therefore about 20 areas were studied to gain a valid description of the sample.

## 3.4 RESULTS AND DISCUSSION

The chemical composition of the pyrite determined by SEM-EDS, AAS and Leco total sulfur analyzer has been reported in Table 2-1 (Section 2.4). The pyrite is fairly pure with small amounts of impurities, mainly silicon.

Figure 3-1 presents a plot of the change in concentration of Fe in solution during treatment of pyrite with 1.23 g/L of Armac T, Armac HR or Armac C. The concentration of Fe leached into the fatty acid amine solutions during the treatment was observed to increase rapidly within the first 5 min and plateau thereafter. The recorded pH of the 1.23 g/L solution of the fatty acid amines were slightly acidic with pH between 4.9 and 5.8. The acidity of the fatty acid amines is due to the presence of carboxylic acid functional group in the surfactants. The pH of these solutions did not change significantly during reaction with the pyrite samples, although minor changes in pH were observed in the first 5 min of the reaction as in the case of Fe concentration in solution. The release of Fe into solution suggest the formation of a sulfur-rich pyrite surface. This phenomenon has been reported by Chander and Briceno (1987).

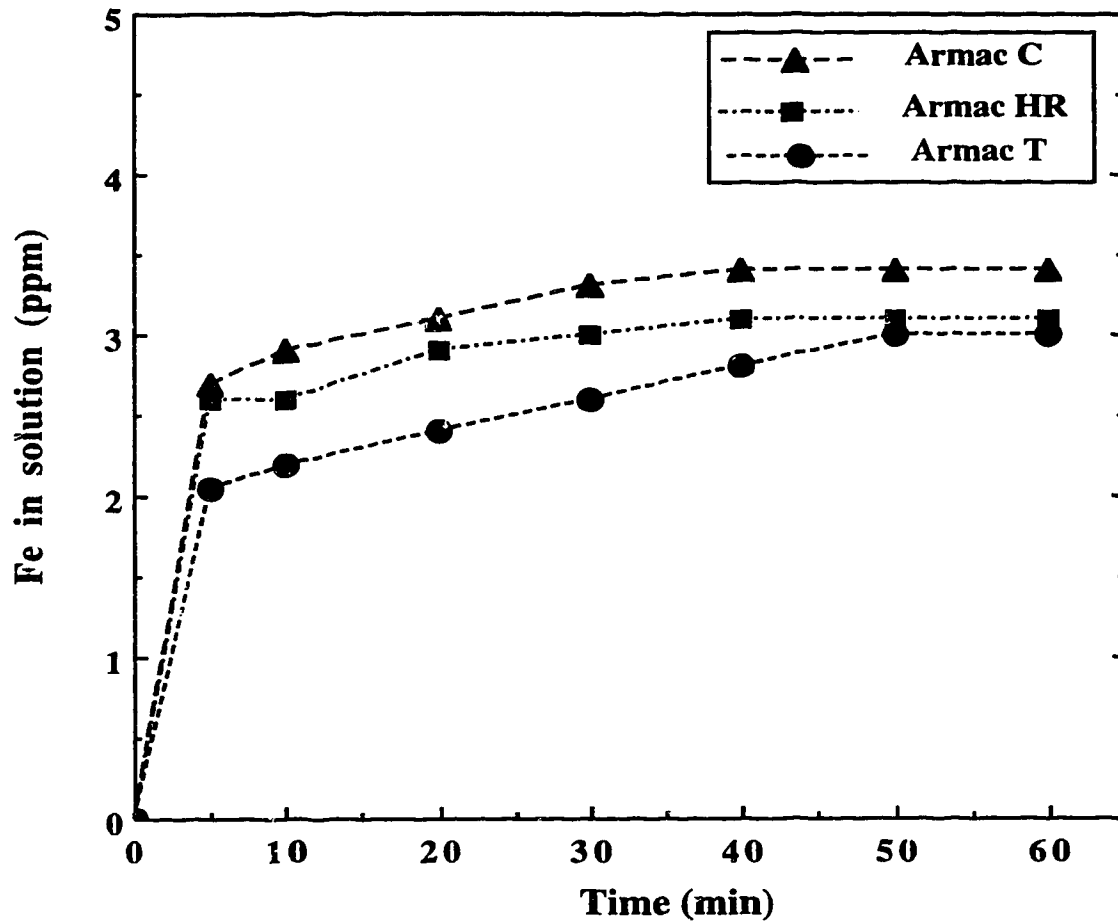


**Figure 3-1. Concentration of iron in solution during deactivation of pyrite with fatty acid amines.**

The changes in the amine values (g of KOH equivalent to the basicity in 1 g) of Armac T, Armac HR and Armac C during treatment of the pyrite samples is illustrated in Figure 3-2. The amine value of Armac C was observed to decrease only slightly in the first 5 min and remain the same for rest of the treatment time. This decrease indicates the adsorption of the surfactant onto the pyrite surface. The amine value of Armac T and Armac HR were observed to decrease significantly with time for the first 30 min and plateau thereafter. The rapid decrease in the amine value of Armac T and Armac HR is due

partly to the uptake of these surfactants by the pyrite, and partly to the formation of micelles (colloidal-sized clusters in solution). The turbidity of the Armac T and Armac HR solutions were observed to increase during the reaction while that of Armac C did not change significantly.

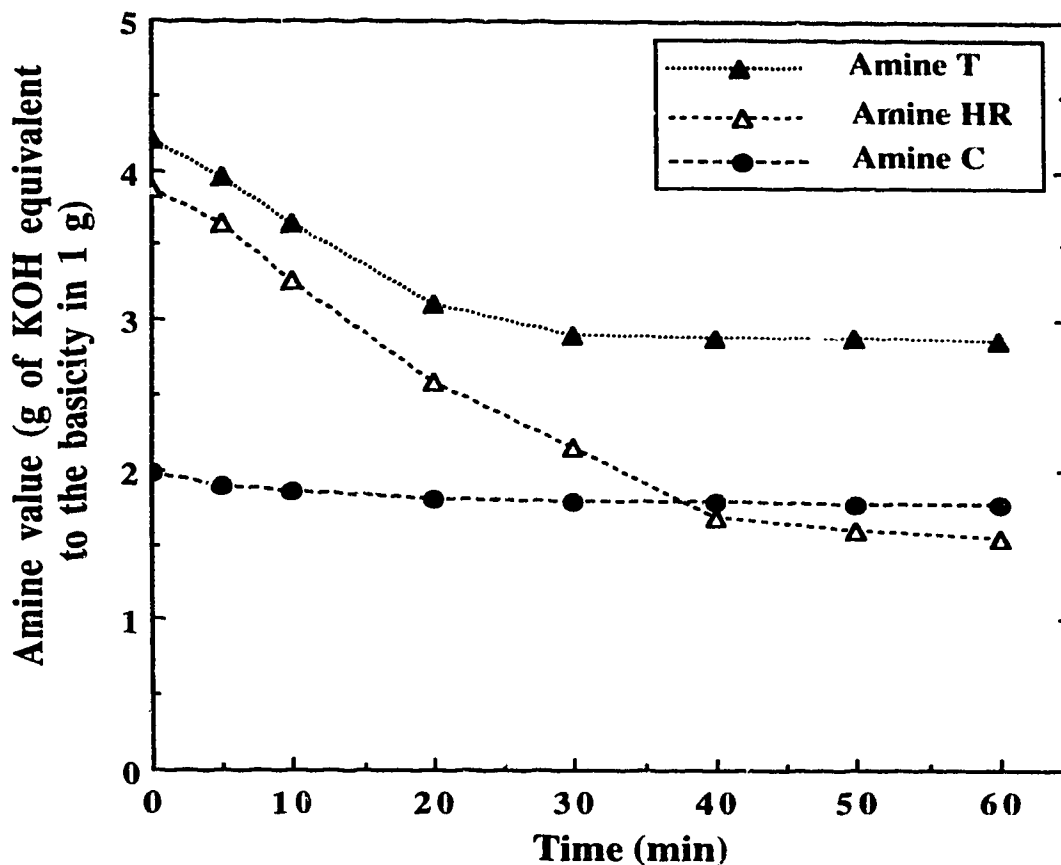
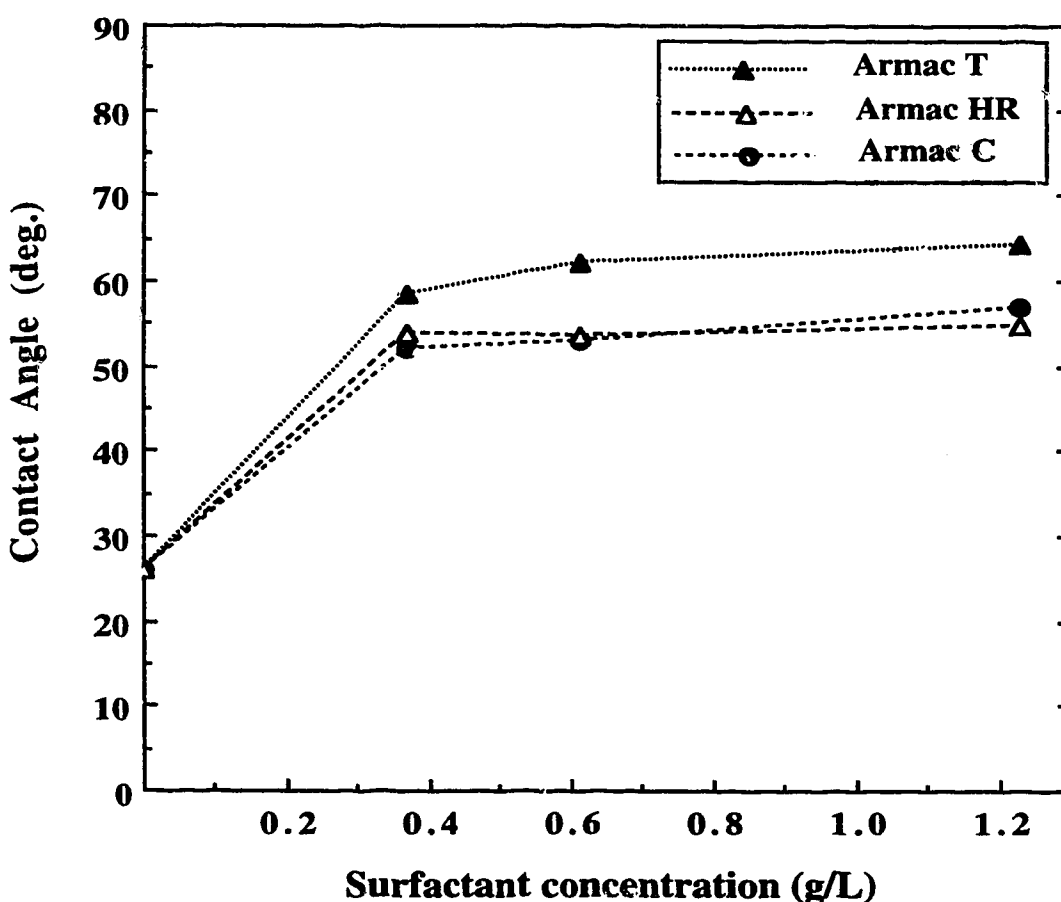


Figure 3-2. Amine value of solution during deactivation of pyrite with fatty acid amine.

Figure 3-3 shows the effect of the concentration of fatty acid amines used for treatment on the contact angle of the treated pyrite particles. Significant increase in the contact angle of the pyrite particles treated with the fatty acids is observed. The untreated pyrite is only slightly hydrophobic with a contact angle of  $26^\circ$  (with reference to silica

sand), whereas fatty acid amine treatment increased the contact angle, thus making the samples highly hydrophobic. The contact angle increased from 26° to 65° when the concentration of Armac T was increased from 0 (untreated) to 1.23 g/L. Contact angle of the pyrite particles also increased from 26° to 57° and 26° to 55° when the concentration of Armac C and Armac HR were increased from 0 to 1.23 g/L, respectively. These increases in the hydrophobicity of the pyrite clearly indicate the adsorption of the surfactants from solution onto the pyrite surface.



**Figure 3-3. Contact angle of untreated and fatty acid amine-treated pyrite particles.**

The effect of 1.23 g/L of Armac T and Armac HR on the zeta potential of the pyrite particles as a function of pH is illustrated in Figure 3-4. The pyrite particles in the absence of the fatty acid amines are positively charged below the pH of 6.5 (point of zero charge) and negatively charged at higher pH. In the presence of Armac T and Armac HR, the pyrite particles become more positively charged throughout the range of pH indicated.

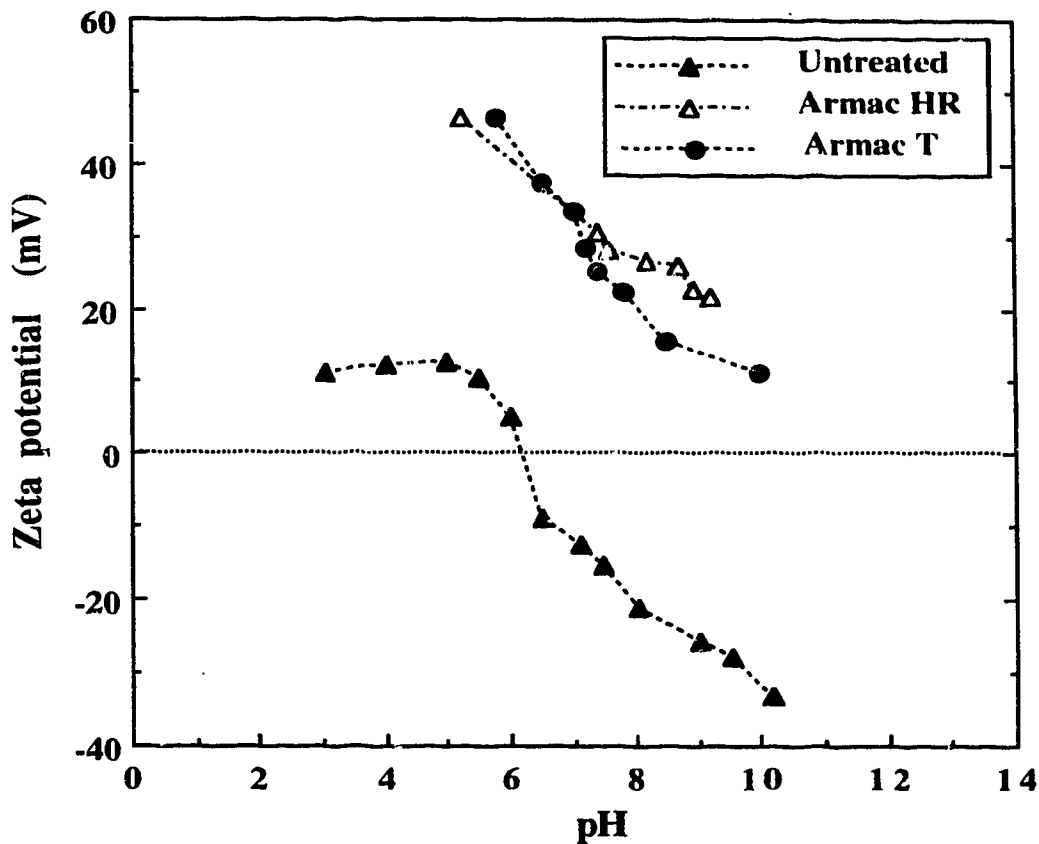
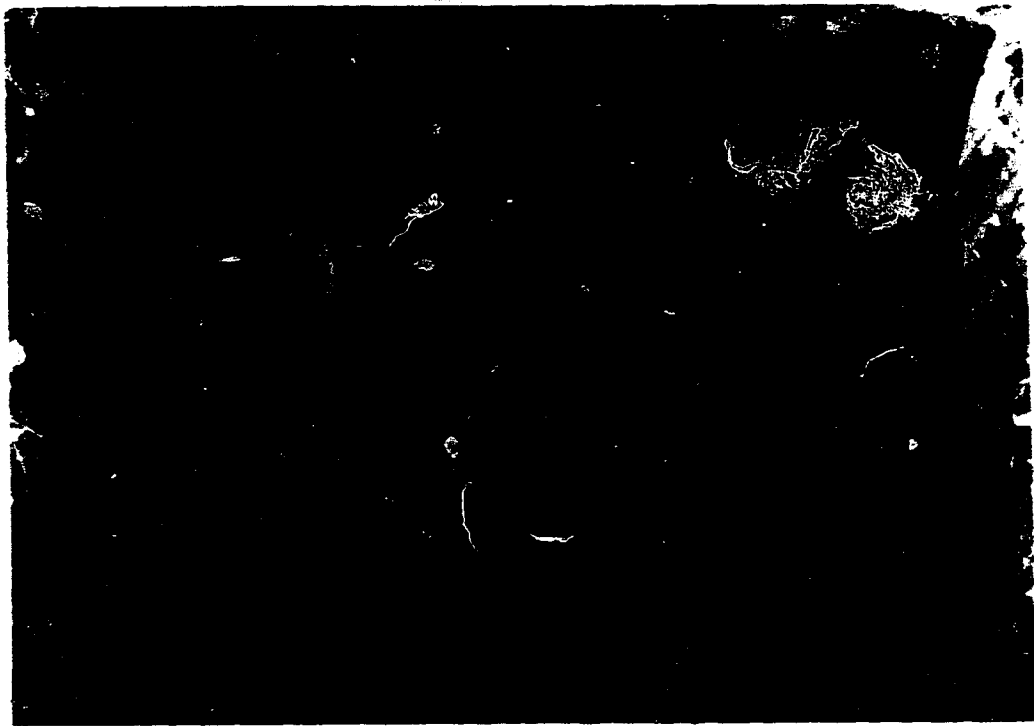


**Figure 3-4. Zeta potential of pyrite as a function of pH in the absence and presence of fatty acid amines.**

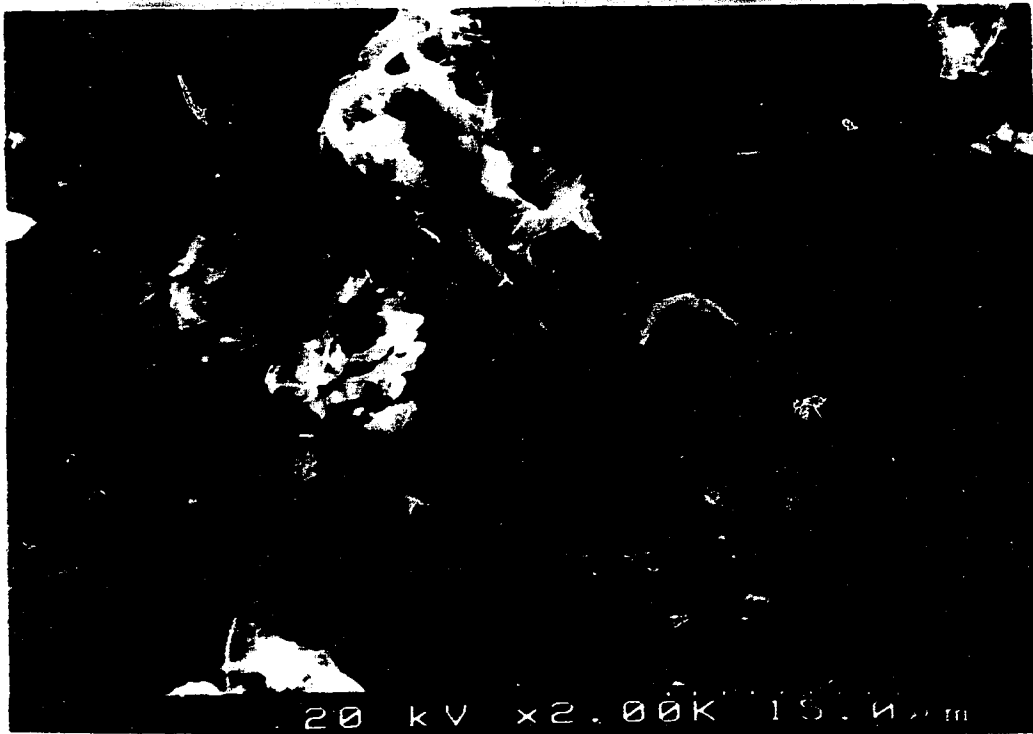
This increase in the zeta potential in the presence of the fatty acid suggests adsorption of the surfactants, which are cationic, onto the surface of the pyrite particles. Armac HR, Armac T and Armac C are primary fatty amine acetates which are weak bases and therefore their

ionization is pH dependent. In the acidic range,  $\text{RNH}_3^+$  species are predominant in solution. These species therefore adsorb onto the surface of the pyrite particles, thus impacting an increased positive charge. The decrease in the zeta potential with increasing pH of the Armac T- and Armac HR-treated pyrite is due to an increased concentration of  $\text{OH}^-$  ions. The  $\text{OH}^-$  ions neutralize some of the positive charges due to adsorbed  $\text{RNH}_3^+$  ions on the surface and reduces the net positive potential. It is suggested from Figures 3-1 and 3-3 that the  $\text{RNH}_3^+$  is adsorbed onto a sulfur-rich pyrite surface. The preferential leaching of Fe from pyrite to produce a sulfur-rich surface in the presence of carboxylic acid functional group has been reported by other investigators (Hamilton and Woods, 1981; Buckley and Woods, 1987). Using XPS, Buckley and Woods (1987) showed the preferential dissolution of Fe from pyrite to form a sulfur-rich surface. The point of attachment of the surfactant to the surface is through the amino head group with the R group (hydrocarbon chain) extending outward. This configuration is responsible for the increased hydrophobic character of the pyrite particles observed through contact angle measurements as shown in Figure 3-4. The attachment of fatty acid amine and other surfactants to soils through the amino group and the resulting increase in hydrophobicity of soils have also been reported by other investigators (Law et al., 1966; Bistline et al., 1983; Bistline and Linfield, 1984).

To determine the hydrophobic reaction products formed on the surface of the pyrite during treatment with the fatty acid amines, the surface of the untreated and treated particles were viewed under the SEM-EDS. The surface morphology of the untreated and Armac T-treated pyrite particles are shown in photomicrographs in Figure 3-5. It is observed that a glassy surface coating forms on the surface of the Armac T-treated pyrite particle. SEM micrographs of Armac HR- and Armac C-treated pyrite particles also showed identical appearances as the Armac T-treated pyrite particles.



a



b

**Figure 3-5. Scanning electron micrographs of (a) untreated and (b) Armac T-treated pyrite samples.**



The stability of fatty acid amine-treated pyrite was evaluated in an autoclave to reduce the time needed for oxidation testing of the samples (Section 2.4). Conditions were chosen such that the hydrophobicity of the treated surfaces is not destroyed. Also, precipitation of Fe during the reaction was to be avoided by using low percent solids (0.6%), since Fe in solution was to be used as a measure of pyrite oxidation. The untreated pyrite particles were first used to obtain the appropriate conditions which were then used to test the treated pyrite particles.

The percent oxidation of the untreated pyrite samples at 24°C, 40°C and 60°C and a pressure of 1000 psi of pure oxygen is shown in Figure 3-6. The figure shows that at

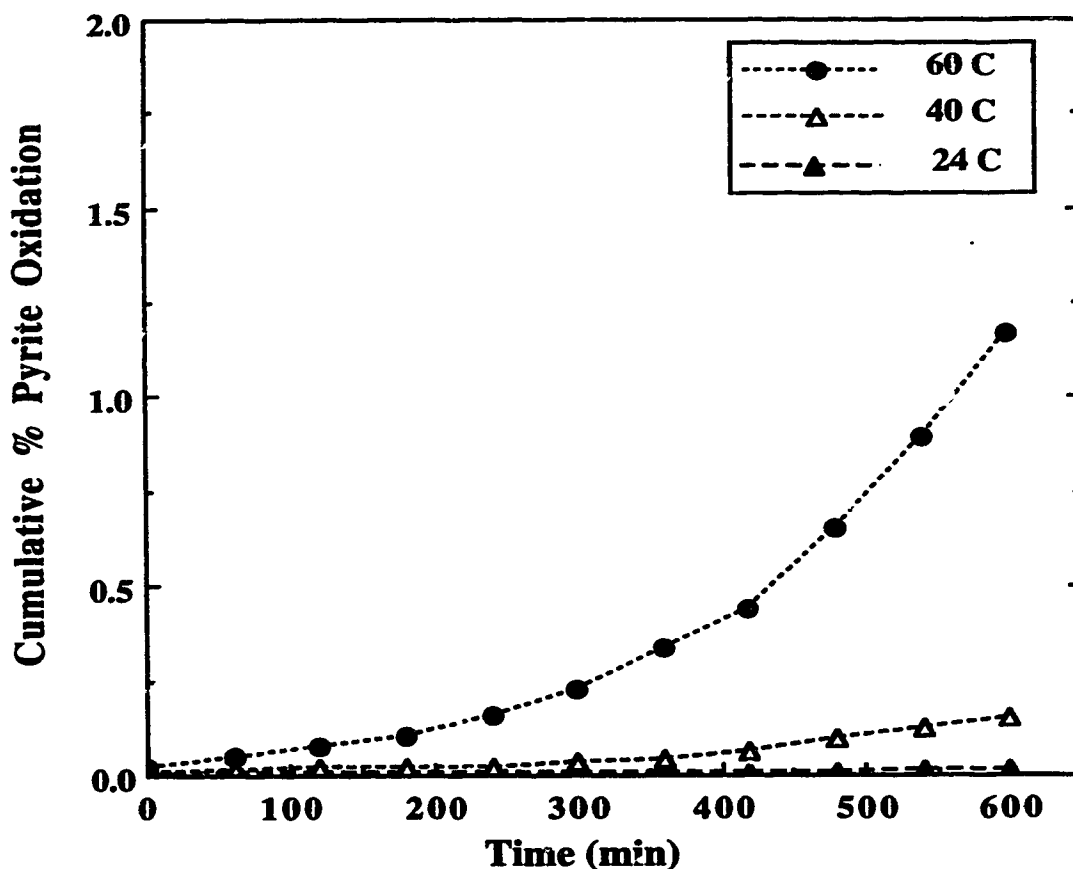


**Figure 3-6. Oxidation of untreated pyrite tested at 25°C, 40°C, and 60°C and 1000 psi of pure oxygen.**

1000 psi and 24°C, an insignificant oxidation of pyrite occurs within 600 min. When the temperature is increased to 40°C, only 0.2% oxidation was obtained after 600 min of reaction time. Increasing the reaction temperature further to 60°C resulted in about 1.2% oxidation of pyrite. Precipitation of Fe was not observed at these temperatures with initial pH of 6 (pH of distilled water).

Figure 3-7 presents the effect of pressure on the oxidation of untreated pyrite at 60°C. As expected, the oxidation of untreated pyrite is observed to increase with oxygen pressure. At 100 psi, the oxidation of pyrite increases steadily throughout the testing

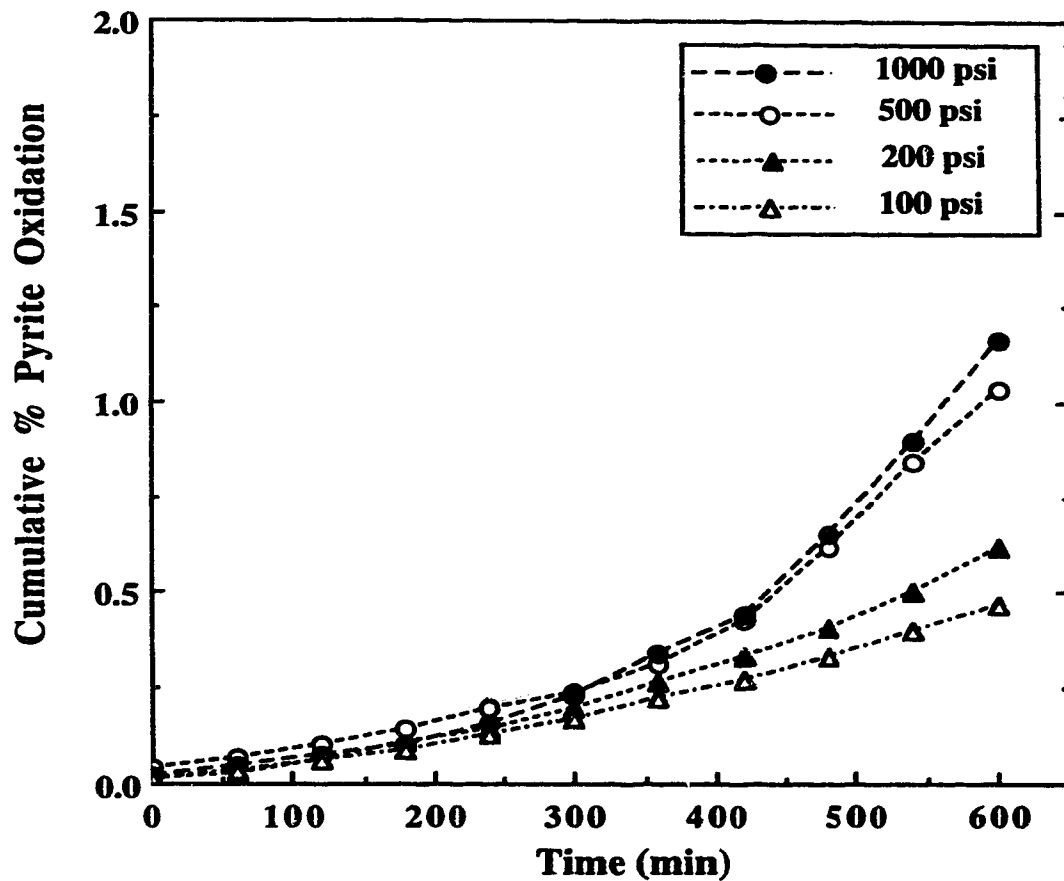
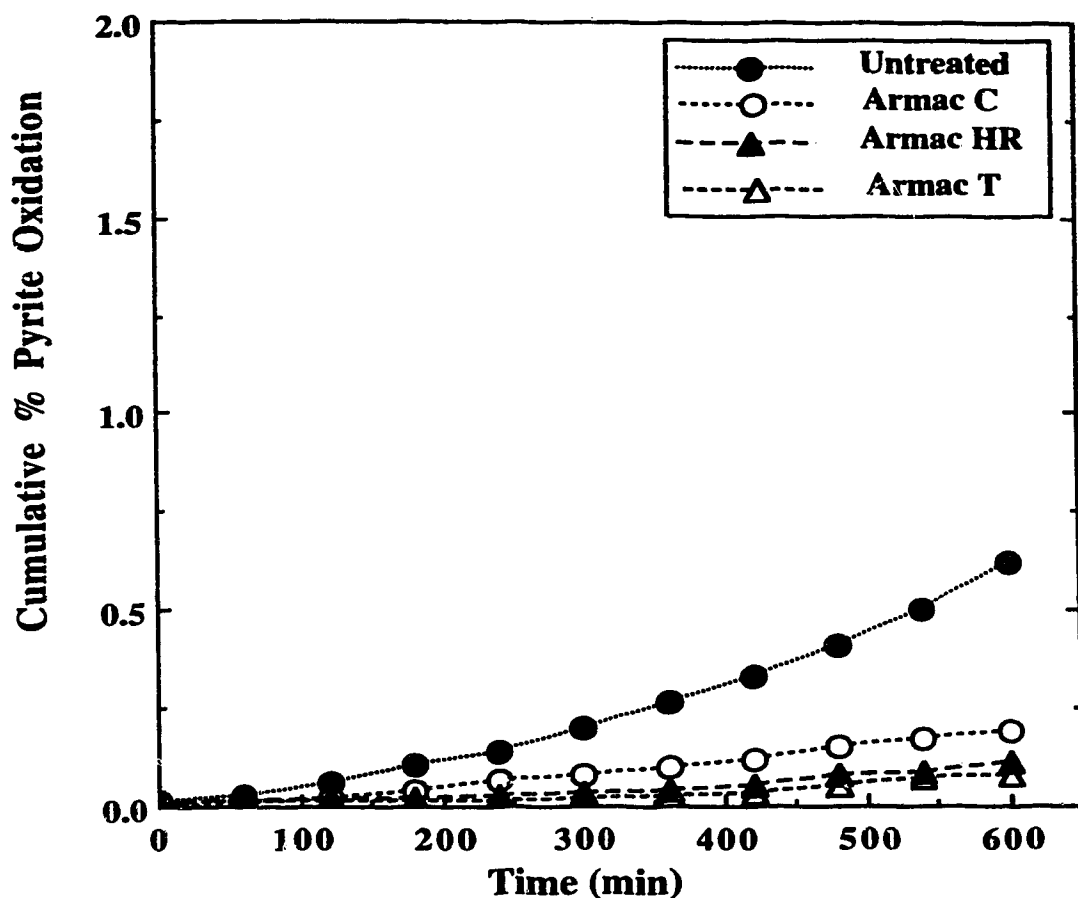


Figure 3-7. Oxidation of untreated pyrite tested at 100 psi, 200 psi, 500 psi and 1000 psi of pure oxygen, and 60°C.

period and 0.5% oxidation was obtained after 600 min of reaction time. A similar trend was observed for 200psi resulting in 0.6% oxidation after 600 min. This trend changes for 500 and 1000 psi, where a steady increase in oxidation is obtained until after 360 min, and a higher oxidation rate is observed thereafter. Based on these results, 60°C and 200 psi were chosen as appropriate conditions for evaluating the stability of the treated pyrite samples in the autoclave, although 200 psi oxygen pressure is high when compared to field conditions. The Armac T-treated samples were also tested at higher pressures.

Figure 3-8 illustrates the oxidation test results for the untreated pyrite and, Armac T-, Armac C- and Armac HR-treated pyrite at 200 psi, 60°C and 600-min reaction time. The rate of oxidation of the untreated pyrite at these conditions was observed to increase rapidly with time. At the end of the 600-min reaction time, 0.7% oxidation was obtained. The rate of oxidation of the Armac T-treated pyrite was observed to be significantly lower than that of the untreated pyrite. The oxidation of the Armac T-treated pyrite increased slowly to about 0.1% after about 400 min of reaction time and remained relatively constant to the end of the 600-min reaction time. A similar trend was observed for the Armac HR-treated pyrite, although the percent oxidation for the Armac-HR treated pyrite was slightly higher than that of the Armac T-treated pyrite. The percent oxidation of the Armac C-treated pyrite was observed to be higher than that of the Armac T- and Armac HR-treated pyrite. The percent oxidation of the Armac C-treated pyrite was also observed to plateau at less than 0.2% after 500 min of oxidation time. After 600 min of reaction time less than 0.1% oxidation was observed for Armac T-treated sample, which translates to about 85% reduction in pyrite oxidation over the untreated pyrite. Both Armac C and Armac HR treatment also suppressed pyrite oxidation, resulting in less than 0.1% and 0.2% oxidation respectively over 600 min. This translates to about 80% and 70% reduction in pyrite oxidation over the untreated pyrite for Armac HR- and Armac C-treated pyrite samples.



**Figure 3-8. Oxidation of untreated and fatty acid amine-treated pyrite tested at 200 psi of pure oxygen and 60°C.**

The stability of the fatty acid amine-treated pyrite under such severe oxidation conditions suggests that the surfactant molecules are not just physically adsorbed onto the surface of the pyrite particles, but are chemisorbed onto the surface. The stability of the treated pyrite is also enhanced by the sulfur-rich layer formed by the preferential leaching of Fe beneath the hydrophobic chemisorbed layer. The attachment of the fatty acid amine onto the sulfur-rich pyrite surface occurs through the amino (N-H) functional group with the long chain hydrocarbon group extending outwards (illustrated in Figure 3-9) as proposed by other investigators (McCaffery and Mungan, 1970; Xu and Somasundaran, 1992).

Suppression of pyrite oxidation by using a cationic surfactant, oleyl imidazoline, an amine, has also been reported by Chander and Zhou (1992) who studied various organic additives, but the mechanism of suppression was not known. McCaffery and Mungan (1970) have also reported irreversibility of the original high degree of hydrophilicity of quartz crystal surfaces after they were treated with octadecylamine.

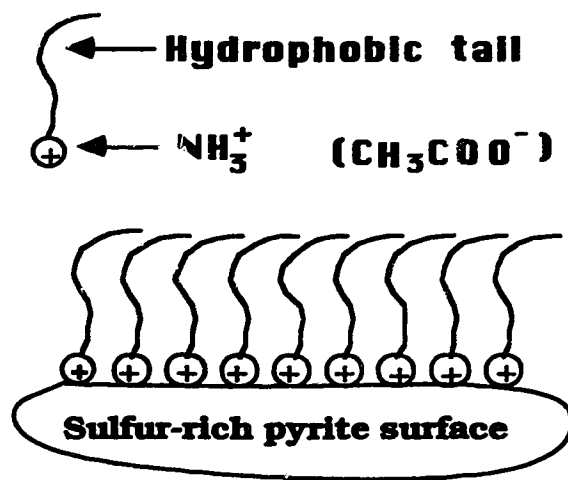


**Figure 3-9. Schematic representation of the chemisorption of fatty acid amine onto pyrite surface.**

Figure 3-10 shows the effect of pressure on the stability of Armac T-treated pyrite samples at 60°C. The rate of pyrite oxidation is observed to increase with pressure. Above 200 psi, the percent oxidation was observed to increase throughout the testing period, whereas below 200 psi the oxidation rate was observed to plateau. The hydrophobic surface coatings fail to protect the pyrite from further oxidation at pressures above 200 psi. Although the percent oxidation of the Armac T-treated pyrite samples increased with pressure, the level of oxidation was still significantly lower than that of the untreated pyrite samples tested under the same conditions (Figure 3-7).

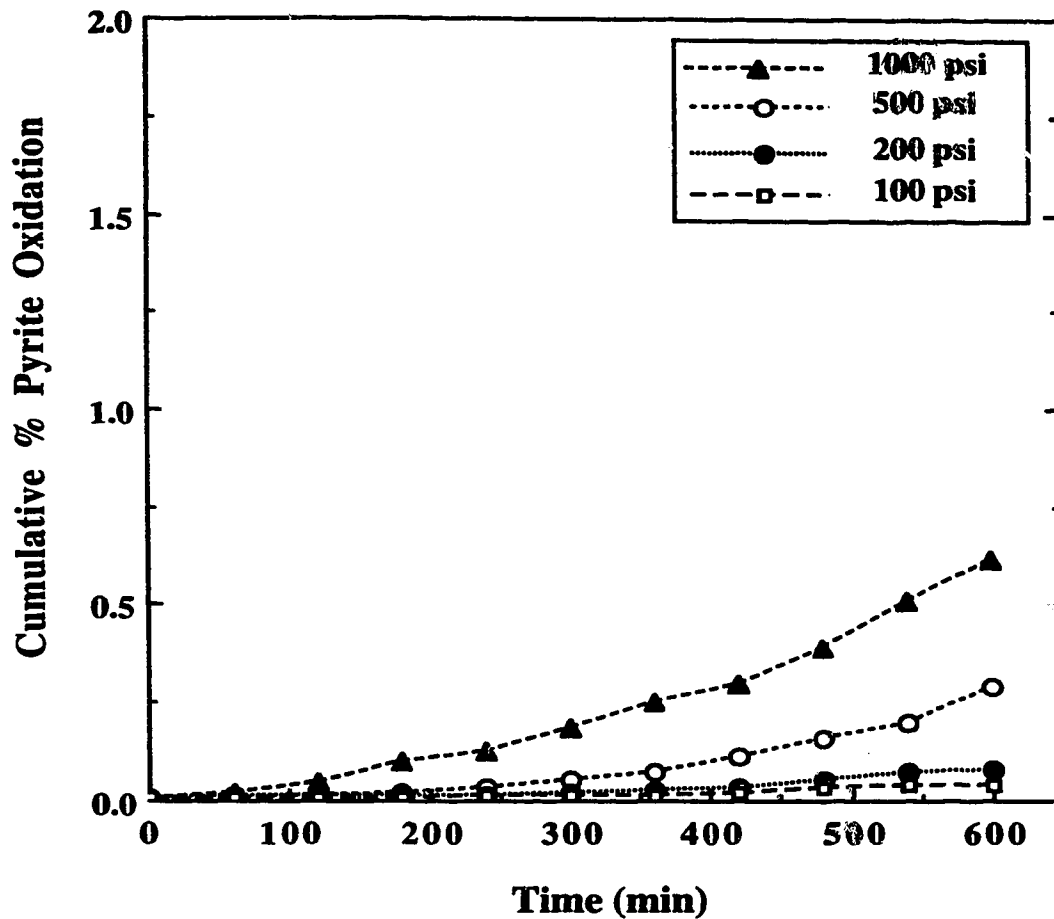


**Figure 3-10. Oxidation of Armac T-treated pyrite tested at 100 psi, 200 psi, 500 psi, and 1000 psi of pure oxygen, and 60°C.**

Figure 3-11 illustrates the cumulative percent oxidation of untreated pyrite samples, and Armac T-, Armac C-, and Armac HR-treated pyrite samples tested in the accelerated oxidation columns over 81 days. The percent oxidation of the untreated pyrite was observed to increase rapidly throughout the testing period. After 81 days 0.45% oxidation was obtained for the untreated pyrite. The oxidation of the Armac T- and Armac C-treated pyrite samples were observed to increase slightly for the first 60 days, where less than 0.1% oxidation was observed, and remained relatively constant for the rest of the testing

period. The percent oxidation of the Armac-HR treated pyrite was observed to be higher than that for Armac C. This trend is a reversal of that observed in the autoclave, where the oxidation of the Armac C-treated pyrite samples were observed to be slightly higher than that of Armac HR-treated pyrite samples (Figure 3-8). The same general trend of

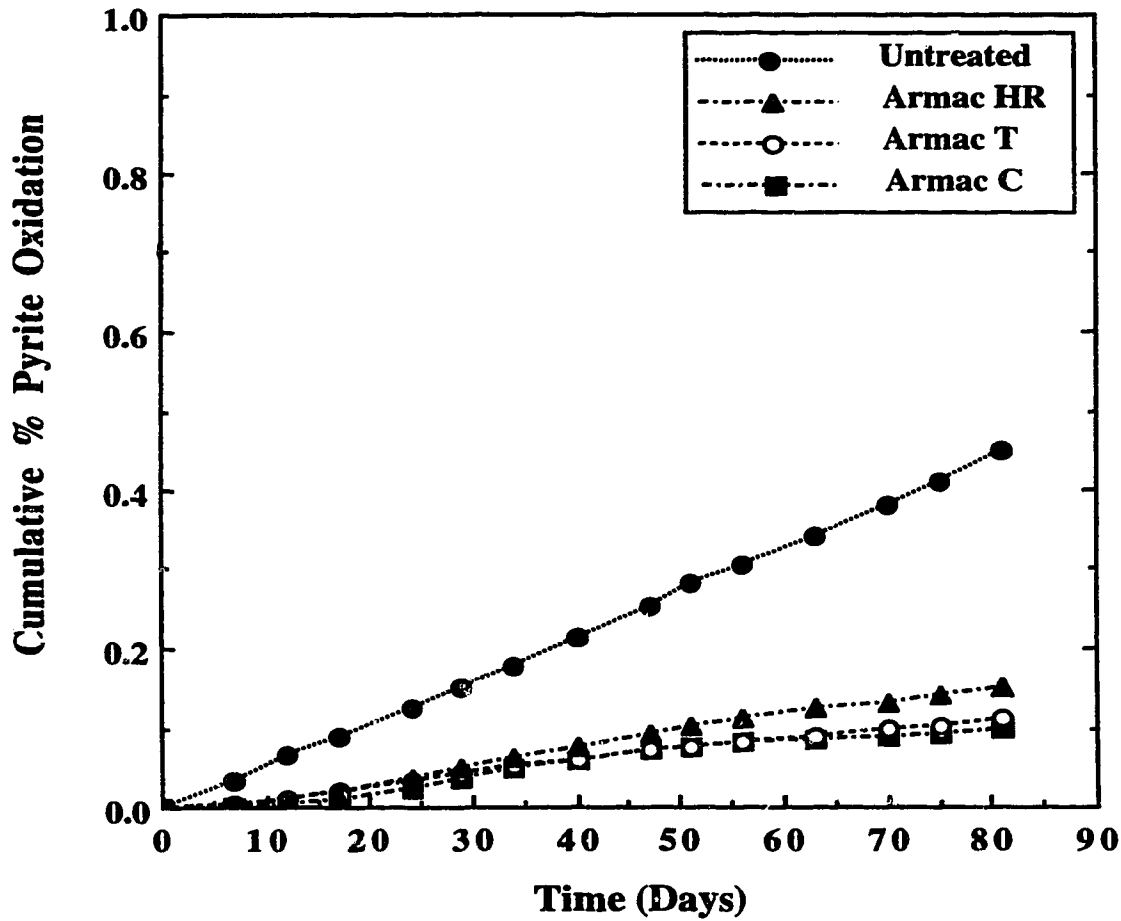


**Figure 3-11. Accelerated column oxidation test of untreated and fatty acid amine-treated pyrite.**

suppression of pyrite oxidation by the fatty acid amine treatment was observed as in the autoclave test. Armac T and Armac C treatment of pyrite resulted in about 75% reduction in oxidation over the untreated pyrite samples, whereas Armac HR treatment resulted in

about 65% reduction at the end of the testing period. This percent reduction in oxidation will most likely increase with time since the oxidation rate of the treated pyrite particles appear to plateau, while the oxidation rate of the untreated pyrite increases.

The accelerated oxidation column test required very long periods for testing the stability of the samples, although the conditions of testing are closer to field conditions than those of the autoclave test. Autoclave oxidation at 60°C and 200 psi increases the rate of oxidation of the untreated pyrite by about 260 times. While the rate of oxidation is about  $2.31 \times 10^{-4}$  % oxidation/h for the untreated pyrite sample tested in the accelerated column oxidation test, it is 0.06 % oxidation/h for the autoclave oxidation at 60°C and 200 psi. The 0.45% oxidation observed after 81 days in the accelerated column test for the untreated pyrite sample, corresponds to about 480 min of oxidation time in the autoclave at 60°C and 200 psi.

### **3.5 SUMMARY OF CHAPTER**

The results of this study have shown that pyrite oxidation and ARD formation can be reduced significantly by treating pyrite with a fatty acid amine. The fatty acid amine treatment has been shown to produce a hydrophobic surface which reduces contact between pyrite and aqueous oxidizing agents, thus preventing or reducing the initiation step for pyrite oxidation and ARD formation. The fatty acid amine, Armac T, was shown to be the most effective in suppressing pyrite oxidation and ARD formation. This fatty acid amine resulted in over 85% reduction in pyrite oxidation over the untreated pyrite when tested at 60°C and 200 psi of pure oxygen for 600 min, and 75% reduction over the untreated pyrite when tested in the accelerated oxidation column for 81 days. The oxidation of the Armac-T treated pyrite remained relatively constant after 400 min in the autoclave test at 60°C and 200 psi of oxygen pressure, and 50 days in the accelerated oxidation column, while the oxidation for the untreated samples increased continuously with time for both test methods.



The use of an autoclave for testing the stability of fatty acid amine treated pyrite particles has also been shown to be a faster and reliable alternative to the conventional column oxidation test. The trend of the results obtained from the autoclave test are comparable with those obtained from the accelerated oxidation column test. Hence autoclave tests can be used as a faster means for screening the effectiveness of reagents used for pyrite oxidation suppression.

### 3.6 REFERENCES

- Ahlberg, E., K. S. E. Forsberg, and X. Wang. 1990. The surface oxidation of pyrite in alkaline solution, *J. Appl. Electrochem.* 20: 1033-1039.
- American Oil Chemist Society. 1979. Quantitative determination of amines. Test Method TF 16-64 and TF 26-64. Am. Chem. Soc., Champaign, IL.
- Biegler, T. 1976. Oxygen reduction on sulphide minerals, Part II. Relation between activity and semiconducting properties of pyrite electrodes. *J. Electroanal. Chem.* 70: 265-275.
- Biegler, T., and D. A. Swift. 1979. Anodic behaviour of pyrite in acid solutions. *Electrochim. Acta.* 24: 415-420.
- Bistline, R. G. Jr., and W. M. Linfield. 1984. Modification by surfactants of soil water absorption. *Structure/Performance Relationships in Surfactants*, M. J. Rosen (ed.). ACS Series 253. pp. 209-223.
- Bistline, R. G. Jr., J. W. Hampson, and W. M. Linfield. 1983. Synthesis and properties of fatty imidazolines and their N-(2-aminoethyl) derivatives. *J. Am. Oil Chemist Soc.* 60: 823-828.
- Buckley, A. N., and R. Woods. 1987. The surface oxidation of pyrite. *Appl. Surf. Sci.* 27: 437-452.
- Chander, S., and A. Briceno. 1987. Kinetics of pyrite oxidation. *Miner. Metallurg. Process.* 4: 171-176.

- Chander, S., and R. Zhou. 1992. Effect of organic additives on acid generation from pyrite waste. Proceedings of the symposium on emerging process technologies for a cleaner environment, S. Chander, P. E. Richardson, and H. El-Shall (eds.). SME, Phoenix, Arizona. pp. 131-139.
- Crundwell, F. K. 1988. The influence of the electronic structure of solids on the anodic dissolution and leaching of semiconducting sulfide minerals. *Hydrometallurgy*. 21: 155-190.
- Garrels, R. M., and M. E. Thompson. 1960. Oxidation of pyrite by iron sulfate solution. *Am. J. Sci.* 258A: 57-67.
- Hamilton, I. C., and R. Woods. 1981. An investigation of surface oxidation of pyrite and pyrrhotite by linear potential sweep voltametry. *J. Electroanal. Chem.* 118: 327-343.
- Healey, P. M., and A. M. Robertson. 1989. A case history of an acid generation abatement program for an abandoned copper mine. Geotechnical aspects of tailings disposal and acid mine drainage. The Vancouver Geotechnical Society, Vancouver, B. C.
- Hiskey, J. B., and W. J. Schlitt. 1982. Aqueous oxidation of pyrite, interfacing technologies in solution mining. Proceedings of the 2nd SME-SPE International solution mining symposium, W. J. Schlitt and J. B. Hiskey (eds.). AIME. pp. 55-74.
- Law, J. P. Jr., M. E. Bloodworth, and J. R. Runkles. 1966. Reactions of surfactants with montmorillonitic soils. *Soil Sci. Soc. Amer. Proc.* 30: 327-332.
- Lowson, R. T. 1982. Aqueous oxidation of pyrite by molecular oxygen. *Chem. Rev.* 82: 461-497.
- Luther, G. W. III. 1987. Pyrite oxidation and reduction: Molecular orbital theory considerations. *Geochim. Cosmochim. Acta.* 51: 3193-3199.
- McCaffery, F. G., and N. Mungan. 1970. Contact angle and interfacial tension studies of some hydrocarbon-water-solid systems. *J. Can. Petrol. Technol.* 9:185-196.
- Mishra, K. K., and K. Osseo-Asare. 1988. Aspects of the electrochemistry of semiconductor pyrite ( $\text{FeS}_2$ ). *J. Electrochem. Soc.* 135: 2502-2509.

- Moses, O. C., and J. S. Herman. 1991. Pyrite oxidation at circumneutral pH. *Geochim. Cosmochim. Acta.* 55: 471-482.
- Murthy, K. S. N., and K. A. Natarajan. 1992. The role of surface attachment of *Thiobacillus ferrooxidans* on the biooxidation of pyrite. *Miner. Metallurg. Process.* 9: 20-24.
- Nicholson, V. R., R. W. Gillham, J. A. Cherry, and E. J. Reardon. 1989. Reduction of acid generation in mine tailings through the use of moisture-retaining cover layer as oxygen barriers. *Can. Geotech.* 26: 1-8.
- Omura, T, T. Umita, J. Aizawa, and M. Onuma. 1991. Biological oxidation of ferrous iron in high acid mine drainage by fluidized bed reactor. *Wat. Sci. Technol.* 23: 1447-1456.
- Osseo-Asare, K. 1992. Semiconductor electrochemistry and hydrometallurgical dissolution processes. *Hydrometallurgy.* 29: 61-90.
- Osseo-Asare, K. 1993. Pyrite in aqueous systems: Semiconductor properties, oxidative dissolution, and environmental control. Proceedings of the 1st international conference on processing materials for properties, H. Henein and T. Oki (eds.). TMS, Honolulu, Hawaii. pp. 83-89.
- Palencia, I., R. Y. Wan, and J. D. Miller. 1991. The electrochemical behavior of a semiconducting natural pyrite in the presence of bacteria. *Metallurg. Trans. B.* 22: 765-774.
- Rosen, M. J. 1978. Surfactants and interfacial phenomena. Wiley-Interscience Publication, New York, NY. pp. 174-199.
- Shaw, D. J. 1969. Electrophoresis. Academic Press Inc., New York, NY. pp. 1-42.
- Shaw, D. J. 1980. Introduction to colloid and surface chemistry. Butterworth Inc., Boston, U. S. 3rd edition. pp. 148-182.
- Springer, G. 1970. Observations on the electrochemical reactivity of semiconducting minerals. *Metallurg. Trans. C.* 79: 11-14.

Vaughan, D. J., and J. R. Craig. 1978. Mineral chemistry of metal sulfides. Cambridge University Press, New York, NY. pp. 36-38.

Xu, Q., and P. Somasundaran. 1992. Adsorption of nonionic/anionic surfactant mixtures and nonionic surfactants and its effect on mineral dispersion and wettability. *Miner. Metallurg. Process.* 9: 29-33.

## CHAPTER 4

### RELATIONSHIP BETWEEN GROWTH PARAMETERS AND FERRIC CONCENTRATION EFFECT ON VIABILITY OF *THIOBACILLUS FERROOXIDANS*

#### 4.1 INTRODUCTION

Increasing demand for metals and energy, and environmental concerns of acid rock drainage (ARD) have had a tremendous impact on research activities involving *Thiobacillus ferrooxidans* and other closely related genera throughout the world. *T. ferrooxidans* is a Gram-negative, acidophilic, chemolithotrophic bacterium which is capable of deriving all its energy from the oxidation of ferrous iron and sulfides, with carbon dioxide and inorganic nitrogen as carbon and nitrogen sources (Silverman, 1967; Baker and Wilshire, 1970; Tuovinen et al., 1978). *T. ferrooxidans* is also capable of utilizing thiosulfate as an alternate energy source (Temple and Colmer, 1951; Silverman and Ehrlich, 1964).

Optimal temperatures for growth vary among different strains and have been reported as 20 to 25°C (Leathen et al., 1956), 28°C (Silverman and Lundgren, 1959a) and 32°C (Kinsell, 1960). Marchlewitz and Schwartz (1961) reported temperatures between 25°C and 45°C. Good growth has been reported to occur at pH ranging from 2.5 to 4.5 (Leathen et al., 1956; Silverman and Lundgren, 1959a; Kinell, 1960; Razzell and Trussell, 1963).

The bacteria are used in the desulfurization of pulverized coal in an aqueous suspension (Mannivannan et al., 1994). In order to maintain satisfactory low SO<sub>2</sub> levels in the atmosphere, *T. ferrooxidans* is used to solubilize pyritic mineral in coal prior to combustion (Dugan and Apel, 1978; Mannivannan et al., 1994). Microbial flotation also utilizes *T. ferrooxidans* to separate coal and pyritic sulfur via the modification of the

surface properties of the minerals (Atkins et al., 1987; Attia, 1990; Ohmura and Saiki, 1994).

Biooxidation has recently progressed to a stage where it has now become a viable process option (Marchant, 1986). In biooxidation processes, *T. ferrooxidans* is employed widely in the pretreatment of refractory ores and concentrates, and in bioleaching of metals from ores and concentrates in heaps, dumps or bioreactors (McCready et al., 1986; Bailey and Handford, 1993; Lawrence, 1994). On the other hand, *T. ferrooxidans* is also partly responsible for ARD formation (Colmer and Hinkle, 1947; Colmer et al., 1950; Temple and Colmer, 1951; Leathen et al., 1953; Temple and Delchamps, 1953; Leathen et al., 1956; Baker and Wilshire, 1970; Singer and Stumm, 1970).

One major obstacle to both fundamental and applied research using these bacteria for bioleaching of metals, pretreatment of refractory ores and concentrates, oxidation kinetics and ARD prevention and control studies, is the correlation between growth parameters. Indirect methods are generally used to determine the activity of the cells and the stage of growth. The main indirect parameters used for bacterial leaching, pretreatment, oxidation kinetics and ARD studies utilizing *T. ferrooxidans* include turbidity (Schnaitman et al., 1969; Atkins et al., 1987), protein concentration (Chang and Myerson, 1982; Bagdigian and Myerson, 1986),  $Fe^{2+}$  and  $Fe^{3+}$  concentration (Kinsell, 1960; Suzuki et al., 1987), direct bacterial counts (Lacey and Lawson, 1970; McCready et al., 1986; Konishi et al., 1994), most probable number (MPN) (Francis et al., 1989; Murr et al., 1977; Dugan, 1987), plate counts (Mishra et al., 1983; Blake et al., 1994) and oxygen concentration (Landesman et al., 1966; Lizama and Suzuki, 1989). Although researchers have used one or more of these parameters to indirectly determine growth stage and cell numbers for oxidation kinetics (Lacey and Lawson, 1970; Suzuki et al., 1987), bioleaching over short and long experimental periods (Torma et al., 1976; Wakao et al., 1983; Rodriguez and Tributsch, 1988), and adsorption studies (Bagdigian and Myerson, 1986;

Ohmura et al., 1993), the correlation between these parameters at various stages of growth have not been studied.

The objective of this study was to investigate the relationship between some of the commonly used parameters in bioleaching, oxidation kinetics and ARD studies during the growth of three strains of *T. ferrooxidans*, and also to study the effect of  $\text{Fe}^{3+}$  on the growth activity of the cells. The study should provide an insight into which parameter is best suited for a particular situation or study.

## 4.2 EXPERIMENTAL METHODS

### 4.2.1 Culture and Medium

Three strains of *T. ferrooxidans*, ATCC 13598, ATCC 13661 and ATCC 14119 were used in this study. All three strains were obtained from the American Type Culture Collection.

The medium used for the growth of the microorganisms consisted of two solutions A and B, prepared separately, autoclaved at  $121^{\circ}\text{C}$  and 30 psi for 20 min and mixed aseptically after cooling. Solution A contained 0.4 g of  $(\text{NH}_4)_2\text{SO}_4$ , 0.2 g of  $\text{K}_2\text{HPO}_4$ , and 0.08 g of  $\text{MgSO}_4 \cdot 7\text{H}_2\text{O}$  per 400 mL of double distilled water. Solution B contained 10 g of  $\text{FeSO}_4 \cdot 7\text{H}_2\text{O}$  per 100 mL of 0.18 M  $\text{H}_2\text{SO}_4$  (ATCC Catalogue, 1982). Each strain was grown separately in 500-mL Erlenmeyer flasks containing 75 mL of growth medium to ensure sufficient diffusion of  $\text{O}_2$  to the bottom of the flask. To each of the flasks, 7.5 mL of cell suspension was added (10% inoculum). The inoculated flasks were shaken on an orbital shaker table at a speed of 200 rpm and a temperature of  $27^{\circ}\text{C}$  in the dark. The stock culture of all strains were maintained by serially transferring into new medium at 5- to 6- day intervals.

#### **4.2.2 Activity and Growth of Strains**

The activity and growth of each of the strains were studied by monitoring the number of viable cells, turbidity, protein concentration, pH, ferrous and total iron concentrations. These parameters were monitored for 9 days after inoculation.

Four-day-old cultures were used for the activity and growth studies. Each strain was inoculated (10%) into sterile growth medium and allowed to grow for 4 days. On the fourth day, a new set of sterile medium was inoculated with each strain in triplicate and samples taken from each flask for days 0 through 6, and day 9. Triplicate control flasks were also incubated with the inoculated flasks.

#### **4.2.3 Agar-growth Medium**

The agar-growth medium consisted of 10 g/L of unwashed or washed agar, and the growth medium described in Section 4.2.1. The washed agar was obtained by washing 10 g of the agar in 1 L of double distilled water and filtering the suspension. The agar and growth medium mixture was then autoclaved at 121°C and 30 psi for 20 min, cooled and poured into sterile petri dishes and allowed to solidify. Small amounts (0.1 mL) of the culture were then spread on the plates with sterilized, bent glass rod. The spread plates were incubated at 27°C for 10 days in the dark.

#### **4.2.4 Most Probable Number Method**

The dilution count method was used to estimate the number of bacteria in the population that are capable of multiplying in a liquid medium. Nine milliliter volumes of sterile growth medium were dispensed into sterile (15 mm diameter x 150 mm) test tubes and 1 mL of the sample taken for each day from a flask was added. After mixing by vortex, 1 mL was transferred to another test tube containing 9 mL of medium using a new sterile pipette; the transfer was continued up to a dilution of  $10^{-9}$ . One milliliter portions of



undiluted and each dilution ( $10^{-1}$  to  $10^{-9}$ ) were then inoculated into triplicate tubes containing 3 mL of sterile medium and incubated under stationary conditions at 27°C for 10 days in the dark. Two sets of sterile controls were also set up. One set was inoculated with samples from the control sterile flasks, while the other was not inoculated. On the tenth day (initial test had shown that the maximum number of tubes with color change occurred after 8 days), both the inoculated and sterile tubes of medium were examined for color changes. Tubes with color changes (rusty color) were considered as positive and assumed to contain at least one iron-oxidizing bacterium/mL of inoculant. MPN table for triplicate culture inoculated with 1-mL aliquots was used to determine the number of cells present in each sample (American Public Health, 1985).

#### **4.2.5 Turbidity and pH**

Turbidity of the samples was determined at 600 nm ( $OD_{600}$ ) after standardization with samples from the sterile control flasks. The turbidity was monitored using a Unicam 8700 series UV/Vis. spectrometer. The pH of the samples were determined by a Cole-Parmer Chemcadet pH/mV meter equipped with a temperature compensation probe.

#### **4.2.6 Total and Ferrous Iron**

Total Fe and  $Fe^{2+}$  in the samples were determined by DR/2000 Spectrophotometer and the total Fe concentration was verified with Atomic Absorption Spectrophotometry (AAS). The procedure used for Fe and  $Fe^{2+}$  analysis is reported in Section 2.3.5.

#### **4.2.7 Protein Analysis**

Protein content of the samples was determined by the method of Lowry et al. (1951). The cells in the samples were lysed prior to analyzing the protein released into solution. Sonic vibration was initially used to rupture the cell walls before protein analysis. ~~Zn~~ <sup>Final</sup> protein analysis of the sonicated samples indicated incomplete lysing of older cells,

since protein content of the samples decreased with time. Sodium hydroxide was therefore used to lyse the cells before protein analysis. The NaOH added also precipitated any residual iron ions in pellets after washing, and therefore reduced the interference of iron during protein analysis. However, NaOH was found to reduce the absorbance when present. The protein standards were therefore prepared by using sterile growth medium to which the same amount of NaOH used to lyse the cells in samples is added. Any iron precipitates or cell material formed after adding NaOH to the pellets were removed by spinning at 13,000 x g for 5 min and the clear solution analyzed for protein. Bovine serum albumin was used to prepare the standards. For protein analysis, 0.5 mL of 1 M NaOH was added to the pellet from 1 mL of the sample and allowed to stand at room temperature for 30 min. The solution was then centrifuged at 13,000 x g for 5 min. To 0.5 mL of the clear solution, 0.5 mL of a solution (containing 4% Na<sub>2</sub>CO<sub>3</sub> in 0.2 N NaOH to which 1 mL of 1.0% CuSO<sub>4</sub>·5H<sub>2</sub>O in 2% sodium tartrate is added) was added, mixed and allowed to stand for 10 min. Folin reagent (0.1 mL) was then added, mixed immediately and allowed to react for 30 min, and the absorbance of the mixture was read at 750 nm (Lowry et al., 1951).

#### **4.2.8 Effect of Initial Ferric Iron**

The effect of Fe<sup>3+</sup> concentration on the number of viable cells was investigated with washed cells. The cultures were incubated for 3 days and harvested. Harvesting of the cells was done by filtering the culture through Whatman no.1 filter paper to remove any precipitate that may be present. The filtrate obtained was then centrifuged at 10,000 x g for 10 min (Du Pout Sorvall RC-5B refrigerated superspeed centrifuge), and the resulting cell pellet washed by resuspending and centrifuging twice with 10<sup>-2</sup> M H<sub>2</sub>SO<sub>4</sub> solution. The cells were finally resuspended in a small volume (4 to 5 mL) of 10<sup>-2</sup> M H<sub>2</sub>SO<sub>4</sub> solution and used for the Fe<sup>3+</sup> concentration experiments. The cell harvesting procedures were all done aseptically.

In the initial ferric iron experiments, different concentrations of  $\text{Fe}^{3+}$  were added to triplicate flasks containing growth medium. The same volume of the resuspended harvested cells was then added to the flasks and incubated at  $27^\circ\text{C}$  in the dark. During incubation, the viable numbers in the cultures were determined by the MPN method.

### 4.3 RESULTS AND DISCUSSION

#### 4.3.1 Change in MPN and $\text{Fe}^{2+}$ Concentration in Batch Cultures.

The MPN method was used to monitor the number of viable cells because growth of the cells on agar plates had failed. Both unwashed and washed agar-growth media plates failed to produce colonies after incubation for 10 days at  $27^\circ\text{C}$ . Failure to obtain growth of *T. ferrooxidans* on solid media has also been reported by other investigators (Silverman and Lundgren, 1959b; Lacey and Lawson, 1970; Tuovinen and Kelly, 1973). Mishra and Roy (1979) had reported growth of some strain of *T. ferrooxidans* on purified agar. Petroff-Hausser counting chamber was used to count bacteria in samples under an optical microscope at 1000x magnification. The microscope counting was considered unsuitable because of counting difficulties due to movement of the cells and the different focal positions for cells at the surface and bottom of the liquid in the counting chamber.

During growth of the three strains of *T. ferrooxidans* in the  $\text{Fe}^{2+}$ -containing medium, MPN and  $\text{Fe}^{2+}$  concentrations were monitored. Control flasks were monitored to determine the amount of autooxidation of  $\text{Fe}^{2+}$  during the experiment. Triplicate culture were used for each strain and the averages plotted. Figure 4-1 presents a plot of the change in the number of viable cells (MPN/mL) and  $\text{Fe}^{2+}$  concentration for both the control (no cells) and inoculated flasks during incubation of strain 13598. The MPN of the control flasks were also monitored during the experiment to ensure that they were not contaminated. The  $\text{Fe}^{2+}$  concentration in the control flasks did not change significantly during the incubation period, while the  $\text{Fe}^{2+}$  concentration of the inoculated flasks was

observed to decrease rapidly after an initial 1-day lag period. This indicates that only microbial oxidation of the  $\text{Fe}^{2+}$  had occurred. Lag periods for *T. ferrooxidans* varies considerably in the literature. Suzuki et al. (1987) report lag time between 2 to 225 h depending on the strain and medium used. The highest rate of decrease in  $\text{Fe}^{2+}$  concentration (2.8 to 0.8 g/L) was observed between days 1 and 2, followed by a slow rate of decrease between days 2 and 5, after which the  $\text{Fe}^{2+}$  concentration remained relatively constant.

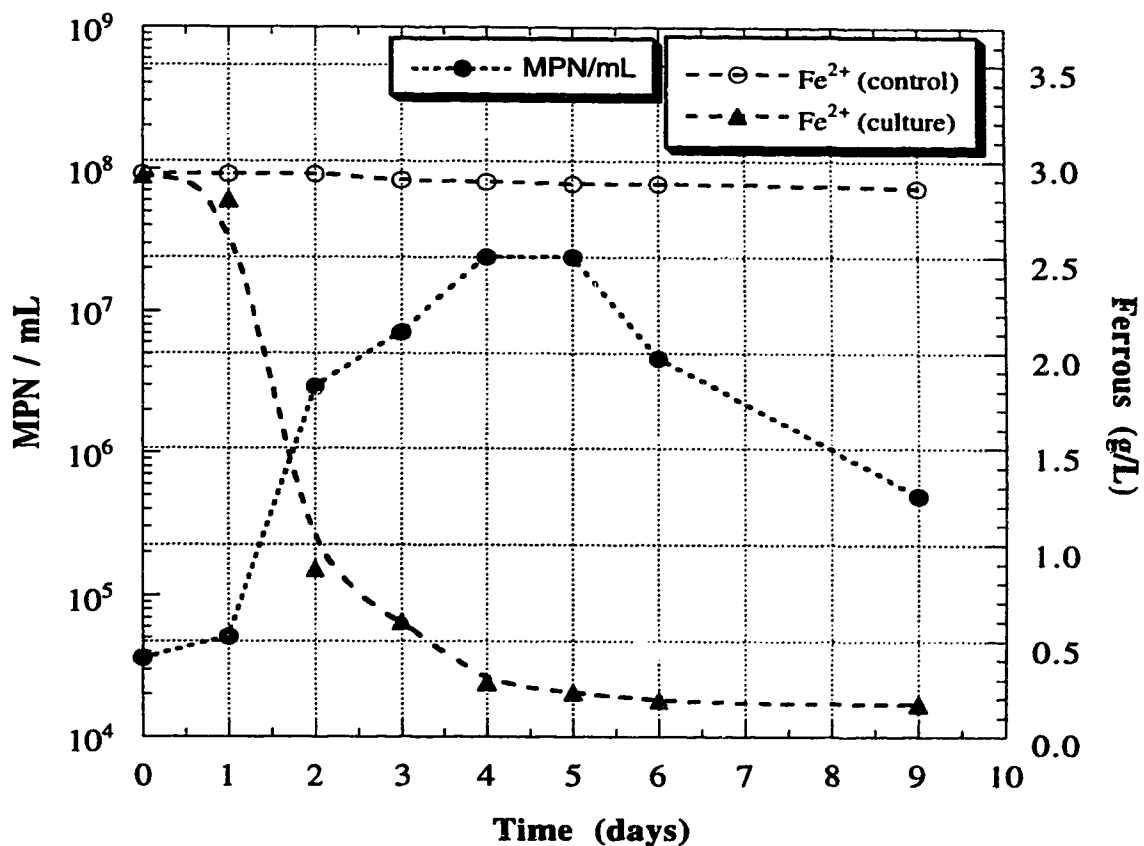


**Figure 4-1. Change in number of viable cells and ferrous concentration during growth of strain 13598.**

The number of viable cells (MPN) showed a lag period of 1 day, during which there was a little change in  $\text{Fe}^{2+}$  concentration. The highest rate of increase in MPN ( $2 \times 10^4$

to  $3 \times 10^6$ /mL) was observed between days 1 and 2 which also coincides with the highest rate of decrease in  $\text{Fe}^{2+}$  concentration. The MPN reached its maximum of  $4 \times 10^7$ /mL after 4 days when the  $\text{Fe}^{2+}$  concentration was close to its lowest concentration. The MPN, however, starts to decrease after day 5 while the  $\text{Fe}^{2+}$  concentration remained relatively constant. While monitoring MPN showed that strain 13598 went through a lag phase between days 0 and 1, a log growth phase between days 1 and 4, a stationary growth phase between days 4 and 5, and a death phase between days 5 and 9, monitoring  $\text{Fe}^{2+}$  concentration only showed a lag, a log growth, and stationary phases. The decreasing viability of a batch culture of iron-oxidizing bacteria with age have been reported by Wakao et al. (1982). The MPN and  $\text{Fe}^{2+}$  concentration plots show that  $\text{Fe}^{2+}$  concentration may be used to give an indication of only the lag and log growth phases. Similar results were obtained for strains 13661 and 14119.

To illustrate the relationship between the MPN and the  $\text{Fe}^{3+}$  concentration (difference between the total Fe and  $\text{Fe}^{2+}$  concentration), the log MPN was plotted against  $\text{Fe}^{3+}$  concentration. Figure 4-2 shows the plot for strain 13598. The plot shows that a positive linear relationship exist between the MPN and  $\text{Fe}^{3+}$  concentration during the log growth phase, and a negative relationship exists after the stationary phase. This relationship implies that while  $\text{Fe}^{3+}$  concentration may be used to indirectly monitor cell numbers during the log growth phase, its use in the stationary and the death phases to monitor cell viability will provide inaccurate results. Because the  $\text{Fe}^{2+}$  and  $\text{Fe}^{3+}$  concentrations are easier to monitor than the MPN or plate counts, most researchers tend to monitor the  $\text{Fe}^{2+}$  and  $\text{Fe}^{3+}$  concentrations and relate it to the activity and number of cells without checking the growth phase of the culture, or whether a positive linear relationship exists between these parameters (McCready et al., 1986; Rodriguez and Tributsch, 1988). A positive correlation between  $\text{Fe}^{3+}$  concentration and  $\text{CO}_2$ -fixed has been reported by Beck (1960),  $\text{CO}_2$ -fixed could therefore be measured in lieu of  $\text{Fe}^{3+}$  concentration.

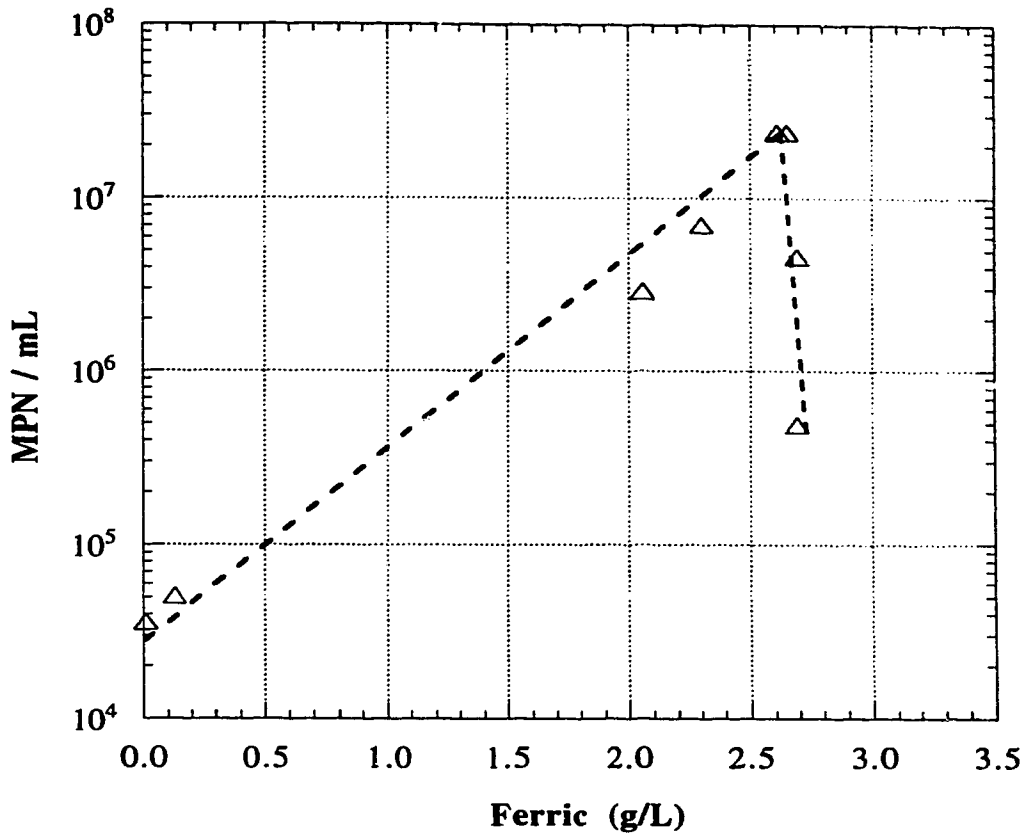


**Figure 4-2. Plot of change in viable cells versus ferric ion concentration, strain 13598.**

#### **4.3.2. Changes in MPN and Turbidity (OD<sub>600</sub>) in Batch Cultures.**

During the incubation of the cultures described above, samples were taken and their turbidity measured. Samples taken from the control flasks (without cells) were used as references for the inoculated samples. The turbidity of the samples was monitored for days 0 through 6 and day 9. Figure 4-3 shows the change in OD<sub>600</sub> and MPN/mL during the incubation of strain 13598. As expected, the turbidity of the culture was observed to increase throughout the incubation period. A sharp increase in turbidity was observed between days 1 and 2 which coincides with the log growth phase of the culture as determined by the MPN. The OD<sub>600</sub>, however, increased throughout the stationary and

death phases when the MPN was constant and decreasing respectively. The increased  $OD_{600}$  during the stationary and death phases is due to the inability of the turbidity measurement to differentiate between viable and dead cells (both the viable and dead cells contribute to the turbidity). The implications of this inverse relationship during the stationary and death phases is that, in experiments which require long durations,  $OD_{600}$  could not be use as a parameter to monitor the number of viable cells beyond the growth

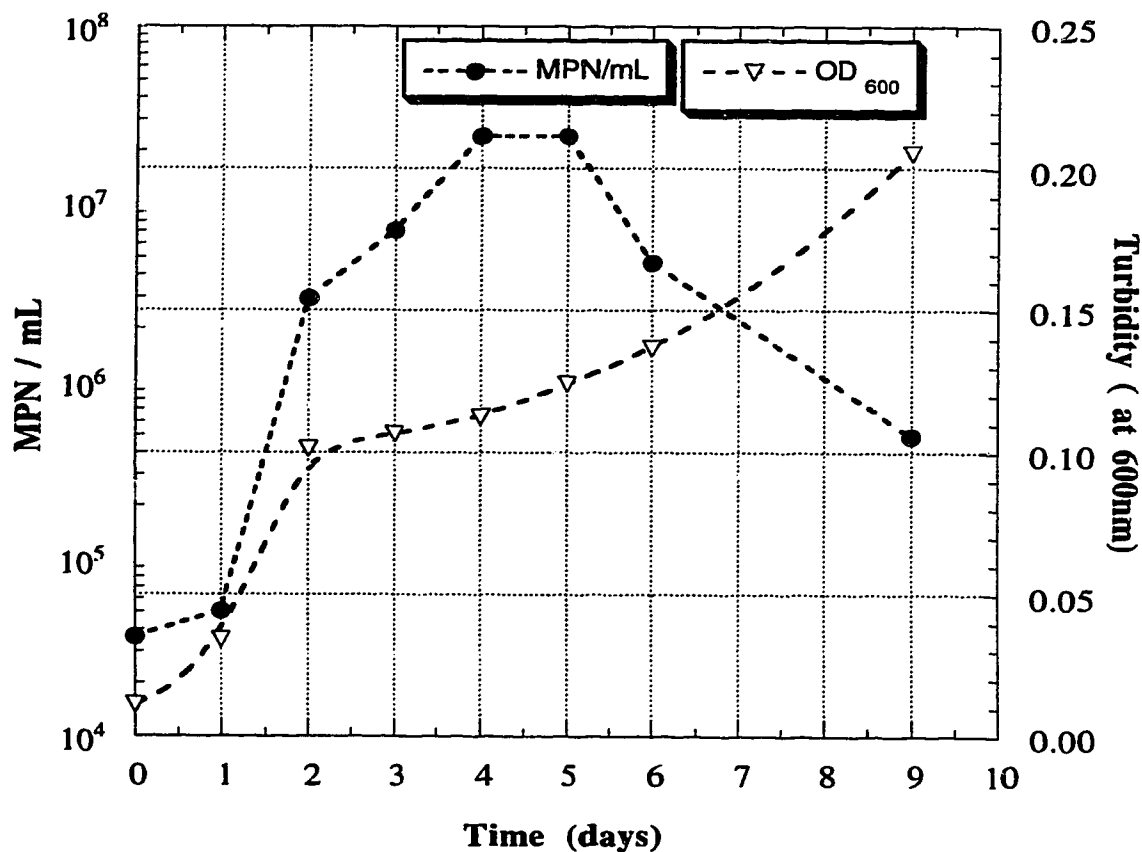


**Figure 4-3. Change in number of viable cells and turbidity during growth of strain 13598.**

phase. Because  $OD_{600}$  is an easily measurable parameter, it has been used in bioleaching, ARD, reaction kinetic and adsorption experiments employing *T. ferrooxidans* (Schnaitman

et al., 1969; Atkins et al., 1987; Pesic and Kim, 1993). The OD<sub>600</sub> measurement identifies only the log growth phase of the culture. Similar trends were observed for samples taken from flasks incubated with strains 13661 and 14119.

#### **4.3.3. Changes in MPN and Protein Concentration in Batch Cultures.**

Figure 4-4 shows the plot of the change in protein concentration and MPN during incubation of strain 13598. The protein concentration was observed to increase throughout the incubation period. The highest rate of increase occurred during the log growth phase. The protein concentration also increased during the stationary and the death phases when the number of viable cells was either constant or decreasing. The protein concentration identifies only the log growth phase and cannot also be used to determine the various growth phases of the culture. The protein concentration measures the total protein content, including those of the dead cells, hence the continuous increase even after the number of viable cells had dropped significantly. This trend was also observed for strains 13661 and 14119.

To illustrate the relationship between the protein concentration and MPN at the various phases of growth, log MPN was plotted against protein concentration for all three strains. The plot for strain 13598 is shown in Figures 4-5. The plot shows that there is a positive linear relationship between the MPN and protein concentration during the growth phase, this relationship is reversed at the stationary phase. Protein concentration is relatively easy to measure, and has been used to monitor *T. ferrooxidans* cell numbers (Myerson and Kline, 1983; Murthy and Natarajan, 1992; Nikolov et al., 1992). The results of this study indicate that the protein concentration correlates well with the viable cell numbers only during the growth phase.



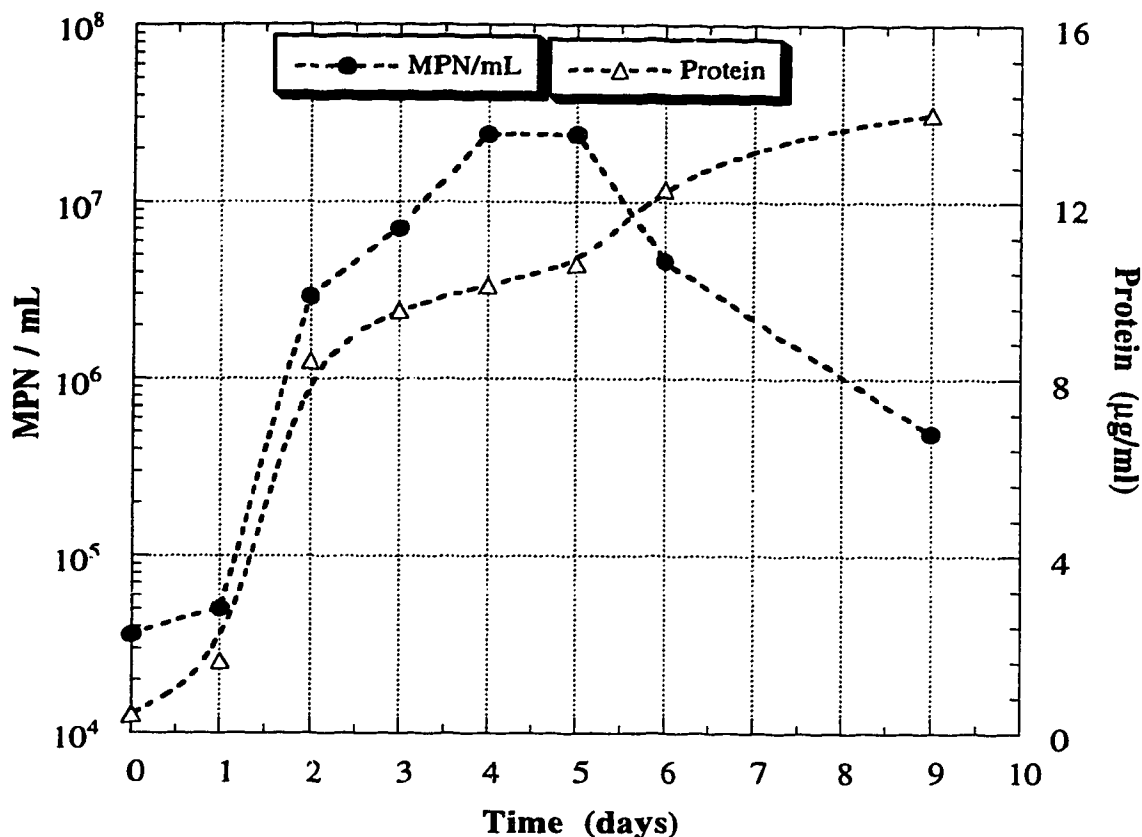


**Figure 4-4. Change in number of viable cells and protein concentration during growth of strain 13598.**

Similar plots for strains 13661 and 14119 showed the same trends. For ARD, bioleach, and ferrous-oxidizing activity experiments which take long experimental periods beyond the log growth phase, the protein concentration cannot be reliably used as a measure of the number of active cells in the culture. The protein concentration continues to increase long after the death phase had commenced, and the number of viable cells had declined significantly. This is because, as with turbidity measurement, the dead cells contribute to the measured protein concentration values. A positive linear correlation between  $\text{Fe}^{3+}$  and protein concentration during the log growth phase has also been reported (Suzuki et al., 1987).

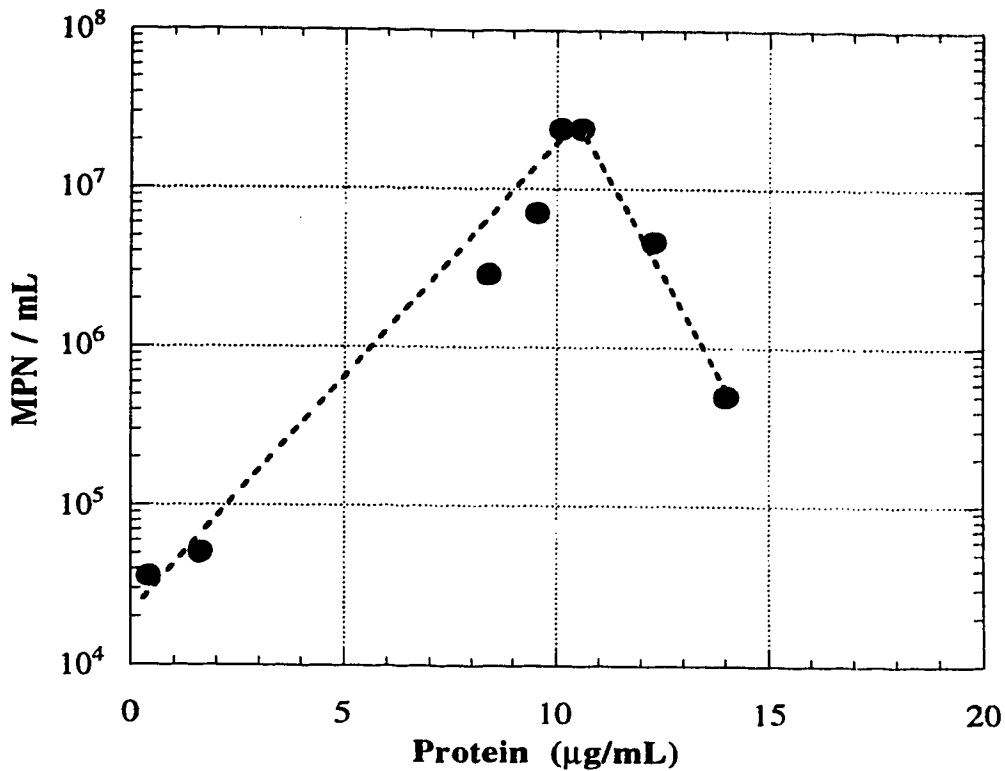


**Figure 4-5. Plot of change in viable cells versus protein concentration, strain 13598.**

#### **4.3.4. Changes in Turbidity and Protein Concentration in Batch Cultures**

The change in protein concentration and turbidity ( $OD_{600}$ ) during incubation of strain 13598 is illustrated in Figure 4-6. Both protein concentration and turbidity were observed to increase throughout the experiment and follow the same trend. The most rapid increase in turbidity (between days 1 and 2) coincides with the sharp increase in protein concentration. Similar trends were obtained for strains 13661 and 14119. The similarity between these two parameters is due to the fact that both measurements do not distinguish between viable and dead cells as noted earlier. The interpretation of this close relationship is that the turbidity of the culture (which is easier to determine) may be monitored in place of the protein concentration throughout the various phases. The only limitation to turbidity

measurement is the possible precipitation of iron oxides and hydroxides at later stages of the log growth phase of the culture (Suzuki et al., 1987). This limitation may be prevented by using low pH media (Razzell and Trussell, 1963; Tuovinen and Kelly, 1973).

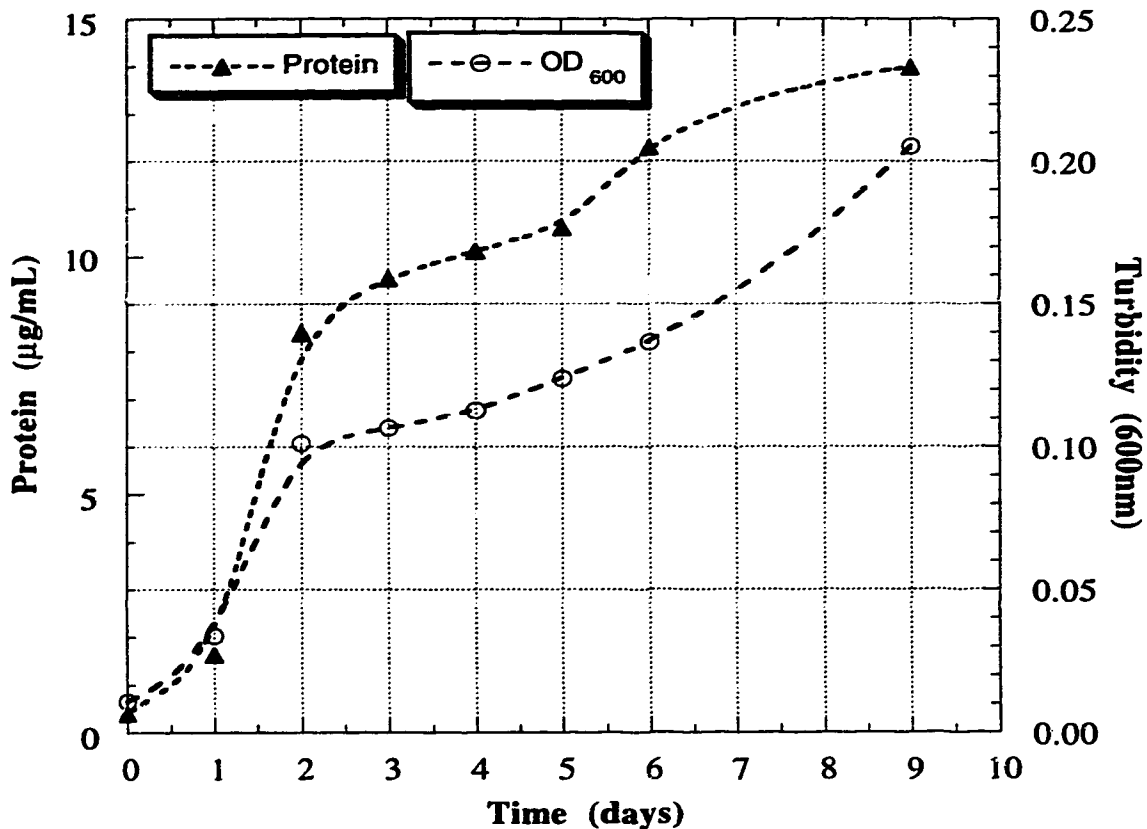


**Figure 4-6. Change in turbidity and protein concentration during growth of strain 13598.**

#### **4.3.5. Changes in Fe<sup>3+</sup> and Protein Concentration in Batch Cultures**

The relationship between protein concentration and Fe<sup>3+</sup> concentration for the three strains is shown in Figure 4-7. A positive linear relationship is observed for all the three strains only during the log growth phase. During the stationary and death phases, a deviation from linearity is observed, where the ferric concentration remains relatively

constant while the protein concentration continues to increase. This is in agreement with the results discussed in Figure 4-1 where ferrous concentration is observed to be constant after the stationary phase, and in Figure 4-4 where protein concentration is observed to increase throughout the stationary and death phases. The conclusion from this is that ferric iron concentration can be monitored in place of protein concentration or vice versa, only during the log growth phase, as reported previously (Suzuki et al., 1987).

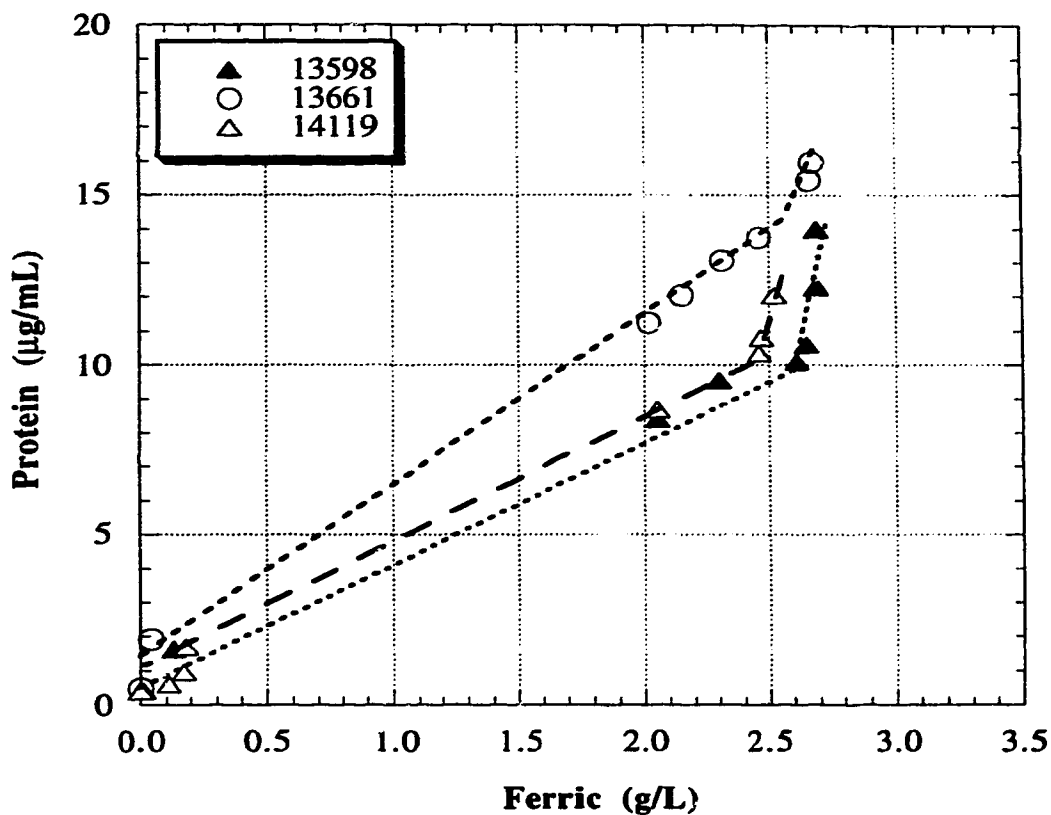


**Figure 4-7. Plot of change in protein versus ferric ion concentration in batch culture of strains 13598, 13661 and 14119.**

#### 4.3.6. Changes in MPN and pH in Batch Cultures

To investigate the cause of the sudden decline of the number of viable cells in Figure 4-1 during the death phase, the pH of the medium was monitored to ascertain if the sudden death of the cells could be attributed to pH changes. A plot of changes in pH and number of viable cells for strain 13598 is shown in Figure 4-8. It is observed that the pH changed only slightly during the lag phase and increased from about 1.7 to 1.9 during the log growth phase. In the stationary and the death phases there was no significant changes

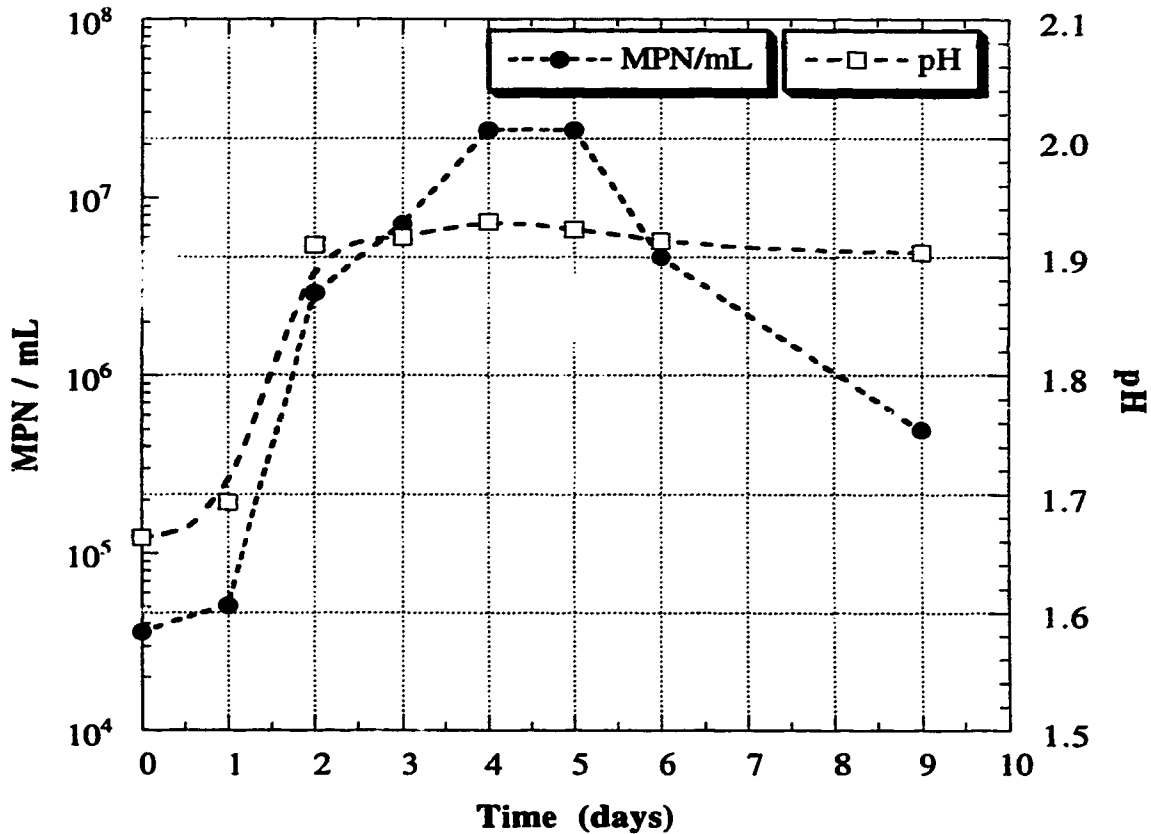


Figure 4-8. Change in number of viable cells and pH during growth of strain 13598.

in pH. The increase in pH during the log growth phase is attributable to H<sup>+</sup> uptake by the cells. The oxidation of Fe<sup>2+</sup> to Fe<sup>3+</sup> results in the removal by the cells of one electron, and in order to maintain balance of electrical neutrality, a proton obtained from the environment of the cell is utilized for the reduction of CO<sub>2</sub> and O<sub>2</sub> (Apel and Dugan, 1987). Depending on the pH of the media, Fe<sub>2</sub>(SO<sub>4</sub>) could be abiotically hydrolyzed and precipitated, releasing H<sup>+</sup> into solution and therefore decreasing pH (Beck, 1960). Strains 13661 and 14119 showed similar trends of slight pH change during the lag phase, a rapid increase during the log growth phase and no significant change during the stationary and death phases. Since there is no significant change in pH during the stationary and death phases, the pH of the medium is unlikely to have caused the sudden decline in the number of viable cells during the death phase.

#### **4.3.7. Effect of Initial Fe<sup>3+</sup> on Number of Viable Cells**

Since the stationary and the death phases coincided with the lowest Fe<sup>2+</sup> concentrations and therefore highest concentrations of Fe<sup>3+</sup> (Figure 4-1), the effect of Fe<sup>3+</sup> concentration on the number of viable cells was investigated. In these experiments, the cultures were grown and the cells were harvested. Equal volumes of the harvested cells were used to inoculate triplicate flasks containing the growth medium. Different concentrations of Fe<sup>3+</sup>, as Fe<sub>2</sub>(SO<sub>4</sub>)<sub>3</sub>, were then added to the cultures and incubated. During incubation the MPN of the cultures were monitored. Figure 4-9 shows a plot of the effect of initial Fe<sup>3+</sup> concentration on the MPN for strain 13598. Although the same number of cells were added to all the flasks, cultures with no initial Fe<sup>3+</sup> showed an increase in MPN after a 1- day lag period. The lag period for the 1.0 g/L initial Fe<sup>3+</sup> flasks was 2 days, while the MPN of the 2.0 g/L initial Fe<sup>3+</sup> flasks decreased for the first 2 days. The MPN of the 2.0 g/L initial Fe<sup>3+</sup> flasks did not increase much above the initial number of viable cells before entering the death phase, while the MPN for the 0 g/L and 1.0 g/L

initial  $\text{Fe}^{3+}$  flasks increased between days 1 and 4, and days 2 and 4 respectively before reaching a stationary phase and subsequent death phase. Similar results were obtained when the test was repeated using strain 13661.

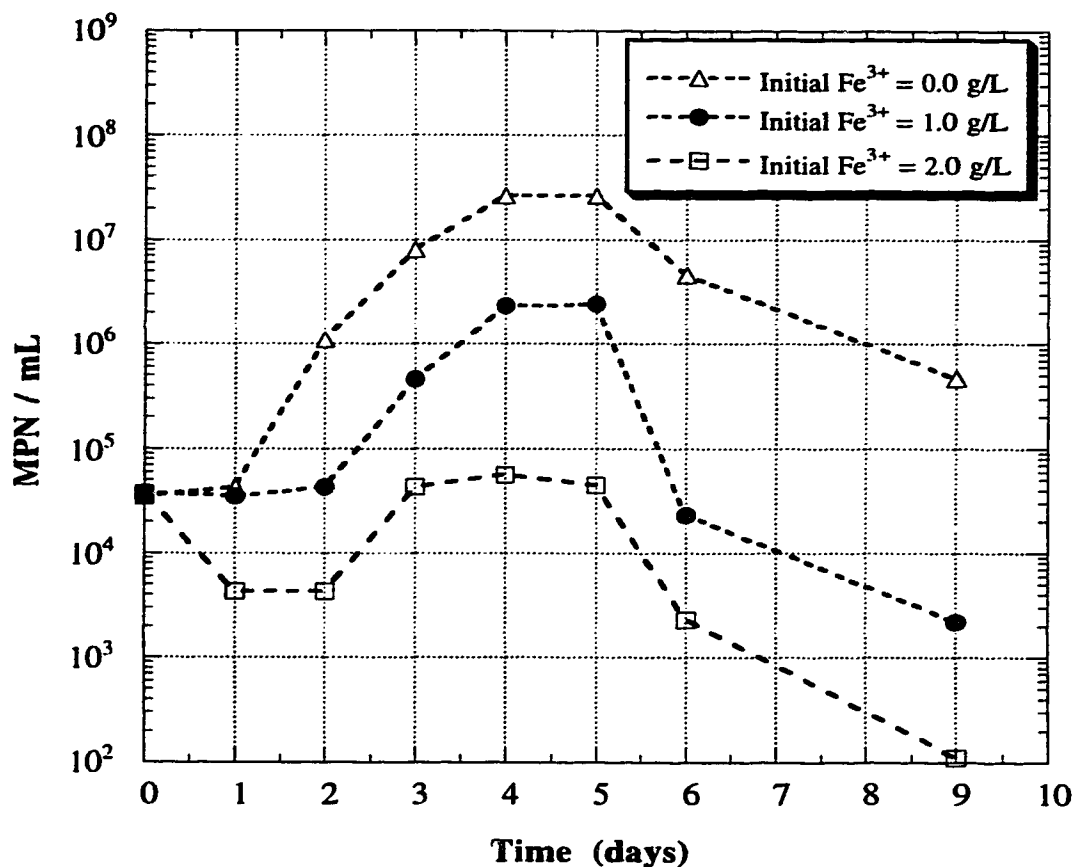


**Figure 4-9. Effect of initial  $\text{Fe}^{3+}$  concentration on the number of viable cells in batch cultures of strain 13598.**

The maximum MPN obtained in each culture was inversely proportional to the initial  $\text{Fe}^{3+}$  concentration as shown in Figure 4-10. The maximum  $\text{Fe}^{3+}$  concentration used in this experiment is equal to the decrease in  $\text{Fe}^{2+}$  concentration in Figure 4-1 (that is, the concentration of  $\text{Fe}^{3+}$  after the log growth phase). This experiment shows that the  $\text{Fe}^{3+}$  produced as a result of the oxidation of  $\text{Fe}^{2+}$  by the cells, which accumulates during the

course of incubation, is responsible for inhibiting the growth of the cells when it exceeds some concentration. An initial  $\text{Fe}^{3+}$  concentration of 2.0 g/L and above will likely be toxic

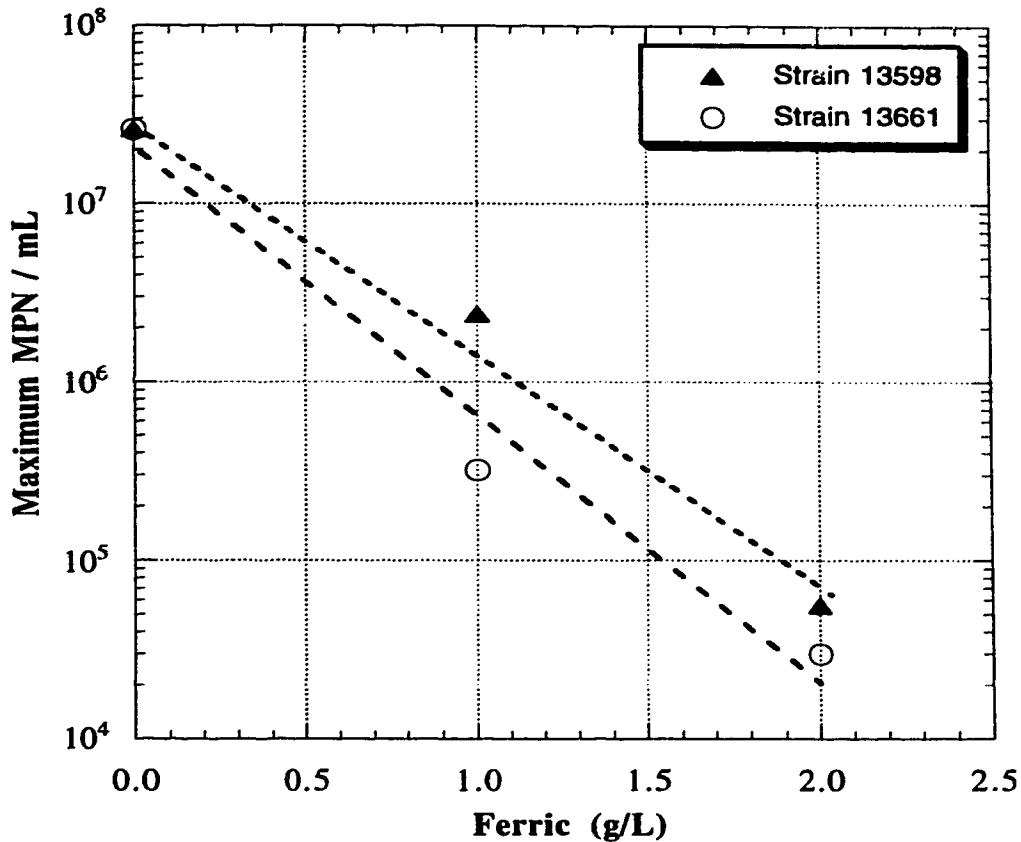


**Figure 4-10. Plot of maximum number of viable cells versus initial  $\text{Fe}^{3+}$  concentration.**

to most of the cells. At an initial concentration of 1 g/L the  $\text{Fe}^{3+}$  also increased the lag period. Increased lag periods were also reported by other investigators (Kelly and Jones, 1978; Kovalenko et al., 1982; Suzuki et al., 1987). The reduced  $\text{Fe}^{2+}$  oxidizing activity of *T. ferrooxidans* in the presence of  $\text{Fe}^{3+}$  observed by Kovalenko et al. (1982) and Suzuki et al. (1987) could be attributed to the reduction in the number of viable cells due to  $\text{Fe}^{3+}$  toxicity. By reducing the amount of  $\text{Fe}^{3+}$  accumulating in situ, using the electrochemical



reduction of  $\text{Fe}^{3+}$  to  $\text{Fe}^{2+}$ , Blake et al. (1994) was able to obtain enhanced *T. ferrooxidans* yields.

#### 4.4 SUMMARY OF CHAPTER

The results of this study have shown that although ferrous iron concentration of a culture may be used to give an indication of the growth phases and to monitor cell numbers and viability during the log growth phase, it cannot be accurately used to monitor changes in cell numbers during the stationary and death phases. The turbidity and protein concentration of the culture showed positive linear relationship with the number of viable cells only during the log growth phase, and could therefore be used as an indication of the cell numbers in the log growth phase only. For experiments which require shorter duration than the log growth phase, protein concentration, ferrous concentration or turbidity may be used as an indirect indication of cell numbers and viability. But, for those that require longer durations than the log growth phase, during which the culture enters the stationary and death phases, protein concentration, ferrous concentration and turbidity will not be adequate for monitoring changes in viable cell numbers. In this case, the MPN should be used.

The protein concentration, and turbidity have positive linear relationships with each other. Therefore, any of these parameters could be monitored in place of the other. The ferric ion concentration correlates well with both the protein concentration and turbidity only during the growth phase, and in this phase any of the three parameters can be used in place of the other.

The pH of the culture increased slightly during the growth of the cells but was not the cause of loss of viability of the cells. The ferric iron generated in situ by the oxidation of ferrous iron by the cells, appears to be responsible for the decreasing viability of the culture and hence indicates some toxic effects of  $\text{Fe}^{3+}$  on *T. ferrooxidans* cells.

#### 4.5 REFERENCES

- American Type Culture Collection. 1982. Catalogue of strains I. 15th edition. Rockville, Maryland, USA. pp. 604.
- Apel, A. W., and R. D. Dugan. 1987. Hydrogen ion utilization by iron-grown *Thiobacillus ferrooxidans*. Metallurgical applications of bacterial leaching and related microbiological phenomena, L. E. Murr, A. E. Torma, and J. A. Brierley (eds.). Academic Press, Inc., New York. pp. 45-59.
- Atkins, A. S., E. W. Bridgwood, and A. J. Davis. 1987. A study of the suppression of pyritic sulphur in coal froth flotation by *Thiobacillus ferrooxidans*. Coal Prep. 5: 1-13.
- Attia, Y. A. 1990. Feasibility of selective biomodification of pyrite floatability in coal desulfurization by froth flotation. Resour. Conserv. Recycl. 3: 169-175.
- Bagdigian, R. M., and A. S. Myerson. 1986. The adsorption of *Thiobacillus ferrooxidans* on coal surfaces. Biotechnol. Bioeng. 28: 467-479.
- Bailey, A. D., and G. S. Handford. 1993. Factors affecting bio-oxidation of sulfide minerals at high concentrations of solid: A Review. Biotechnol. Bioeng. 42: 1164-1174.
- Baker, R. A., and A. G. Wilshire. 1970. Microbiological factor in acid mine drainage formation: A pilot plant study. Environ. Sci. Technol. 4: 401-407.
- Beck, J. V. 1960. A ferrous-ion-oxidizing bacterium. I. Isolation and some general physiological characteristics. J. Bacteriol. 79: 502-509.
- Bell, A., K. D. Phinney, K. Ferguson, A. Gosselin, J. Ingles, and J. S. Scott. 1987. Mine and mill wastewater treatment. Mining, Mineral and Metallurgical Process Division, Environmental Protection, Environment Canada. Report EPS 3/HA.
- Blake, C. R. II, T. G. Howard, and S. McGinness. 1994. Enhanced yields of iron-oxidizing bacteria by in situ electrochemical reduction of soluble iron in the growth medium. Appl. Environ. Microbiol. 60: 2704-2710.

- Chang, C. Y., and S. A. Myerson. 1982. Growth models of the continuous bacterial leaching of iron pyrite by *Thiobacillus ferrooxidans*. *Biotechnol. Bioeng.* 24: 889-902.
- Colmer, A. R., and M. E. Hinkle. 1947. The role of microorganisms in acid mine drainage: A preliminary report. *Science.* 106: 253-256.
- Colmer, A. R., K. L. Temple, and M. E. Hinkle. 1950. An iron-oxidizing bacterium from the acid drainage of some bituminous coal mines. *J. Bacteriol.* 59: 317-328.
- Dugan, P. R. 1987. Prevention of formation of acid drainage from high-sulfur coal refuse by inhibition of iron-and sulfur-oxidizing microorganisms, II. Inhibition in "Run of Mine" refuse under simulated field conditions. *Biotechnol. Bioeng.* 29: 49-54.
- Dugan, P. R., and W. A. Apel. 1978. Microbiological desulfurization of coal. *Metallurgical applications of bacterial leaching and related Microbiological phenomena*, L. E. Murr, A. E. Torma, and J. A. Brierley (eds.). Academic Press, Inc., New York. pp. 223-250.
- Francis, A. J., C. J. Dodge, A. W. Rose, and A. J. Ramirez. 1989. Aerobic and anaerobic microbial dissolution of toxic metals from coal wastes: mechanism of action. *Environ. Sc. Tech.* 23: 435-441.
- Jensen, M. L., and A. M. Bateman. 1979. *Economic mineral deposits*. John Wiley & Sons, Inc., New York. pp. 41-59.
- Kelly, D. P., and C. A. Jones. 1978. Factors affecting metabolism and ferrous iron oxidation in suspensions and batch cultures of *Thiobacillus ferrooxidans*: relevance to ferric iron leach solution regeneration. *Metallurgical applications of bacterial leaching and related microbiological phenomena*, L. E. Murr, A. E. Torma, and J. A. Brierley (eds.). Academic Press Inc., New York. pp. 19-44.
- Kinsell, N. A. 1960. New sulfur oxidizing iron bacterium: *Ferrobacillus sulfooxidans* sp. N. *J. Bacteriol.* 80: 628-632.

- Konishi, Y., Y. Takasaka, and S. Asai. 1994. Kinetics of growth and elemental sulfur oxidation in batch culture of *Thiobacillus ferrooxidans*. *Biotechnol. Bioeng.* 44: 667-673.
- Kovalenko, T. V., G. I. Karavailo, and V. P. Piskunov. 1982. Effect of Fe<sup>3+</sup> ions in the oxidation of ferrous iron by *Thiobacillus ferrooxidans* at various temperatures. *Mikrobiol.* 51: 156-160.
- Lacey, D. T., and F. Lawson. 1970. Kinetics of the liquid-phase oxidation of acid ferrous sulfide by the bacterium *Thiobacillus ferrooxidans*. *Biotechnol. Bioeng.* 12: 29-50.
- Landesman, J., D. W. Duncan, and C. C. Walden. 1966. Iron oxidation by washed cell suspensions of the chemoautotroph, *Thiobacillus ferrooxidans*. *Can. J. Microbiol.* 12: 25-33.
- Lawrence, R. W. 1994. Biooxidation for the treatment of refractory gold ores and concentrates - A Canadian perspective. *CIM Bulletin.* 87: 58-65.
- Leathen, W. W., S. Braley Sr., and L. D. McInyre. 1953. The role of bacteria in the formation of acid from certain surfuritic constituents associated with bituminous coal; part 2, ferrous iron oxidizing bacteria. *Appl. Microbiol.* 1: 65-68.
- Leathen, W. W., A. N. Kinsel, and S. A. Braley Sr. 1956. *Ferrobacillus ferrooxidans* : A chemosynthetic autotrophic bacterium. *J. Bacteriol.* 72: 700-704.
- Lizama, M. H., and I. Suzuki. 1989. Synergistic competitive inhibition of ferrous iron oxidation by *Thiobacillus ferrooxidans* by increasing concentrations of ferric iron and cells. *Appl. Environ. Microbiol.* 55: 2588-2591.
- Lowry, O. H., N. J. Rosebrough, A. L. Farr, and R. J. Randall. 1951. Protein measurement with the folin phenol reagent. *J. Biol. Chem.* 193: 265-275.
- Mannivannan, T., S. Sandhya, and R. A. Pandey. 1994. Microbial desulfurization of coal by chemoautotrophic *Thiobacillus ferrooxidans* - An iron mine isolate. *J. Environ. Sci. Health.* A29: 2045-2061.

- Marchant, P. B. 1986. Commercial piloting and the economic feasibility of plant scale continuous tank leaching at Equity Silver Mines Limited. Fundamental and applied biohydrometallurgy, R. W. Lawrence, R. M. R. Branion and H. G. Ebner (eds.). Elsevier, Amsterdam. pp. 53-76.
- Marchlewitz, B., and W. Schwartz. 1961. Microbe association of acid mine waters. Z. Allg. Mikrobiol. 1: 100-114.
- McCready, R. G. L., D. Wadden, and A. Marchbank. 1986. Nutrient requirement for the in-place leaching of uranium by *Thiobacillus ferrooxidans*. Hydrometallurgy. 17: 61-71.
- Mishra, K. A., R. Pampa, and S. S. R. Mahapatra. 1983. Isolation of *Thiobacillus ferrooxidans* from various habitats and their growth pattern on solid medium. Current Microbiology. 8: 147-152.
- Mishra, K. A., and P. Roy. 1979. A note on the growth of *Thiobacillus ferrooxidans* on solid medium. J. Appl. Bacteriol. 47: 289-292.
- Murr, L. E. L. M. Cathles, D. A. Reese, J. B. Hiskey, C. J. Popp, J. A. Brierley, D. Bloss, V. K. Berry, W. J. Schlitt, and P-C. Hsu. 1977. Chemical, biological, and metallurgical aspects of large-scale column leaching experiments for solution mining and in-situ leaching. In Situ. 1: 209-233.
- Murthy, K. S. N., and K. A. Natarajan. 1992. The role of surface attachment of *Thiobacillus ferrooxidans* on the biooxidation of pyrite. Miner. Metallurg. Processing. 9: 20-24.
- Myerson, S. A., and P. Kline. 1983. The adsorption of *Thiobacillus ferrooxidans* on solid particles. Biotechnol. Bioeng. 25: 1669-1676.
- Nikolov, L. N., and D. G. Karamanev. 1992. Kinetics of the ferrous iron oxidation by resuspended cells of *Thiobacillus ferrooxidans*. Biotechnol. Prog. 8: 252-255.
- Ohmura, N., K. Kitamura, and H. Saiki. 1993. Selective adhesion of *Thiobacillus ferrooxidans* to pyrite. Appl. Environ. Microbiol. 59: 4044-4050.

- Ohmura, N., and H. Saiki. 1994. Desulfurization of coal by microbial column flotation. *Biotechnol. Bioeng.* 44: 125-131.
- Pesic, B., and I. Kim. 1993. Electrochemistry of *Thiobacillus ferrooxidans* interactions with pyrite. *Metallurg. Trans. B.* 24: 717-727.
- Razzell, W. E., and P. C. Trussell. 1963. Isolation and properties of an iron-oxidizing *Thiobacillus*. *J. Bacteriol.* 85: 595-603.
- Rodriguez, L., and H. Tributsch. 1988. Morphology of bacterial leaching patterns by *Thiobacillus ferrooxidans* on synthetic pyrite. *Arch. Microbiol.* 149: 401-405.
- Schnaitman, C. A., M. S. Korczynski, and D. G. Lundgren. 1969. Kinetic studies of iron oxidation by whole cells of *Ferrobacillus ferrooxidans*. *J. Bacteriol.* 99: 552-557.
- Silverman, M. P. 1967. Mechanism of bacterial pyrite oxidation. *J. Bacteriol.* 94: 1046-1051.
- Silverman, M. P., and H. L. Ehrlich. 1964. Microbial formation and degradation of minerals. *Adv. Appl. Microbiol.* 6: 153-206.
- Silverman, M. P., and D. G. Lundgren. 1959a. Studies on the chemoautotrophic iron bacterium *Ferrobacillus ferrooxidans*, II. Manometric studies. *J. Bacteriol.* 78: 326-331.
- Silverman, M. P., and D. G. Lundgren. 1959b. Studies on the chemoautotrophic iron bacterium *Ferrobacillus ferrooxidans*. *J. Bacteriol.* 77: 642-647.
- Singer, P. C., and W. Stumm. 1970. Acid mine drainage: The rate-determining step. *Science.* 167: 1121-1123.
- Suzuki, I., J. K. Oh, P. D. Tackaberry, and H. Lizama. 1987. Determination of activity parameters in *Thiobacillus ferrooxidans* strains as criteria for mineral leaching efficiency. I. Growth characteristics and effects of metals on growth and on sulfur of ferrous iron oxidation. Proceedings of the 4th Annual General Meeting of Biominet, R. G. L. McCready (ed.). CANMET, SP87-10. pp. 179-209.

- Temple, L. K., and W. E. Delchamps. 1953. Autotrophic bacteria and the formation of acid in bituminous coal mines. *Appl. Microbiol.* 1: 255-258.
- Temple, L. K., and R. A. Colmer. 1951. The autotrophic oxidation of iron by a new bacterium: *Thiobacillus ferrooxidans*. *J. Bacteriol.* 62: 605-611.
- Torma, A. E. G. G. Gabra, R. Guay, and M. Silver. 1976. Effects of surface active agents on the oxidation of chalcopyrite by *Thiobacillus ferrooxidans*. *Hydrometallurgy* 1: 301-309.
- Tuovinen, H. O., and P. D. Kelly. 1973. Studies on the growth of *Thiobacillus ferrooxidans*. 1. Use of membrane filters and ferrous iron agar to determine viable numbers, and comparison with  $^{14}\text{CO}_2$ -fixation and iron oxidation as measures of growth. *Arch. Mikrobiol.* 88: 285-298.
- Tuovinen, H. O., D. P. Kelly, C. S. Dow, and M. Eccleston. 1978. Metabolic transitions in cultures of acidophilic *Thiobacilli*. *Metallurgical applications of bacterial leaching and related microbiological phenomena*, L. E. Murr, A. E. Torma, and J. A. Brierley (eds.). Academic Press, Inc., New York. pp. 61-81.
- Wakao, N., M. Mishina, Y. Sakurai, and H. Shiota. 1982. Bacterial pyrite oxidation. I. The effect of pure and mixed cultures of *Thiobacillus ferrooxidans* and *Thiobacillus thiooxidans* on release of iron. *J. Gen. Appl. Microbiol.* 28: 331-343.
- Wakao, N., M. Mishina, Y. Sakurai, and H. Shiota. 1983. Bacterial pyrite oxidation. II. The effect of various organic substances on release of iron from pyrite by *Thiobacillus ferrooxidans*. *J. Gen. Appl. Microbiol.* 29: 177-185.

## CHAPTER 5

### KINETICS OF FERROUS IRON OXIDATION BY *THIOBACILLUS FERROOXIDANS* \*

#### 5.1 INTRODUCTION

The oxidizing property of ferric ion makes it one of the most useful reagents in hydrometallurgy and it is used widely for the leaching of metals from their ores and concentrates (Torma, 1983; Morrison, 1989; Crundwell, 1987). However, during the oxidation reactions, the ferric ion is reduced to ferrous ion and has to be reoxidized to regain its oxidizing power. In many leaching systems, the reoxidation of ferrous to ferric ions plays a central role (Kelly and Jones, 1978), and chemical catalysts such as mixtures of O<sub>2</sub> and SO<sub>2</sub>, and Cu<sup>2+</sup> have been used to improve the rate of regeneration of ferric ion (Tiwari et al., 1979). Lately however, the bacterium *Thiobacillus ferrooxidans*, which is capable of deriving its energy from the oxidation of ferrous ions (Silverman, 1967) has been investigated for use as a biocatalyst in the regeneration of ferric ions in leaching systems (Marchant, 1986; McCready et al., 1986).

Another area where the oxidation of ferrous to ferric ion plays an important role is in acid rock drainage (ARD) formation (Colmer and Hinkle, 1947; Leathen et al., 1956; Baker and Wilshire, 1970). Two mechanisms of bacterial sulfide oxidation and ARD formation have been proposed; the indirect and direct contact mechanisms (Silverman and Ehrlich, 1964). The indirect contact mechanism involves the oxidation of sulfides by ferric ions, and the bacteria enter the reaction by reoxidizing ferrous ions generated from the sulfide-ferric ion reaction to the ferric state, thereby regenerating the primary ferric ion

---

\* A version of this chapter, co-authored with N. O. Egiebor and P. M. Fedorak, has been resubmitted to the Canadian Journal of Microbiology.



oxidant. Ferrous to ferric ion oxidation is also utilized in the cleanup of ARD effluents, where the ferrous ions are converted to the ferric ions under low pH, and the ferric ions precipitated as insoluble hydroxide by the addition of calcium carbonate (Omura et al., 1991).

A good knowledge of the mechanism of ARD formation, regeneration of ferric ions and consequent leaching of metals will require an understanding of the kinetics of the chemical and the microbiological reactions of oxidation of ferrous to ferric ions. The kinetics of the chemical oxidation of ferrous ions in sulfate medium (Huffman and Davidson, 1956) and chloride medium (Colborn and Nicol, 1973) have been studied, and shown to be very slow at acidic pH (Pesic et al., 1989). The kinetics of the biological oxidation of ferrous ions by *T. ferrooxidans* has generally been studied and reported in terms of the Michaelis-Menten kinetic analysis (Kelly and Jones, 1978; Suzuki et al., 1989). However, Pesic et al. (1989) reported that ferrous oxidation to ferric ions in the presence of *T. ferrooxidans* followed a first order rate expression. They suggested that the deviation from the Michaelis-Menten kinetics may be due to the much lower concentrations of ferrous ions used in their reaction. The Michaelis-Menten kinetic analysis involves the use of initial velocities of ferrous oxidation, whereas the first order kinetic analysis employs an integration method, where the kinetic parameters are estimated from a single time course experiment.

The work reported in this chapter was aimed to study the kinetics of the microbiological oxidation of ferrous ions using a wide range of ferrous and cell concentrations in an attempt to determine whether or not the kinetics of *T. ferrooxidans* oxidation of ferrous ions varies with the concentrations of either the ferrous ions or the active cells. The study monitored ferrous concentration, a direct parameter, instead of oxygen consumption, an indirect parameter that is commonly used with the Michaelis-Menten kinetic analysis of ferrous ion oxidation (Kelly and Jones, 1978; Lizama and Suzuki, 1989; Suzuki et al., 1989).

## 5.2 THEORY AND BACKGROUND

The oxidation of ferrous ions to ferric ion by *T. ferrooxidans* to ferric ions can be represented by the reaction:



Assuming that  $\text{Fe}^{2+}$  oxidation by whole cells of *T. ferrooxidans* can be considered as a simple enzyme reaction which can be described by a sequence represented by:



where E is the  $\text{Fe}^{2+}$ -oxidizing enzyme (from *T. ferrooxidans* cells), S is the substrate ( $\text{Fe}^{2+}$ ), ES is the intermediate product, and P is the product ( $\text{Fe}^{3+}$ ). Since the catalyzed rate of  $\text{Fe}^{2+}$  oxidation is several orders of magnitude greater than the uncatalyzed rate at acidic pH (Leathen et al., 1953; Singer and Stumm, 1970), the kinetic equations based on Reaction (5-1) may be restricted to:

$$\frac{dS}{dt} = k_2 [ES] - k_1 [E] [S] \quad (5-2)$$

$$\frac{dE}{dt} = (k_2 + k_3) [ES] - k_1 [E] [S] \quad (5-3)$$

$$\frac{dES}{dt} = k_1 [E] [S] - (k_2 + k_3) [ES] \quad (5-4)$$

$$\frac{dP}{dt} = k_3 [ES] \quad (5-5)$$

and, the conservation equation for the enzyme,

$$[E_t] = [E] + [ES] \quad (5-6)$$

where [E],  $[E_t]$ , [S], [ES] and [P] are the concentrations of the enzyme, total enzyme, substrate ( $\text{Fe}^{2+}$ ), intermediate product and product ( $\text{Fe}^{3+}$ ), respectively. At steady-state, with low concentration of  $E_t$  as compared with [S],

$$\frac{dE}{dt} \text{ and } \frac{dES}{dt} \approx 0 \quad (5-7)$$

therefore,

$$\frac{dES}{dt} = k_1 [E] [S] - (k_2 + k_3) [ES] \approx 0 \quad (5-8)$$

Substituting  $[E_t] - [ES] = [E]$  into Equation (5-8) and rearranging results in,

$$[ES] = \frac{k_1 [E_t] [S]}{k_1 [S] + k_2 + k_3} \quad (5-9)$$

Equations (5-2) and (5-5) are equal, and represents the velocity of  $Fe^{2+}$  oxidation,  $v$ .

$$v = \frac{-dS}{dt} = \frac{dP}{dt} = k_3 [ES] \quad (5-10)$$

Substituting the value of  $[ES]$  from Equation (5-9) into Equation (5-10) results in,

$$v = \frac{-dS}{dt} = \frac{k_1 k_3 [E_t] [S]}{k_1 [S] + k_2 + k_3} = \frac{(k_3 [E_t]) [S]}{(k_2 + k_3)/k_1 + [S]} \quad (5-11)$$

If each *T. ferrooxidans* cell has  $\beta$  number of the enzyme E capable of oxidizing the substrate S ( $Fe^{2+}$ ) to product P ( $Fe^{3+}$ ), then  $[E_t] = \beta[C]$ , where  $[C]$  is the total concentration of viable *T. ferrooxidans* cells. Equation (5-11) can therefore be written as,

$$v = \frac{\beta k_3 [C] [S]}{(k_2 + k_3)/k_1 + [S]} \quad (5-12)$$

Equation (5-12) may be rewritten in a simpler form as,

$$v = \frac{\eta [S]}{K_m + [S]} \quad (5-13)$$

where  $\eta = \beta k_3 [C]$  and  $K_m = (k_2 + k_3)/k_1$  is the Michaelis constant. Inverting Equation (5-13) results in the double-reciprocal type equation (Lineweaver and Burke, 1934), given as:

$$\frac{1}{v} = \frac{K_m}{\eta} \left( \frac{1}{[S]} \right) + \frac{1}{\eta} \quad (5-14)$$

If a constant concentration of cells is used for an experiment in which all parameters except the substrate concentration are kept constant, Equation (5-14) predicts that  $\eta$  remains constant and an enzymatically-catalyzed reaction should show a variation in initial rates with substrate concentration,  $[S]$ . Thus, plots of  $1/v$  versus  $1/[S]$  at different cell

concentrations, [C], should show a family of lines with slopes of  $K_m/\eta$ , and intercepts on the  $1/v$  and  $1/[S]$  axes at  $1/\eta$  and  $-1/K_m$ , respectively.

While the enzyme kinetics method of treating such data involves the use of initial velocities only (the initial velocities are obtained at several concentrations of the substrates), in theory, all the necessary information on the kinetics could be obtained from a single time course experiment using an integrated equation.

Replacing  $v$  by  $-dS/dt$ , Equation (5-13) becomes,

$$-\eta dt = \left( \frac{K_m}{[S]} + 1 \right) dS \quad (5-15)$$

rearranging Equation (5-15),

$$-\eta dt = K_m \frac{dS}{[S]} + dS \quad (5-16)$$

Integrating Equation (5-16) gives,

$$\eta t = K_m \left( \ln \frac{[S]_0}{[S]} \right) + ([S]_0 - [S]) \quad (5-17)$$

Where  $[S]_0$  is the initial concentration of the substrate, and  $[S]$  is the concentration of the substrate at any time  $t$ . Rearranging Equation (5-17):

$$\frac{[S]_0 - [S]}{t} = -K_m \frac{\ln ([S]_0 / [S])}{t} + \eta \quad (5-18)$$

Simplifying Equation (5-18):

$$\psi = -K_m \lambda + \eta \quad (5-19)$$

where  $\psi = \frac{[S]_0 - [S]}{t}$  and  $\lambda = \frac{\ln ([S]_0 / [S])}{t}$ . A plot of  $\psi$  against  $\lambda$  should result in a straight line with a slope of  $-K_m$  and an intercept of  $\eta$  on the  $\psi$  axis. However, the integrated equation has no provision for inhibition of the reaction by products, in this case  $Fe^{3+}$  formed in situ (Kelly and Jones, 1978), pH changes during the oxidation reaction,

and also approach to equilibrium. This form of integrated equation has been used in the biohydrometallurgical analysis of  $\text{Fe}^{2+}$  oxidation by *T. ferrooxidans* and has resulted in the first order reaction rate (Pesic et al., 1989).

## **5.3 MATERIALS AND METHODS**

### **5.3.1 Culture and Medium**

The three strains of *T. ferrooxidans* used in this study were obtained from the American Type Culture Collection: ATCC 13598, ATCC 13661 and ATCC 14119. Details of the medium used for the growth of the microorganisms has been reported in Section 4.2.1.

### **5.3.2 Determination of Growth Phases of Strains**

The growth phases of each of the strains were studied by monitoring the number of viable cells in batch cultures by the most probable number method (MPN). Four-day-old cultures were used for the activity and growth studies. Each strain was inoculated (10%) into sterile growth medium and allowed to grow for 4 days. On the fourth day, a new set of sterile medium was inoculated with each strain in triplicates and samples taken from each flask for days 0 through 6, and on day 9 for MPN determinations. Triplicate sterile control flasks were also incubated with the inoculated flasks.

### **5.3.3 Most Probable Number Method**

The numbers of *T. ferrooxidans* in cultures and cell suspensions were determined by a 3-tube MPN method (Table given in American Public Health Association 1985). Details of the MPN procedure has been reported in Section 4.2.3. Ten-fold dilutions were prepared in sterile growth medium, and then 1-mL portions of each dilution were

inoculated into three tubes containing 3 mL of growth medium. The small volume of medium ensured aerobic conditions throughout the tubes. The cultures were incubated for 10 days at 27°C and growth was indicated by a change in the color of the medium from colourless to rust.

#### **5.3.4 Preparation of Cell Suspension**

Cultures of each strain were grown in three 500-mL Erlenmeyer flasks, containing 75 mL of growth medium and 10% inoculum each, at 27°C and 200 rpm in the dark. When the cultures had reached their log growth phase, after 2 or 3 days of incubation, the cells in the triplicate cultures were harvested. Harvesting of the cells was done by filtering the cultures of each strain through Whatman no.1 filter paper to remove any precipitate that may be present. The filtrate obtained was then centrifuged at 10,000 x g for 10 min (Du Pout Sorvall RC-5B refrigerated superspeed centrifuge), and the resulting cell pellet washed twice by resuspending with 0.01 M H<sub>2</sub>SO<sub>4</sub> solution and centrifuging. The cells were finally resuspended in a small volume (4 to 5 mL) of 0.01 M H<sub>2</sub>SO<sub>4</sub> solution and used for the Fe<sup>2+</sup> oxidation rate experiments. The cell harvesting procedures were all done aseptically.

#### **5.3.5 Determination of Time for Initial Linear Drop in Fe<sup>2+</sup> Concentration**

The time for initial linear drop in Fe<sup>2+</sup> concentration was obtained by monitoring the change in Fe<sup>2+</sup> concentration with time. These experiments were conducted in 500-mL Erlenmeyer flasks using 100 mL of predetermined Fe<sup>2+</sup> concentration and cells suspension. Samples were taken periodically for 6 h and the Fe<sup>2+</sup>-time curves plotted for each initial Fe<sup>2+</sup> and cell concentrations. The Fe<sup>2+</sup>-time curves were used to estimate the time required for the initial linear drop in Fe<sup>2+</sup> concentration. These times were used to design initial oxidation rate experiments.

### **5.3.6 Determination of Initial Oxidation Rates and pH**

The initial rate experiments were conducted in loosely capped 15 mm diameter x 150 mm test tubes. A set of 5 test tubes were used for each  $\text{Fe}^{2+}$  and cell concentrations. Approximate volumes of the growth medium were measured into the tubes and the volumes made up to 5 mL with sterile 0.01 M  $\text{H}_2\text{SO}_4$  to predetermined  $\text{Fe}^{2+}$  concentrations. The test tubes were then inoculated with different volumes of prepared cells suspension. A set of tubes consisting of one tube from each concentration batch was not inoculated and used as controls to determine the actual initial  $\text{Fe}^{2+}$  concentration and also any autooxidation of  $\text{Fe}^{2+}$  that may occur. Another set of inoculated tubes were used to determine the initial number of viable cells by the MPN method. The remaining tubes were incubated at  $27^\circ\text{C}$  in a rotary shaker at 200 rpm in the dark. At predetermined times (obtained from the  $\text{Fe}^{2+}$ -time curves), a set of tubes were taken and the  $\text{Fe}^{2+}$  concentrations determined. The initial and final  $\text{Fe}^{2+}$  concentrations, and the reaction times were used to determine the initial rate of  $\text{Fe}^{2+}$  oxidation for the various initial  $\text{Fe}^{2+}$  and cell concentrations.

All the  $\text{Fe}^{2+}$  oxidation experiments were carried out at pH 2.0. The pH of each sample was determined using a Cole-Parmer Chemcadet pH/mV meter equipped with a temperature compensation probe.

### **5.3.7 Total and Ferrous Iron**

Total Fe and  $\text{Fe}^{2+}$  in the samples were determined by DR/2000 Spectrophotometer and the total Fe concentrations was verified with Atomic Absorption Spectrophotometry (AAS). The procedure used for Fe and  $\text{Fe}^{2+}$  analysis is reported in Section 2.3.5.

## 5.4 RESULTS AND DISCUSSION

### 5.4.1 Change in the Number of Viable Cells During Growth of Cultures

Figure 5-1 shows the change in MPN with time for *T. ferrooxidans* strains 13598, 13661, and 14119. It was observed that the number of viable cells in the 13598 culture increases steadily after an initial 1-day lag period and reaches a maximum number of viable cells of  $1.5 \times 10^7$  MPN/mL after 4 days before starting to decrease. Since the 13598 culture was in log growth phase after 2 days, the 13598 cells used for the experiments were harvested after 2 days of incubation. Figure 5-1 shows that strain 13661 also followed a

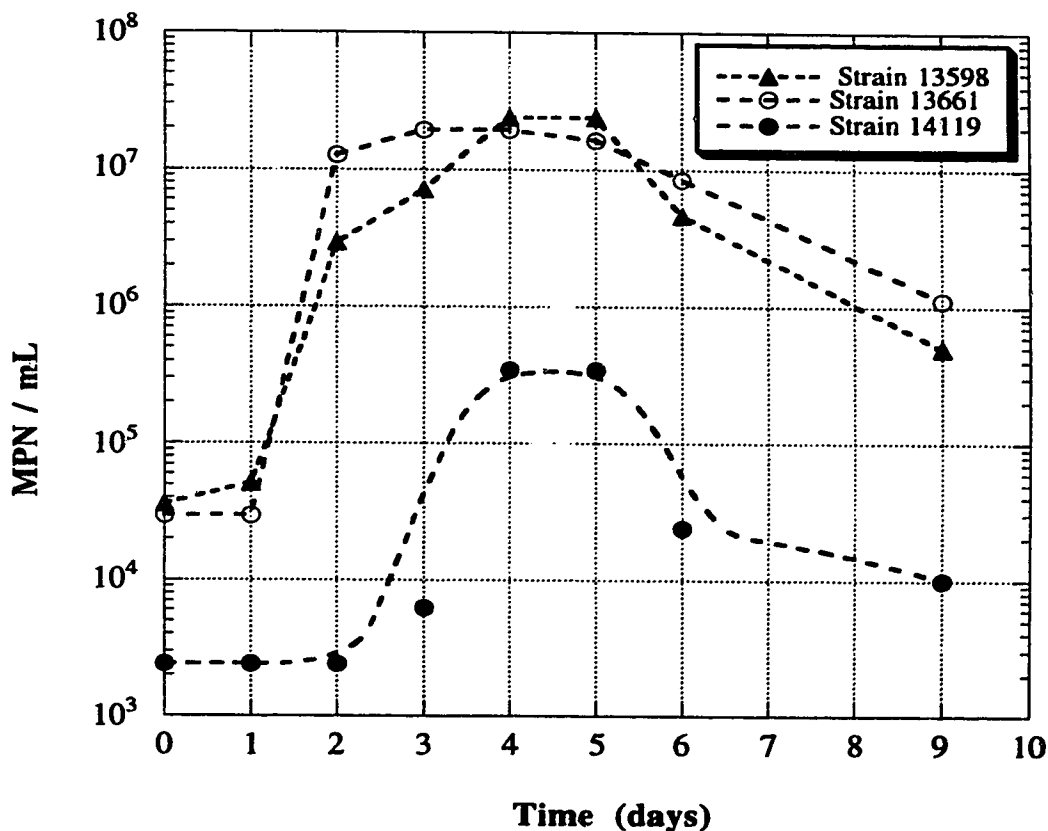


Figure 5-1. Change in the number of viable cells during incubation of *T. ferrooxidans* strains 13598, 13661, and 14119.



similar growth path as strain 13598. The 13661 culture reached a maximum number of viable cells ( $1.1 \times 10^7$  MPN/mL) after 3 days and starts to decline after day 4. The 13661 culture also was in log growth phase after 2 days of incubation, after an initial 1-day lag period. The 13661 cultures were therefore harvested after 2 days of incubation and used in the subsequent experiments. Strain 14119 showed a longer lag period of 2 days. This culture reached its maximum number of viable cells of  $2.5 \times 10^5$  MPN/mL after 4 days of incubation and then decreases to day 9. Figure 5-1 shows that the 14119 culture was in log growth phase after 3 days of incubation. Cultures of strain 14119 were therefore incubated for 3 days before the cells were harvested and used in the subsequent experiments. Ferrous-oxidizing activity of *T. ferrooxidans* have been shown to be highest during the log growth phase (Beck 1960; Landesman et al., 1966), hence cells in their log growth phase were targeted for use in the  $\text{Fe}^{2+}$  oxidation kinetics study.

#### **5.4.2 Determination of Kinetic Parameters**

The initial  $\text{Fe}^{2+}$  oxidation velocities obtained from the tubes were used to determine the kinetic parameters because of errors due to  $\text{Fe}^{3+}$  inhibition, pH changes, and approach to equilibrium associated with the single time course approach ( $\text{Fe}^{2+}$ -time curves). Figure 5-2 shows the change in  $\text{Fe}^{2+}$  concentration with time using an initial cell concentration of  $4.3 \times 10^5/\text{mL}$  (0.2 mL) and  $\text{Fe}^{2+}$  concentration of 12 mg/L. An initial  $\text{Fe}^{2+}$  concentration drop time of less than 2 h was obtained and used for the initial  $\text{Fe}^{2+}$  oxidation rate experiment.

Since Equation (5-14) shows that a plot of  $1/v$  versus  $1/[S]$  at different cell concentrations,  $[C]$ , should result in a family of straight lines, these values were plotted for each strain of *T. ferrooxidans*. The plots of  $1/v$  versus  $1/[S]$  were divided into three groups, low initial  $\text{Fe}^{2+}$  concentration and low cell concentration, low initial  $\text{Fe}^{2+}$  concentration and high cell concentration, and high initial  $\text{Fe}^{2+}$  concentration and low cell concentration. Cell suspensions of 10  $\mu\text{L}$ , 20  $\mu\text{L}$ , 50  $\mu\text{L}$ , 100  $\mu\text{L}$ , 200  $\mu\text{L}$  and 400  $\mu\text{L}$

used in the tests resulted in viable cell concentrations of  $4.3 \times 10^5/\text{mL}$ ,  $9.3 \times 10^5/\text{mL}$ ,  $2.3 \times 10^6/\text{mL}$ ,  $2.3 \times 10^7/\text{mL}$ ,  $9.3 \times 10^7/\text{mL}$ , and  $1.1 \times 10^9/\text{mL}$ , respectively.

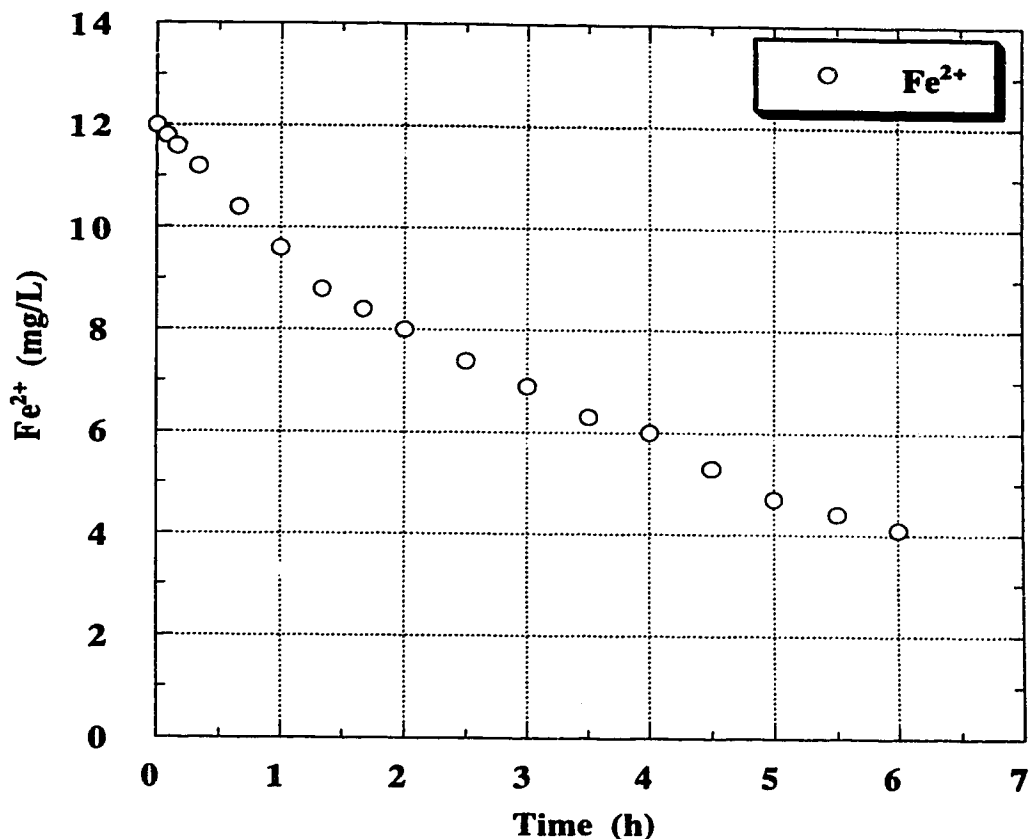


**Figure 5-2. Change in Fe<sup>2+</sup> concentration with time. (Initial Fe<sup>2+</sup> and cell concentrations of 12 mg/L and  $4.3 \times 10^5/\text{mL}$  respectively)**

#### **5.4.2.1 Low initial Fe<sup>2+</sup> concentration and low cell concentration**

Figure 5-3 shows  $1/v$  versus  $1/[S]$  plot for strain 13598 using low initial Fe<sup>2+</sup> concentrations of 0.06 mM to 0.58 mM and low viable cell concentrations of  $4.3 \times 10^5/\text{mL}$  (10  $\mu\text{L}$ ) to  $2.3 \times 10^6/\text{mL}$  (50  $\mu\text{L}$ ). It is observed that the double-reciprocal rate ( $v$ ) versus [Fe<sup>2+</sup>] plot is linear as expected from the standard Michaelis-Menten kinetics, Equation (5-14). Increasing the cell concentration, [C], at a constant Fe<sup>2+</sup> concentration, increases the

rate of  $\text{Fe}^{2+}$  oxidation. The lines intercept the  $1/[\text{Fe}^{2+}]$  axis at  $-2.5 \text{ mM}^{-1}$ , resulting in a Michaelis constant,  $K_m$ , value of  $0.40 \text{ mM}$ . Similar plots were obtained for strains 14119 and 13661 with  $K_m$  values of  $0.29$  and  $0.67 \text{ mM}$  respectively (Table 5-1). The  $K_m$  data show a range of  $K_m$  values between  $0.29$  and  $0.67$  for the three strains. The apparent  $K_m$  values for  $\text{Fe}^{2+}$  oxidation by *T. ferrooxidans* reported in the literature vary from  $0.28$  to  $0.8 \text{ mM}$  (Suzuki et al., 1989) and  $0.43$  to  $9.4 \text{ mM}$  (Kelly and Jones, 1978). The results indicate that with low initial ferrous, and cell concentrations, the oxidation of ferrous to ferric ions by *T. ferrooxidans* follows the Michaelis-Menten kinetics.

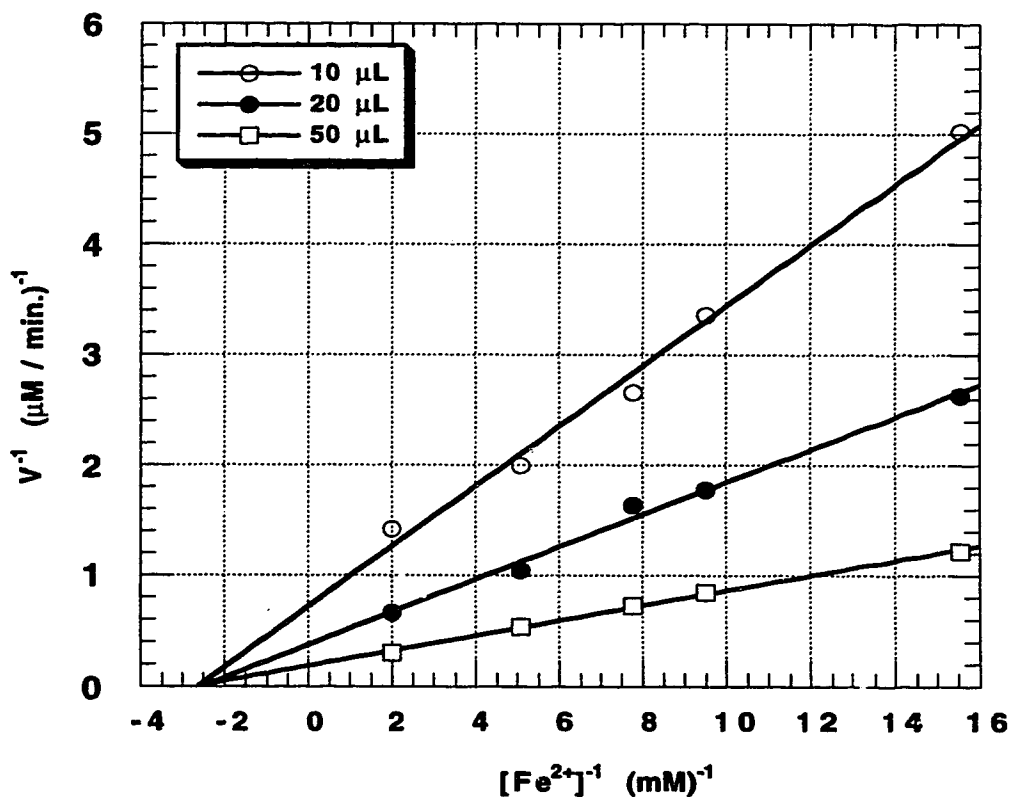


**Figure 5-3.** The effect of low initial  $\text{Fe}^{2+}$  and low cell concentrations on the rate of  $\text{Fe}^{2+}$  oxidation with strain 13598.

**Table 5-1. Michaelis constants for Fe<sup>2+</sup> oxidation by *T. ferrooxidans*.**

Strain	K <sub>m</sub> (mM Fe <sup>2+</sup> )
ATCC 14119	0.29
ATCC 13598	0.40
ATCC 13661	0.67

#### 5.4.2.2 Low initial Fe<sup>2+</sup> concentration and high cell concentration

Figure 5-4 illustrates the effect of using low initial [Fe<sup>2+</sup>] (0.06 mM to 0.5 mM) and higher cell concentrations, {4.3 x 10<sup>7</sup>/mL (100 μL) and 9.3 x 10<sup>7</sup>/mL (200 μL)} on the rate of oxidation of Fe<sup>2+</sup> by strain 13598. For each cell concentration used, the plot of 1/v versus 1/[S] shows a straight line passing through the origin. This set of plots clearly show a pseudo-first order kinetics (straight line passing through the origin) for the *T. ferrooxidans* oxidation of ferrous ions at low Fe<sup>2+</sup> concentrations and relatively high cell concentrations. Similar results were obtained for strains 14119 and 13661. The pseudo-first order rate constants for the three strains at cell concentrations ranging from 2.3 x 10<sup>7</sup>/mL (100 μL) to 1.1 x 10<sup>9</sup>/mL (400 μL) are shown in Table 5-2. At 2.3 x 10<sup>7</sup>/mL (100 μL) cell concentrations, all three strains show similar first order rate constants, K<sub>n</sub>, from 1.5 x 10<sup>-2</sup>/min for strain 13598 to 1.6 x 10<sup>-2</sup>/min for strain 13661. As expected, when the cell concentrations were doubled to 9.3 x 10<sup>7</sup>/mL (200 μL), the rate constant, K<sub>n</sub>, increases to between 1.9 x 10<sup>-2</sup>/min and 2.0 x 10<sup>-2</sup>/min. It is interesting to note that while the 1/v versus 1/[S] plots for low initial Fe<sup>2+</sup> concentrations, [Fe<sup>2+</sup>], of 0.06 mM to 0.58 mM, and cell concentrations, [C], of 9.3 x 10<sup>4</sup>/mL (10 μL) to 10<sup>6</sup>/mL (50 μL) follows the standard Michaelis-Menten kinetics, the intercept on the 1/[Fe<sup>2+</sup>] shifts as the [C] is increased beyond a certain cell concentration, and a pseudo-first order kinetics with a straight line passing through the origin is obtained. Thus, the kinetics of ferrous oxidation by *T. ferrooxidans* depend on the relative concentrations of ferrous ions and active cells.

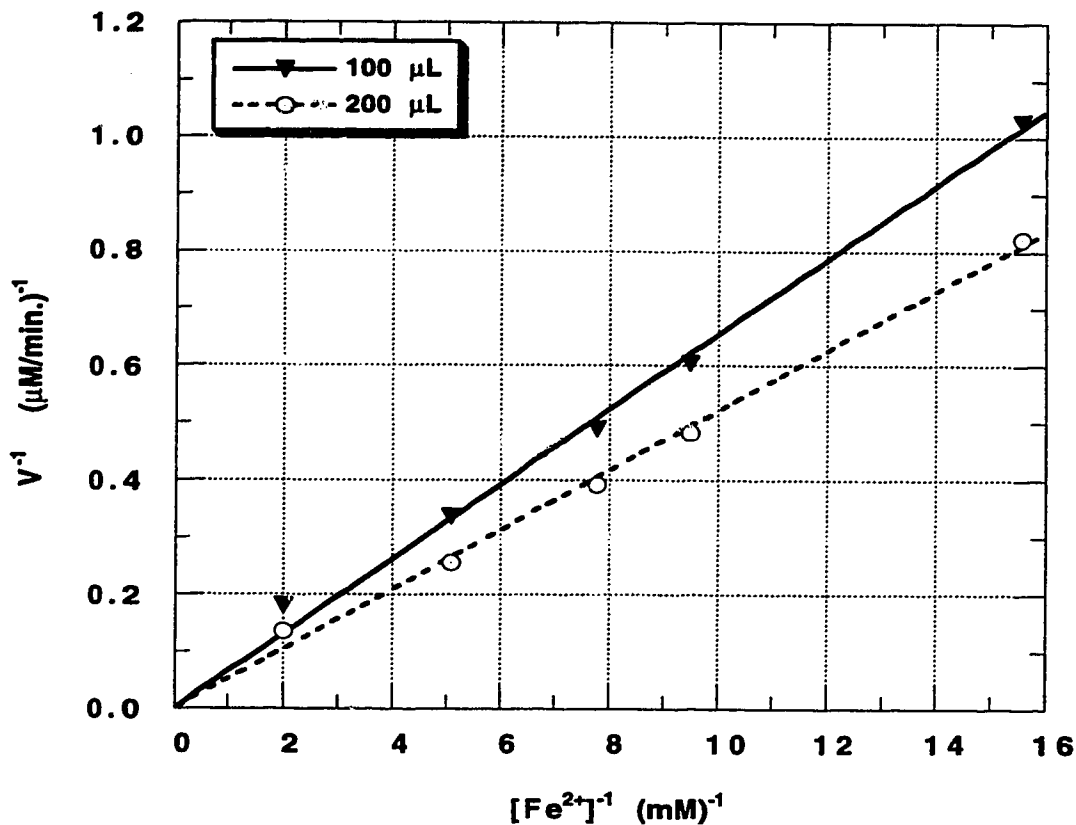


Figure 5-4. The effect of low initial Fe and high cell concentrations on the rate of Fe<sup>2+</sup> oxidation with strain 13598.

Table 5-2. First order rate constant\* ( $k_d$ ) for Fe<sup>2+</sup> oxidation by *T. ferrooxidans*.

Strain	Cell concentrations (volume of cell suspensions)		
	2.3x10 <sup>7</sup> /mL (100 μL)	9.3x10 <sup>7</sup> /mL (200 μL)	1.1x10 <sup>9</sup> /mL (400 μL)
ATCC 14119	1.6 x 10 <sup>-2</sup> /min	1.9 x 10 <sup>-2</sup> /min	nt
ATCC 13598	1.5 x 10 <sup>-2</sup> /min	1.9 x 10 <sup>-2</sup> /min	nt
ATCC 13661	1.6 x 10 <sup>-2</sup> /min	2.0 x 10 <sup>-2</sup> /min	3.2 x 10 <sup>-2</sup> /min

nt = not tested.

### 5.4.2.3 High Initial Fe<sup>2+</sup> Concentration

Figure 5-5 shows a plot of  $1/v$  versus  $1/S$  using high initial Fe<sup>2+</sup> concentration,  $S$ , of 1.3 mM to 73 mM, and cell concentrations of  $4.3 \times 10^5/\text{mL}$  ( $10 \mu\text{L}$ ) to  $9.3 \times 10^7/\text{mL}$  ( $200 \mu\text{L}$ ) of strain 13598. It was observed that at these high ferrous concentrations, as the  $[C]$  is increased, the Fe<sup>2+</sup> oxidation kinetics shifts from a Michaelis-Menten type ( $4.3 \times 10^5/\text{mL}$  ( $10 \mu\text{L}$ ) to  $2.3 \times 10^6/\text{mL}$  ( $50 \mu\text{L}$ )) to a pseudo-first order kinetics ( $4.3 \times 10^7/\text{mL}$  ( $100 \mu\text{L}$ ) to  $9.3 \times 10^7/\text{mL}$  ( $200 \mu\text{L}$ )). The plots from strains 14119 and 13661 also gave similar results.

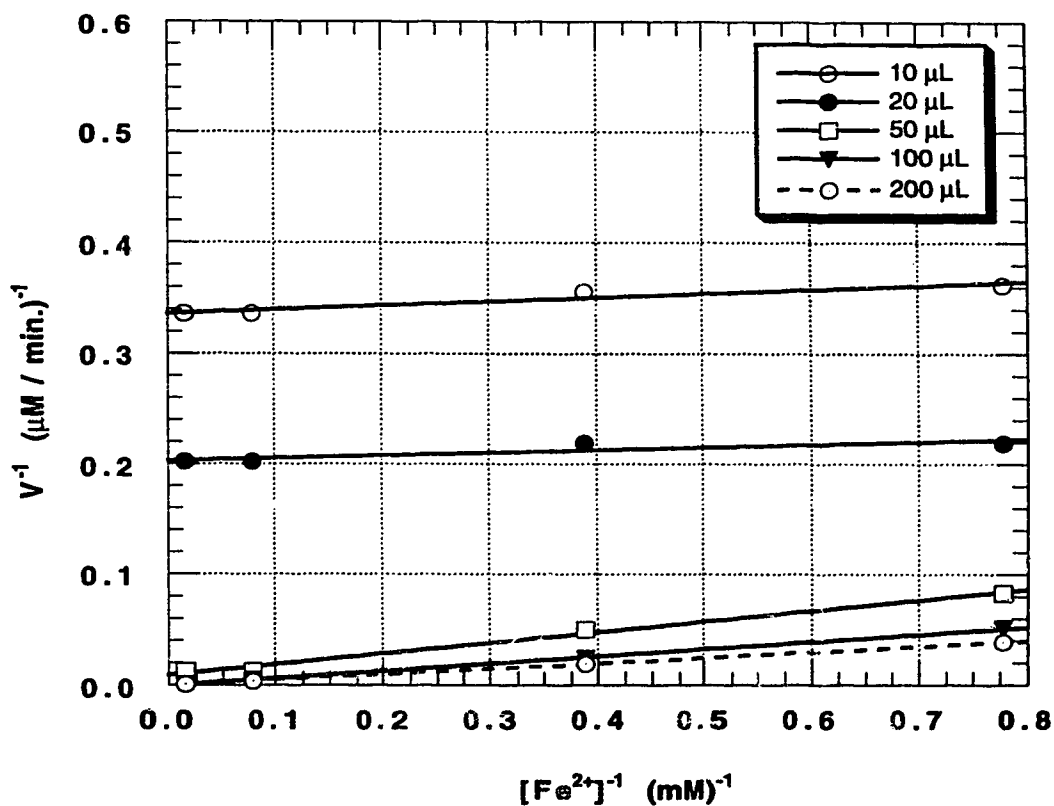


Figure 5-5. The effect of high initial Fe and various cell concentrations on the rate of Fe<sup>2+</sup> oxidation with strain 13598.

The results from Figures 5-3 to 5-5 show that with low  $\text{Fe}^{2+}$  concentrations, and relatively low cell concentrations,  $\text{Fe}^{2+}$  oxidation by *T. ferrooxidans* follows the Michaelis-Menten kinetics represented by Equation (5-14). As the cell concentration is increased at low initial  $\text{Fe}^{2+}$  concentration (Figure 5-4), the kinetics of  $\text{Fe}^{2+}$  oxidation shifts to a pseudo-first order rate. These results can be explained on the basis of the Michaelis-Menten kinetics using Equation (5-13). At a relatively high cell concentration,  $[C]$ , and low initial ferrous or substrate concentration,  $[S]$ , the Michaelis constant,  $K_m$ , becomes very large, i.e.  $K_m \gg [S]$ . Hence Equation (5-13) can be written as:

$$v = \frac{\eta [S]}{K_m + [S]} \approx \frac{\eta [S]}{[S]}, \quad (K_m \gg [S])$$

or

$$v = K_n [S] \quad (5-20)$$

where  $K_n = \eta/K_m$  approaches a first order rate constant. Thus, a plot of  $1/v$  versus  $1/[S]$  should give a straight line passing through the origin with a slope of  $1/K_n$ . This explains the pseudo-first order rate kinetics obtained in Figure 5-3.

Similarly, at high ferrous or substrate concentrations,  $[S]$ , and relatively low cell concentrations,  $[C]$ , the rate of oxidation becomes so low that the Michaelis constant,  $K_m$ , becomes insignificant, i.e.  $[S] \gg K_m$ . Equation 5-13 can then be written as:

$$v = \frac{\eta [S]}{K_m + [S]} \approx \frac{\eta [S]}{[S]}, \quad ([S] \gg K_m)$$

or

$$v = \eta \quad (5-21)$$

Equation (5-21) shows that at sufficiently high ferrous concentration, relative to cell concentration, the Michaelis-Menten kinetics approaches zero order. This explains the

flattening of the rate curves in Figure 5-5 as the cell concentration is reduced with high concentrations of ferrous ions. The approach of the Michaelis-Menten kinetics to zero order at high ferrous concentration has also been reported by Macdonald and Clark (1970). Note that the extrapolation of the curves for  $4.3 \times 10^5/\text{mL}$  (10  $\mu\text{L}$ ) and  $9.3 \times 10^5/\text{mL}$  (20  $\mu\text{L}$ ) cell concentrations in Figure 5-5 to the ferrous concentration axis, will result in a very low Michaelis constant,  $K_m$ , value.

The observed pseudo-first order kinetics reported by Pesic et al., (1989) is clearly due to the very low ferrous concentrations employed relative to the cell concentrations. The resulting pseudo-first order kinetics is an approximation of the Michaelis-Menten kinetics, and it applies only when the Michaelis constant,  $K_m$ , is very large. Conversely, when the ferrous concentration is very large, relative to cell concentrations, the Michaelis constant,  $K_m$ , becomes negligible and the oxidation of ferrous ions by *T. ferrooxidans* approach a zero order kinetics. The dependence of kinetic parameters on cell and  $\text{Fe}^{2+}$  concentrations during  $\text{Fe}^{2+}$  oxidation by *T. ferrooxidans* has also been noted by other investigators (Macdonald and Clark, 1970; Kelly and Jones, 1978). Some investigators have attributed the change in kinetic parameters with increasing  $\text{Fe}^{2+}$  concentration to the inhibitory effects of high concentrations of  $\text{Fe}^{2+}$  (Landesman et al., 1966; Kelly and Jones, 1978). Suzuki et al. (1989) reported inhibition of  $\text{Fe}^{2+}$  oxidation by high *T. ferrooxidans* cell concentrations.

## 5.5 CHAPTER SUMMARY

The results obtained in this study have shown that the kinetics of ferrous oxidation by *T. ferrooxidans* shifts from the standard Michaelis-Menten rate kinetics to a first order rate kinetics depending on the relative ferrous and cells concentrations used for the analysis.

The first order analysis used mainly by metallurgists is an approximation of the Michaelis-Menten rate kinetics used by microbiologists. The first order approximation of



the Michaelis-Menten kinetics holds only above a certain concentration of cell relative to the ferrous concentration. At very high ferrous concentrations and relatively low cell concentrations, the Michaelis-Menten kinetic equation approximates a zero order rate.

## 5.6 REFERENCES

- American Public Health Association. 1985. Standard methods for the examination of water and wastewater. APHA, Washington, DC.
- Baker, R. A., and A. G. Wilshire. 1970. Microbiological factor in acid mine drainage formation: A pilot plant study. Environ. Sci. Technol. 4: 401-407.
- Beck, J. V. 1960. A ferrous-ion-oxidizing bacterium. I. Isolation and some general physiological characteristics. J. Bacteriol. 79: 502-509.
- Colborn, R. P., and M. J. Nicol. 1973. An investigation into the kinetics and mechanism of the oxidation of iron (II) by oxygen in aqueous chloride solutions. J. S. Afr. Inst. Min. Met. 73: 281-289.
- Colmer, A. R., and M. E. Hinkle. 1947. The role of microorganisms in acid mine drainage: A preliminary report. Science. 106: 253-256.
- Crundwell, F. K. 1987. Kinetics and mechanism of the oxidative dissolution of a zinc sulfide concentration in ferric sulfate solutions. Hydrometallurgy. 19: 227-242.
- Huffman, R. E., and N. Davidson. 1956. Kinetic of the ferrous iron-oxygen reaction in sulfuric acid solution. J. Am. Chem. Soc. 78: 4836-4845.
- Kelly, D. P., and C. A. Jones. 1978. Factors affecting metabolism and ferrous iron oxidation in suspensions and batch cultures of *Thiobacillus ferrooxidans*: Relevance to ferric iron leach solution regeneration. Metallurgical applications of bacterial leaching and related microbiological phenomena, L. E. Murr, A. E. Torma, and J. A. Brierley (eds.). Academic Press, New York. pp. 19-44.

- Landesman, J., D. W. Duncan, and C. C. Walden. 1966. Iron oxidation by washed cell suspensions of the chemoautotroph, *Thiobacillus ferrooxidans*. *Can. J. Microbiol.* 12: 25-33.
- Leathen, W., S. Braley Sr., and L. D. McIntyre. 1953. The role of bacteria in the formation of acid from certain surfuritic constituents associated with bituminous coal; Part 2, ferrous iron oxidizing bacteria. *Appl. Microbiol.* 1: 65-68.
- Leathen, W. W., A. N. Kinsel, and S. A. Braley Sr. 1956. *Ferrobacillus ferrooxidans*: A chemosynthetic autotrophic bacterium. *J. Bacteriol.* 72: 700-704.
- Lineweaver, H., and D. Burke. 1934. Determination of enzyme dissociation constants. *J. Am. Chem. Soc.* 56: 658-666.
- Lizama, H. M., and I. Suzuki. 1989. Synergistic competitive inhibition of ferrous oxidation by *Thiobacillus ferrooxidans* by increasing concentrations of ferric iron and cells. *Appl. Environ. Microbiol.* 55: 2588-2591.
- MacDonald, D. G., and R. H. Clark. 1970. The oxidation of aqueous ferrous sulfate by *Thiobacillus ferrooxidans*. *Can. J. Chem. Eng.* 48: 669-676.
- Marchant, P. B. 1986. Commercial piloting and the economic feasibility of plant scale continuous tank leaching at Equity Silver Mines Limited. *Fundamental and applied biohydrometallurgy*, R. W. Lawrence, R. M. R. Branion, and H. G. Ebner (eds.). Elsevier, Amsterdam. pp. 53-76.
- McCready, R. G. L., D. Wadden, and A. Marchbank. 1986. Nutrient requirement for the in-place leaching of uranium by *Thiobacillus ferrooxidans*. *Hydrometallurgy.* 17: 61-71.
- Morrison, R. M. 1989. The dissolution of silver in ferric sulfate-sulfuric acid media. *Hydrometallurgy.* 22: 67-85.
- Omura, T., T. Umita, V. Nenov, J. Aizawa, and M. Onuma. 1991. Biological oxidation of ferrous iron in high acid mine drainage by fluidized bed reactor. *Wat. Sci. Tech.* 23: 1447-1456.

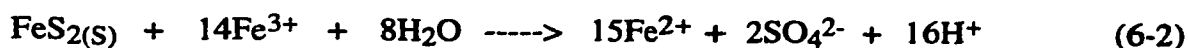
- Pesic, B., D. J. Oliver, and P. Wichlacz. 1989. An electrochemical method of measuring the oxidation rate of ferrous to ferric iron with oxygen in the presence of *Thiobacillus ferrooxidans*. *Biotechnol. Bioeng.* 33: 428-439.
- Silverman, M. P. 1967. Mechanism of bacterial pyrite oxidation. *J. Bacteriol.* 94: 1046-1051.
- Silverman, M. P., and Ehrlich, H. L. 1964. Microbial formation and degradation of minerals. *Adv. Appl. Microbiol.* 6: 153-206.
- Singer, P. C., and W. Stumm. 1970. Acid mine drainage: The rate-determining step. *Science.* 167: 1121-1123.
- Suzuki, I., M. H. Lizama, and D. P. Tackaberry. 1989. Competitive inhibition of ferrous iron oxidation by *Thiobacillus ferrooxidans* by increasing concentrations of cells. *Appl. Environ. Microbiol.* 55: 1117-1121.
- Tiwari, B. L., J. Kolbe, and H. W. Hayden Jr. 1979. Oxidation of ferrous sulfate in acid solution by a mixture of sulfur dioxide and oxygen. *Metallurg. Trans. B.* 10: 607-612.
- Torma, A. E. 1983. Biotechnology applied to mining of metal. *Biotechnol. Adv.* 1: 73-80.

## CHAPTER 6

### THE EFFECT OF FERRIC ION ON THE RATE OF FERROUS OXIDATION BY *THIOBACILLUS FERROOXIDANS* \*

#### 6.1 INTRODUCTION

During acid rock drainage (ARD) formation and the bioleaching of metals from ores and concentrates, ferrous and ferric ions are always present in the system. During ARD formation, ferrous ions serve as a substrate for the bacterium, *Thiobacillus ferrooxidans*, which is capable of deriving its energy from the oxidation of ferrous ions (Temple and Delchamps, 1953; Cox and Brand, 1984; Ingledew, 1986). The ferric ions produced as a result of the growth of the bacteria in turn serves as a lixiviant for the oxidation of the sulfides and ferrous ions are regenerated in the process (Temple and Delchamps, 1953; Silverman and Ehrlich, 1964; Silverman, 1967; Singer and Stumm, 1970). Thus a ferrous oxidation-sulfide degradation cycle is established during ARD formation (Singer and Stumm, 1970). This cyclical process can be represented by the chemical reactions:



Since the rate of ferric generation by the bacteria, Equation (6-1), and the rate of ferric consumption by the sulfide oxidation reaction, Equation (6-2), are not equal, ferric ions may accumulate over time, depending on the pH of the system. Above a pH of about 4.5 the  $\text{Fe}^{3+}$  formed may be precipitated by the reaction (Kleinmann et al., 1981),

---

\* A version of this chapter, co-authored with N. O. Egiebor and P. M. Fedorak, has been accepted for publication in Applied Microbiology and Biotechnology.



However, under acidic conditions, at which *T. ferrooxidans* is most active (Razzell and Trusell, 1963), the  $\text{Fe}^{3+}$  ions remain in the ionic state and participate in sulfide oxidation. In the presence of the bacteria at acidic pH,  $\text{Fe}^{3+}$  oxidation of the sulfide is the rate-limiting step (Silverman, 1967) and therefore  $\text{Fe}^{3+}$  ions accumulate in the system. In bioleaching, the ferric ions produced by the bacteria are utilized in the leaching of metals from ores and concentrates (Bailey and Handford, 1993; Lawrence, 1994), and ferrous ions produced are in turn used by the bacteria for their growth and  $\text{Fe}^{3+}$  is regenerated. Thus, in both processes, the bacteria comes in contact with increasing ferric/ferrous concentration ratios.

In ARD control and prevention, the aim is to slow down the growth of *T. ferrooxidans*, and its ability to oxidize  $\text{Fe}^{2+}$  to  $\text{Fe}^{3+}$  (Singer and Stumm, 1970; Klienmann and Erickson, 1983; Dugan, 1987) and the subsequent oxidation of sulfides. Conversely, in bioleaching the goal is to improve the growth of *T. ferrooxidans* and its ability to oxidize ferrous to ferric ion (Norris and Kelly, 1978) and the subsequent oxidation of metals from ores and concentrates.

Although some investigators have reported improved  $\text{Fe}^{2+}$  oxidation rates in the presence of low  $\text{Fe}^{3+}$  concentrations (Landesman et al., 1966; Kelly and Jones, 1978), others have reported inhibition at all  $\text{Fe}^{3+}$  concentrations (Kovalenko et al., 1982; Suzuki et al., 1987). The inhibitory effect of  $\text{Fe}^{3+}$  has also been reported to be both competitive and non-competitive (Kelly and Jones, 1978). Lizama and Suzuki (1989) suggested that  $\text{Fe}^{2+}$  oxidation was inhibited by both  $\text{Fe}^{3+}$  ions and *T. ferrooxidans* cells.

Since ARD formation and bioleaching processes involve the production of ferric ions from ferrous ions, the effect of ferric ions on the ability of *T. ferrooxidans* to oxidize ferrous ions is important to both processes. Furthermore, a good knowledge of the mechanism of ARD formation and bioleaching processes will require an understanding of

the effect of  $\text{Fe}^{3+}$ , which is a product of the system, on the oxidation of  $\text{Fe}^{2+}$  ions. The objective of this study was to investigate the effect of ferric ion and cell concentrations on the oxidation kinetics of ferrous ions by *T. ferrooxidans* in acidic medium. The study monitored ferrous concentration, a direct parameter, instead of oxygen consumption, an indirect parameter which has been monitored by others (Landesman et al., 1966; Kelly and Jones, 1978; Lizama and Suzuki, 1989).

## **6.2 MATERIALS AND METHODS**

### **6.2.1 Culture and Medium**

The two strains of *T. ferrooxidans* used in this study were obtained from the American Type Culture collection: ATCC 13598 and ATCC 13661. The composition and condition of the growth medium used is the same as reported in Chapter 4.2.1.

### **6.2.2 Most Probable Number (MPN) Method**

The numbers of *T. ferrooxidans* in cultures and cell suspensions were determined by a 3-tube MPN method. Details of the method has been reported in Section 4.2.3.

### **6.2.3 Preparation of Cell Suspension**

The procedure used for the preparation of cell suspension has been outlined in Section 5.3.4.

### **6.2.4 Determination of Initial Oxidation Rates and pH**

The procedure used for the initial rate of  $\text{Fe}^{2+}$  oxidation in the absence and presence of  $\text{Fe}^{3+}$  ions is the same as described in Section 5.3.5.

### 6.2.5 Total, Ferrous and Ferric Iron Determination

Total Fe and Fe<sup>2+</sup> in the samples were determined by DR/2000 Spectrophotometer and the total Fe verified with Atomic Absorption Spectrophotometry (AAS). Details of the procedure have been reported in Section 2.3.5.

### 6.2.6 Theory and Background

The oxidation of Fe<sup>2+</sup> to Fe<sup>3+</sup> ions by *T. ferrooxidans* can be represented by Equation (6-1). Assuming that Fe<sup>2+</sup> oxidation by whole cells of *T. ferrooxidans* can be considered as a simple enzyme reaction, it can be described by a sequence of reactions represented by:



where E is the Fe<sup>2+</sup>-oxidizing enzyme (from *T. ferrooxidans* cells), S is the substrate (Fe<sup>2+</sup>), ES is the intermediate product, and P is the product (Fe<sup>3+</sup>). If an inhibitor molecule, I, can also combine with the enzyme (E) by the reaction,



in such a way that EI, the product, can no longer bind the substrate (S), and ES cannot bind I, then Equation (6-4) and (6-5) describe the condition of fully competitive inhibition. The oxidizing enzyme, E, will bind only I or only S but not both, and ES will only break down to products. If this is the case, the total enzyme, [E<sub>t</sub>] is given by,

$$[E_t] = [E] + [ES] + [EI] \quad (6-6)$$

However, if the affinity of the enzyme for the substrate is not affected by complexation with the inhibitor (I), and vice versa, then a noncompetitive inhibition results and the total enzyme,  $[E_t]$  is give by,

$$[E_t] = [E] + [ES] + [EI] + [EIS] \quad (6-7)$$

Considering the earlier case, from Equation (6-5), the dissociation constant (inhibition constant),  $K_i$ , is given by,

$$K_i = \frac{[E][I]}{[EI]} = \frac{k_{ii}}{k_i} \quad (6-8a)$$

thus,

$$[EI] = \frac{[E][I]}{K_i} \quad (6-8b)$$

From Equation (6-4),

$$[ES] = \frac{k_1 [E][S]}{(k_2 + k_3)} = \frac{[E][S]}{K_m} \quad (6-9)$$

where  $K_m = \{(k_2 + k_3)/k_1\}$  is the Michaelis constant. Substituting Equations (6-8b) and (6-9) into Equation (6-6) results in,

$$[E_t] = [E] \left( 1 + \frac{[S]}{K_m} + \frac{[I]}{K_i} \right) \quad (6-10a)$$

$$[E] = \frac{[E_t]}{\left( 1 + \frac{[S]}{K_m} + \frac{[I]}{K_i} \right)} \quad (6-10b)$$

Substituting for  $[E]$  in Equation (6-9),

$$[ES] = \frac{[E_t][S]}{K_m \left( 1 + \frac{[S]}{K_m} + \frac{[I]}{K_i} \right)} \quad (6-11a)$$



$$[ES] = \frac{[E_t][S]}{[S] + K_m \left( 1 + \frac{[I]}{K_i} \right)} \quad (6-11t)$$

From Equation (6-4),

$$v = -\frac{dS}{dt} = \frac{dP}{dt} = k_3 [ES] \quad (6-12)$$

therefore, substituting for ES from Equation (6-11b), gives,

$$v = \frac{k_3 [E_t][S]}{K_m \left( 1 + \frac{[I]}{K_i} \right) + [S]} \quad (6-13)$$

If each *T. ferrooxidans* cell has  $\beta$  number of the enzyme, E, capable of oxidizing the substrate, S, to product, P, then  $[E] = \beta[C]$ , where  $[C]$  is the total concentration of viable *T. ferrooxidans* cells. Equation (6-13) therefore becomes,

$$v = \frac{\beta k_3 [C][S]}{K_m \left( 1 + \frac{[I]}{K_i} \right) + [S]} \quad (6-14)$$

Simplifying Equation (6-14),

$$v = \frac{\eta [S]}{K_m \left( 1 + \frac{[I]}{K_i} \right) + [S]} \quad (6-15)$$

where  $\eta = \beta k_3 [C]$ . Inverting Equation (6-15) results in the double-reciprocal type equation (Lineweaver and Burke 1934),

$$\frac{1}{v} = \frac{K_m}{\eta} \left( 1 + \frac{[I]}{K_i} \right) \left( \frac{1}{[S]} \right) + \frac{1}{\eta} \quad (6-16)$$

From Equation (6-16), a plot of  $1/v$  versus  $1/[S]$ , at constant cell concentration and different inhibitor concentrations,  $[I]$ , should give a straight line intercepting the  $1/v$  axis at  $1/\eta$  with the slopes,  $\{K_m/\eta(1+[I]/K_i)\}$ , increasing with the inhibitor concentration.

Also from Equation (6-16),

$$\text{Slope} = \frac{K_m}{\eta} \left( 1 + \frac{[I]}{K_i} \right) \quad (6-17)$$

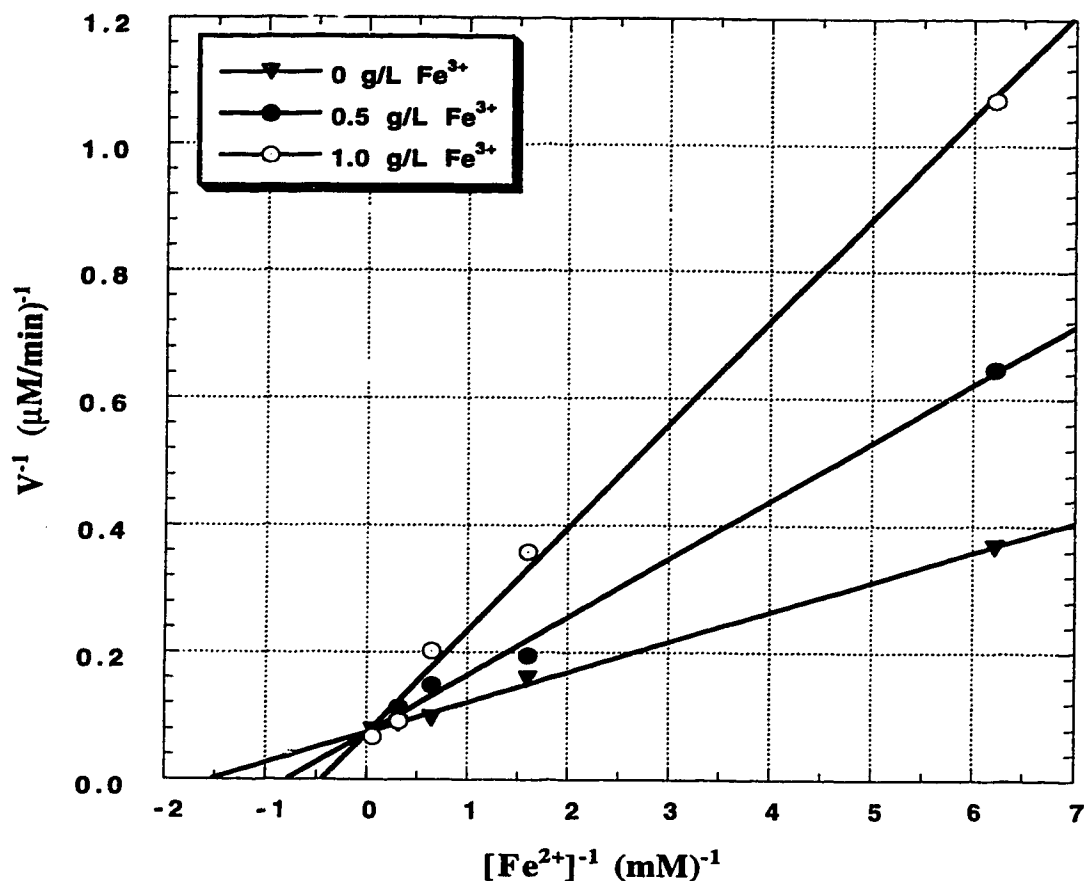
therefore,

$$\text{Slope} = \frac{K_m}{\eta} + \frac{K_m}{\eta K_i} [I] \quad (6-17b)$$

A plot of the slopes (from Equation (6-16)) versus [I] at constant cell concentration should give a straight line with intercepts on the slope and [I] axes of  $K_m/\eta$  and  $-K_i$  (inhibitor constant), respectively.

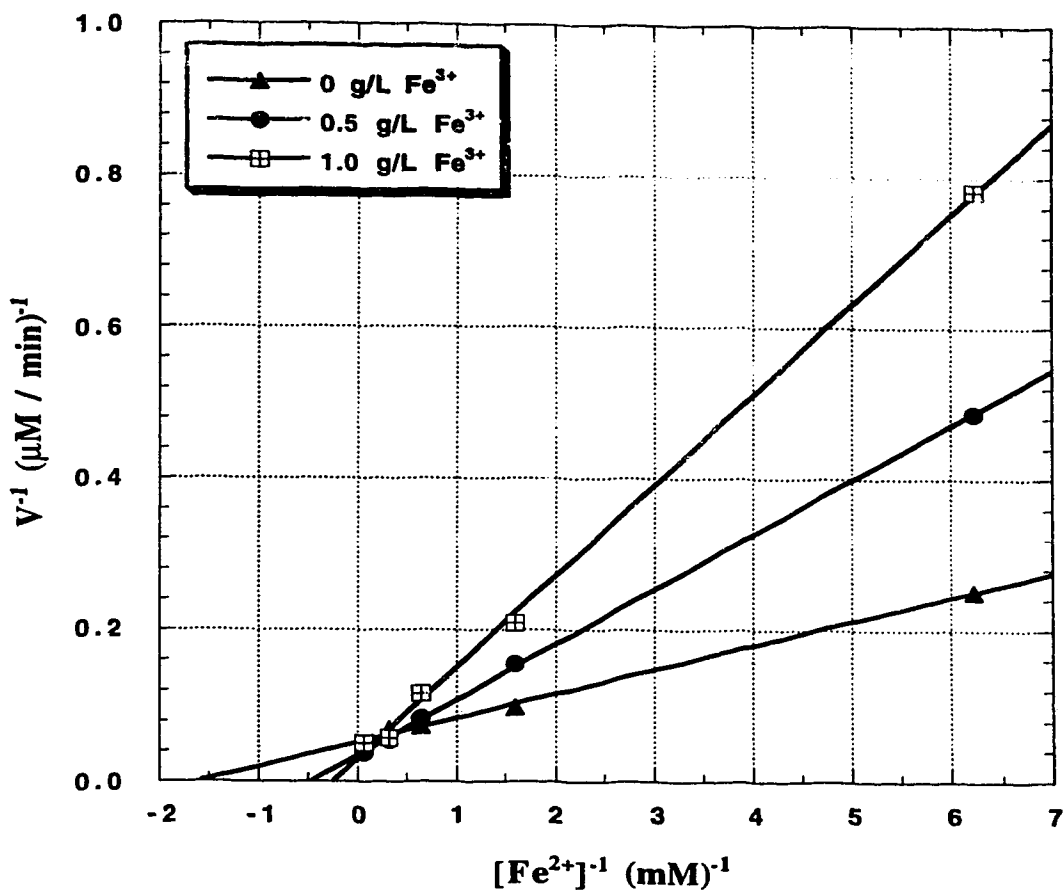
### 6.3 RESULTS AND DISCUSSION

Because Equation (6-16) predicts that a plot of  $1/v$  versus  $1/[S]$  at different inhibitor concentrations, [I], should result in a family of straight lines with slopes of  $\{K/\eta(1+[I]/K_i)\}$ , and an intercept of  $1/\eta$  on the  $1/v$  axis, these values were plotted for each strain of *T. ferrooxidans*. Figure 6-1 shows  $1/v$  versus  $1/[S]$  plot for strain 13598 using  $4.3 \times 10^5/\text{mL}$  of cell concentration and 0, 0.5, and 1.0 g/L  $\text{Fe}^{3+}$ . The double-reciprocal rate ( $v$ ) versus  $[\text{Fe}^{2+}]$  plot show straight lines of increasing slopes with increasing  $\text{Fe}^{3+}$  concentration. The straight lines for the various  $\text{Fe}^{3+}$  concentrations intercept the  $1/v$  axis at a common point, while the absolute values of the intercept on the  $1/[S]$  axis decrease with increasing  $\text{Fe}^{3+}$  concentration. The apparent  $K_m(1+[I]/K_i)$  values therefore increase with increasing concentration of  $\text{Fe}^{3+}$  as expected from Equation (6-16). The 0 g/L  $\text{Fe}^{3+}$  line intercepts the  $1/[S]$  axis at  $-1.5 \text{ mM}^{-1}$  which results in an apparent Michaelis constant,  $K_m$ , value of 0.67 mM  $\text{Fe}^{2+}$ . Figure 6-1 follows a typical competitive inhibition kinetics, since only the slopes vary with  $\text{Fe}^{3+}$  concentration (Zeffren and Hall, 1973).



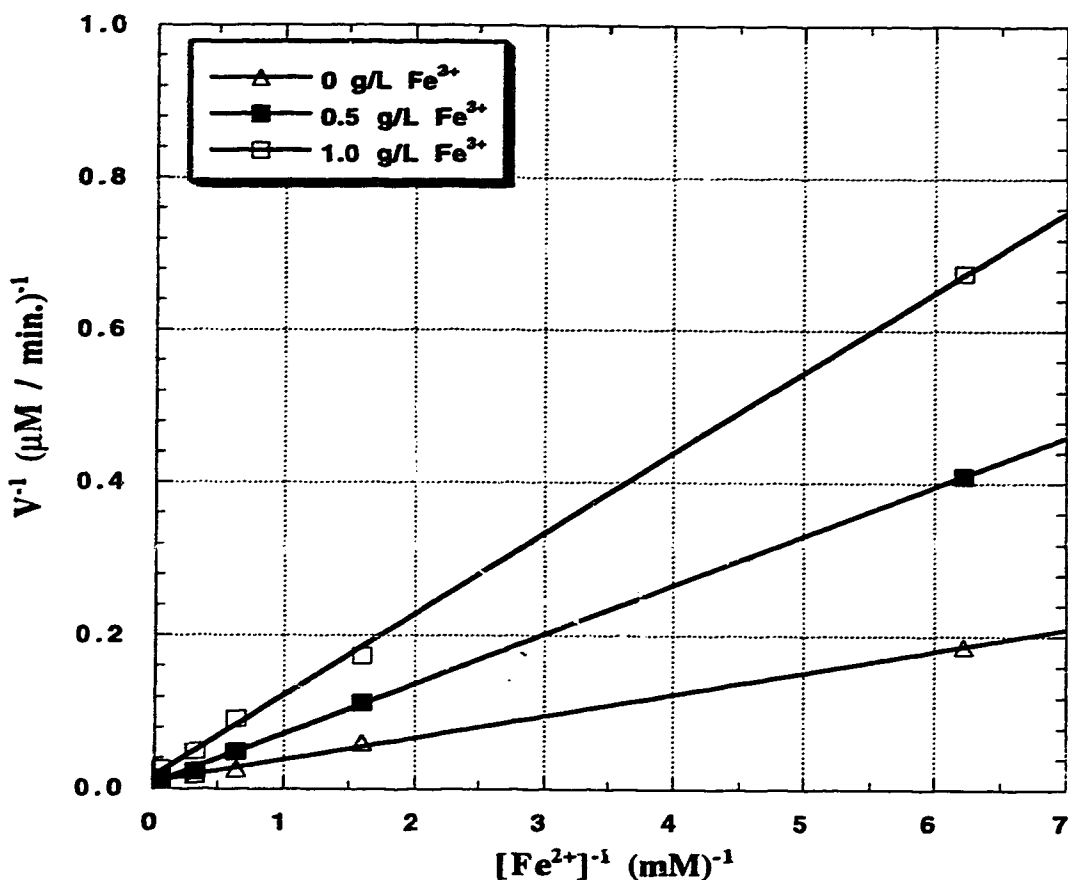
**Figure 6-1. The effect of Fe<sup>3+</sup> concentration on the initial rate of Fe<sup>2+</sup> oxidation using cell concentration of 4.3x10<sup>5</sup>/mL, strain 13598.**

A plot of 1/v versus 1/[S] using 2.3 x 10<sup>6</sup>/mL of cell concentration and Fe<sup>3+</sup> concentrations of 0, 0.5 and 1.0 g/L is shown in Figure 6-2. The plot results in straight lines of increasing slopes with increasing Fe<sup>3+</sup> concentration as was obtained for the 4.3 x 10<sup>5</sup>/mL cell concentration. The 0 g/L Fe<sup>3+</sup> plot intercepts the 1/[S] axis at -1.5 mM<sup>-1</sup>, resulting in a K<sub>m</sub> value of 0.67 mM Fe<sup>2+</sup>. The same K<sub>m</sub> value was obtained for the lower cell concentration, 4.3 x 10<sup>5</sup>/mL, in Figure 6-1.



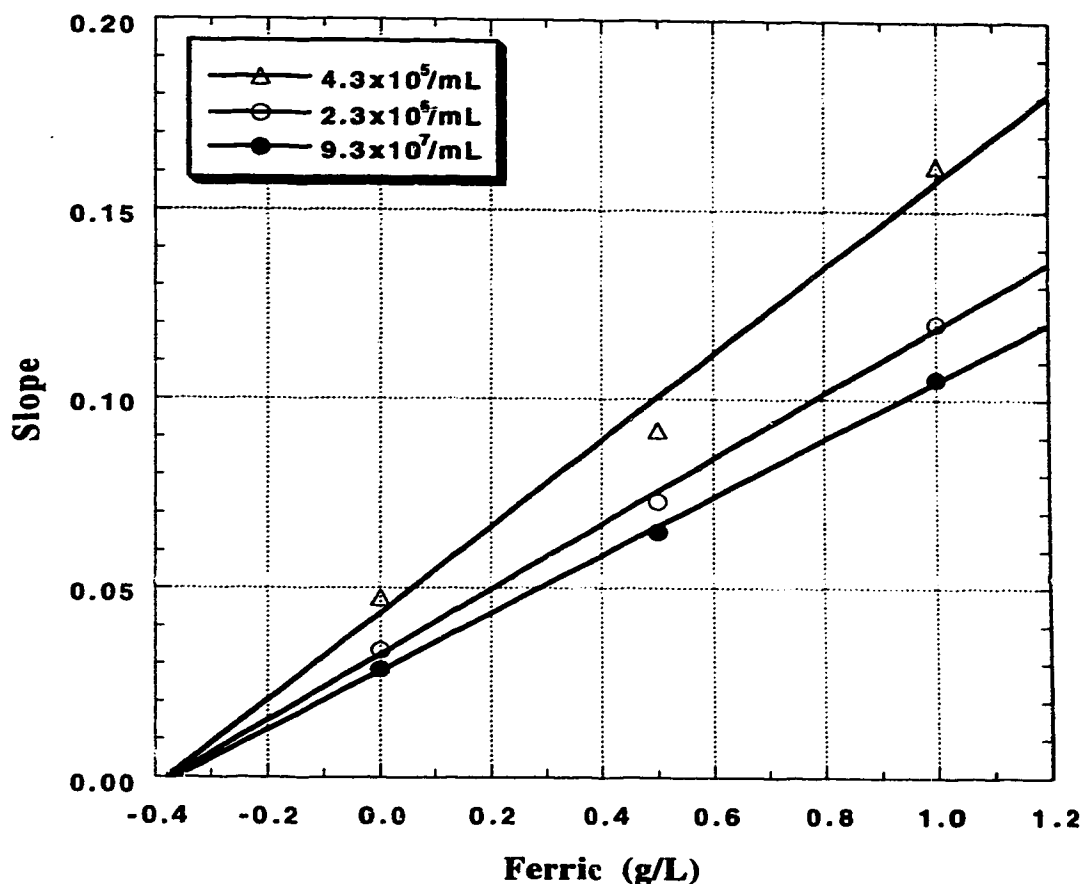
**Figure 6-2. The effect of Fe<sup>3+</sup> concentration on the initial rate of Fe<sup>2+</sup> oxidation using cell concentration of 2.3x10<sup>6</sup>/mL, strain 13598.**

Figure 6-3 illustrates the double reciprocal plot using 9.3 x 10<sup>7</sup>/mL of cell concentration and 0, 0.5, and 1.0 g/L Fe<sup>3+</sup>. At this cell concentration, the double reciprocal plot shows straight lines passing through the origin. The slopes of the lines increased with increasing Fe<sup>3+</sup> concentration. The plot follows a pseudo-first order kinetics with respect to [Fe<sup>2+</sup>] at constant Fe<sup>3+</sup> concentration.



**Figure 6-3. The effect of Fe<sup>3+</sup> concentration on the initial rate of Fe<sup>2+</sup> oxidation using cell concentration of 9.3x10<sup>7</sup>/mL, strain 13598.**

Figure 6-4 shows a plot of the slopes for the 4.3 x 10<sup>5</sup>/mL, 2.3 x 10<sup>6</sup>/mL, and 9.3 x 10<sup>7</sup>/mL cell concentrations against Fe<sup>3+</sup> concentration. The slope plot results in straight lines of decreasing slopes with increasing cell concentration. The linear plots for the various cell concentrations intercept the [Fe<sup>3+</sup>] axis at a common point. A replot of the slopes from Figure 6-4 against the reciprocal of cell concentration, 1/[C], is illustrated in Figure 6-5. The plot shows a straight line with a positive intercept on the slope axis. The slope values increase with the reciprocal of the cell concentrations.



**Figure 6-4. Plot of slopes from double reciprocal graphs at various cell concentrations versus  $\text{Fe}^{3+}$  concentration, strain 13598.**

The test was repeated using *T. ferrooxidans* strain 13661 with similar results as strain 13598. A  $K_m$  value of 0.5 mM  $\text{Fe}^{2+}$  was obtained for cell concentrations of  $2.4 \times 10^6/\text{mL}$  and  $4.3 \times 10^6/\text{mL}$ . At a cell concentration of  $4.3 \times 10^8/\text{mL}$  a pseudo-first order rate kinetics was observed in the presence and absence of  $\text{Fe}^{3+}$ .

While the  $1/v$  versus  $1/[S]$  plots for cell concentrations of  $4.3 \times 10^5/\text{mL}$  and  $2.3 \times 10^6/\text{mL}$  follow a typical Michaelis-Menten kinetics at the  $\text{Fe}^{2+}$  and  $\text{Fe}^{3+}$  concentrations investigated, increasing the cell concentration to  $10^8/\text{mL}$ , results in pseudo-first order approximation of the Michaelis-Menten kinetics. The plots for the  $4.3 \times 10^5/\text{mL}$  and  $2.3 \times$

$10^6/\text{mL}$  cell concentrations for both strains show typical competitive inhibition of  $\text{Fe}^{2+}$  oxidation by  $\text{Fe}^{3+}$  ions. From Equation (6-17b), a plot of slopes (from Equation 6-16) against  $\text{Fe}^{3+}$  concentration should result in straight lines with intercept on the  $[\text{Fe}^{3+}]$  axis of  $-K_i$ , the inhibitor constant, if competitive inhibition assumptions are satisfied.

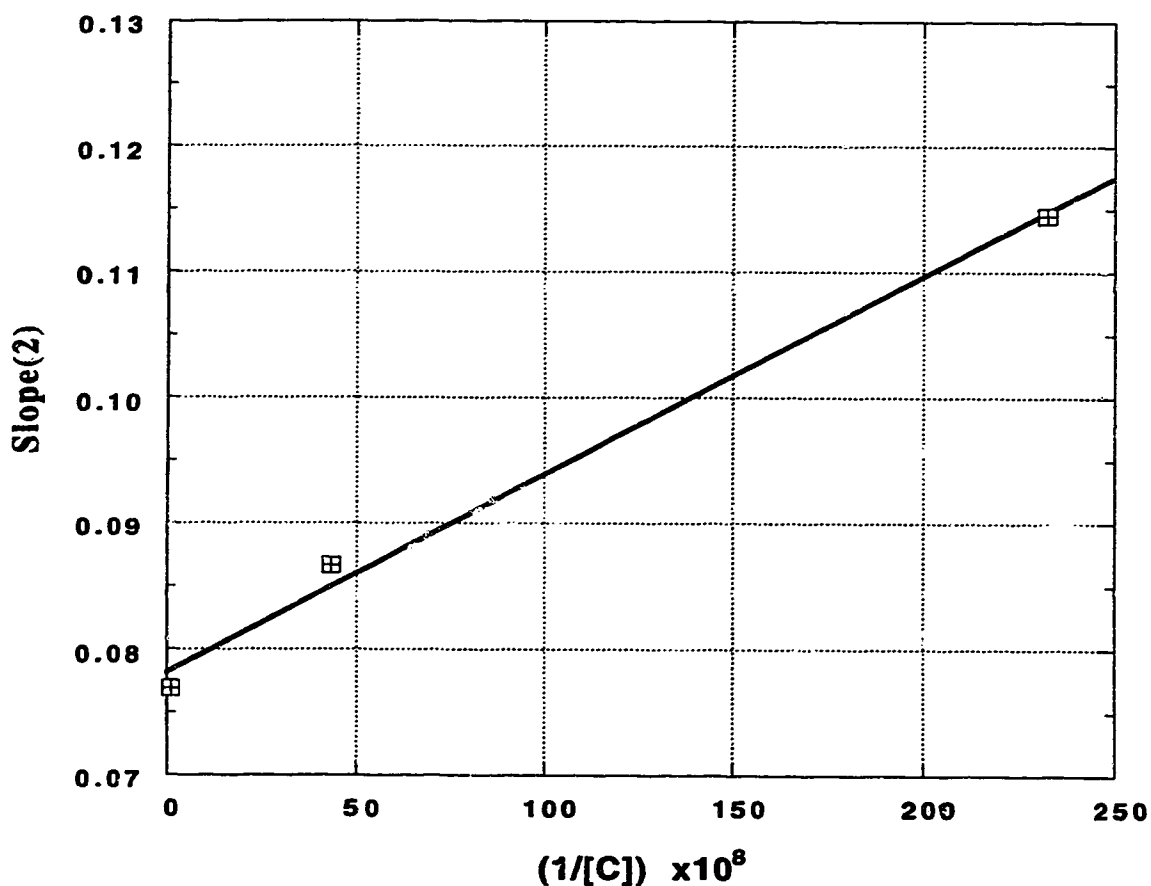


**Figure 6-5. Plot of secondary slopes from Figure 6-4 versus reciprocal of cell concentration, strain 13598.**

Strain 13598, therefore, gave an inhibitor constant,  $K_i$ , of 0.35 g/L (6.3 mM)  $\text{Fe}^{3+}$ , from Figure 6-4. The intercept of -0.4 g/L on the  $[\text{Fe}^{3+}]$  axis for strain 13661, (graph not shown), results in an inhibitor constant,  $K_i$ , of 0.4 g/L (7.1 mM)  $\text{Fe}^{3+}$ . The apparent

inhibitor constant for  $\text{Fe}^{3+}$  varies in the literature. Suzuki et al. (1987) report  $K_i$  values of 1.5 to 10 mM  $\text{Fe}^{3+}$  for different strains of *T. ferrooxidans*, while values of 8 to 10 mM  $\text{Fe}^{3+}$  were reported earlier by Kelly and Jones (1978). By considering both *T. ferrooxidans* cells and  $\text{Fe}^{3+}$  as inhibitors of  $\text{Fe}^{2+}$  oxidation, Lizama and Suzuki (1989) reported a  $K_i$  value of 0.64 mM. The inhibition by the *T. ferrooxidans* cells was, however, attributed to the introduction of  $\text{Fe}^{3+}$  ions with the cells.

Replotting the slopes from Equation (6-17b), results in:

$$\text{Slope}(2) = \frac{K_m}{\eta K_i} = \frac{K_m}{\beta K_i k_3 [C]} = \frac{K_I}{[C]} \quad (6-18)$$

where  $K_I = \frac{K_m}{\beta K_i k_3}$ , and slope(2) is the slope from Equation (6-17b). Therefore from Equation (6-18), replotting slope(2) versus the reciprocal of cell concentration should theoretically result in a straight line passing through the origin. However, plots of slope(2) against  $1/[C]$ , for both strains (Figure 6-5 and a plot for strain 13661 not shown) resulted in straight lines with positive intercepts on the slope(2) axis. The straight lines from Figures 6-5 and that for strain 13661 can therefore be represented by the equation:

$$\text{Slope}(2) = \frac{K_I}{[C]} + \xi \quad (6-19)$$

where  $\xi$  is the intercept on the slope(2) axis. It is important to note the difference between Equation (6-18) and (6-19).

In theory, as the cell concentration approaches infinity (i.e.  $1/[C]$  approaches zero), slope(2), which is the reciprocal of the rate of  $\text{Fe}^{2+}$  oxidation in the absence or presence of  $\text{Fe}^{3+}$  should approach zero (Equation 6-18). However, in practice, as the cell concentration is increased, the reciprocal of the rate of oxidation approaches a fixed value,  $\xi$ , and not zero. A similar straight line plot with a positive intercept on the slope axis was obtained by Lizama and Suzuki (1989) using a mine strain of *T. ferrooxidans*. Figure 6-5 shows that increasing cell concentration in the absence or presence of  $\text{Fe}^{3+}$  increases the



rate of  $\text{Fe}^{2+}$  oxidation. Thus, the inhibitory effect of  $\text{Fe}^{3+}$  is reduced by increasing cell concentration at constant  $\text{Fe}^{3+}$  concentration. The  $\text{Fe}^{3+}$  ions compete with the  $\text{Fe}^{2+}$  ions for the enzyme active sites on the *T. ferrooxidans* cells. Increasing cell concentration at a fixed  $\text{Fe}^{3+}$  concentration therefore increases the initial rate of  $\text{Fe}^{2+}$  oxidation by increasing the number of enzymatic active sites available. The increased number of enzyme active sites at constant  $\text{Fe}^{3+}$  concentration translates into reduced inhibitory effect of the  $\text{Fe}^{3+}$  ions when the cell concentration is increased. The inhibitor constant (EI dissociation constant), however, does not change with increasing cell concentration (Figures 6-4). Changes in the inhibitor constant with temperature were reported by Kovalenko et al. (1982).

Because of the experimental design to determine the initial  $\text{Fe}^{2+}$  oxidation rates, insignificant  $\text{Fe}^{3+}$  had formed from the oxidation of  $\text{Fe}^{2+}$  in situ, and the  $\text{Fe}^{3+}$  inhibition can be attributed to the  $\text{Fe}^{3+}$  ions added. In practice therefore, as the  $\text{Fe}^{2+}/\text{Fe}^{3+}$  concentration ratio decreases in a system, the rate of  $\text{Fe}^{2+}$  oxidation also decreases (Beck, 1960; Mishra and Roy, 1979; Pesic et al., 1989). In ARD control and prevention, while the decrease in  $\text{Fe}^{2+}$  oxidation rate with decreasing  $\text{Fe}^{2+}/\text{Fe}^{3+}$  ratio is desirable, in bioleaching processes it is not. The bacteria, however, reduce the inhibitory effect of  $\text{Fe}^{3+}$  during ARD formation by the formation of ferric hydroxysulfates and jarosite (Pesic and Kim, 1993; Bhatti et al., 1993) which reduces the  $\text{Fe}^{3+}$  concentration in solution.

#### 6.4 CHAPTER SUMMARY

The results of the study shows that  $\text{Fe}^{3+}$  competitively inhibits the oxidation of  $\text{Fe}^{2+}$  by *T. ferrooxidans*. Increasing the concentration of cells does not change the inhibitor constant, however, increasing cell concentration at a constant inhibitor concentration increases the rate of  $\text{Fe}^{2+}$  oxidation. Thus increasing cell concentration decreases the inhibitory effect of  $\text{Fe}^{3+}$  on  $\text{Fe}^{2+}$  oxidation by the bacteria.

## 6.5 REFERENCES

- Bailey, A. D., and G. S. Hansford. 1993. Factors affecting bio-oxidation of sulfide minerals at high concentrations of solid: A review. *Biotech. Bioeng.* 42: 1164-1174.
- Beck, J. V. 1960. A ferrous-ion-oxidizing bacterium. I. Isolation and some general physiological characteristics. *J. Bacteriol.* 79: 502-509.
- Bhatti, M. T. , J. M. Bigham, L. Carlson, and O. H. Tuovinen. 1993. Mineral products of pyrrhotite oxidation by *Thiobacillus ferrooxidans*. *Appl. Environ. Microbiol.* 59: 1984-1990.
- Cox, J. C., and M. D. Brand. 1984. Iron oxidation and energy conservation in the chemoautotroph *Thiobacillus ferrooxidans*. *Microbial Chemoautotrophy*, W. R. Strohl and O. H. Tuovinen (eds.). Ohio State University Press, Columbus. pp. 31-46.
- Dugan, P. R. 1987. Prevention of formation of acid drainage from high-sulfur coal refuse by inhibition of iron- and sulfur-oxidizing microorganisms. II. Inhibition in "run of mine" refuse under simulated field conditions. *Biotech. Bioeng.* 29: 49-45.
- Ingledeavor, W. J. 1986. Ferrous iron oxidation by *Thiobacillus ferrooxidans*. *Biotech. Bioeng. Symp.* 16: 23-33.
- Kelly, D. P., and C. A. Jones. 1978. Factors affecting metabolism and ferrous iron oxidation in suspensions and batch cultures of *Thiobacillus ferrooxidans*: relevance to ferric iron leach solution regeneration. *Metallurgical applications of bacterial leaching and related microbiological phenomena*, L. E. Murr, A. E. Torma, and J. A. Brierley (eds). Academic Press, Inc., New York. pp. 19-44.
- Kleinmann, R. L. P., D. A. Crerar, and R. R. Pacelli. 1981. Biogeochemistry of acid mine drainage and a method to control acid formation. *Min. Eng.* 33: 300-305.
- Kleinmann, R. L. P., and P. M. Erickson. 1983. Control of acid drainage from coal refuse using anionic surfactants. U. S. Bureau of Mines RI 8847.

- Kovalenko, T. V., G. I. Karavaiko, and V. P. Piskunov. 1982. Effect of Fe<sup>3+</sup> ions in the oxidation of ferrous iron by *Thiobacillus ferrooxidans* at various temperatures. *Mikrobiol.* 51: 156-160.
- Landesman, J., D. W. Duncan, and C. C. Walden. 1966. Iron oxidation by washed cell suspensions of the chemoautotroph, *Thiobacillus ferrooxidans*. *Can. J. Microbiol.* 12: 25-33.
- Lawrence, R. W. 1994. Biooxidation for the treatment of refractory gold ores and concentrates - A Canadian perspective. *CIM Bulletin.* 87: 58-65.
- Lineweaver, H., and D. Burke. 1934. Determination of enzyme dissociation constants. *J. Am. Chem. Soc.* 56: 658-666.
- Lizama, M. H., and I. Susuki. 1989. Synergistic competitive inhibition of ferrous iron oxidation by *Thiobacillus ferrooxidans* by increasing concentrations of ferric iron and cells. *Appl. Environ. Microbiol.* 55: 2588-2591.
- Mishra, K. A., and P. Roy. 1979. A note on the growth of *Thiobacillus ferrooxidans* on solid medium. *J. Appl. Bacteriol.* 47: 289-292.
- Norris, P. R., and M. P. Kelly. 1978. Toxic metals in leaching systems. Metallurgical applications of bacterial leaching and related microbiological phenomena, L. E. Murr, A. E. Torma, and J. A. Brierley (eds.). Academic Press, Inc., New York. pp. 83-102.
- Pesic, B., and I. Kim. 1993. Electrochemistry of *Thiobacillus ferrooxidans* interactions with pyrite. *Metallurg. Trans. B.* 24: 717-727.
- Pesic, B., D. J. Oliver, and P. Wichlacz. 1989. An electrochemical method of measuring the oxidation rate of ferrous to ferric iron with oxygen in the presence of *Thiobacillus ferrooxidans*. *Biotechnol. Bioeng.* 33: 428-439.
- Razzell, W. E., and P. C. Trussell. 1963. Isolation and properties of an iron-oxidizing *Thiobacillus*. *J. Bacteriol.* 85: 595-603.

- Silverman, M. P. 1967. Mechanism of bacterial pyrite oxidation. *J. Bacteriol.* 94: 1046-1051.
- Silverman, M. P., and H. L. Ehrlich. 1964. Microbial formation and degradation of minerals. *Adv. Appl. Microbiol.* 6: 153-206.
- Singer, P. C., and W. Stumm. 1970. Acid mine drainage: The rate-determining step. *Science.* 167: 1121-1123.
- Suzuki, I., J. K. Oh, P. D. Tackaberry, and H. Lizama. 1987. Determination of activity parameters in *Thiobacillus ferrooxidans* strains as criteria for mineral leaching efficiency. I. Growth characteristics and effects of metals on growth and on sulfur of ferrous iron oxidation. Proceedings of the 4th Annual General Meeting of Biominet, R. G. L. McCready (ed.). CANMET, SP87-10. pp. 179-209.
- Temple, L. K., and W. E. Delchamps. 1953. Autotrophic bacteria and the formation of acid in bituminous coal mines. *Appl. Microbiol.* 1: 255-258.
- Zeffren, E., and P. L. Hall. 1973. The study of enzyme mechanisms. John Wiley & Sons, Inc., New York. pp. 53-99.

## CHAPTER 7

### MECHANISM OF MICROBIAL OXIDATION OF PYRITE DURING ACID ROCK DRAINAGE FORMATION\*

#### 7.1 INTRODUCTION

Since its isolation by Colmer and Hinkle (1947), *Thiobacillus ferrooxidans* has been regarded as a possible agent in acid rock drainage (ARD) formation. It was initially thought that it merely accelerated the precipitation of  $\text{Fe}(\text{OH})_3$  (Colmer et al., 1950; Temple and Colmer, 1951). Later experiments showed that *T. ferrooxidans* also increased the rate of pyrite oxidation (Leathen, 1953). However, it was not until about two decades after its isolation that Silverman and Ehrlich (1964) proposed two possible mechanisms of bacterial oxidation of sulfides; the indirect and direct contact mechanisms. According to the indirect contact mechanism, ferric ions are the primary oxidants, oxidizing metal sulfides while being reduced in turn to the ferrous state. The bacteria then enter the reaction by oxidizing ferrous ions to the ferric state, thereby regenerating the primary oxidant. Colmer et al. (1950) had earlier observed that the oxidation of  $\text{FeSO}_4$  to  $\text{Fe}_2(\text{SO}_4)_3$  was prevented when the growth of the organism was stopped. Singer and Stumm (1970) later reported that the rate of oxidation of  $\text{Fe}^{2+}$  to  $\text{Fe}^{3+}$  was accelerated by a factor of more than  $10^6$  in the presence of *T. ferrooxidans* when compared to its absence. The direct contact mechanism is said to be independent of ferric ions, requiring intimate physical contact between the bacteria and the sulfide mineral; i.e. a direct oxidative attack on the metal sulfide. Silverman (1967) suggested that the two mechanisms operate concurrently. However, in contrast to the indirect mechanism, Schaeffer et al. (1963) had earlier reported that bacteria

---

\* A version of this chapter, co-authored with N. O. Egiebor and P. M. Fedorak, has been published in the proceedings of sessions and symposia sponsored by The Extraction and Processing Division, edited by G. W. Warren, TMS Annual Meeting in Anaheim, CA. Feb. 4-9, pp. 269-287, 1996.

exerted their catalytic effect only while attached to the pyrite surface. Brierley (1978) also suggested that bacterial adhesion to the sulfide mineral surface is the initial step in the bacterial oxidation of sulfides.

Although it has been known that *T. ferrooxidans* plays an important role in the desulfurization of coal (Mannivannan et al., 1994), microbial flotation (Ohmura and Saiki, 1994; Atkins et al., 1987; Attia, 1990), bioleaching (Marchant, 1986), pretreatment of refractory ores/concentrates (Bailey and Hansford, 1993; Lawrence, 1994; McCready et al., 1986), and ARD formation (Colmer et al., 1950; Temple and Delchamp, 1953; Baker and Wilshire, 1970), the actual mechanism involved in these oxidation processes is still not well understood. While on the one hand the direct attachment of bacteria is said to accelerate sulfide oxidation (Shrihari et al, 1991; Murthy and Natarajan, 1992), on the other hand some researchers have reported that such direct attachments could reduce the rate of sulfide oxidation (Wakao et al., 1984). In spite of the controversies surrounding the mechanism of sulfide oxidation, both the indirect and direct mechanisms have been accepted without full verification (Vitaya and Toda, 1991; Devasia et al., 1993). Most investigators have accepted the direct contact mechanism as proposed based on observing *T. ferrooxidans* attachment onto sulfides minerals (Murr and Berry, 1976). Others have supported the mechanism after observing pitting of sulfides during bioleaching and concluded that the pits were caused by direct attack of bacteria on the sulfides (Bartels et al., 1989; Bennett and Tributsch, 1978).

While there are doubts as to the viability of the direct oxidation mechanism (Wakao et al., 1984), there has been no successful verification of this mechanism. The difficulty in verifying the direct contact mechanism arises from the perceived interdependence of the two mechanisms (Murthy and Natarajan, 1992). The indirect mechanism however has been verified by other investigators (Colmer et al. 1950; Singer and Stumm 1970; Ingledew, 1986). The object of this study was to ascertain whether or not the direct contact

mechanism plays a significant role in the *T. ferrooxidans* assisted oxidation of pyrite during ARD formation.

## 7.2 THEORY AND BACKGROUND

The two mechanisms of sulfide oxidation by *T. ferrooxidans* can only be investigated if the various reactions and reactants that contribute to sulfide oxidation can be identified and separated. The main reactants are bacteria, oxygen, sulfide, ferric iron and  $H^+$ . The two possible pathways by which sulfides can be oxidized are the chemical and the microbiological pathways. The chemical pathway of oxidation of sulfides depend on the pH, oxygen, and  $Fe^{3+}$  concentrations. Oxygen and  $Fe^{3+}$  may oxidize sulfides directly depending on the pH of the medium (Razzell and Trussell, 1963; Silverman, 1967; Lawson, 1982). The microbiological pathway for sulfide oxidation is closely associated with the microbial oxidation of  $Fe^{2+}$  to  $Fe^{3+}$  and possibly the direct oxidation of sulfides by bacteria via the direct contact mechanisms as has been proposed by some researchers (Silverman and Ehrlich, 1964).

To study the chemical and biological pathways of sulfide oxidation, the  $E_h$ -pH diagram for Fe-S- $H_2O$  system was used to design experiments such that one pathway was eliminated while the other was studied. Figure 7-1 shows the  $E_h$ -pH diagram for  $FeS_2$  at 25°C and 1 atmospheric pressure (Hem, 1967). Increasing positive potentials are considered to represent increasing oxidizing conditions. From this diagram (Figure 7-1), both chemical and biological oxidation of dissolved  $Fe^{2+}$  to  $Fe^{3+}$  can be investigated at pH between 0 and 2 depending on the  $E_h$  of the system. At pH 0 to 2, the  $Fe^{2+}$  ions that are oxidized to  $Fe^{3+}$  are not precipitated as  $Fe(OH)_3$  and can be monitored without prior acidification of the samples. For the biological oxidation of  $Fe^{2+}$  to  $Fe^{3+}$ , the other condition that has to be satisfied is the activity of the bacteria in this pH range. *T. ferrooxidans* has been reported to be active at pH between 1 and 5 (Razzell and Trussell, 1963). Razzell and Trussell (1963) reported that the pH limit within which *T. ferrooxidans*

will grow depends on the medium, since iron salts become insoluble above pH 4.0. Both biological and chemical pathways of ferrous oxidation could therefore be studied at pH below 2.

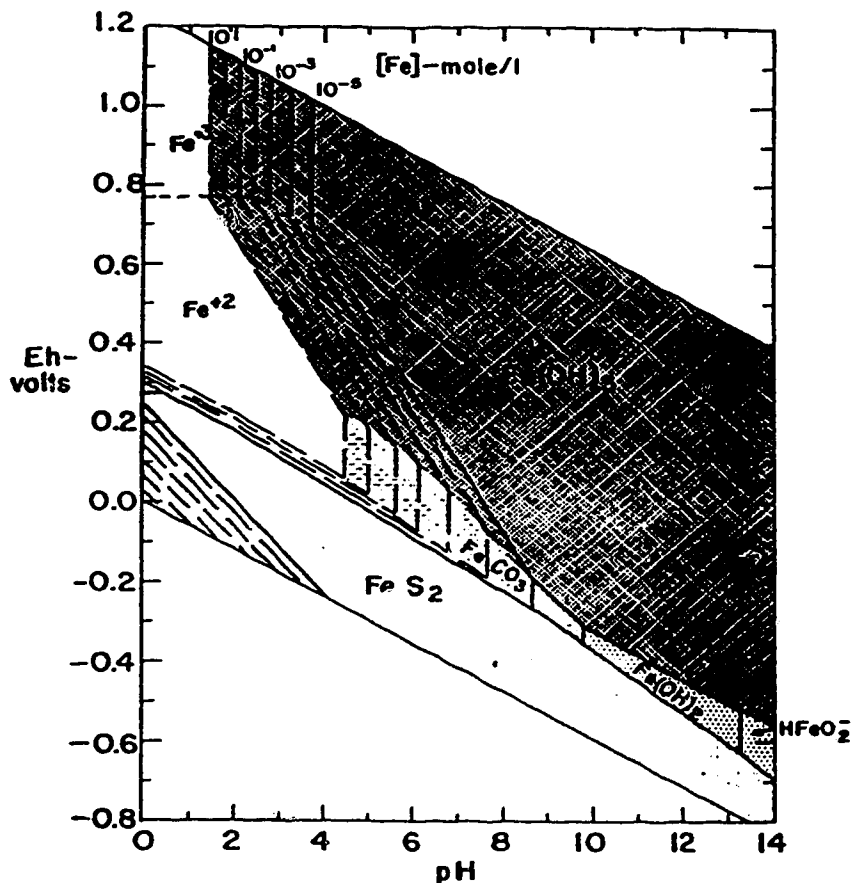


Figure 7-1. Eh-pH diagram for Fe-S-H<sub>2</sub>O system at 25°C and 1 atmosphere.

The chemical oxidation of sulfide can be investigated at pH between 0 and 4 using pyrite, since pyrite is the most abundant sulfide mineral in the earth's crust and has been extensively studied (Vanghan and Craig, 1978). The biological dissolution of pyrite can also be studied by working at pH above 4, and E<sub>h</sub> between 0 and 0.3 V (Figure 7-1). At pH above about 4 and E<sub>h</sub> between 0 and 0.3 V, the chemical oxidation of the pyrite is insignificant, and the direct bacterial attack on the pyrite (direct contact mechanism) can be investigated. Working at pH above 4 will also ensure that any chemical oxidation of the



pyrite during the direct contact mechanism studies, which will result in  $\text{Fe}^{2+}$  generation, will be precipitated as  $\text{Fe}(\text{OH})_3$  after being oxidized by the bacteria to  $\text{Fe}^{3+}$  (Figure 7-1), and therefore not available to chemically oxidize the pyrite. Under this experimental condition, iron solubilization will be due solely to the direct biological oxidation of the pyrite. The only limitation to how high a pH could be used for studying the direct attack mechanism of the pyrite is the activity range of the *T. ferrooxidans* cells which could be investigated. Figure 7-2 shows the pH regions in which thiobacilli is active (Atlas and Bartha, 1993). Superimposing Figures 7-1 and 7-2, it is observed that theoretically, both pathways can be verified with experiments carried out at pH between 1.5 and 5.0.

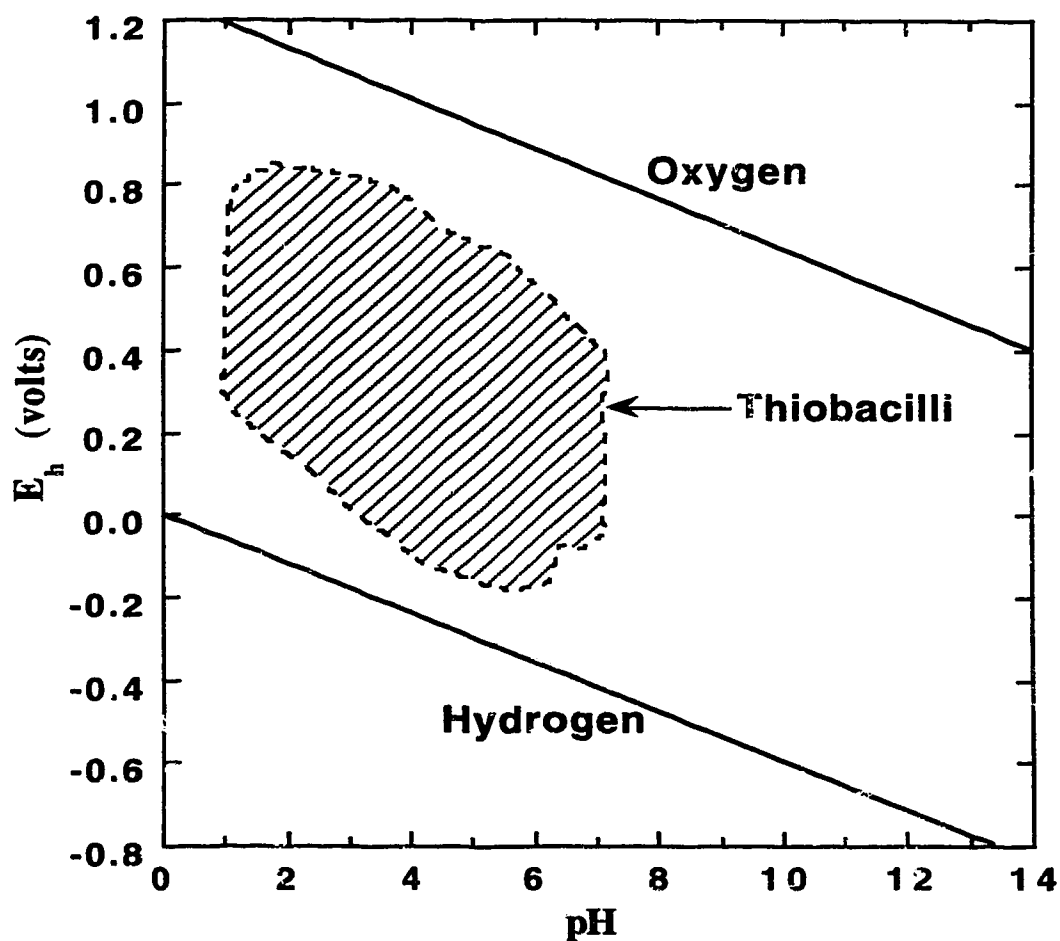


Figure 7-2. The pH and  $E_h$  tolerance contours of thiobacilli. Adapted from Atlas and Bartha (1993).

## 7.3 EXPERIMENTAL

### 7.3.1 Materials

The natural pyrite used for the experiments is the same as that described in Section 2.3.1. All chemical reagents were annular grade obtained from Fisher Scientific, Edmonton, Canada, and used without further purification. The pyrite was ground in a jaw crusher and separated into different size fractions by dry sieving, and stored under nitrogen gas. The -355 +300  $\mu\text{m}$  size fraction was used for this study.

### 7.3.2 Culture and Medium

The *T. ferroxidans* strain ATCC 13661 used in this study, was obtained from the American Type Culture Collection. The medium used for the growth of the microorganisms consisted of two solutions A and B, prepared separately, autoclaved at 121°C and 30 psi for 20 min and mixed aseptically after cooling. Details of the composition of the medium is reported in Section 4.2.1. The mixture of solutions A and B is referred to as the +Fe<sup>2+</sup> growth medium, while solution A is the -Fe<sup>2+</sup> medium. The microorganisms were grown in 500-mL Erlenmeyer flasks containing 75 mL of +Fe<sup>2+</sup> growth medium to ensure sufficient diffusion of oxygen to the bottom of the flask. The inoculated flasks were shaken on an orbital shaker table at a speed of 200 rpm and a temperature of 27°C in the dark.

### 7.3.3 Most Probable Number (MPN) Method

The numbers of viable *T. ferroxidans* cells in cultures and cell suspensions were determined by a 3-tube MPN method. Details of the MPN method are reported in Section 4.2.3.

### **7.3.4 Ferrous-oxidizing Activity of Fe<sup>2+</sup>- and FeS<sub>2</sub>-grown and Colonized Cells**

The ferrous-oxidizing activity of Fe<sup>2+</sup>- and FeS<sub>2</sub>-grown cells and FeS<sub>2</sub>-colonized cells were investigated with Fe<sup>2+</sup>- and FeS<sub>2</sub>-grown and harvested cells, and FeS<sub>2</sub>-attached cells, respectively. The Fe<sup>2+</sup>-grown cells were obtained by growing *T. ferrooxidans* in Fe<sup>2+</sup> medium until the log phase, which occurred after 2 to 3 days of incubation. The cells were harvested by filtering the cultures through Whatman no. 1 filter paper to remove any precipitate that may be present. The filtrate obtained was then centrifuged at 10,000 x g for 10 minutes (Du Pout Sorvall RC-5B refrigerated superspeed centrifuge). The resulting cell pellet was washed by resuspending and centrifuging twice with H<sub>2</sub>SO<sub>4</sub> solution of pH 2. The cells were finally resuspended in a small volume (4 to 5 mL) of H<sub>2</sub>SO<sub>4</sub> solution of pH 2 and used for Fe<sup>2+</sup> oxidation, FeS<sub>2</sub> oxidation, FeS<sub>2</sub> colonization and generation of FeS<sub>2</sub>-grown cells.

The FeS<sub>2</sub>-grown cells were obtained by growing the cells on FeS<sub>2</sub>. The Fe<sup>2+</sup> grown and harvested cells were used to inoculate flasks containing -Fe<sup>2+</sup> medium, growth medium without Fe<sup>2+</sup>, and FeS<sub>2</sub> added as the Fe source and incubated for 12 days. Cells harvested from the first cycle (12 days) flasks were used to inoculate flasks with -Fe<sup>2+</sup> medium and FeS<sub>2</sub> for two more cycles. During the fourth cycle, the MPN, total Fe and Fe<sup>2+</sup> were monitored. At the end of the incubation, the suspension was filtered and the cells in the filtrate harvested. The cells attached to the pyrite particles are referred to as the colonized pyrite cells. The colonized FeS<sub>2</sub> particles which remained on the filter were washed gently with H<sub>2</sub>SO<sub>4</sub> solution of pH 2. Both the harvested cells and the colonized FeS<sub>2</sub> particles were used in Fe<sup>2+</sup> and FeS<sub>2</sub> oxidation tests.

### **7.3.5 Pyrite Oxidation by FeS<sub>2</sub>-Colonized and Fe<sup>2+</sup>-grown Cells**

Pyrite oxidation by FeS<sub>2</sub>-colonized cells experiments involve mixing different portions of the colonized FeS<sub>2</sub> and fresh FeS<sub>2</sub> in -Fe<sup>2+</sup> medium and monitoring the total Fe

concentration in solution. During the test, MPN of the solution was monitored. Pyrite oxidation experiments with  $\text{Fe}^{2+}$ -grown cells employed  $\text{Fe}^{2+}$  grown and harvested cells.

### **7.3.6 Solid and Liquid Phase Relative Activities**

The solid and liquid phase relative activities were investigated by incubating  $\text{Fe}^{2+}$ -grown cells with  $\text{FeS}_2$  in  $-\text{Fe}^{2+}$  medium for 8 days. During incubation, MPN and total Fe concentration were monitored. At the end of the 8th day, two 10-mL and one 40-mL volumes of the suspension were withdrawn into three separate 50-mL flasks. The colonized pyrite from the incubation flask was washed gently and added to one of the 10-mL cell suspensions. The incubation flask was then rinsed with  $\text{H}_2\text{SO}_4$  solution of pH 2, and 20 mL of  $+\text{Fe}^{2+}$  growth medium was added to each of the four flasks and incubated. During incubation, samples were taken for  $\text{Fe}^{2+}$  analysis. The test was performed to give an indication of the viability of cells attached to glass and  $\text{FeS}_2$  surfaces, and whether the activity of cells during  $\text{FeS}_2$  oxidation is in suspension or on the solid surface.

### **7.3.7 Effect of pH on $\text{Fe}^{2+}$ -oxidizing Activity of $\text{Fe}^{2+}$ -grown Cells**

The effect of pH on the activity of the cells was studied by using  $-\text{Fe}^{2+}$  and  $+\text{Fe}^{2+}$  growth medium. The two growth media were mixed in proportions that resulted in a pH 4.5 medium. Drops of  $\text{H}_2\text{SO}_4$  were then added to obtain medium of pH 2.5, 1.5 and 1.0 with the same  $\text{Fe}^{2+}$  concentrations. Two sets of flasks were then set up for each pH using the different pH medium, one set was used as a control, and the other inoculated with cells. All the flasks were incubated in the dark at  $27^\circ\text{C}$ . During incubation, the  $\text{Fe}^{2+}$  concentrations were monitored for each flask.

### **7.3.8 Effect of pH on Chemical and Microbial Oxidation of $\text{FeS}_2$**

In these experiments, the  $\text{FeS}_2$  was washed with  $\text{H}_2\text{SO}_4$  solution of pH 2 for 24 h to remove any soluble Fe. The  $\text{FeS}_2$  suspension was filtered and washed with distilled

water, and the washed FeS<sub>2</sub> weighed into -Fe<sup>2+</sup> growth media of pH 1.5 and 4.5. Harvested Fe<sup>2+</sup>-grown cells were then added to one set of flasks and the other set was used as control, and all the flasks incubated. During incubation, total Fe, soluble Fe, Fe<sup>2+</sup>, E<sub>h</sub>, pH, and the viability (Fe<sup>2+</sup> oxidizing ability) of cells at the initial pH of the test medium were monitored. The viability of cells at the pH 4.5 experiment was monitored by drawing aliquots (1 mL) from the flask. These aliquots were then used to inoculate tubes with Fe<sup>2+</sup> medium also at pH 4.5, and the Fe<sup>2+</sup> concentration remaining in the tubes after 24 h was recorded.

### **7.3.9 Total and Ferrous Iron Analysis**

Total iron was determined by the addition of HCl to the sample to dissolve any iron precipitates formed. The resulting solution was then analyzed for Fe by the use of DR/2000 spectrophotometer after the addition of hydroxylamine hydrochloride, o-phenanthroline and sodium acetate. Details of the method has been reported in Section 4.2.5.

### **7.3.10 Surface Area and Density**

The density of the pyrite was determined with a pynometer (ASTM D167, 1982). The total surface area of FeS<sub>2</sub> particles was determined by BET method and a calculation based on the assumption that each particle is spherical. The average opening of the passing and retaining sieves was used as the average diameter of the particles (Wills, 1988).

### **7.3.11 Scanning Electron Microscopy**

Pyrite samples from the flasks were washed gently with H<sub>2</sub>SO<sub>4</sub> solution of pH 2 and transferred into vials with 2.5% gluteraldehyde to fix the cells. After 24 h, the excess gluteraldehyde was drained, the samples freeze dried, and sputter coated with gold. The

samples were then viewed and photographed with a Hitachi S-2700 scanning electron microscope.

## 7.4 RESULTS AND DISCUSSION

### 7.4.1 Pyrite Oxidation by $\text{Fe}^{2+}$ - and $\text{FeS}_2$ -grown Cells

Figure 7-3 illustrates the oxidation of pyrite in the presence of  $\text{Fe}^{2+}$ - and  $\text{FeS}_2$ -grown *T. ferrooxidans* cells at an initial pH of 2.5 for 20 days, taking the initial number of viable cells (MPN) into consideration. Equal optical densities at 600 nm ( $\text{OD}_{600}$ ) of 0.23 of the  $\text{Fe}^{2+}$ - or  $\text{FeS}_2$ -grown cell suspensions were used in each experiments. The  $\text{OD}_{600}$

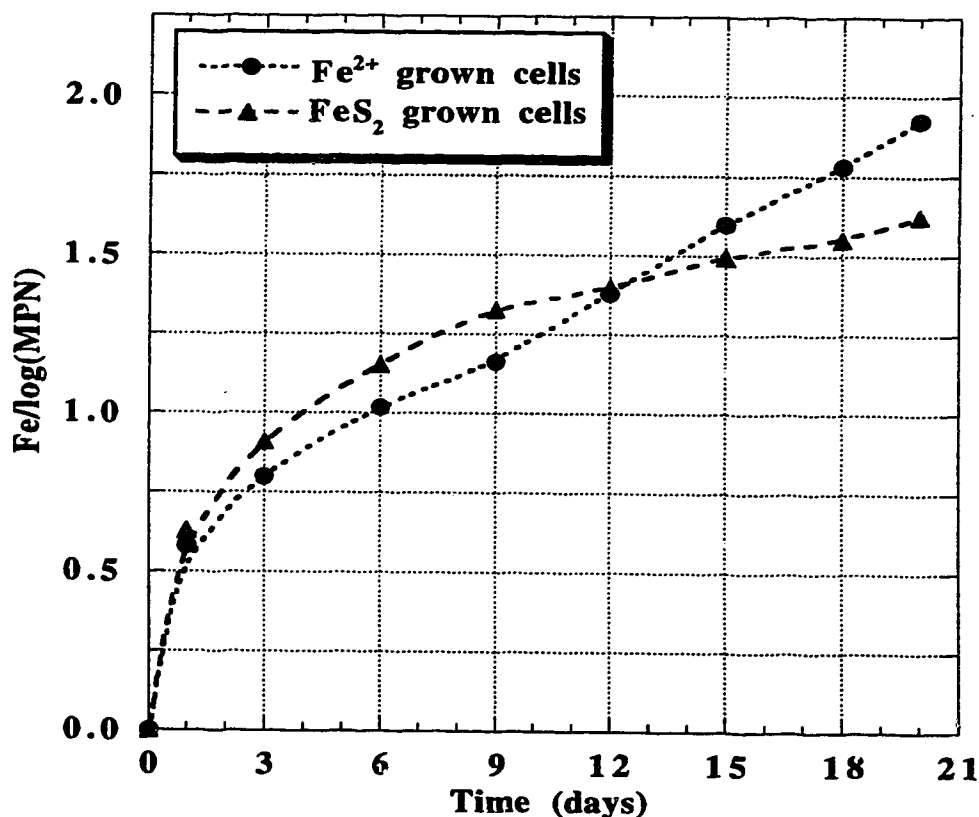


Figure 7-3. Pyrite oxidation of  $\text{Fe}^{2+}$ - and  $\text{FeS}_2$ -grown cells at initial of pH 2.5.

of 0.23 translates to  $1.1 \times 10^7/\text{mL}$  and  $2.1 \times 10^7/\text{mL}$  (statistically the same) of viable cells for the  $\text{Fe}^{2+}$ - and  $\text{FeS}_2$ -grown cell suspensions respectively. Both cultures were harvested in the log growth phase. The figure shows that the  $\text{FeS}_2$ -oxidizing activity (concentration of Fe leached into solution) for both the  $\text{Fe}^{2+}$ - and  $\text{FeS}_2$ -grown cells are almost identical. While it has been reported that the mineral-grown cells are more hydrophobic than the ferrous-grown cells (Devasia et al., 1993), there does not seem to be any significant difference in their pyrite-oxidizing activity. The test results indicates that the  $\text{Fe}^{2+}$ -grown cells are as active in oxidizing  $\text{FeS}_2$  as the pyrite-grown cells over the test period.

#### **7.4.2 Ferrous Oxidation by $\text{Fe}^{2+}$ - and $\text{FeS}_2$ -grown Cells**

The change in the MPN, total Fe and  $\text{Fe}^{2+}$  concentration during colonization of  $\text{FeS}_2$  for 12 days with cell suspension of initial pH of 2.4 is shown Figure 7-4. During colonization, oxidation of the  $\text{FeS}_2$  occurs as is shown by the increasing Fe concentration. The total Fe leached into solution is predominantly in the  $\text{Fe}^{3+}$  state because of bacterial oxidation of  $\text{Fe}^{2+}$  to  $\text{Fe}^{3+}$ . The number of viable cells in suspension was observed to decrease during the colonization due to attachment of bacteria to the solid surfaces.

Figure 7-5 shows  $\text{Fe}^{2+}$ -oxidizing activity by  $\text{Fe}^{2+}$ - and  $\text{FeS}_2$ -grown cells, and  $\text{FeS}_2$ -colonized cells. It is observed that the  $\text{Fe}^{2+}$ - and  $\text{FeS}_2$ -grown cells, and  $\text{FeS}_2$ -colonized cells are capable of oxidizing  $\text{Fe}^{2+}$  in solution. The  $\text{FeS}_2$ -attached cells were therefore viable. The viable cell count of the  $\text{FeS}_2$ -colonized suspension showed  $4.0 \times 10^7/\text{mL}$  on the 8th day, implying that some of the attached cells detached from the  $\text{FeS}_2$  surface and may have multiplied in the liquid medium. The results show that there are active cells in both the liquid medium and on the solid surface.

The rate of the  $\text{Fe}^{2+}$  oxidation by cells in the liquid media and cells attached to  $\text{FeS}_2$  are difficult to compare. However if it is assumed that 45% of the  $\text{FeS}_2$  surface is colonized by active cells (Chang and Myerson, 1982; Ohmuru et al., 1993), and the  $\text{FeS}_2$  particles are spherical, a total surface area of  $9.2 \times 10^8 \mu\text{m}^2$  is calculated for the 0.5 g used.

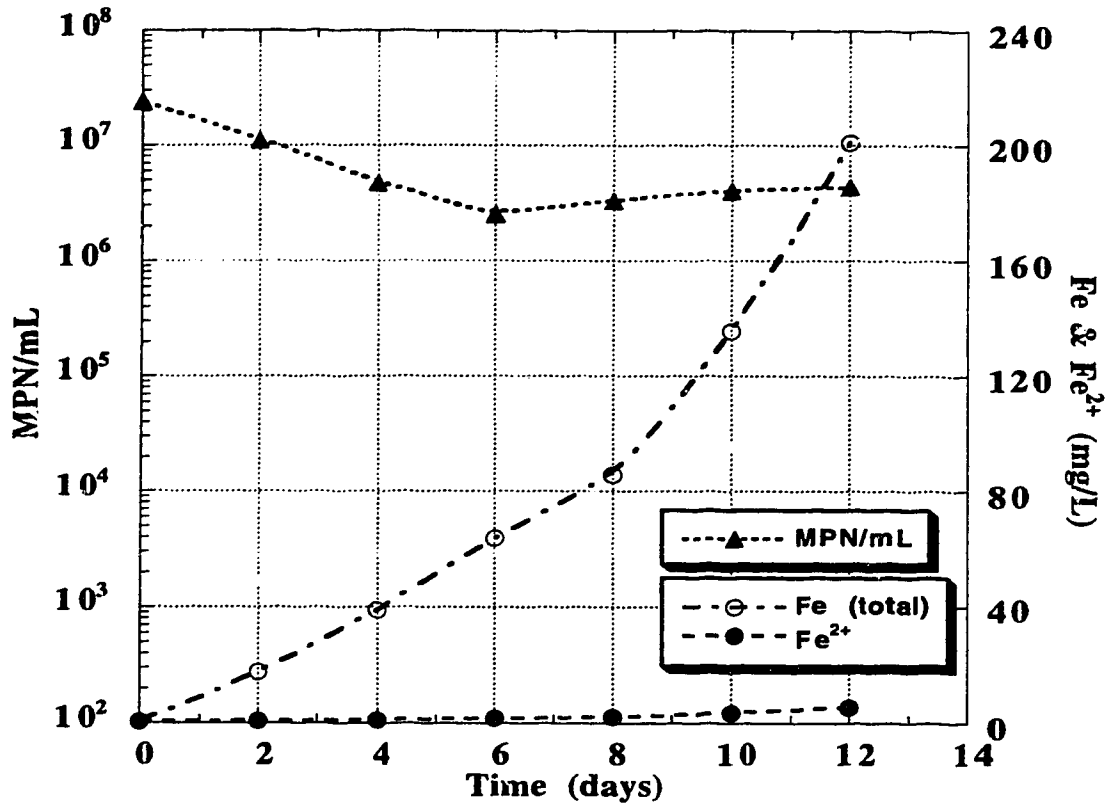


**Figure 7-4. Change in MPN, ferrous and total Fe concentration during colonization of pyrite, initial pH of 2.4.**

The specific gravity of the pyrite used is 4.95. Considering that *T. ferrooxidans* cells are rod shaped with average size of 0.5 by 1.0  $\mu\text{m}$  (Kelly and Harrison, 1989), an average cell covers 0.5  $\mu\text{m}^2$ . It is therefore estimated that a total of  $8.2 \times 10^8$  cells were initially attached to the 0.5 g of pyrite used in the  $\text{Fe}^{2+}$  oxidation experiment. A plot of the  $[\text{Fe}^{2+}]/\log$  (initial viable cells numbers) against time showed that there is a significant difference in the  $\text{Fe}^{2+}$ -oxidizing activity of the  $\text{Fe}^{2+}$ -grown and the  $\text{FeS}_2$ -grown cells (plot same as Figure 7-5). The rate of oxidation of  $\text{Fe}^{2+}$  by the  $\text{FeS}_2$ -colonized cells is lower than those cells already in solution ( $\text{Fe}^{2+}$ -grown and  $\text{FeS}_2$ -grown). The  $\text{FeS}_2$ -colonized cell curve also shows an initial lag phase, when the cells are detaching from the solid substrate.



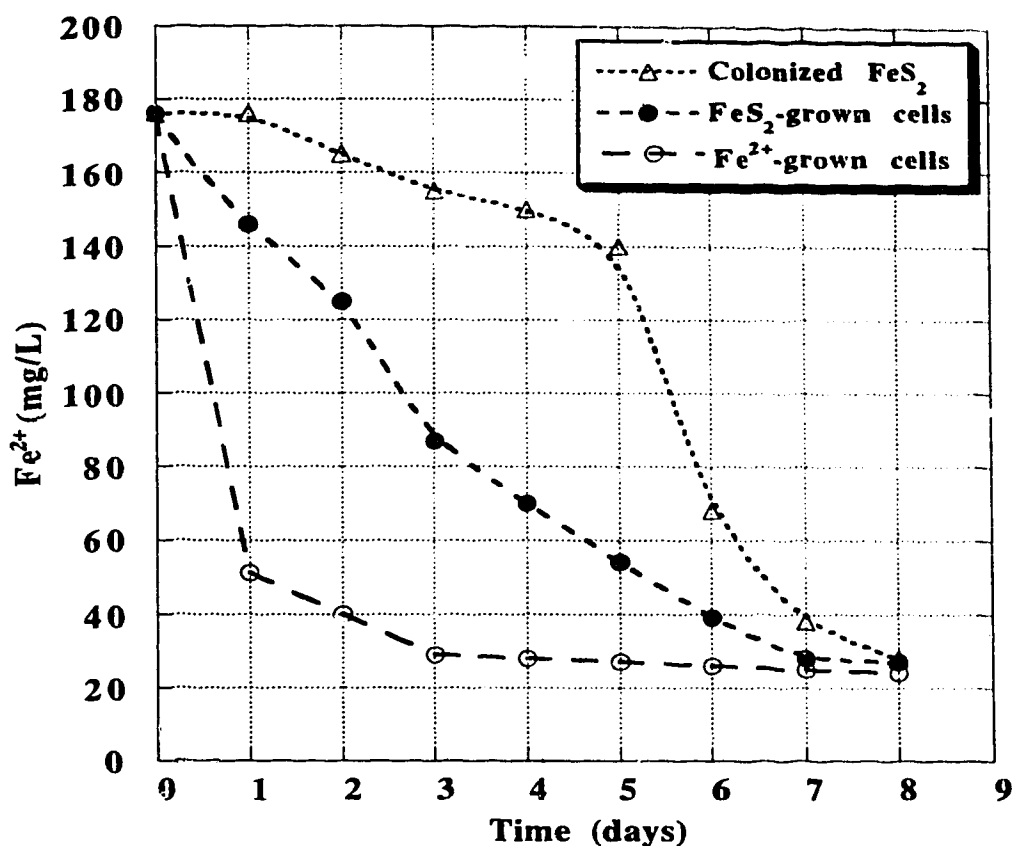
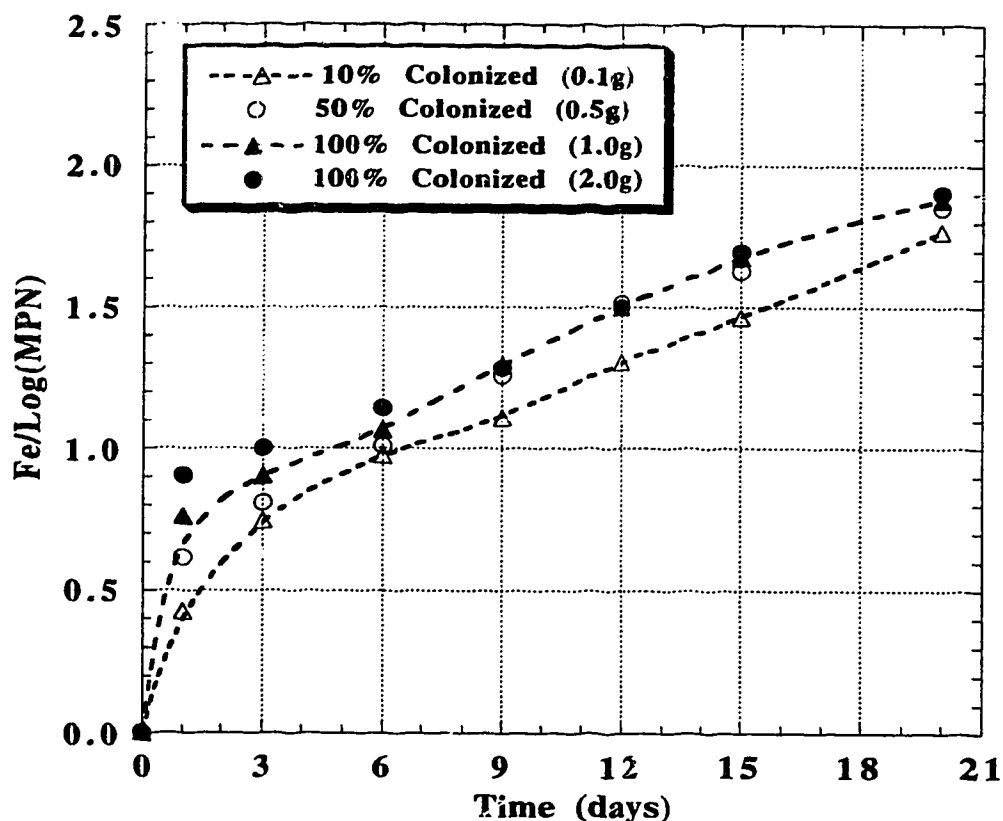


Figure 7-5. Ferrous oxidation by Fe<sup>2+</sup>-grown, FeS<sub>2</sub>-grown, and FeS<sub>2</sub>-colonized cells. (Initial MPN of 2.4x10<sup>9</sup>/mL, 1.2x10<sup>9</sup>/mL and 8.2x10<sup>8</sup>/mL respectively)

#### 7.4.3 Oxidation of FeS<sub>2</sub> by FeS<sub>2</sub>-colonized Cells

To investigate pyrite oxidizing activity of FeS<sub>2</sub>-colonized cells, portions of the colonized pyrite were mixed with fresh FeS<sub>2</sub> in -Fe<sup>2+</sup> growth medium of pH 2.5 and incubated. Figure 7-6 shows a plot of the rate of oxidation taking the initial number of viable cells into consideration, when 10% (0.1 g), 50% (0.5g), 100% (1.0 g) and 100% (2.0 g) colonized FeS<sub>2</sub> were used. The 2 g (100%), 1 g (100%) and 0.5 g (50%) of colonized pyrite show identical rates. All the flasks showed positive MPN results at the

end of the test period, indicating liquid phase activity due to the detachment of some viable cells from the FeS<sub>2</sub> surface.



**Figure 7-6. Pyrite oxidation by FeS<sub>2</sub>-colonized cells. (Initial MPN of  $1.7 \times 10^8/\text{mL}$ ,  $8.2 \times 10^8/\text{mL}$ ,  $1.6 \times 10^9/\text{mL}$ , and  $3.3 \times 10^{10}/\text{mL}$  respectively).**

#### 7.4.4 Effect of Initial Cell Concentration on FeS<sub>2</sub> and Fe<sup>2+</sup> Oxidation

Figure 7-7 shows the effect of initial cell concentration on the oxidation of the FeS<sub>2</sub> at an initial pH of 2.4. Although there is an increase in the rate of oxidation of the FeS<sub>2</sub> with increasing cell concentration from  $2.6 \times 10^5/\text{mL}$  to  $4.6 \times 10^6/\text{mL}$ , there is no significant increase in the pyrite oxidation rate by increasing cell concentration from  $4.6 \times 10^6/\text{mL}$  to  $1.1 \times 10^9/\text{mL}$ . However, increasing cell concentration increased the rate of dissolved Fe<sup>2+</sup> oxidation irrespective of the range in which the increase occurs. Figure 7-8 shows that the

rate of oxidation of  $\text{Fe}^{2+}$  in solution by cells increased with increasing cell concentrations from  $4.3 \times 10^3/\text{mL}$  to  $4.6 \times 10^9/\text{mL}$ . The insignificant increase in  $\text{FeS}_2$  oxidation when the cell concentration is increased beyond  $10^6/\text{mL}$ , and the measureable increase in  $\text{Fe}^{2+}$  oxidation by increasing cell concentration support the mechanistic proposition that the indirect mechanism is the predominant mode in the presence of bacteria. If the direct contact mechanism occurred to a significant extent, an increase in bacterial concentration should give a proportionate increase in rate of  $\text{FeS}_2$  oxidation unless  $\text{FeS}_2$  surface is completely covered at  $4.6 \times 10^6/\text{mL}$ , which is very unlikely as shown from surface area calculations.

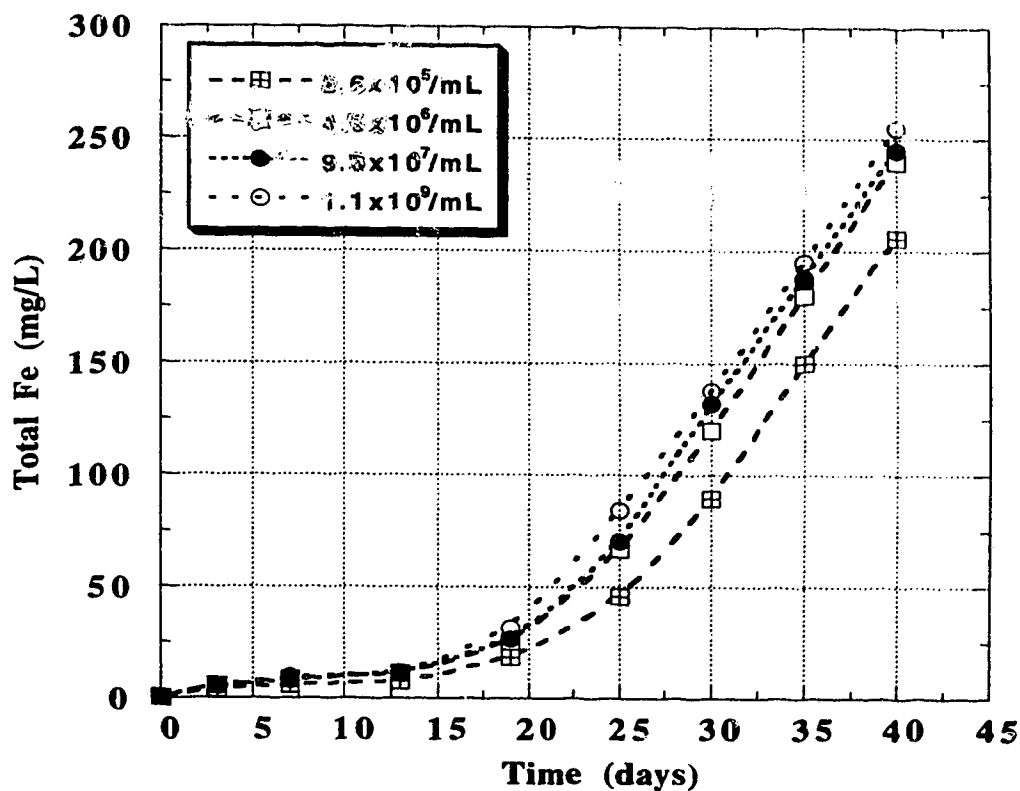


Figure 7-7. The effect of initial cell concentration on pyrite oxidation.

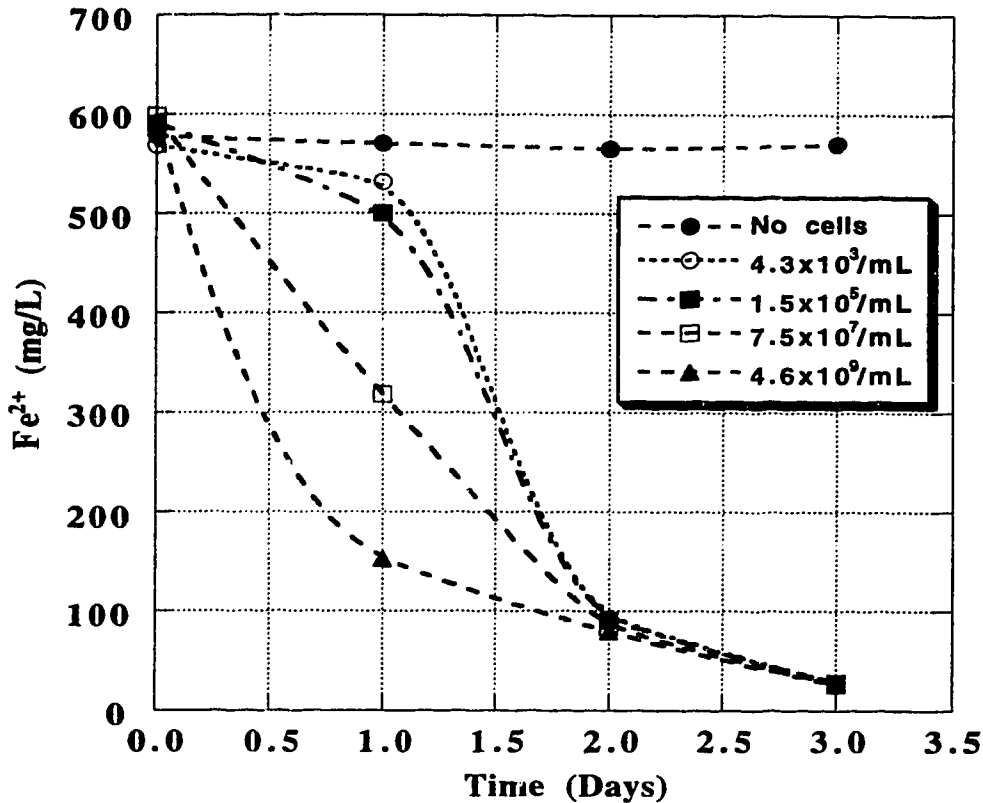


Figure 7-8. The effect of initial cell concentration on ferrous oxidation.

#### 7.4.5 Comparison of Activity of Attached and Suspended Cells

Figure 7-9 shows  $\text{Fe}^{2+}$ -oxidizing activity of suspended,  $\text{FeS}_2$ -colonized and glass-attached cells at initial pH of 2.4. The  $\text{FeS}_2$  particles were colonized for 10 days with  $\text{Fe}^{2+}$  cell suspension of initial pH of 2.4. The 40-mL cell suspension showed higher  $\text{Fe}^{2+}$ -oxidizing activity than 10-mL cell suspension as expected. However, the 10-mL cell suspension without colonized  $\text{FeS}_2$  and the 10-mL suspension with 5 g of colonized  $\text{FeS}_2$  showed similar  $\text{Fe}^{2+}$ -oxidizing activity, with the one without colonized  $\text{FeS}_2$  showing slightly better activity. The results show that the  $\text{FeS}_2$ -colonized cells did not improve the  $\text{Fe}^{2+}$  oxidation rate to any appreciable extent. These results suggest that the liquid phase oxidation activity is higher than that of the solid phase activity as had been reported by

Wakao et al. (1984). The rinsed flask also showed  $\text{Fe}^{2+}$ -oxidizing activity, although at a lower rate, which was attributable to the cells attached to the flask. The glass-attached cells are therefore viable and capable of oxidizing the  $\text{Fe}^{2+}$ . The results show that *T. ferrooxidans* attaches to a variety solid surfaces and not necessarily to pyrite or sulfides only. The attachment of *T. ferrooxidans* to pyrite or sulfides surfaces does not therefore necessarily imply direct oxidation of pyrite (direct mechanism). The attachment of *T. ferrooxidans* to  $\text{SiO}_2$  particles (Myerson and Kline, 1983) and *Sulfolobus* strains to glass surfaces (Wesis, 1973) have been reported. Some investigators have accepted the direct contact mechanism as proposed based on observing *T. ferrooxidans* attachment onto sulfide minerals (Murr and Berry, 1976).

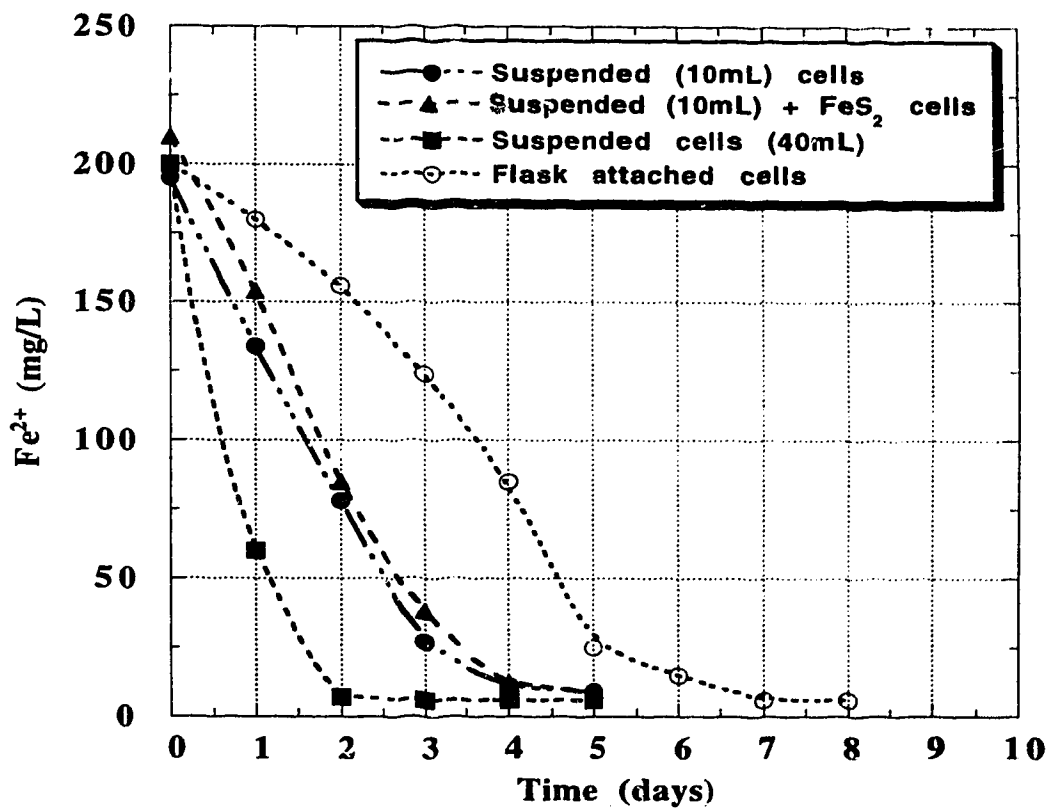


Figure 7-9. Ferrous-oxidizing activity of suspended and attached cells.

#### 7.4.6 Effect of pH on Fe<sup>2+</sup>-oxidizing Activity

Figure 7-10 shows the effect of pH on the Fe<sup>2+</sup>-oxidizing activity of *T. ferrooxidans*. Controls (no cells added) were also incubated for each pH to eliminate errors due to chemical oxidation of Fe<sup>2+</sup>. It is observed that the *T. ferrooxidans* cells are viable and capable of oxidizing Fe<sup>2+</sup> at pH between 1.0 to 4.5, although the rates are slightly higher for pH 1.0 and 1.5, than pH 2 and pH 4.5. There was insignificant chemical oxidation of Fe<sup>2+</sup> in the controls during the experimental period. The results show that Fe<sub>2</sub>S<sub>3</sub> oxidation experiments with *T. ferrooxidans* could be carried out at pH up to 4.5 without compromising the activity of the cells. At these pH and low Fe concentrations, insignificant chemical oxidation of Fe<sup>2+</sup> to Fe<sup>3+</sup> occurs.

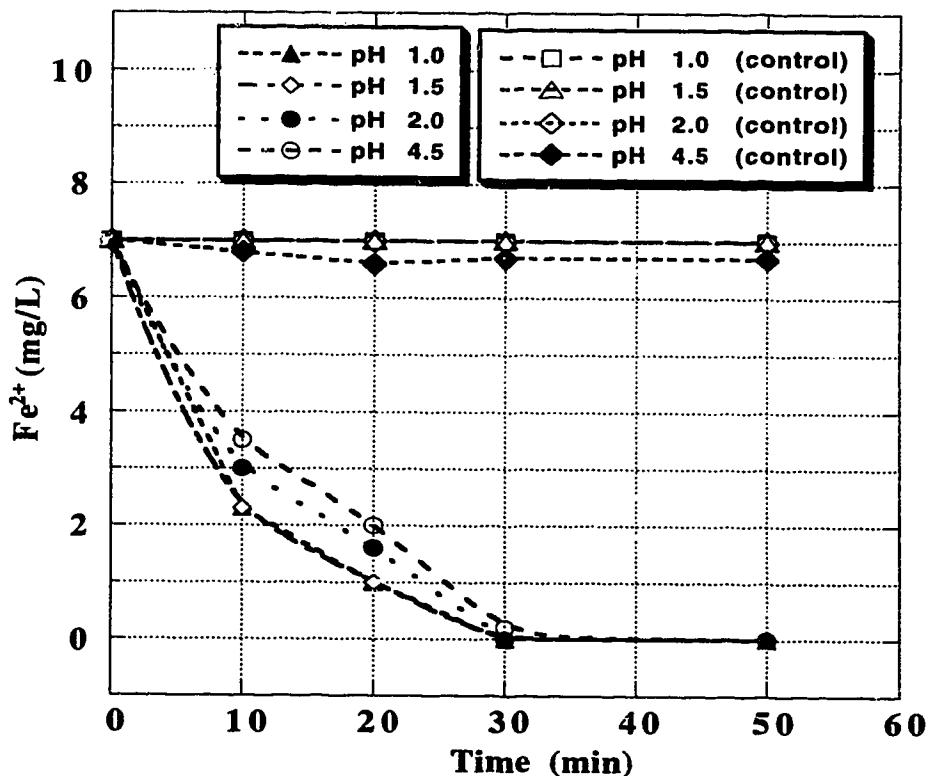


Figure 7-10. Effect of pH on ferrous-oxidizing activity of cells.

### 7.4.7 Effect of pH on Biotic and Abiotic FeS<sub>2</sub> Oxidation

To investigate the direct oxidation mechanism of FeS<sub>2</sub> by cells, biotic and abiotic oxidation of FeS<sub>2</sub> was carried out at pH of 1.5 and 4.5. The FeS<sub>2</sub> particles were washed with H<sub>2</sub>SO<sub>4</sub> (pH 2) for 24 h prior to the oxidation test to remove soluble free Fe. During the test, total Fe, Fe<sup>2+</sup>, pH, E<sub>h</sub>, and viability of cells at the initial pH of the flasks were monitored. Figure 7-11 shows the change in total Fe concentration during abiotic and biotic oxidation of the washed pyrite for 11 days. At pH 1.5, the total Fe concentration for the biotic oxidation is significantly higher than that of the abiotic, while at pH 4.5, both the biotic and abiotic tests showed the same rates without significant oxidation of pyrite after 11 days of testing.

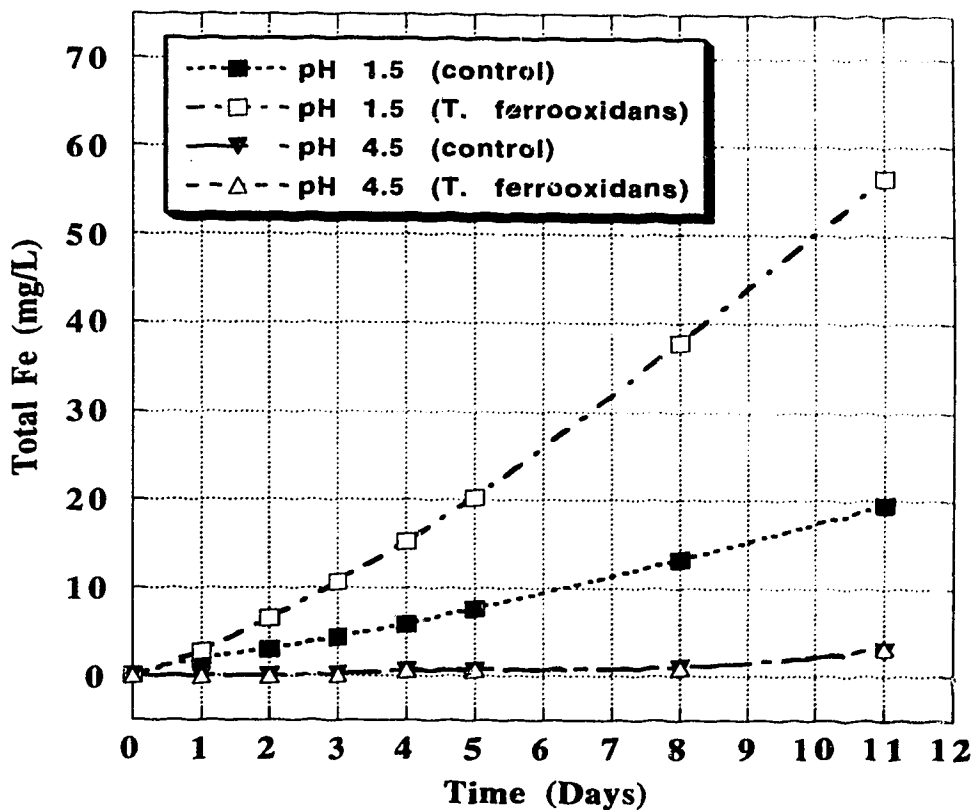
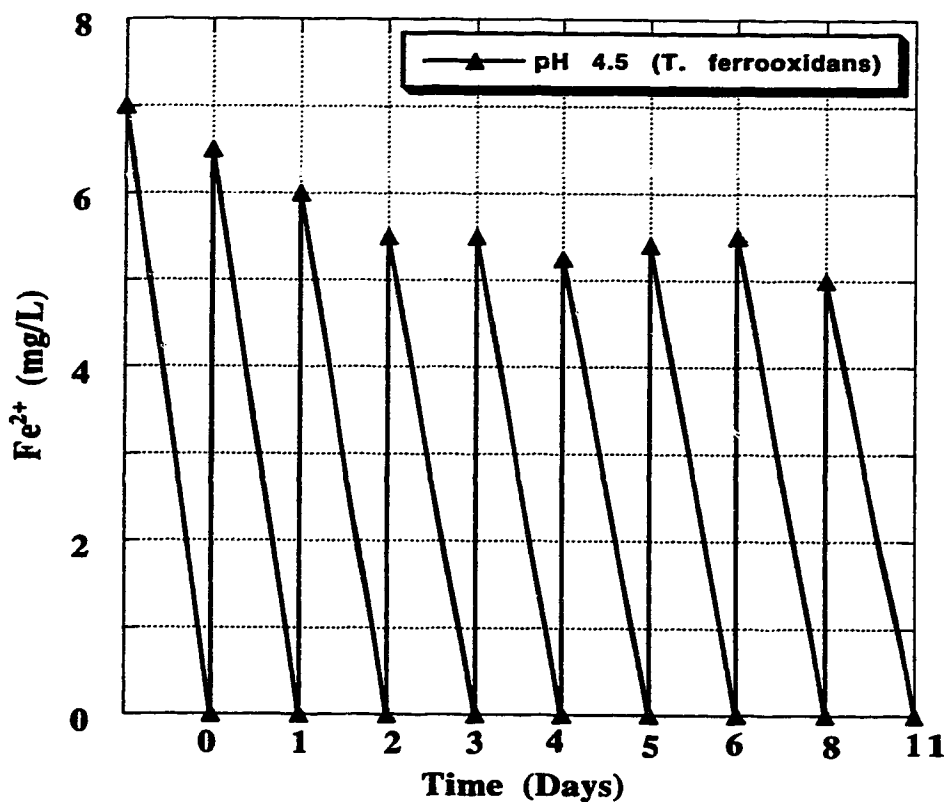


Figure 7-11. Effect of pH on abiotic and biotic oxidation of H<sub>2</sub>SO<sub>4</sub> washed pyrite.

In order to check the viability of the pH 4.5 test cells, samples were taken to inoculate  $\text{Fe}^{2+}$  growth medium at the same pH. These tests were carried out daily for 11 days using fresh  $\text{Fe}^{2+}$  growth medium. Figure 7-12 illustrates the ability of the cells to oxidize dissolved  $\text{Fe}^{2+}$  at the pH of 4.5. The figure shows that the cells in the pH 4.5 tests were capable of oxidizing  $\text{Fe}^{2+}$  throughout the experimental period. Therefore, the cells incubated with pyrite at pH 4.5 remained viable over the 11-day test period and these results suggest that



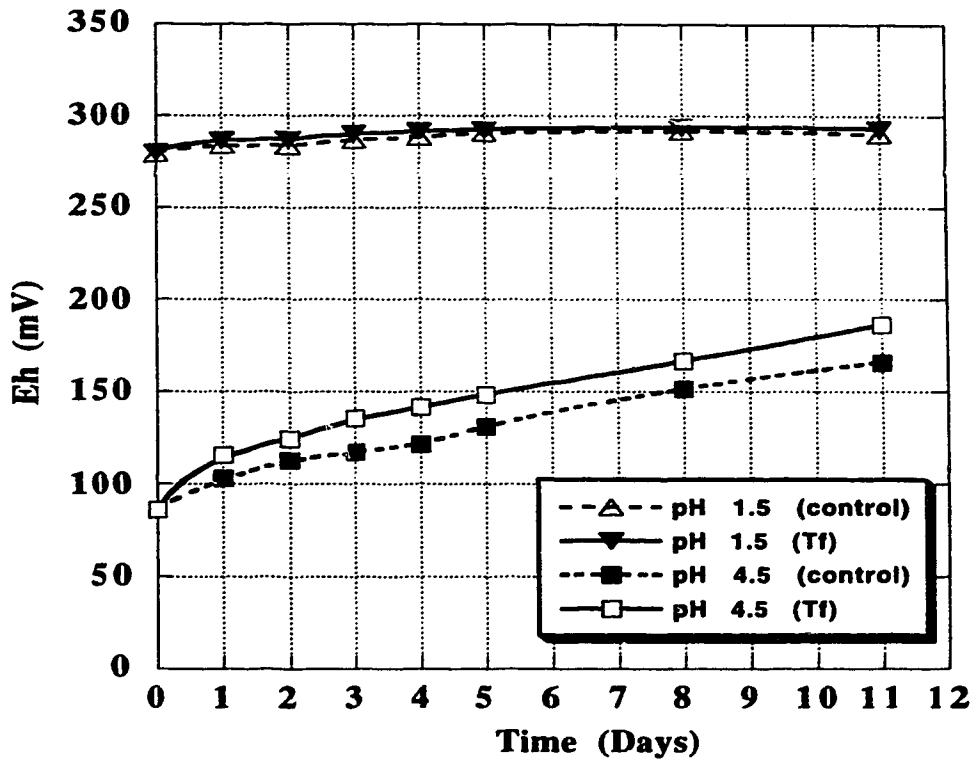
.. **Figure 7-12. Viability of cells tested at pH 4.5 during oxidation of  $\text{H}_2\text{SO}_4$  washed pyrite.**

the cells are only capable of participating in  $\text{FeS}_2$  oxidation after chemical oxidation of the  $\text{FeS}_2$  is initiated to produce  $\text{Fe}^{2+}$  which cannot occur at an appreciable rate at pH 4.5. Razzel and Trussell (1963) also reported that biological oxidation of chalcopyrite did not



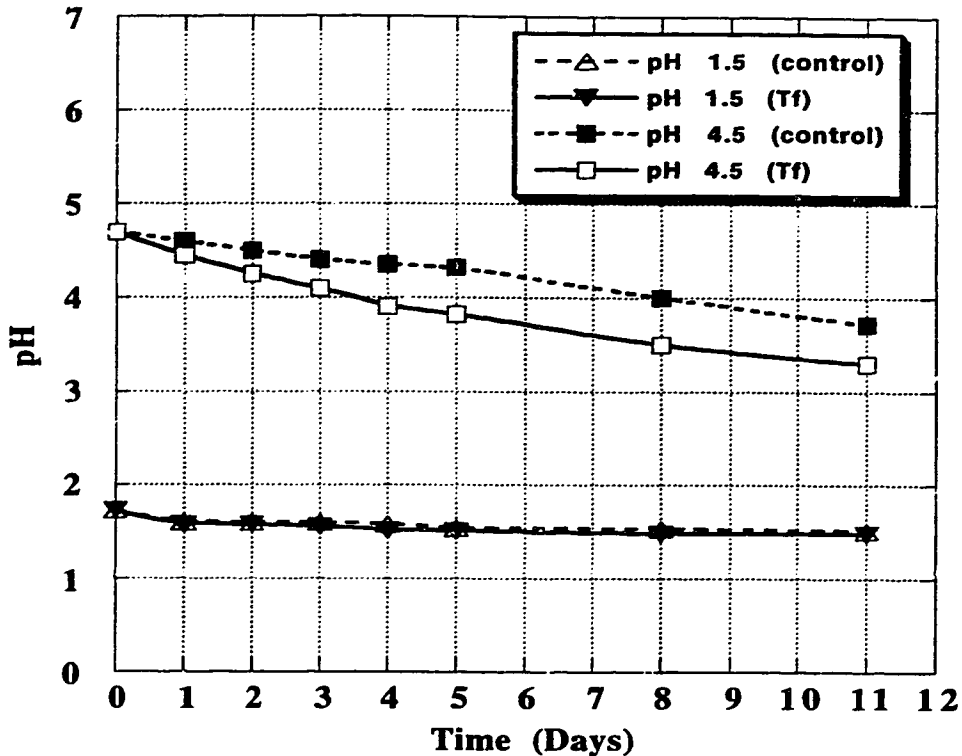
occur at pH above 5. The inability of the cells to oxidize chalcopyrite was however attributed to the inability of the cells to attach to chalcopyrite at pH above 4.

Figure 7-13 shows the changes in  $E_h$  during the experiments. There are no significant differences in the  $E_h$  of the abiotic and biotic flasks of initial pH of 1.5. At pH 4.5, the  $E_h$  of the biotic test is consistently higher than the  $E_h$  of the abiotic test, indicating higher oxidizing conditions.



**Figure 7-13. Change in  $E_h$  during biotic and abiotic oxidation of  $H_2SO_4$  washed pyrite. (Tf denotes *T. ferrooxidans*)**

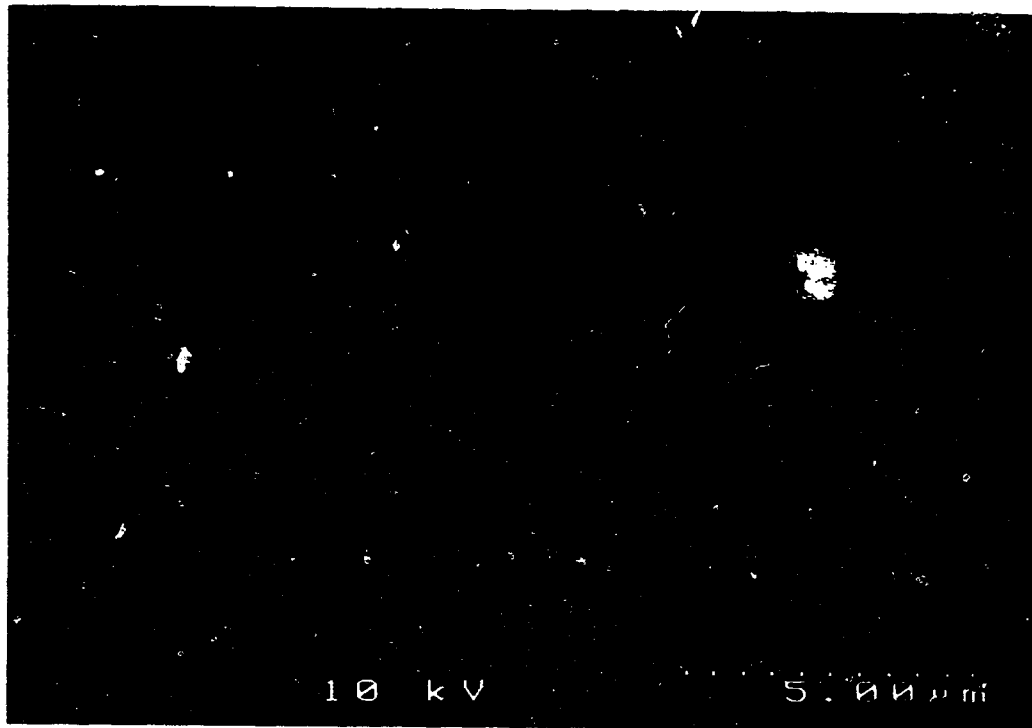
The pH changes (Figure 7-14) also show a similar trend as the  $E_h$ . The pH of the abiotic and the biotic tests with initial pH of 1.5 are the same. At initial pH of 4.5, however, the biotic test shows a lower pH than the abiotic after 1 day of incubation.



**Figure 7-14. Change in pH during biotic and abiotic oxidation of  $H_2SO_4$  washed pyrite. (Tf denotes *T. ferrooxidans*)**

#### 7.4.8 Scanning Electron Microscopy (SEM)

Figure 15a shows SEM micrograph of pyrite particles leached for 6 months in  $-Fe^{2+}$  medium of initial pH of 2.3 without *T. ferrooxidans* cells. It is observed that there is no pitting of the pyrite. Figure 15b, c and d show SEM micrographs of pyrite particles taken from *T. ferrooxidans* inoculated medium with initial pH of 2.3 after 1 month, 2 months and 6 months respectively. Pitting of the  $FeS_2$  can be observed in these micrographs, with bacteria cells in some of the pits. While pitting had been attributed to the direct contact mechanism by other investigators (Bennett and Tributsch, 1978; Bartels et al., 1989), the inability of the cells to oxidize  $FeS_2$  at pH 4.5 where chemical oxidation is eliminated and the uniform oxidation of  $FeS_2$  in the control growth medium (without cells)

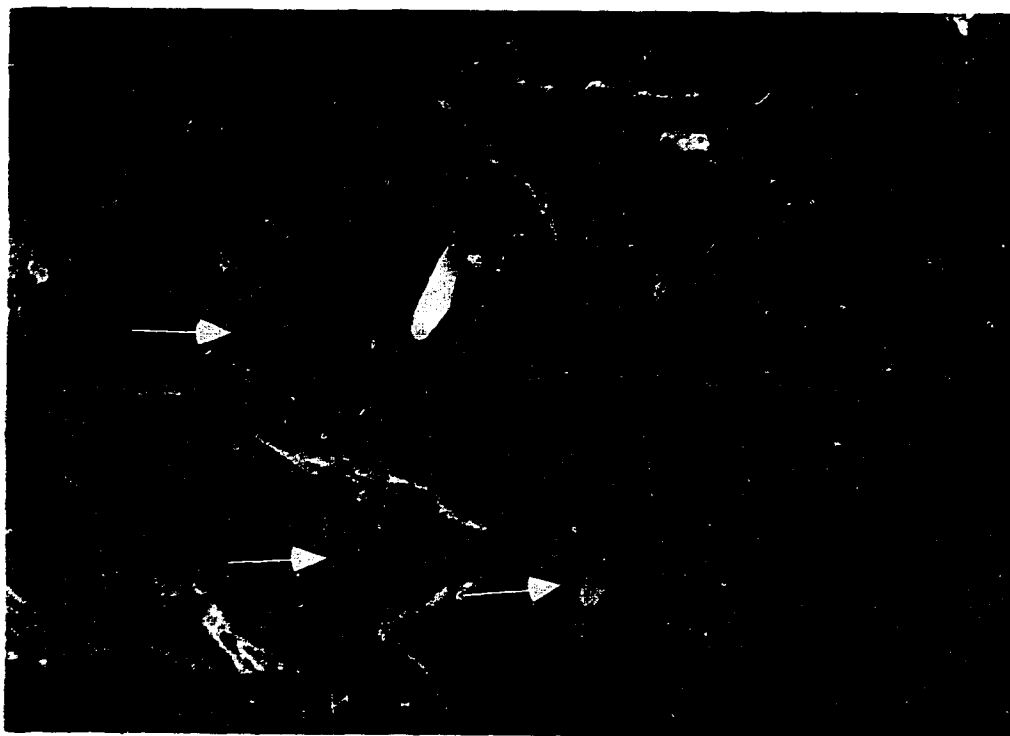


a

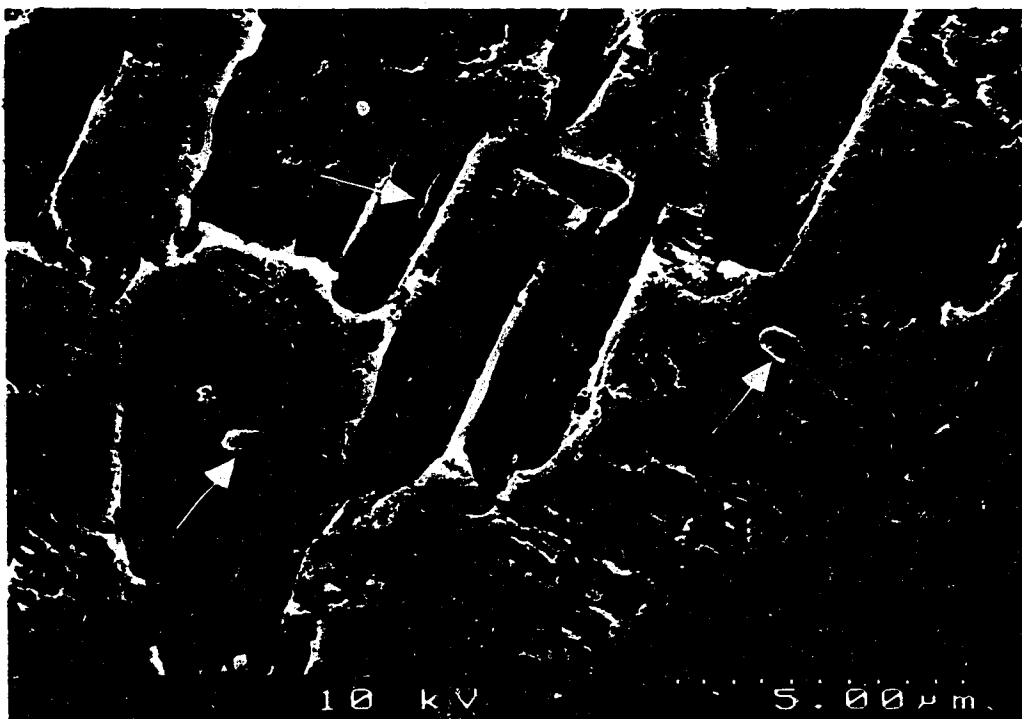


b

**Figure 7-15** Scanning electron micrographs of (a) pyrite in sterile control medium for 6 months and (b) pyrite in inoculated medium for 1 month. Arrows point to bacterial cells.



c



d

**Figure 7-15** Scanning electron micrographs of (c) pyrite in inoculated medium for 2 months and (d) pyrite in inoculated medium for 6 months. Arrows point to bacterial cells

suggests that the pitting of the  $\text{FeS}_2$  is likely due to the high concentration of  $\text{Fe}^{3+}$  at the vicinity where bacteria attach to the  $\text{FeS}_2$  particles. The high  $\text{Fe}^{3+}$  concentration at bacteria attached sites results in the pitting of the  $\text{FeS}_2$  due to  $\text{Fe}^{3+}$  induced oxidation.

It is well known that accelerated oxidation occurs at imperfections, and bacteria has also been reported to preferably attach to solid surfaces at dislocations and grain boundaries (Andrews, 1988; Berry and Murr, 1975). Bagdigian and Myerson (1986) suggested that selective adsorption of bacteria is influenced by surface energy and electrostatic effects. Because of this preferred attachment, concentration gradients of  $\text{Fe}^{3+}$  will exist at different sites on the surface of the sulfide. High  $\text{Fe}^{3+}$  concentration at bacterial attached sites resulting from bacterial oxidation of  $\text{Fe}^{2+}$  (chemically generated) to  $\text{Fe}^{3+}$  at these sites leads to the pitting of the sulfides. Furthermore,  $\text{H}_2\text{SO}_4$  is generated during the oxidation of  $\text{Fe}^{2+}$  to  $\text{Fe}^{3+}$  and also enhances the pitting of the mineral. The  $\text{Fe}^{3+}$  generated does not react with the entire surface of the sulfide particle as suggested by Bartels et al. (1989) who attributed pitting to direct attack of sulfides. The attachment of *T. ferrooxidans* to sulfide minerals and the pitting of sulfide do not constitute evidence of the direct oxidation mechanism and may not be essential for the microbial oxidation of sulfides.

## 7.5 SUMMARY OF CHAPTER

The results of this study have shown that although *T. ferrooxidans* attaches to sulfide and glass surfaces it does not directly oxidize the sulfides as proposed by the direct contact mechanism. The pitting of the pyrite in the presence of *T. ferrooxidans* which had been used to support the direct contact mechanism is likely due to the high concentration gradient of  $\text{Fe}^{3+}$  in the vicinity of the bacteria attachment. The highest concentrations of  $\text{Fe}^{3+}$  occurs at bacteria attached sites because of the rapid oxidation of the chemically generated  $\text{Fe}^{2+}$  to  $\text{Fe}^{3+}$  by the bacteria. The results presented in this chapter indicate that oxidation of  $\text{FeS}_2$  is mainly by chemical means, with the bacteria acting as a catalyst in

converting  $\text{Fe}^{2+}$  to  $\text{Fe}^{3+}$  which in turn oxidizes  $\text{FeS}_2$  and generates  $\text{H}_2\text{SO}_4$ . This mechanistic proposition is supported by the inability of viable cells to oxidize  $\text{FeS}_2$  when initial chemical oxidation of  $\text{FeS}_2$  is eliminated above pH of about 4.0. The insignificant increase in pyrite oxidation with increase cell concentration beyond  $10^6/\text{mL}$  also supports the indirect contact mechanism.

The ferrous-oxidizing activity of the bacterial cells is shown to occur both in suspension and when attached to solids. It can be concluded from this study, that the indirect mechanism is the predominant pathway during sulfide oxidation and ARD formation in the presence of bacteria.

## 7.6 REFERENCES

- American society for testing and materials. 1982. Annual book of ASTM standards, part 26. Philadelphia, PA. pp. 205-208.
- Andrews, G. F. 1988. The selective adsorption of thiobacilli to dislocation sites on pyrite surfaces. *Biotechnol. Bioeng.* 31: 378-381.
- Atlas, R. M. and R. Bartha. 1993. *Microbial Ecology*. The Benjamin/Cummings Publishing, Co. Inc., New York, NY. 3rd edition. pp. 234-235.
- Atkins, A. S., E. W. Bridgwood, and A. J. Davis. 1987. A study of the suppression of pyritic sulphur in coal froth flotation by *Thiobacillus ferrooxidans*. *Coal Prep.* 5: 1-13.
- Attia, Y. A. 1990. Feasibility of selective biomodification of pyrite floatability in coal desulfurization by froth flotation. *Resour. Conserv. Recycl.* 3: 169-175.
- Bagdigian, R. M., and A. S. Myerson. 1986. The Adsorption of *Thiobacillus ferrooxidans* on Coal Surfaces. *Biotech. Bioeng.* 28: 467-479.
- Bailey, A. D., and G. S. Hansford. 1993. Factors affecting bio-oxidation of sulfide minerals at high concentrations of solid: A review. *Biotech. Bioeng.* 42: 1164-1174.
- Baker, R. A., and A. G. Wilshire. 1970. Microbiological factor in acid mine drainage formation: A pilot plant study. *Environ. Sci. Technol.* 4: 401-407.

- Bartels, C. C., G. Chatzitheodorou, M. Rodriguez-Leiva, and H. Tributsch. 1989. Novel technique for investigation and quantification of bacterial leaching by *Thiobacillus ferrooxidans*. *Biotech. Bioengin.* 33: 1196-1204.
- Bennett, J. C., and H. Tributsch. 1978. Bacterial leaching patterns on pyrite crystal surfaces. *J. Bacteriol.* 134: 310-317.
- Berry, V. K., and L. E. Murr. 1975. Bacterial attachment of molybdenite: An electron microscope study. *Metallurg. Trans. B.* 6: 488-490.
- Brierley, C. L. 1978. Bacterial leaching. *CRC Critical Rev. Microbiol.* 6: 207-262.
- Chang, C. Y., and S. A. Myerson. 1982. Growth models of the continuous bacterial leaching of iron pyrite by *Thiobacillus ferrooxidans*. *Biotech. Bioeng.* 24: 889-902.
- Colmer, A. R., and M. E. Hinkle. 1947. The role of microorganisms in acid mine drainage: A preliminary report. *Science.* 106: 253-256.
- Colmer, A. R., K. L. Temple, and M. E. Hinkle. 1950. An iron-oxidizing bacterium from the acid drainage of some bituminous coal mines. *J. Bacteriol.* 59: 317-328.
- Devasia, P., K. A. Natarajan, D. N. Sathyanarayana, and G. R. Rao. 1993. Surface chemistry of *Thiobacillus ferrooxidans* relevant to adhesion on mineral surfaces. *Appl. Environ. Microbiol.* 59: 4051-4055.
- Hem, J. D. 1967. Equilibrium chemistry of iron in ground water. Principles and application of water chemistry, S. D. Faust and J. D. Lands (eds.). John Wiley & Sons, Inc., New York. pp. 625-643.
- Ingledeu, W. J. 1986. Ferrous Iron Oxidation by *Thiobacillus ferrooxidans*. *Biotech. Bioeng. Symp.* 16: 23-33.
- Lawrence, R. W. 1994. Biooxidation for the treatment of refractory gold ores and concentrates - A Canadian perspective. *CIM Bulletin.* 87: 58-65.
- Leathen, W., S. Braley Sr., and L. D. McIntyre. 1953. The role of bacteria in the formation of acid from certain sulfidic constituents associated with bituminous coal; Part 2, Ferrous iron oxidizing bacteria. *Appl. Microbiol.* 1: 65-68.

- Lowson, T. R. 1982. Aqueous oxidation of pyrite by molecular oxygen. *Chem. Rev.* 82: 461-497.
- Mannivannan, T., S. Sandhya, and R. A. Pandey. 1994. Microbial desulfurization of coal by chaemoautotrophic *Thiobacillus ferrooxidans* - An iron mine isolate. *J. Environ. Sci. Health.* A29: 2045-2061.
- Marchant, P. B. 1986. Commercial piloting and the economic feasibility of plant scale continuous tank leaching at Equity Silver Mines Limited. *Fundamental and applied biohydrometallurgy*, R. W. Lawrence, R. M. R. Branion and H. G. Ebner (eds.). Elsevier, Amsterdam. pp. 53-76.
- McCready, R. G. L., D. Wadden, and A. Marchbank. 1986. Nutrient requirement for the in-place leaching of uranium by *Thiobacillus ferrooxidans*. *Hydrometallurgy.* 17: 61-71.
- Murr, L. E., and V. K. Berry. 1976. Direct observation of selective attachment of bacteria on low-grade sulfide ores and other mineral surfaces. *Hydrometallurgy.* 2: 11-24.
- Murthy, K. S. N., and K. A. Natarajan. 1992. The role of surface attachment of *Thiobacillus ferrooxidans* on the biooxidation of pyrite. *Miner. Metallurg. Process.* 9: 20-24.
- Myerson, S. A., and P. Kline. 1983. The Adsorption of *Thiobacillus ferrooxidans* on solid particles. *Biotechnol. Bioeng.* 25: 1669-1676.
- Ohmura, N., K. Kitamura, and H. Saiki. 1993. Selective adhesion of *Thiobacillus ferrooxidans* to Pyrite. *Appl. Environ. Microbiol.* 59: 4044-4050.
- Ohmura, N., and H. Saiki. 1994. Desulfurization of coal by microbial column flotation. *Biotech. Bioeng.* 44: 125-131.
- Razzell, W. E., and P. C. Trussell. 1963. Isolation and properties of an iron-oxidizing *Thiobacillus*. *J. Bacteriol.* 85: 595-603.
- Schaeffer, W. I., P. E. Holbert, and W. W. Umbreit. 1963. Attachment of *Thiobacillus thiooxidans* to sulfur crystals. *J. Bacteriol.* 85: 137-140.



- Silverman, M. P. 1967. Mechanism of bacterial pyrite oxidation. *J. Bacteriol.* 94: 1046-1051.
- Silverman, M. P., and H. L. Ehrlich. 1964. Microbial formation and degradation of minerals. *Adv. Appl. Microbiol.* 6: 153-206.
- Singer, P. C., and W. Stumm. 1970. Acid Mine Drainage: The rate-determining step. *Science.* 167: 1121-1123.
- Temple, L. K., and W. E. Delchamps. 1953. Autotrophic bacteria and the formation of acid in bituminous coal mines. *Appl. Microbiol.* 1: 255-258.
- Temple, L. K., and R. A. Colmer. 1951. The autotrophic oxidation of iron by a new bacterium: *Thiobacillus ferrooxidans*. *J. Bacteriol.* 62: 605-611.
- Vaughan, D. J., and J. R. Craig. 1978. Mineral chemistry of metal sulfides. Cambridge University Press, New York, NY. pp. 36-38.
- Vitaya, V.B., and K. Toda. 1991. Kinetics and mechanism of the adsorption of *Sulfolobus acidocaldarius* on coal surfaces. *Biotechnol. Prog.* 7: 427-433.
- Wakao, N., M. Mishina, Y. Sakurai, and H. Shiota. 1984. Bacterial pyrite oxidation. III. Adsorption of *Thiobacillus ferrooxidans* cells on solid surfaces and its effect on iron release from pyrite. *J. Gen. Appl. Microbiol.* 30: 63-77.
- Weiss, R. L. 1973. Attachment of bacteria to sulphur in extreme environments. *J. Gen. Microbiol.* 77: 501-507.
- Wills, B. A. 1988. Mineral processing technology. Pergamon Press, New York. 4th edition. pp. 166-199.

## CHAPTER 8

### SUPPRESSION OF MICROBIAL PYRITE OXIDATION BY FATTY ACID AMINE TREATMENT\*

#### 8.1 INTRODUCTION

Techniques directed towards prevention of acid rock drainage (ARD) at-source have been found to be more promising than the treatment methods since, if achieved, they can provide permanent solutions to ARD problem and will therefore not require treatment facilities after mine closure. These at-source prevention techniques depend on the creation of conditions which chemically, biochemically or physically retard the rate of oxidation of sulfide minerals. Based on this, many approaches have been investigated, including: complexation of ferric ions in solution or at the surface of the pyrite so that they are not available for oxidation (Chander and Zhou, 1992; Nebgen et al., 1981); creation of fully anoxic environments by using clay liners, plastic liners, and asphalt (Nicholson et al., 1989; Healey and Robertson, 1989); coating of the surface of pyrite with ferric phosphate (Evangelou and Huang, 1992; Nyavor and Egiebor, 1995; Chapter 2); addition of Portland cement (Nebgen et al., 1981; Amaratunga, 1991); electrochemical passivation by addition of copper and silver ions (Lalvani and Shami, 1987); passivation by treatment with acetyl acetone and humic acid (Lalvani et al., 1990); and production of highly hydrophobic surfaces by the use of fatty acid (Nyavor and Egiebor, 1994; Chapter 3).

Although *Thiobacillus ferrooxidans* plays an important role and is unavoidable in ARD formation (Colmer et al., 1950; Temple and Delchamp, 1953; Baker and Wilshire, 1970), none of these at-source ARD prevention and control techniques have been evaluated

---

\* A version of this chapter, co-authored with N. O. Egiebor and P. M. Fedorak, has been accepted for publication in *Science of the Total Environment*.

in the presence of bacteria. The objective of this study was to evaluate the stability of fatty acid amine treated pyrite in the presence of *T. ferrooxidans*. The theory and background of the fatty acid amine treatment method has been reported elsewhere (Nyavor and Egiebor, 1994; Chapter 3).

## **8.2 EXPERIMENTAL METHODS**

### **8.2.1 Culture and Medium**

The three strains of *T. ferrooxidans* used are the same as those described in Section 4.2.1. Details of the medium used for growth of the microorganisms are also reported in Section 4.2.1.

The medium used for the pyrite stability test consist of solution A only, adjusted to a pH of 2.3 to 2.5 with H<sub>2</sub>SO<sub>4</sub> and referred to as -Fe<sup>2+</sup> medium. All chemical reagents used were analar grade obtained from Fisher Scientific, Edmonton, Canada and used without further purification.

### **8.2.2 Pyrite and Surfactants**

The natural pyrite described in Section 2.3.1 was used for the experiments. The pyrite was ground in a jaw crusher and separated into different size fractions by dry sieving, and stored under nitrogen. The -355 +300 μm size fraction was used for this study. Primary fatty acid amine surfactants, Armac T and Armac HR, obtained from Akzo Chemicals Ltd. were used to treat the pyrite. These surfactants have a general chemical formula of RNH<sub>3</sub><sup>+</sup>CH<sub>3</sub>COO<sup>-</sup> where R represents tallow and hydrogenated rapeseed derivatives in Armac T and Armac HR, respectively.

### **8.2.3 Pyrite Treatment**

The pyrite was treated with the surfactant in a cylindrical glass reactor. Details of the treatment procedure have been reported elsewhere (Section 3.3.2; Nyavor and Egiebor, 1994). The pyrite samples were treated with 1.23 g/L of Armac T or Armac HR and used in the control (no cells added) and inoculated experiments.

### **8.2.4 Most Probable Number (MPN) Method**

The numbers of *T. ferrooxidans* in cultures and cell suspensions were determined by a 3-tube MPN method. Details of the method is reported in Section 4.2.3.

### **8.2.5 Preparation of Cell Suspension**

Details of the preparation of the cell suspension used for the pyrite stability experiments are reported in Section 5.3.4.

### **8.2.6 Stability Tests**

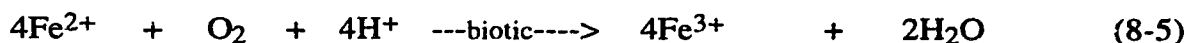
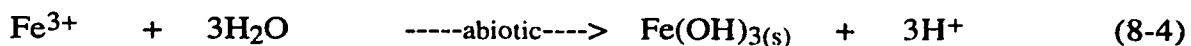
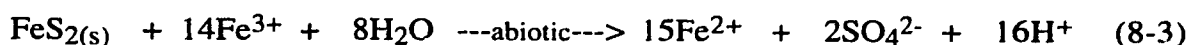
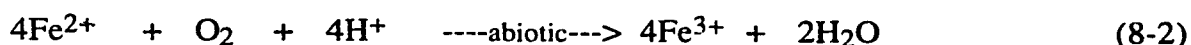
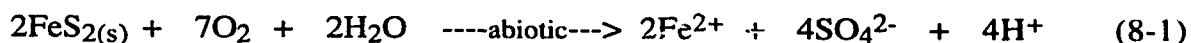
The stability tests on untreated and treated pyrite samples, in the absence and presence of *T. ferrooxidans*, were done in 500-mL Erlenmeyer flasks. Equal volumes of  $\text{-Fe}^{2+}$  medium (100 mL) were measured into flasks and 1 g of untreated or treated pyrite added. Equal volumes of prepared cell suspension (1 to 3 mL) were then added to one set of the flasks, the other set was used as sterile control. The flasks were then incubated at 27°C on an orbital shaker table at a speed of 200 rpm. Samples were taken before and during incubation from all flasks for total Fe, soluble  $\text{Fe}^{2+}$ , pH and MPN analysis. The stability experiments were done in duplicate. The results were within 5% deviation.

### 8.2.7 Chemical Analysis and pH

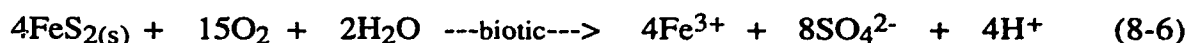
Total Fe and Fe<sup>2+</sup> in the leached solutions were determined by DR/2000 Spectrophotometer and the total Fe verified with Atomic Absorption Spectrophotometry (AAS). Details of the procedure is reported in Section 2.3.5. The pH of the leached solutions were determined by a Cole-Parmer Chemcadet pH/mV meter equipped with a temperature compensation probe.

### 8.2.8 Theory and Background

In order to evaluate the stability of fatty acid amine treated pyrite in the presence of *T. ferrooxidans*, all the reactions occurring during pyrite oxidation (both chemical and biological) have to be considered. Based on proposed mechanisms of chemical and biological oxidation of sulfides (Silverman and Ehrlich, 1964), the possible reactions that may occur during abiotic and biotic oxidation of pyrite are (Kleinman et al., 1981; Bell et al., 1987):



and possibly, the direct bacterial attack on the pyrite,



Depending on the conditions of the system, such as, pH and E<sub>h</sub>, some of these reactions may be eliminated as possible reactions during pyrite oxidation.

### 8.3 RESULTS AND DISCUSSION

Chemical analysis of the natural pyrite by AAS, Leco total sulfur analyzer and Scanning Electron Microscope/Energy-Dispersive X-Ray Spectrometer showed that it contained 46.9% of Fe, 52.4% of S, and small amounts of impurities, mainly silicon (Section 2.4). The S/Fe mole ratio of 1.96 illustrates that the pyrite is fairly pure. Pyrite does not generally conform to the ideal composition of  $\text{FeS}_2$ , the variation in composition has been reported to be in the direction of sulfur deficiency within the limits of  $\text{FeS}_{2.0}$  to  $\text{FeS}_{1.94}$  (Smith, 1942).

An initial series of experiments were done on the untreated pyrite using the three strains of *T. ferrooxidans* to determine the rate of pyrite oxidation and variations in the number of suspended viable cells during the oxidation. Control experiments (no cells added) were also run simultaneously. Results from these initial experiments should give an indication of how long the stability tests will be run, and if cells suspension should be added periodically. During the initial experiments, samples were taken periodically for total Fe ( $\text{Fe}^T$ ) analysis and the number of viable suspended cells by the MPN method. Figure 8-1 shows a plot of the change in  $\text{Fe}^T$  concentration for the three strains of *T. ferrooxidans* and the control experiment for 40 days. As expected, the presence of the bacteria enhanced the rate of oxidation of the untreated pyrite, with more Fe leached into solution in the inoculated experiments than the control. The rate of oxidation of the untreated pyrite with strain 14119 is slightly lower than that of strain 13598 and 13661. The number of suspended viable cells did not change significantly during the experiment for strains 13598 and 13661. At the start of the experiment,  $3.0 \times 10^6/\text{mL}$  of strains 13598 and 13661 were in suspension, and about the same number of viable cells were in suspension at the end of the experiment, although the number of cells fluctuated during the course of the experiment. Strain 14119, however, generally increased throughout the experiment. The low cell concentration ( $10^5/\text{mL}$ ) for strain 14119, compared to strains 13598 and 13661, at the start of the experiment may have resulted in the lower rate of

pyrite oxidation for strain 14119. At the end of the experiment the number of suspended cells of strain 14119 had increased to  $10^6$ /mL. The initial experiments indicated that the bacterial systems could be incubated for 40 days without the need to add fresh cells during the course of the experiment.

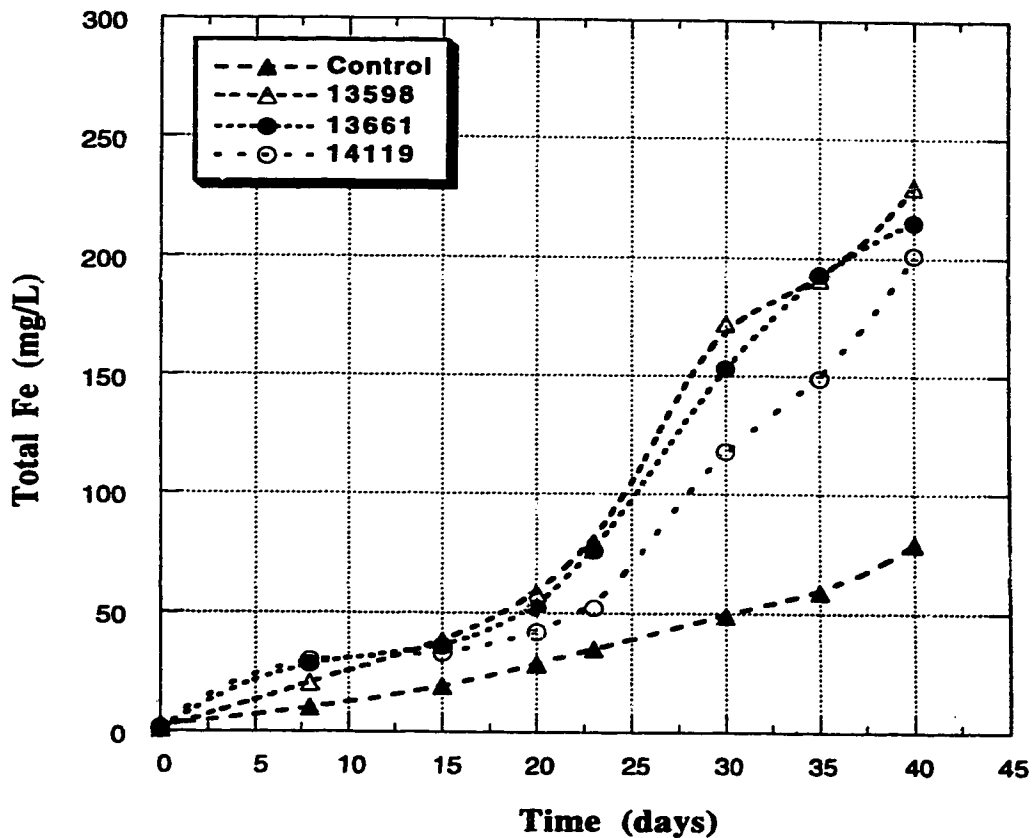


**Figure 8-1. Change in total Fe concentration during oxidation of untreated pyrite (initial pH =2.4)**

The effect of initial cell concentration on the oxidation of untreated pyrite and  $Fe^{2+}$  was reported in Section 7.4.4. The results showed that there is no significant increase in the pyrite oxidation rate by increasing cell concentration from  $4.6 \times 10^6$ /mL to  $1.1 \times 10^9$ /mL. However, increasing cell concentration from  $4.3 \times 10^3$ /mL to  $4.6 \times 10^9$ /mL resulted in significant increase in the rate of  $Fe^{2+}$  oxidation irrespective of the range in which the

increase occurs. The insignificant increase in pyrite oxidation rate when the cell concentration is increased beyond  $10^6/\text{mL}$ , and the measureable increase in  $\text{Fe}^{2+}$  oxidation rate by increasing cell concentration implies that the rate-limiting step in pyrite oxidation in the presence of bacteria is  $\text{Fe}^{3+}$  oxidation of the pyrite (Equation 8-3). The oxidation of pyrite by  $\text{Fe}^{3+}$  has also been reported to be the rate-limiting step in the oxidation of sulfides in the presence of *T. ferrooxidans* (Silverman, 1967). The knowledge of the rate-limiting step was used in designing the stability tests in terms of the optimum cell concentration.

The stability of the fatty acid amine (Armac T and Armac HR) treated pyrite was tested with each of the three strains separately. For each strain, two sets of experiments (inoculated and control) were run simultaneously. Each set of experiments consisted of the untreated, Armac T treated, and Armac HR treated pyrite, all incubated under the same conditions. The control experiments were used for monitoring chemical oxidation only, while the inoculated experiments were used for monitoring the total oxidation (chemical and biological). The stability tests were incubated for 40 days at optimum conditions obtained from the initial cell concentration (Section 7.4.4) and oxidation experiments (Figure 8.1). Samples taken during the experiment were analyzed for total Fe ( $\text{Fe}^{\text{T}}$ ),  $\text{Fe}^{2+}$ , pH and number of suspended viable cells.

Figures 8-2 and 8-3 illustrate results from the control experiment (no cells added) for the untreated and treated pyrite samples. The release of Fe during the oxidation experiment is shown in Figure 8-2. It is observed from the plot that the fatty acid amine treatment reduces the rate of chemical oxidation of the pyrite. Less than half the total Fe leached into solution with the untreated is observed with the treated samples under similar conditions. The  $\text{Fe}^{2+}$  concentration shows the same trend as the  $\text{Fe}^{\text{T}}$  concentration with generally lower  $\text{Fe}^{2+}$  concentrations from the treated pyrite than the untreated pyrite.



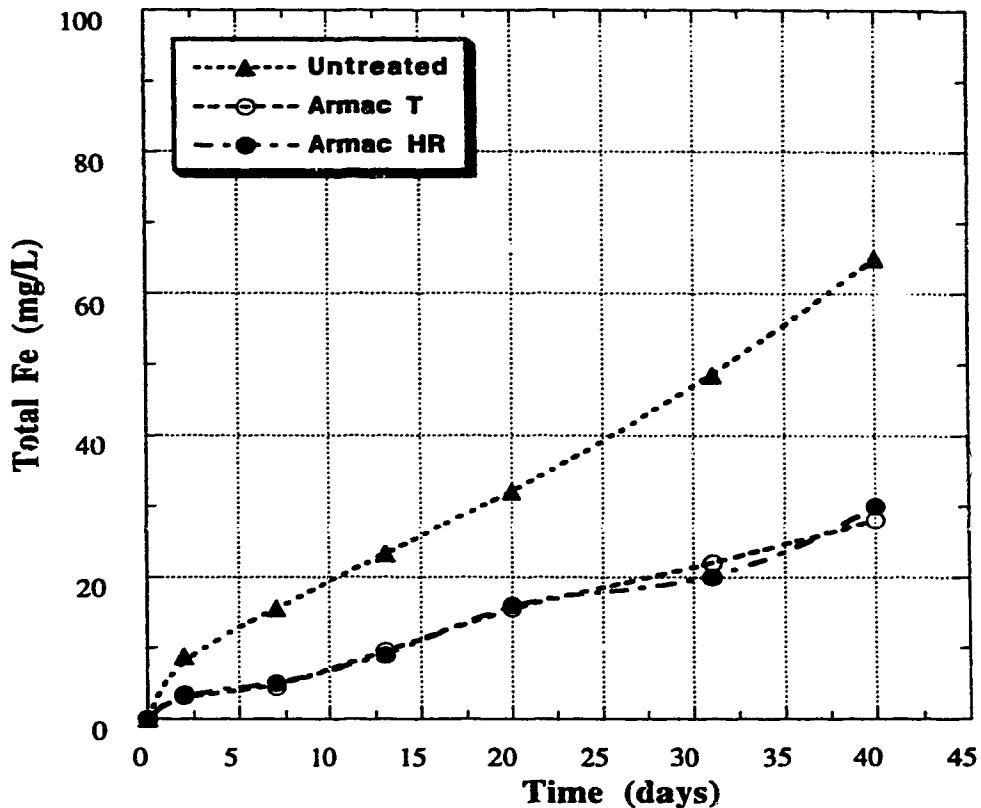


**Figure 8-2. Change in total Fe concentration during leaching of untreated and treated pyrite (no cells added).**

A plot of the percentage of the total Fe as  $Fe^{2+}$  ( $\% Fe^{2+}$ ) during the experiment is shown in Figure 8-3. The plot shows that greater than 80% of the Fe is in the  $Fe^{2+}$  state during the oxidation of both the treated and the untreated pyrite in the absence of bacteria. Wakao et al. (1982) reported an average  $\%Fe^{3+}$  of 20% (i.e.  $\%Fe^{2+}$  of 80%) in uninoculated controls during oxidation of pyrite. During the chemical oxidation of pyrite in the absence of bacteria, oxygen oxidation of  $Fe^{2+}$  to  $Fe^{3+}$  (Equation 2) is the only pathway for generating the  $Fe^{3+}$  oxidant. The chemical oxidation of  $Fe^{2+}$  under acidic pH and ambient condition is extremely slow (Colborn and Nicol, 1973) and therefore this oxidation reaction becomes the rate-limiting step. The  $Fe^{2+}$  ion therefore accumulates in the system and this explains the high  $\%Fe^{2+}$  obtained in the absence of bacteria. The pH of both the

untreated and treated pyrite solutions decreased continuously during the experiment. No significant difference in pH is observed between the untreated, which decreased from a pH of 2.6 to 2.1 and the treated pyrite solutions which decreased by the same amount, over the course of the experiment.

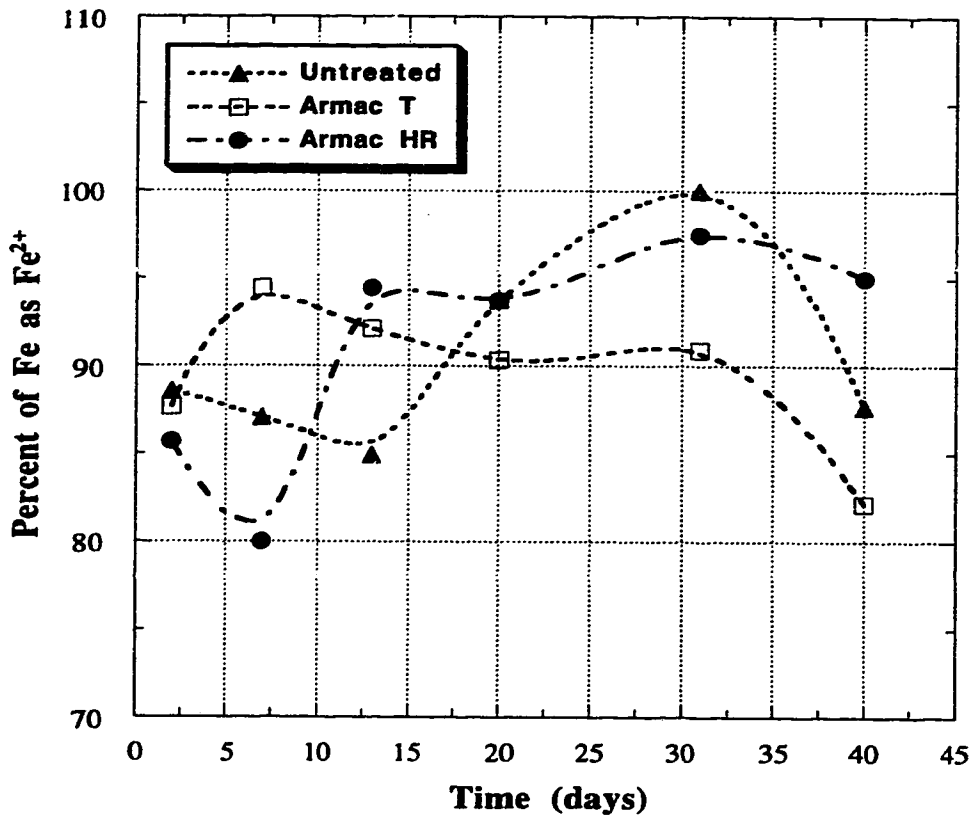


**Figure 8-3. Percentage of total Fe as ferrous during leaching of untreated and treated pyrite (no cells added).**

Figures 8-4 and 8-5 show results from the inoculated experiments for the untreated and treated samples incubated with strain 13661. Figure 8-4 shows the change in total Fe concentration during leaching of the untreated and treated pyrite samples. The figure shows that the rate of oxidation of the pyrite is reduced significantly by the fatty acid treatment. About 85% reduction in pyrite oxidation is observed with fatty acid treatment

over 40 days. Both the Armac T and Armac HR treatment resulted in a similar level of protection of the pyrite. The number of suspended viable cells fluctuated during the experiments; however, about the same number of viable cells ( $10^8$ /mL) were in suspension at the end of the experiments.

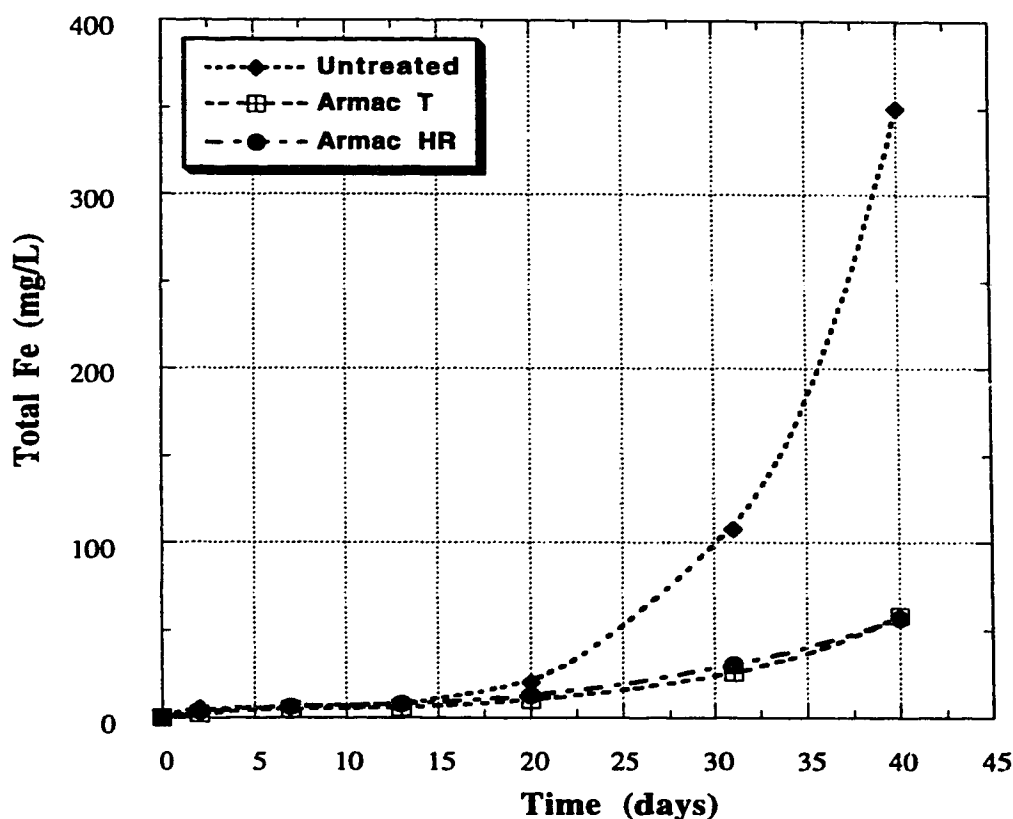


**Figure 8-4. Change in total Fe concentration during bioleaching of untreated and treated pyrite (strain 13661).**

The percentage of the total Fe concentration that is  $Fe^{2+}$  is shown in Figure 8-5. It is observed that in contrast to the control experiments (without cells), the percent  $Fe^{2+}$  for the inoculated experiments is below 8% throughout the experiment. An average value of 10%  $Fe^{2+}$  (90%  $Fe^{3+}$ ) was reported by Wakao et al. 1984. The percent  $Fe^{2+}$  decreased during the experiment until after day 30 when the % $Fe^{2+}$  starts to increase (Figure 8-5). This is attributable to the increased rate of pyrite oxidation after day 30, as illustrated in

Figure 8-4. The low percent  $\text{Fe}^{2+}$ , less than 10%, for both the untreated and the treated pyrite in the presence of bacteria indicates that over 90% of the total Fe is in the  $\text{Fe}^{3+}$  state. In the presence of *T. ferrooxidans*, the bacteria acts as a catalyst in the oxidation of  $\text{Fe}^{2+}$  to  $\text{Fe}^{3+}$  (Equation 8-5); however,  $\text{Fe}^{3+}$  oxidation of pyrite (Equation 8-3) to produce additional  $\text{Fe}^{2+}$  is slow, and therefore  $\text{Fe}^{3+}$  accumulates in the system; hence the low percent  $\text{Fe}^{2+}$ . The pH of both the untreated and treated pyrite solutions decreased with time during the experiment. The pH of the untreated pyrite solution however decreased more rapidly than treated pyrite solutions, thus indicating that the fatty acid amines suppress acid production resulting from pyrite oxidation. Similar results were obtained for the untreated and treated pyrite samples using strains 13598 and 14119.

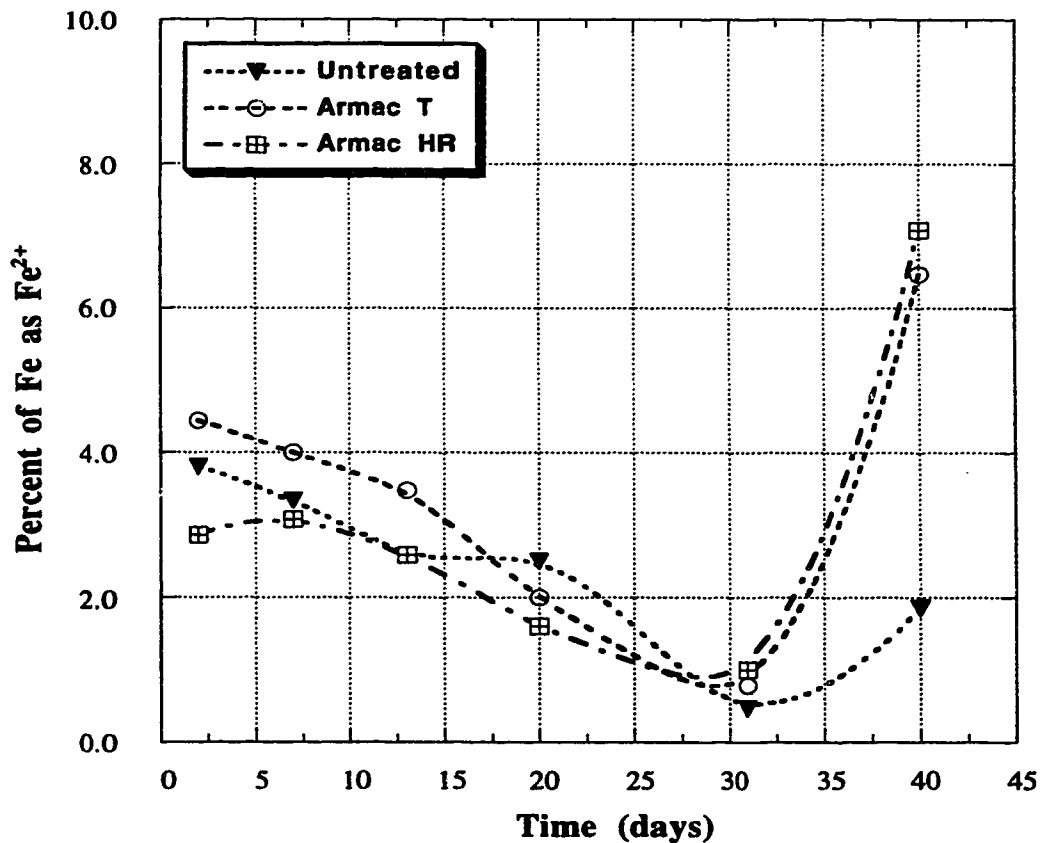


Figure 8-5. Percentage of total iron as ferrous during bioleaching of untreated and treated pyrite (strain 13661).

The fatty acid amine decreases the rate of both chemical and biological oxidation of the treated pyrite samples. Fatty acid amine treatment of pyrite has been shown to impart hydrophobicity to the treated pyrite particles (Nyavor and Egiebor, 1994; Chapter 3). Since the initial adsorption of ions or molecules on the surface of the pyrite is the initiation step of pyrite oxidation (Garrels and Thompson, 1960; Biegler and Swift, 1979), the fatty acid amine treatment reduces the rate of chemical oxidation by repelling molecules and ions from the pyrite surface during oxidation in the absence of bacteria.

The oxidation rate of the treated pyrite in the presence of bacteria (chemical and biological oxidation) is also reduced by fatty acid amine treatment because contact between the  $\text{Fe}^{3+}$  ion (produced by the bacteria) and the pyrite is still required for oxidation to occur. Although some investigators have reported improved sulfide oxidation by increasing contact between the bacteria and the sulfide surface (Duncan and Trussell, 1964), others have reported improved oxidation rates by decreasing contact between the sulfide surface and the bacteria (Torma et al., 1976). Duncan et al. (1964) reported that surface active agents, Tween 40, 60, and 80 wetted the surface of chalcopyrite permitting more rapid contact and more intimate association by the bacteria, thus increasing the oxidation of the sulfide. The increased wetting of the surface of the sulfide by the surfactant is the same as increasing the hydrophilicity of the sulfide and thus, supports the oxidation suppression mechanism reported in this study. The relative contribution of the direct contact mechanism (direct bacterial attack on pyrite) to the overall oxidation rate is also a subject of controversy. Some investigators have suggested that the contribution of the direct contact mechanism is negligible (Wakao et al. 1984). It is important to note that increasing hydrophilicity also improves contact between the oxidizing ions and the surface of the sulfides, and therefore depending on the possibility of direct bacterial attack, contact between the bacteria and the surface of the pyrite may not be important.

In both the untreated and treated pyrite inoculated experiments,  $\text{Fe}^{3+}$  accumulates in the system, since  $\text{Fe}^{3+}$  oxidation of pyrite is the rate-limiting step. Making the pyrite

highly hydrophobic reduces the contact between the  $\text{Fe}^{3+}$  and the pyrite surface and reduces the oxidation of the pyrite further. It is important to note that the fatty acid amine treated pyrite particles were washed to remove any residual reagent and dried before the stability experiments. The control of ARD by controlling bacterial activity has not been successful because of repopulation of the bacteria (Klienmann and Erickson, 1983; Silver and Ritcey, 1985; Siwik et al., 1989). The control scheme presented here utilizes the alteration of the sulfide surface by making the pyrite highly hydrophobic, rather than controlling the bacterial population which is normally difficult to achieve over long periods.

#### **8.4 SUMMARY OF CHAPTER**

In the absence of *T. ferrooxidans*, the rate-limiting reaction during pyrite oxidation is the chemical oxidation of ferrous to ferric ion. The ferrous to ferric ion oxidation limiting reaction results in the accumulation of ferrous ion in the system. Conversely, in the presence of bacteria, ferric ion oxidation of the pyrite is the rate-limiting reaction during the oxidation of pyrite. This rate-limiting reaction results in the accumulation of ferric ion in the system, and therefore a small proportion exits as  $\text{Fe}^{2+}$  ions.

Fatty acid amine treatment suppresses the rate of both chemical and biological oxidation of the pyrite by making the pyrite surface highly hydrophobic. The hydrophobic surface repels the oxidizing ions, thus reducing the rate of oxidation of the treated pyrite.

## 8.5 REFERENCES

- Amaratunga, M. L. 1991. A novel concept of safe disposal of acid generating tailings by agglomeration and encapsulating alkaline and bacterial additives. *Mineral Bioprocessing*, R. W. Smith and M. Misra (eds.). TMS. pp. 389-400.
- Baker, R. A., and A. G. Wilshire. 1970. Microbiological factor in acid mine drainage formation: A pilot plant study. *Environ. Sci. Technol.* 4: 401-407.
- Bell, A., K. D. Phinney, K. Ferguson, A. Gosselin, J. Ingles, and J. S. Scott. 1987. Mine and mill wastewater treatment. *Mining, Mineral and Metallurgical Process Division, Environ. Protect., Environment Canada. Report EPS 3/HA.* pp. 3-8.
- Biegler, T., and D. A. Swift. 1979. Anodic behaviour of pyrite in acid solutions. *Electrochim. Acta.* 24: 415-420.
- Chander, S., and R. Zhou. 1992. Effect of organic additives on acid generation from pyrite waste. *Proceedings of the symposium on emerging process technologies for a cleaner environment*, S. Chander, P. E. Richardson, and H. El-Shall (eds.). SME, Phoenix, Arizona. pp. 131-139.
- Colborn, R. P., and M. J. Nicol. 1973. An investigation into the kinetics and mechanism of the oxidation of iron (II) by oxygen in aqueous chloride solution. *J. S. Afr. Inst. Min. Metal.* 73: 281-289.
- Colmer, A. R., K. L. Temple, and M. E. Hinkle. 1950. An iron-oxidizing bacterium from the acid drainage of some bituminous coal mines. *J. Bacteriol.* 59: 317-328.
- Duncan, D. W., and P. C. Trussell. 1964. Advances in the microbiological leaching of sulphide ores. *Can. Met. Quart.* 3: 43-55.
- Duncan, D. W., P. C. Trussell, and C. C. Walden. 1964. Leaching of chalcopyrite with *Thiobacillus ferrooxidans* : Effect of surfactant and shaking. *Appl. Microbiol.* 12: 122-126.
- Evangelou, V. P., and X. Huang. 1992. A new technology for armoring and deactivating pyrite. *Environmental issues and waste management in energy and minerals*

- production, R. K. Singhal, A. K. Mehrotra, K. Fytas, and J-C. Collins (eds.). Calgary, Alberta. Balkema, Rotterdam. pp. 413-417.
- Garrels, R. M., and M. E. Thompson. 1960. Oxidation of pyrite by iron sulfate solution. *Am. J. Sci.* 258A: 57-67.
- Healey, P. M., and A. M. Robertson. 1989. A case history of an acid generation abatement program for an abandoned copper mine. Geotechnical aspects of tailings disposal and acid mine drainage. The Vancouver Geotechnical Society, B. C.
- Kleinmann, R. L. P., D. A. Crerar, and R. P. Pacelli. 1981. Biogeochemistry of acid mine drainage and a method to control acid formation. *Min. Eng.* 33: 300-305.
- Kleinmann, R. L. P., and P. M. Erickson. 1983. Control of acid drainage from coal refuse using anionic surfactants. U. S. Bureau of Mines, RI8847.
- Lalvani, S. B., B. A. Deneve, and A. Weston. 1990. Passivation of pyrite due to surface treatment. *Fuel.* 69: 1567-1569.
- Lalvani, S. B., and M. Shami. 1987. Passivation of pyrite oxidation with metal cations. *J. Mat. Sci.* 22: 3503-3507.
- Nebgen, J. W., W. H. Engelmann, and D. F. Weatherman. 1981. Inhibition of acid mine drainage formation: The role of insoluble iron compounds. *J. Environ. Sci.* 24: 23-27.
- Nicholson, V. R., R. W. Gillham, J. A. Cherry, and E. J. Reardon. 1989. Reduction of acid generation in mine tailings through the use of moisture-retaining cover layer as oxygen barriers. *Can. Geotech.* 26: 1-8.
- Nyavor, K., and N. O. Egiebor. 1994. Suppression of pyrite oxidation by fatty acid amine treatment. Extraction and processing for the treatment and minimization of wastes, J. P. Hager, B. J. Hansen, W. P. Imrie, J. F. Pusateri, and V. Ramachandran (eds.). TMS, San Francisco, California. pp. 773-790.
- Nyavor, K., and N. O. Egiebor. 1995. Control of pyrite oxidation by phosphate coating. *Sci. Total Environ.* 162: 225-237.



- Silver, M., and G. M. Ritcey. 1985. Effects of iron-oxidizing bacteria and vegetation on acid generation in laboratory lysimeter tests on pyrite-containing uranium tailings. *Hydrometallurgy*. 15: 255-264.
- Silverman, M. P. 1967. Mechanism of bacterial pyrite oxidation. *J. Bacteriol.* 94: 1046-1051.
- Silverman, M. P., and H. L. Ehrlich. 1964. Microbial formation and degradation of minerals. *Adv. Appl. Microbiol.* 6: 153-206.
- Siwik, R., S. Payant, and K. Wheeland. 1989. Control of acid generation from reactive waste rock with the use of chemicals. Tailings and effluent management, Proceedings of the international symposium on tailings and effluent management, M. E. Chalkley, B. R. Conard, V. I. Lakshmanan, and K. G. Wheeland (eds.), CIM, Halifax. Pergamon, New York. pp. 181-193.
- Smith, G. F. 1942. Variation in the properties of pyrite. *Am. Mineralogist*. 27: 1-18.
- Temple, K. L., and A. R. Colmer. 1951. The autotrophic oxidation of iron by a new bacterium: *Thiobacillus ferrooxidans*. *J. Bacteriol.* 62: 605-611.
- Temple, L. K., and W. E. Delchamps. 1953. Autotrophic bacteria and the formation of acid in bituminous coal mines. *Appl. Microbiol.* 1: 255-258.
- Torma, A. E., G. G. Gabra, R. Guay, and M. Silver. 1976. Effects of surface active agents on the oxidation of chalcopyrite by *Thiobacillus ferrooxidans*. *Hydrometallurgy*. 1: 301-309.
- Wakao, N., M. Mishina, Y. Sakurai, and H. Shiota. 1982. Bacterial pyrite oxidation. I. The effect of pure and mixed cultures of *Thiobacillus ferrooxidans* and *Thiobacillus thiooxidans* on release of iron. *J. Gen. Appl. Microbiol.* 28: 331-343.
- Wakao, N., M. Mishina, Y. Sakurai, and H. Shiota. 1984. Bacterial pyrite oxidation. III. Adsorption of *Thiobacillus ferrooxidans* cells on solid surfaces and its effect on iron release from pyrite. *J. Gen. Appl. Microbiol.* 30: 63-77.

## CHAPTER 9

### STABILITY OF PHOSPHATE COATED PYRITE IN THE PRESENCE OF *THIOBACILLUS FERROOXIDANS* \*

#### 9.1 INTRODUCTION

Throughout the world, large sums of money are spent for the treatment, prevention and control of acid rock drainage (ARD). Sulfide oxidation and ARD formation have been shown to follow two main pathways; the chemical and the microbiological pathways (Silverman and Ehrlich, 1964; Singer and Stumm, 1970; Hiskey and Schlitt, 1982). The rate of ferrous oxidation and ARD formation is known to be accelerated in the presence of bacteria, *Thiobacillus ferrooxidans* (Singer and Stumm, 1970, Kleinmann and Crerar, 1979).

The need to prevent and control ARD formation has led to investigations into various oxidation suppression techniques (Peeler, 1963; Tyco Laboratories, 1971; Lalvani and Shami, 1987; Nyavor and Egiebor, 1994; Chapter 3). One of these oxidation suppression techniques is phosphating (Nyavor and Egiebor, 1995; Chapter 2; Evangelou, 1995). Sulfide phosphating results in the formation of iron phosphate coating on the sulfides, thus suppressing its oxidation.

Although sulfide oxidation and ARD formation have been shown to be due to both chemical and microbiological oxidation of sulfide and ferrous ion, only the chemical pathway of oxidation of the phosphate technique for the control and prevention of ARD has been evaluated. The objective of this study was to investigate the stability of phosphate-

---

\* A version of this chapter, co-authored with N. O. Egiebor and P. M. Fedorak, has been submitted to the Science of the Total Environment.

coated pyrite in the presence of  $\text{H}_2\text{SO}_4$  and *T. ferrooxidans*, which are both unavoidable in ARD formation.

## **9.2 THEORY AND BACKGROUND**

The theory and background of the phosphating technique for controlling and preventing ARD at-source has been reported in Section 2.2 (Nyavor and Egiebor, 1995).

## **9.3 EXPERIMENTAL METHODS**

### **9.3.1 Culture and Medium**

*T. ferrooxidans* strain ATCC 13661 was used in this study. The composition of the medium used for the growth of the bacteria is reported in Section 4.2.1. The medium used for the phosphate coated pyrite stability test has also been reported in Section 8.2.1. All chemical reagents used were analar grade obtained from Fisher Scientific, Edmonton, Canada and used without further purification.

### **9.3.2 Pyrite and Phosphate Coating**

The origin of the pyrite used in this study and its preparation has been reported in Section 8.2.2. Pyrite particles of -355 +300  $\mu\text{m}$  size fraction were used in the study.

Phosphate coating of pyrite samples was carried out in a cylindrical glass reactor. Details of the coating procedure has been reported elsewhere (Section 2.3.2; Nyavor and Egiebor, 1995). The pyrite samples were treated with 0.1 M  $\text{KH}_2\text{PO}_4$  and 2%  $\text{H}_2\text{O}_2$  at 25°C and 40°C, and used in the control (no cells added) and inoculated experiments.

### **9.3.3 Most Probable Number (MPN) Method**

The MPN method used to monitor the number of viable *T. ferrooxidans* cells in cultures and cell suspensions has been outlined in Section 4.2.3.

### **9.3.4 Preparation of Cell Suspension**

Details of the preparation of cell suspension used for the pyrite stability experiments has been reported in Section 5.3.4.

### **9.3.5 Stability Tests**

Details of the stability test of the untreated and phosphate coated pyrite samples in the absence and presence of *T. ferrooxidans* is similar to that reported in Section 8.2.6. Samples were taken before and during incubation for total Fe, soluble Fe<sup>2+</sup>, PO<sub>4</sub><sup>3-</sup>, pH and MPN analysis. The stability experiments were carried out in duplicate and average values reported. The results from the duplicate experiments were within 5% deviation.

### **9.3.6 Chemical Analysis and pH**

Total Fe and Fe<sup>2+</sup> in the leached solutions were determined by DR/2000 Spectrophotometer and the total Fe verified with Atomic Absorption Spectrophotometry (AAS). Details of the procedure is reported in Section 2.3.5. The phosphate concentration of leached solutions were determined by the vanadomolybdophosphoric acid method (American Public Health Association, 1975). The pH of the leached solutions were determined by a Cole-Parmer Chemcadet pH/mV meter equipped with a temperature compensation probe.

## **9.4 RESULTS AND DISCUSSION**

Chemical analysis of the natural pyrite used in the experiments by AAS, Leco total sulfur analyzer and Scanning Electron Microscope/Energy-Dispersive X-Ray Spectrometer has been reported in Section 2.4.

A series of experiments were initially done on the untreated pyrite with and without *T. ferrooxidans* to determine the rate of pyrite oxidation and variations in the number of

suspended viable cells during the oxidation. The initial experimental results were to be used to design phosphate-coated pyrite stability experiments. Figure 9-1 shows a plot of the change in total Fe and  $\text{Fe}^{2+}$  concentration with and without *T. ferrooxidans* for 40 days. From the plot, it is observed that the presence of the bacteria enhanced the rate of oxidation of the untreated pyrite, with more Fe leached into solution in the inoculated experiments than the control (no cells) experiments. In the control experiments, the total Fe and  $\text{Fe}^{2+}$  concentrations are similar throughout the incubation period, while with the inoculated experiments very little of the Fe is in the  $\text{Fe}^{2+}$  state.

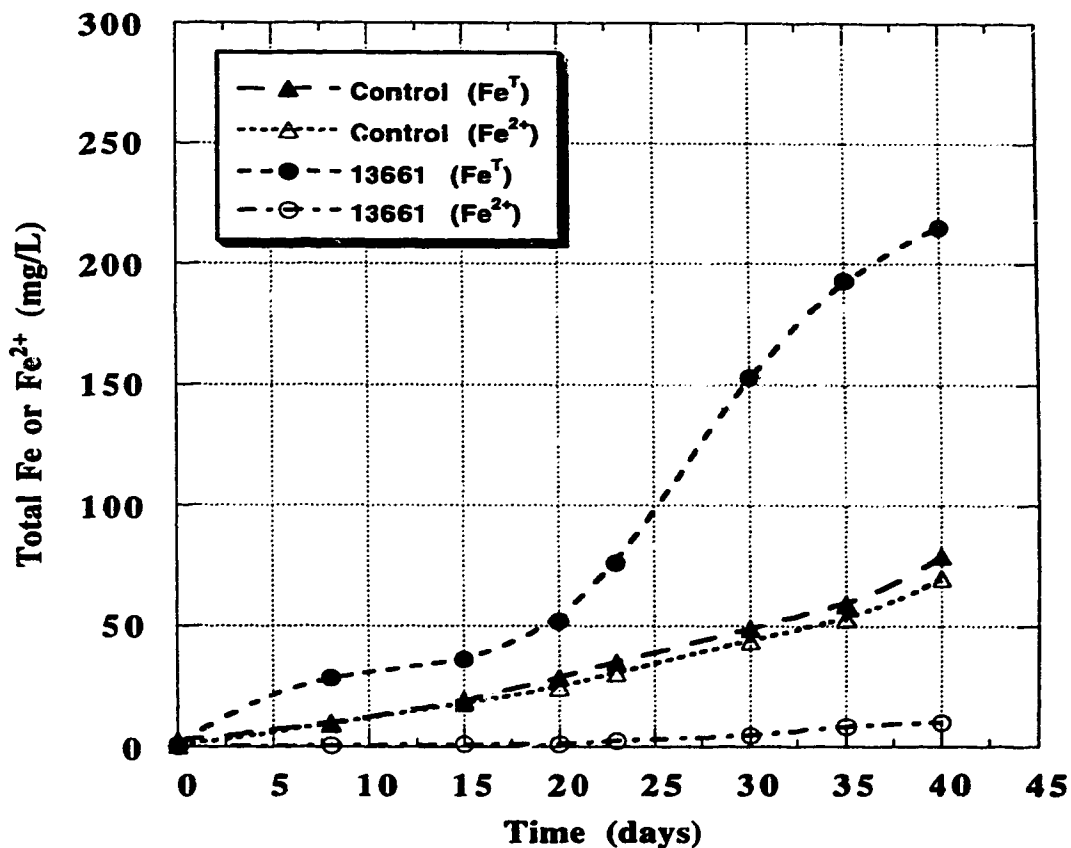


**Figure 9-1. Change in total Fe ( $\text{Fe}^T$ ) and ferrous ( $\text{Fe}^{2+}$ ) concentration during oxidation of untreated pyrite, initial pH of 2.4.**

This demonstrates that in the absence of bacteria, most of the iron in solution is in the  $\text{Fe}^{2+}$  state. Whereas in the presence of bacteria, the leached  $\text{Fe}^{2+}$  is rapidly converted to  $\text{Fe}^{3+}$ . At the start of the inoculated experiments,  $3.0 \times 10^6/\text{mL}$  of viable cells were in suspension, about the same number  $2.5 \times 10^6/\text{mL}$  were in suspension at the end of the experiment, although the number of cells fluctuated during the course of the experiment. The initial experiments indicated that the bacteria systems could be incubated for 40 days without the need to add fresh cells.

The effect of initial cell concentration on the oxidation of untreated pyrite was reported in Section 7.4.4. While there was an increase in the rate of oxidation of the untreated pyrite with increasing cell concentration from,  $2.6 \times 10^5/\text{mL}$  to  $4.6 \times 10^6/\text{mL}$ , there was no significant increase in the pyrite oxidation rate by increasing cell concentration above  $4.6 \times 10^6/\text{mL}$ . Cell concentrations above  $4 \times 10^6/\text{mL}$  were therefore used in the stability evaluation experiments.

The stability of the phosphate-coated pyrite samples was tested in the absence and presence of *T. ferrooxidans*. Two sets of experiments (inoculated and control) were incubated simultaneously, each set of experiments consisted of the untreated pyrite, phosphate-coated pyrite prepared at  $25^\circ\text{C}$ , and phosphate-coated pyrite prepared at  $40^\circ\text{C}$ , with all runs under the same conditions. The control experiments were used for monitoring chemical oxidation of the untreated and treated pyrite in the presence of  $\text{H}_2\text{SO}_4$ , while the inoculated experiments were used for monitoring total oxidation, both chemical and microbiological. The stability tests were incubated for 40 days at optimum conditions obtained from the initial experiments (Section 7.4.4 and Figure 9-1). Samples were drawn during the experiment and were analyzed for total Fe,  $\text{Fe}^{2+}$ ,  $\text{PO}_4^{3-}$ , pH and number of suspended viable cells.

Figures 9-2 and 9-3 illustrate results from the control experiment (no cells added) for the untreated,  $25^\circ\text{C}$  phosphate-coated, and  $40^\circ\text{C}$  phosphate-coated pyrite samples. The release of Fe during the oxidation experiment is shown in Figure 9-2. The plot shows that

the 40°C phosphate treatment does not reduce the rate of chemical oxidation of the pyrite in the  $-Fe^{2+}$  medium. The 40°C phosphate treatment resulted in a slight increase in the rate of pyrite oxidation over the untreated. The release of Fe into solution increased above that of the untreated pyrite after 10 days of leaching. The 25°C phosphate treatment slightly reduced the rate of pyrite oxidation, less Fe is leached into solution of the 25°C phosphate

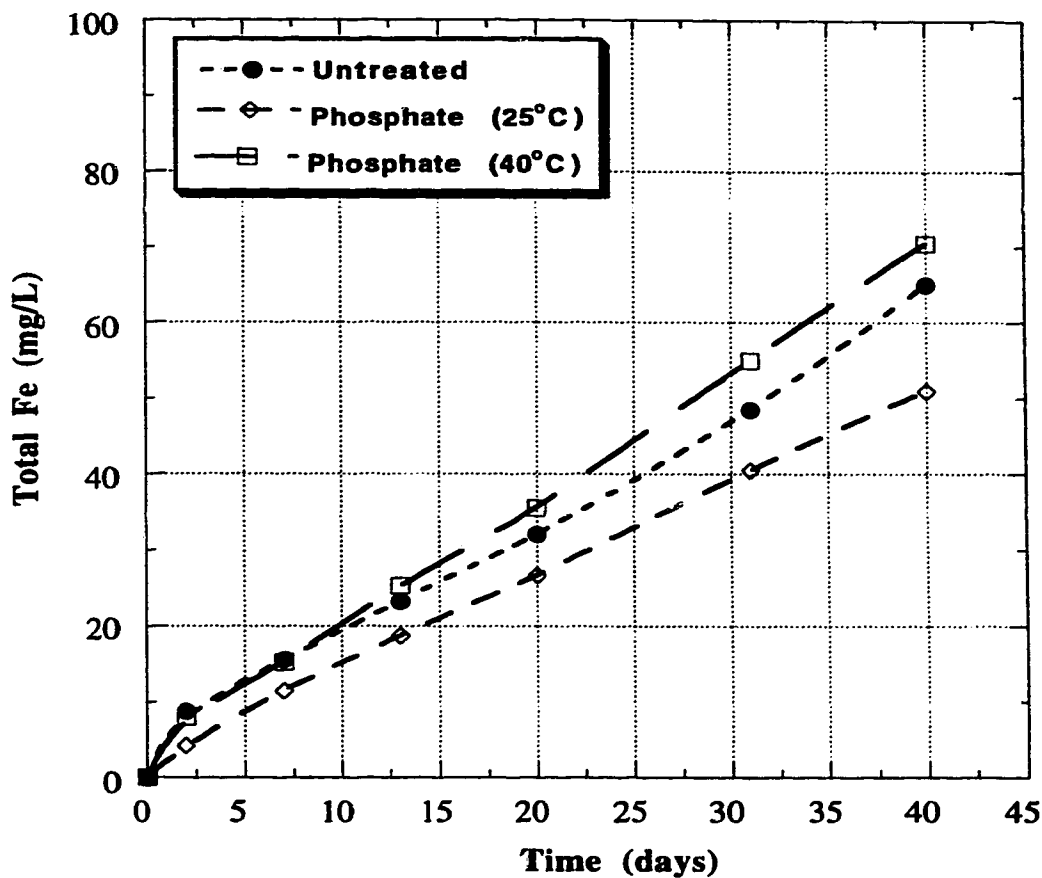


**Figure 9-2. Effect of phosphate coating at 25°C and 40°C on the oxidation of pyrite (no cells added, initial pH of 2.5).**

treated pyrite than the untreated pyrite and 40°C phosphate treated pyrite under the same conditions. The  $Fe^{2+}$  concentration during the experiment showed the same trend as the total Fe concentration with lower  $Fe^{2+}$  concentrations from the 25°C phosphate treated pyrite than the untreated and 40°C phosphate-treated pyrite (figure not shown). The higher

Fe released rate for the 40°C treated pyrite sample is due to the cracking of the coatings formed at higher temperatures (Figures 2-8 and 2-9) and the dissolution of the Fe-phosphate complex.

Figure 9-3 shows a plot of the percentage of the total Fe as  $\text{Fe}^{2+}$  in solution during the experiment. The plot shows that greater than 80% of the Fe is in the  $\text{Fe}^{2+}$  state during the oxidation of both the phosphate-treated and the untreated pyrite in the absence of bacteria. During chemical oxidation of untreated and phosphate-treated pyrite in the absence of bacteria, oxygen oxidation of ferrous to ferric is the only pathway for generating ferric ions. However, the chemical oxidation of ferrous under acidic pH and ambient condition is extremely slow (Colborn and Nicol, 1973). Ferrous ions therefore accumulate in the system and this explains the high proportion of  $\text{Fe}^{2+}$  obtained in the absence of the bacteria. Wakao et al. (1982) also reported an average percent  $\text{Fe}^{2+}$  value of 80% in uninoculated controls during oxidation of pyrite. The pH of both the untreated and phosphate-treated pyrite solutions decreased continuously during the control oxidation experiment. No significant difference in pH was observed between the untreated pyrite solution, which decreased from a pH of 2.6 to 2.1 and the phosphate-treated pyrite solutions which decreased by the same amount, over the course of the experiment. Though the 40°C phosphate-treated pyrite generally released more Fe into solution than the untreated and the 25°C phosphate treated pyrite, no significant difference in the concentration of phosphate was observed between these solutions during the course of the experiment. Since the -Fe<sup>2+</sup> medium contained 0.1 g/L of  $\text{KH}_2\text{PO}_4$ , it was difficult to detect additional phosphate concentrations due to leaching of the phosphate coating. Dissolution of the coating in the presence of  $\text{H}_2\text{SO}_4$  could therefore not be ruled out.



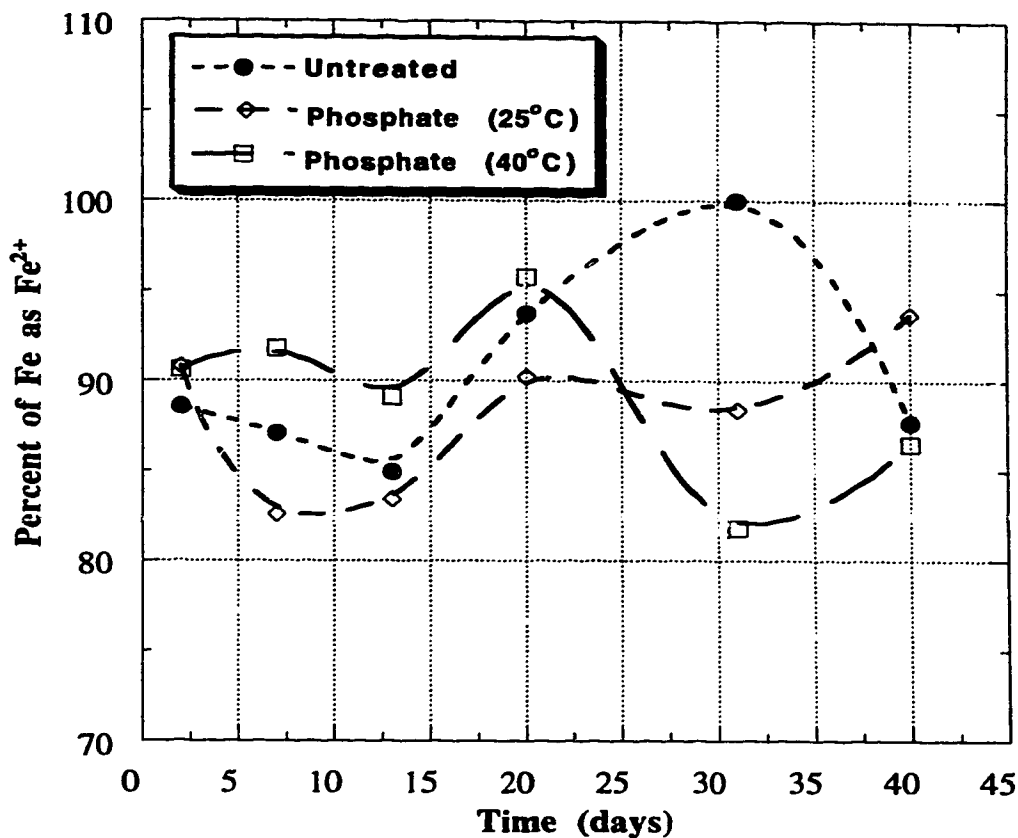


**Figure 9-3. Percentage of total Fe as ferrous during leaching of untreated, 25°C and 40°C phosphate-treated pyrite (no cells added).**

The results from the inoculated experiments for the untreated and phosphate-treated pyrite samples are shown in Figures 9-4 and 9-5. Figure 9-4 shows the change in total Fe concentration during bioleaching of the untreated and phosphate-treated pyrite samples. It is observed that the rate of oxidation of the pyrite is slightly reduced by the 25°C phosphate treatment. The 40°C phosphate treatment did not reduce the rate of pyrite oxidation over the untreated pyrite during the experimental period. Generally the same concentration of Fe was released into solution from the 40°C phosphate treated and untreated pyrite samples. The number of suspended viable cells fluctuated during the experiments; however, about the same number of viable cells were in suspension at the end of the experiments. At the

start of the experiment,  $4 \times 10^8$ /mL of viable cells were in suspension, while at the end to the experiment,  $1 \times 10^8$ /mL,  $5 \times 10^7$ /mL, and  $3 \times 10^7$ /mL were in the untreated, 25°C phosphate-treated, and 40°C phosphate-treated pyrite suspensions, respectively.

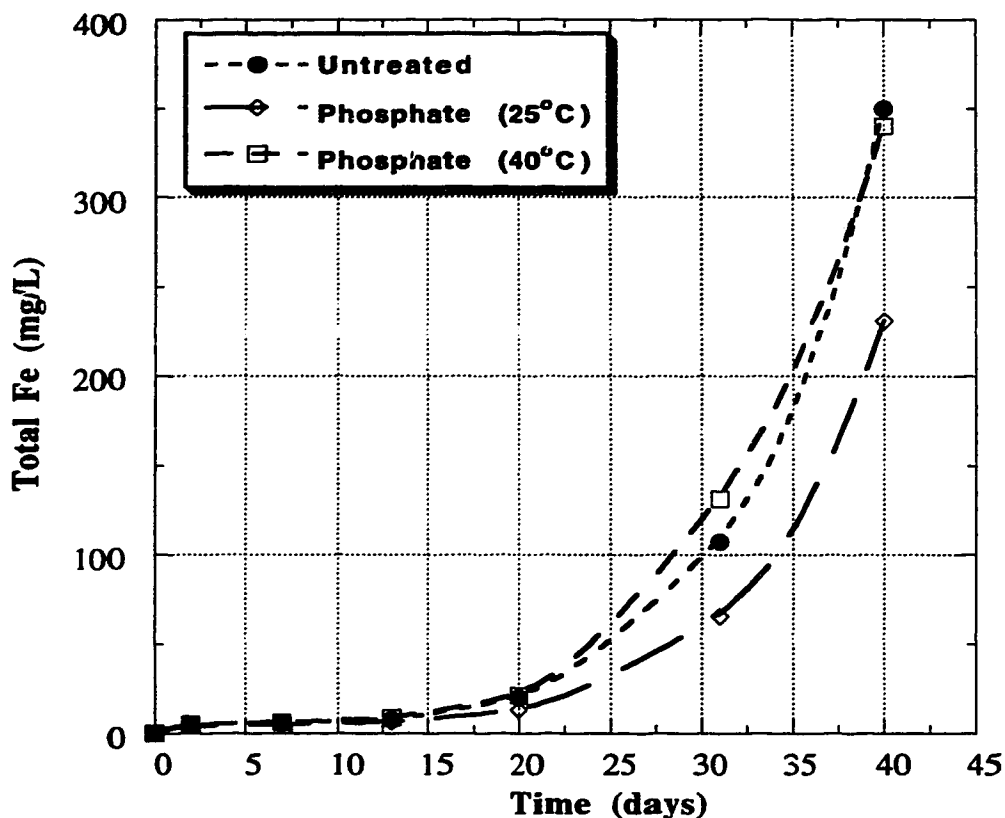


**Figure 9-4. Change in total Fe concentration during bioleaching of untreated, 25°C and 40°C phosphate-treated pyrite, initial pH of 2.5.**

Figure 9-5 shows a plot of the percentage of the total Fe concentration as  $Fe^{2+}$  during the inoculated experiments. In contrast to the control experiments (without cells), proportion of  $Fe^{2+}$  for the inoculated experiments are below 4% throughout the experiment. The low percent of  $Fe^{2+}$ , for both the untreated and the phosphate treated pyrite in the presence of bacteria indicates that over 95% of the total Fe is in the  $Fe^{3+}$  state. In the inoculated experiments for both the untreated and treated pyrite, the bacteria acts as a

catalyst in the oxidation of ferrous to ferric ion; however, ferric ion oxidation of the untreated and treated pyrite to produce additional ferrous ion is slow and therefore ferric ion accumulates in the system; hence the low percent  $\text{Fe}^{2+}$ . The pH of both the untreated and phosphate-treated pyrite solutions decreased with time during the experiment, and no significant differences were observed. No significant difference in phosphate concentration of leach solutions was observed between the phosphate-treated and the untreated pyrite solutions throughout the experiment.

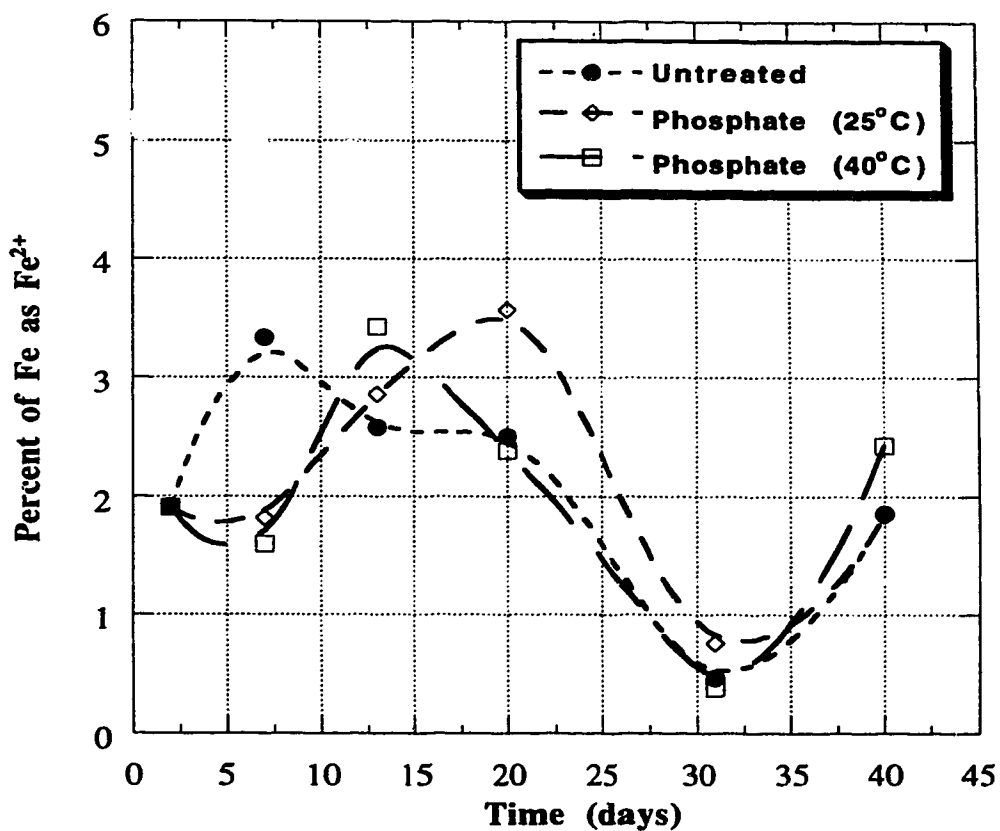


**Figure 9-5. Percentage of total iron as ferrous during bioleaching of untreated, 25°C and 40°C phosphate-treated pyrite, initial pH of 2.5.**

Phosphating of pyrite has been shown to form ferric-phosphate coatings on the pyrite surface (Nyavor and Egiebor, 1995; Chapter 2). Since the initial adsorption of ions or molecules on the surface of the pyrite is the initiation step of pyrite oxidation (Garrels and Thompson, 1960; Biegler and Swift, 1979), the phosphate coatings reduce the rate of chemical oxidation by keeping the molecules and ions from the pyrite surface during oxidation in the absence of bacteria. Since protection of the pyrite by the phosphate coatings is by physical means, reduced oxidation rates may only be achieved with low-crack, low-porosity coatings. Furthermore, the leaching test solution should not react with the coating material. The phosphate coatings had previously been tested at near-neutral pH under ambient and elevated temperature and pressures. Under these conditions, the coatings formed at 25°C, 40°C and 80°C significantly reduced the rate of pyrite oxidation (Nyavor and Egiebor, 1995; Chapter 2). Evangelou (1995) also tested phosphate-coated pyrite under stationary condition with H<sub>2</sub>O<sub>2</sub> at pH 4 for 16 h and reported reduced rates of oxidation over untreated pyrite.

The phosphate coatings, however, did not significantly reduce the rate of chemical and microbiological oxidation of the pyrite samples under the acidic conditions used in this experiment. To sustain the growth of the bacteria, the pH of the stability test solution was reduced with H<sub>2</sub>SO<sub>4</sub> to a pH of about 2.5 and other nutrients, (NH<sub>4</sub>)<sub>2</sub>SO<sub>4</sub>, K<sub>2</sub>HPO<sub>4</sub> and MgSO<sub>4</sub>, were added. Furthermore the stability experiments were conducted on orbital shaker tables at a speed of 200 rpm to ensure sufficient oxygen supply to the bacteria. Though phosphating of pyrite at higher temperatures have been shown to form thicker coatings and are expected to result in better protection of the pyrite, the higher temperature phosphating also produce cracked coatings (Nyavor and Egiebor, 1995; Chapter 2). The poor protection of the 40°C coating compared to the 25°C coating may partly be due to this factor. The strong acid test solution may also dissolve the phosphate coating, although no significant increase in phosphate concentration was observed in these solutions because of

the high background phosphate concentration in the medium. The dissolution of ferric-phosphate coatings on pyrite in HCl solution has been reported by Evangelou (1995).

In the presence of bacteria, the oxidation rates of the phosphate-treated pyrites, were higher than in the absence of the bacteria (Figures 9-2 and 9-4). In the presence of *T. ferrooxidans*, the phosphate coatings have to withstand not only the chemical constituents of the leach test solution ( $\text{Fe}^{2+}$  medium), but also the high concentrations of  $\text{Fe}^{3+}$  (a strong oxidant) produced by the bacteria oxidation of  $\text{Fe}^{2+}$ , and possibly, the bacterial attack on the coating material directly. The high  $\text{Fe}^{3+}$  concentration of the leach solutions in the presence of bacteria are shown by the low proportion of  $\text{Fe}^{2+}$  in the presence of the bacteria (Figure 9-5). These factors resulted in the higher oxidation rates of the coated pyrite samples in the presence of the bacteria than in its absence. The bacteria therefore increased the oxidation rates of both the 25°C and 40°C phosphate treated pyrite, and the untreated pyrite samples.

## 9.5 SUMMARY OF CHAPTER

The results of this study have shown that the phosphate coatings formed on the pyrite samples were not stable under the physical, chemical and biological conditions used in this test. The coatings formed at 25°C only slightly reduced the rate of chemical oxidation of the pyrite in the absence of bacteria, whereas the 40°C phosphate coatings slightly increased the rate of chemical oxidation of the pyrite. In the presence of bacteria, the 25°C phosphate coating also slightly reduced the rate of pyrite oxidation over the 40°C coated pyrite and the untreated pyrite which generally showed the same oxidation rate. The rate of oxidation of both the 25°C and 40°C phosphate coated pyrite and the untreated pyrite were all higher in the presence of the bacteria than in its absence. While in the absence of bacteria the Fe leached into solution is generally in the  $\text{Fe}^{2+}$  state, in presence of the bacteria the dissolved Fe is generally in the  $\text{Fe}^{3+}$  state.

## 9.6 REFERENCES

- American Public Health Association. 1985. Standard methods for the examination of water and wastewater. APHA, Washington, DC.
- Biegler, T., and D. A. Swift. 1979. Anodic behaviour of pyrite in acid solutions. *Electrochim. Acta.* 24: 415-420.
- Colborn, R. P. and M. J. Nicol. 1973. An investigation into the kinetics and mechanism of the oxidation of iron (II) by oxygen in aqueous chloride solution. *J. S. Afr. Inst. Min. Metal.* 73: 281-289.
- Evangelou, V. P. 1995. Potential microencapsulation of pyrite by artificial inducement of ferric phosphate coatings. *J. Environ. Qual.* 24: 535-542.
- Garrels, R. M., and M. E. Thompson. 1960. Oxidation of pyrite by iron sulfate solution. *Am. J. Sci.* 258A: 57-67.
- Kleinmann, R. L. P., and D. A. Crerar. 1979. *Thiobacillus ferrooxidans* and the formation of acidity in simulated coal mine environments. *J. Geomicrobiol.* 1: 373-388.
- Lalvani, S. B., and M. Shami. 1987. Passivation of pyrite oxidation with metal cations. *J. Materials Sci.* 22: 3503-3507.
- Nyavor, K., and N. O. Egiebor. 1994. Suppression of pyrite oxidation by fatty acid amine treatment. Extraction and processing for the treatment and minimization of wastes, J. P. Hager B. J. Hansen, W. P. Imrie, J. F. Pusateri, and V. Ramachandran (eds). TMS, San Francisco, California. pp. 773-790.
- Nyavor, K., and N. O. Egiebor. 1995. Control of pyrite oxidation by phosphate coating. *Sci. Total Environ.* 162: 225-237.
- Peeler, C. E. Jr. 1963. Treatment of earth strata containing acid forming chemicals. U. S. Pat. 3,094,846.
- Singer, P. C., and W. Stumm. 1970. Acid mine drainage: The rate-determining step. *Science.* 167: 1121-1123.

Tyco Laboratories Inc. 1971. Silicate treatment of sulfide refuse piles. Water Pollution Control Research Services. U. S. EPA, report no. 14010DL101/71.

Wakao, N., M. Mishina, Y. Sakurai, and H. Shiota. 1982. Bacterial pyrite oxidation. I. The effect of pure and mixed cultures of *Thiobacillus ferrooxidans* and *Thiobacillus thiooxidans* on release of iron. J. Gen. Appl. Microbiol. 28: 331-343.

## CHAPTER 10

### GENERAL DISCUSSION AND CONCLUSIONS

#### 10.1 Bacteria Growth Parameters

The results of the *T. ferrooxidans* growth study have shown that ferrous iron concentration of a culture may be used to give an indication of the growth phases and to monitor cell numbers and viability during the log growth phase. However, it cannot be accurately used to monitor changes in viable cell numbers during the stationary and death phases.

The turbidity and protein concentration of the culture showed positive linear relationship with the number of viable cells only during the log growth phase, and could therefore be used as an indication of the cell numbers in the log growth phase only. For experiments which require shorter duration than the log growth phase, protein concentration, ferrous concentration or turbidity may be used as an indirect indication of cell numbers and viability. But, for those that require longer durations than the log growth phase, during which the culture enters the stationary and death phases, protein concentration, ferrous concentration and turbidity will not be adequate for monitoring changes in viable cell numbers. In this case, the most probable number (MPN) should be used.

The protein concentration and turbidity have positive linear relationships with each other. Either of these parameters could therefore be monitored in place of the other. The ferric iron concentration correlates well with both the protein concentration and turbidity only during the growth phase, and in this phase any of the three parameters can be used in place of the other (Chapter 4).



The ferric iron generated in situ by the oxidation of ferrous iron by the cells, was, in part, responsible for the decreasing viability of the culture and hence indicates some toxic effects of  $\text{Fe}^{3+}$  on *T. ferrooxidans* cells.

## 10.2 Phosphating of Pyrite

Pyrite phosphating forms an iron phosphate coating on the particles. The phosphate coating controls the ingress of oxidants into the pyrite matrix, which in turn reduces the rate of pyrite oxidation in the absence of bacteria and under circumneutral pH (Chapter 2; Nyavor and Egiebor, 1995).

High temperature phosphating of pyrite forms thicker coatings; however, these thicker coatings do not significantly improve the protection of the pyrite over thinner coatings formed under ambient conditions (Chapter 2; Nyavor and Egiebor, 1995). Phosphating at high temperatures results in cracked coatings on the pyrite surface.

In the presence of *T. ferrooxidans* and  $\text{H}_2\text{SO}_4$ , the rate of oxidation of the untreated and phosphate-coated pyrite were higher than in the presence of only  $\text{H}_2\text{SO}_4$ .

The coatings were less stable in the presence of bacteria and  $\text{H}_2\text{SO}_4$  than under circumneutral pH in the absence of the bacteria (Chapter 9). The coatings formed at  $25^\circ\text{C}$  only slightly reduced the rate of oxidation of the pyrite in the presence of bacteria, while the  $40^\circ\text{C}$  phosphate-coatings generally showed the same oxidation rate as the untreated pyrite. Under the acidic conditions used in the bacterial experiments, both the coating material and the pyrite are attacked through the cracks in the coating formed at high temperatures. In the absence of bacteria, the iron leached into solution is generally in the ferrous state, whereas in the presence of the bacteria, the dissolved iron is generally in the ferric state.

### **10.3 Fatty Acid Amine Treatment**

The treatment of pyrite with fatty acid amine significantly reduced the rate of oxidation of the pyrite. Fatty acid amine treatment produced a hydrophobic surface which reduces contact between pyrite and aqueous oxidizing agents. The reduced contact results in reduced rate of pyrite oxidation in the absence of bacteria and at circumneutral pH (Chapter 3; Nyavor and Egiebor 1994).

In the presence of bacteria and under acidic conditions ( $H_2SO_4$ ), the fatty acid amine treatment suppresses the rate of both chemical and microbiological oxidation of the pyrite. The hydrophobic surface formed by the fatty acid amine treatment of the pyrite repels the oxidizing ions, thus reducing the rate of oxidation of the treated pyrite (Chapter 8).

The use of an autoclave for testing the stability of treated sulfide particles, in terms of chemical oxidation has been shown to be a faster, and reliable alternative to the conventional column oxidation test. The trend of the results obtained from the autoclave test were comparable with those obtained from the accelerated oxidation column test. Hence autoclave tests can be used as a faster means for screening the effectiveness of reagents used for pyrite oxidation suppression.

### **10.4 Comparison of Phosphate and Fatty Acid Amine Treatment**

Both the phosphate and fatty acid amine treatment suppresses the rate of chemical oxidation of the pyrite near-neutral pH under ambient and elevated temperature and pressures. The phosphate treatment did not significantly reduce the rate of chemical and biological oxidation of the pyrite under acidic conditions (Chapter 9). However, the fatty acid amine treatment suppressed the rate of both chemical and biological oxidation of the pyrite under acidic conditions (Chapter 8).

Michaelis-Menten rate kinetics to a first order rate kinetics depending on the ferrous and cells concentrations used for the analysis.

The pseudo-first order kinetics is an approximation of the Michaelis-Menten and it applies only when the Michaelis constant  $K_m$ , is very large. Conversely, if ferrous concentration is very large, relative to cell concentrations, the Michaelis constants become negligible and the oxidation of ferrous ions by *T. ferrooxidans* follows zero order kinetics (Chapter 5).

The first order analysis used mainly by metallurgists is an approximation of the Michaelis-Menten rate kinetics used by microbiologists.

### **Effect of Ferric Ion on Ferrous Oxidation Kinetics**

Ferric ion competitively inhibits the oxidation of ferrous by *T. ferrooxidans*. As the concentration of cells does not change the inhibitor constant; however, as cell concentration at a constant inhibitor concentration increases the rate of  $Fe^{2+}$  oxidation (Chapter 6). Thus increasing cell concentration decreases the inhibitory effect of  $Fe^{3+}$  on  $Fe^{2+}$  oxidation by the bacteria. The  $Fe^{3+}$  ions compete with the  $Fe^{2+}$  ions for the active site on the *T. ferrooxidans* cells.

### **Mechanism of Acid Mine Drainage Formation**

Two possible mechanisms of bacterial oxidation of sulfides and AMD formation have previously been proposed; the indirect and direct contact mechanisms. For the indirect mechanism, ferric ions are the primary oxidants, oxidizing metal sulfides while being reduced to the ferrous state. *T. ferrooxidans* then oxidized ferrous to ferric as discussed in Chapter 5. The indirect mechanism can be represented by Figure 10-1:

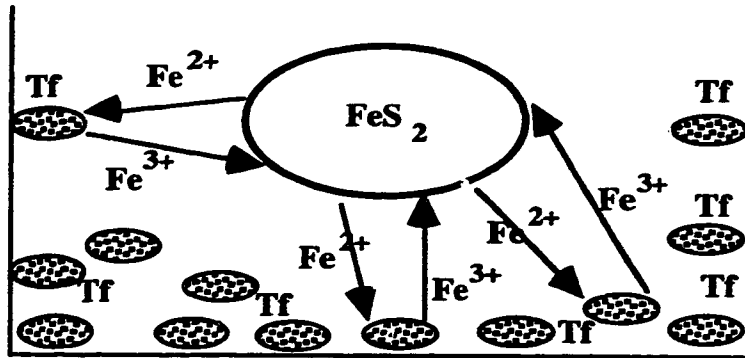


**Figure 10.1. Representation of the indirect contact mechanism.**  
(Tf denotes *T. ferrooxidans* cells)

In Figure 10.1, the chemical oxidation of the pyrite results in the generation of  $\text{Fe}^{2+}$  into solution, which is then oxidized by *T. ferrooxidans* to  $\text{Fe}^{3+}$  in solution. The  $\text{Fe}^{3+}$  produced by the oxidation of  $\text{Fe}^{2+}$  by the bacteria in turn oxidizes the pyrite to produce  $\text{Fe}^{2+}$  which is again oxidized by the bacteria, resulting in a cyclical process.

For the indirect contact mechanism, direct contact between the bacteria and the pyrite is not required. However, for the direct contact mechanism, intimate contact between the bacteria and the surface of the sulfide mineral is necessary. Figure 10-2 illustrates the direct contact mechanism. The *T. ferrooxidans* cells attach onto the surface of the pyrite and carries out the pyrite oxidation from the surface. From a practical standpoint, the difference between these two conceptual models lies in the fact that, in the indirect case, the total number of bacteria in a given system is potentially a rate-determining factor, while in the direct model, only those bacteria attached to the pyrite surface will directly affect oxidation rates.

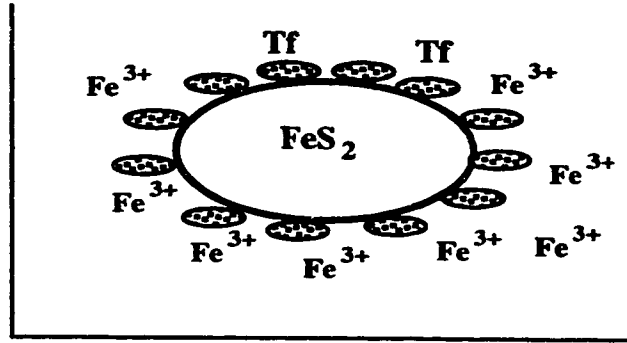


**Figure 10.2. Representation of the direct contact mechanism.**  
 (Tf denotes *T. ferrooxidans* cells)

Results of the mechanistic studies (Chapter 7) suggest that although *T. ferrooxidans* attaches to sulfide and glass surfaces it may not directly oxidize the sulfides as proposed by the direct contact mechanism.

The pitting of the pyrite (Figure 7-15) in the presence of *T. ferrooxidans* which had been used to support the direct contact mechanism is likely due to the high concentration gradient of  $\text{Fe}^{3+}$  in the vicinity of the bacteria attachment. The highest concentrations of  $\text{Fe}^{3+}$  occurs at bacteria attached sites because of the rapid oxidation of the chemically generated  $\text{Fe}^{2+}$  to  $\text{Fe}^{3+}$  by the bacteria.

The results presented in Chapter 7 indicate that oxidation of  $\text{FeS}_2$  is mainly by chemical means, with the bacteria acting as a catalyst in converting  $\text{Fe}^{2+}$  to  $\text{Fe}^{3+}$  which in turn oxidizes  $\text{FeS}_2$  and generates  $\text{H}_2\text{SO}_4$ . This mechanistic proposition is supported by the inability of viable cells to oxidize  $\text{FeS}_2$  when initial chemical oxidation of  $\text{FeS}_2$  is suppressed above pH of about 4.0. The insignificant increase in pyrite oxidation with increase in cell concentration beyond  $10^6/\text{mL}$  also supports the indirect contact mechanism.

suspension and when attached to solids. It can be concluded from the study, that the indirect mechanism is the predominant pathway during sulfide oxidation and AMD formation in the presence of bacteria.

The study showed that in the absence of *T. ferrooxidans*, the rate-limiting reaction during pyrite oxidation is the chemical oxidation of ferrous to ferric ion. The ferrous to ferric ion oxidation limiting reaction results in the accumulation of ferrous ion in the system. Conversely, in the presence of bacteria, ferric ion oxidation of the pyrite is the rate-limiting reaction during the oxidation of pyrite. This rate-limiting reaction results in the accumulation of ferric ion in the system, and therefore low abundance of  $Fe^{2+}$ . Figure 10-1 therefore illustrates the proposed mechanism of sulfide oxidation and AMD formation.

## **CHAPTER 11**

### **RECOMMENDATIONS FOR FURTHER STUDIES**

Based on the results of this study, the following suggestions for further studies are recommended:

- A. To further investigate the predominance of the chemical pathway of AMD formation, the rate of oxidation of sulfide by ferric ions at various concentrations in the absence and presence of bacteria should be investigated. This study should further clarify the relative contribution of the direct and indirect contact mechanisms of sulfide oxidation and AMD formation.
- B. The phosphate coatings significantly reduced the chemical oxidation of the sulfide particles in columns, but failed to appreciably reduce its oxidation during agitation in the absence and presence of bacteria. It will be important to evaluate the stability of the phosphated sulfide particles under stationary conditions in columns in the presence of bacteria. This project should give an indication of the effects of vigorous agitation on the stability of the coating. Agitation may result in the removal of loosely formed phosphate coatings.
- C. Increasing hydrophobicity of the sulfide particles reduces the rate of its oxidation in the absence and presence of bacteria. The other factor that may be attributed to the reduced rate of oxidation is the surfactant used. It should be interesting to investigate the effect of the fatty acid amine on the viability of the cells, and the rate of chemical and biological oxidation of ferrous ion and sulfide in the presence and absence of fatty acid amine.
- D. Any technique which would modify the surface properties of the sulfides and result in the reduction of the rate of oxidation of the sulfide should result in the control of

**AMD. Silicates are very stable compounds and are used for stabilizing wastes. The formation of a stable silicate coating on the surface of the sulfides and evaluating the stability of these coatings in terms of sulfide oxidation in the absence and presence of bacteria should be an interesting project. Preliminary experiments showed reduced oxidation rates after silicate treatment in the absence and presence of bacteria.**



## APPENDIX

### (DATA USED IN FIGURES)

#### CHAPTER 2

**Figure 2-5**

Time (mins)	pH	Total Fe (mg/L)
0	4.17	0.00
5	2.70	93.70
10	2.44	77.75
20	2.12	32.50
30	1.93	30.20
40	1.70	35.50
50	1.68	37.80
60	1.69	36.50

**Figure 2-11**

Time (days)	untreated Pyrite Fe(mg/l)	T=25°C Per=2% Fe(mg/l)	T=40°C Per=2% Fe(mg/l)	T=80°C Per=1% Fe(mg/l)	T=80°C Per=2% Fe(mg/l)	untreat Cum. %	T=25C Cum. %	T=40C Cum. %	T=80C Cum. %	T=80C Cum. %
0	0.00	0.00	0.00	0.00	0.00	0.000	0.000	0.000	0.000	0.000
2	1.74	0.31	0.75	0.61	0.96	0.007	0.001	0.003	0.003	0.004
5	1.47	0.27	0.89	1.28	1.23	0.014	0.002	0.007	0.008	0.009
10	2.71	0.50	0.61	0.98	0.86	0.025	0.005	0.010	0.012	0.013
14	4.23	0.64	0.53	1.10	0.87	0.043	0.007	0.012	0.017	0.017
18	4.17	0.81	0.50	1.05	0.96	0.061	0.011	0.014	0.021	0.021
21	2.99	0.78	0.57	0.94	0.50	0.074	0.014	0.016	0.025	0.023

Figure 2-11 (cont.)

Time (days)	untreated Pyrite Fe(mg/l)	T=25°C Per=2% Fe(mg/l)	T=40°C Per=2% Fe(mg/l)	T=80°C Per=1% Fe(mg/l)	T=80°C Per=2% Fe(mg/l)	untreat Cum. %	T=25C Cum. %	T=40C Cum. %	T=80C Cum. %	T=80C Cum. %
25	4.42	0.96	0.68	1.07	0.67	0.093	0.018	0.019	0.030	0.026
28	3.61	0.91	0.75	1.17	0.83	0.108	0.022	0.023	0.035	0.029
32	4.50	1.17	0.92	1.38	0.92	0.127	0.027	0.026	0.041	0.033
36	4.81	1.12	0.78	1.57	0.98	0.148	0.032	0.030	0.048	0.038
40	5.46	1.18	1.40	2.36	1.42	0.171	0.037	0.036	0.058	0.044
44	8.21	1.58	1.23	2.10	1.23	0.206	0.044	0.041	0.067	0.049
48	4.70	1.60	1.34	1.64	1.19	0.226	0.051	0.047	0.074	0.054
52	6.37	1.65	1.60	1.86	1.44	0.254	0.058	0.054	0.082	0.060
56	4.44	1.63	1.44	1.78	1.49	0.273	0.065	0.060	0.089	0.066
61	7.79	2.54	2.14	2.81	1.82	0.306	0.075	0.069	0.101	0.074
67	9.06	3.15	2.97	3.52	2.33	0.344	0.089	0.082	0.116	0.084
74	10.24	3.74	3.53	4.24	3.49	0.388	0.105	0.097	0.134	0.099
81	12.72	5.78	4.58	5.13	3.57	0.442	0.129	0.116	0.156	0.114

Figure 2-12

Time (days)	untreated Pyrite Acid/mg	untreated Cum. acidity	T=25°C Per=2% Acid/mg	T=25°C Cum. acidity	T=40°C Per=2% Acid/mg	T=40C Cum. acidity	T=80C Pe=1% Acid	T=80C Cum. acidity	T=80C Pe=2% Acid	T=80C Cum. acidity
0	0.00	0.00	0.00	0.00	0.00	0.00	0.00	0.00	0.00	0.00
2	2.45	2.45	0.90	0.90	9.20	9.20	6.10	6.10	6.90	6.90
5	3.81	6.26	1.04	1.94	7.33	16.53	5.16	11.26	6.15	13.05
10	5.56	11.82	2.54	4.48	4.66	21.19	3.56	14.82	4.57	17.62
14	11.70	23.52	3.05	7.53	4.45	25.64	1.22	16.04	6.09	23.71
18	11.42	34.94	3.81	11.34	4.75	30.39	4.61	20.65	6.04	29.75

**Figure 2-12 (cont.)**

Time (days)	untreated Pyrite Acid/mg	untreated Cum. acidity	T=25°C Per=2% Acid/mg	T=25°C Cum. acidity	T=40°C Per=2% Acid/mg	T=40°C Cum. acidity	T=80°C Pe=1% Acid	T=80°C Cum. acidity	T=80°C Pe=2% Acid	T=80°C Cum. acidity
21	10.46	45.40	4.07	15.41	6.06	36.45	4.83	25.48	3.97	33.72
25	12.37	57.77	5.13	20.54	5.97	42.42	6.30	31.78	4.98	38.70
28	11.98	69.75	5.53	26.07	7.12	49.54	6.61	38.39	5.91	44.61
32	13.98	83.73	5.34	31.41	7.12	56.66	6.06	44.45	6.33	50.94
36	15.14	98.87	6.09	37.50	7.71	64.37	8.21	52.66	7.43	58.37
40	17.62	116.49	5.69	43.19	9.19	73.56	9.98	62.64	8.01	66.38
44	23.97	140.46	6.67	49.86	8.15	81.71	8.90	71.54	7.41	73.79
48	15.43	155.89	7.98	57.84	7.71	89.42	6.83	78.37	7.30	81.09
52	20.58	176.47	6.99	64.83	8.60	98.02	9.85	88.22	8.77	89.86
56	14.74	191.21	6.62	71.45	7.68	105.7	7.55	95.77	8.04	97.90
61	25.16	216.37	9.83	81.28	10.98	116.7	11.47	107.2	9.36	107.3
67	28.91	245.28	12.71	93.99	13.05	129.7	13.51	120.8	10.80	118.1
74	33.25	278.53	14.21	108.20	15.76	145.5	16.56	137.3	16.20	134.3
81	55.45	333.98	19.80	128.00	17.68	163.2	18.53	155.8	13.50	147.8

**Figure 2-13**

Time (mins)	25°C Untreated	40°C Untreated	60°C Untreated
0	0.003	0.009	0.022
60	0.005	0.015	0.048
120	0.006	0.020	0.078
180	0.007	0.023	0.105
240	0.007	0.024	0.156
300	0.008	0.036	0.230
360	0.008	0.044	0.339
420	0.009	0.065	0.441
480	0.010	0.094	0.653
540	0.011	0.125	0.896
600	0.012	0.150	1.166

**Figure 2-14**

Time (mins)	100 psi	200 psi	500 psi	1000 psi
0	0.015	0.015	0.044	0.022
60	0.031	0.025	0.071	0.048
120	0.060	0.060	0.104	0.078
180	0.089	0.107	0.142	0.105
240	0.128	0.141	0.195	0.156
300	0.172	0.198	0.240	0.230
360	0.222	0.262	0.313	0.339
420	0.269	0.331	0.426	0.441
480	0.334	0.410	0.620	0.653
540	0.403	0.504	0.843	0.896
600	0.470	0.619	1.032	1.166

**Figure 2-15**

Time (mins)	Untreated	25°C Phosphate	40°C Phosphate	80°C Phosphate
0	0.015	0.010	0.010	0.010
60	0.025	0.016	0.014	0.012
120	0.060	0.023	0.021	0.018
180	0.107	0.042	0.039	0.030
240	0.141	0.064	0.060	0.050
300	0.198	0.088	0.080	0.065
360	0.262	0.122	0.100	0.085
420	0.331	0.172	0.142	0.125
480	0.410	0.226	0.190	0.160
540	0.504	0.306	0.250	0.220
600	0.619	0.369	0.300	0.250

**Figure 2-16**

Time (mins)	Untreated	25°C Phosphate	40°C Phosphate	80°C Phosphate
0	0.022	0.030	0.060	0.030
60	0.048	0.034	0.082	0.040
120	0.078	0.036	0.095	0.050
180	0.105	0.059	0.112	0.090
240	0.156	0.095	0.144	0.100
300	0.230	0.146	0.187	0.150
360	0.339	0.213	0.245	0.220
420	0.441	0.270	0.298	0.275
480	0.653	0.371	0.387	0.388
540	0.896	0.501	0.563	0.510
600	1.166	0.663	0.777	0.600

**CHAPTER 3**

**Figure 3-1**

Time (mins)	Armac T	Armac C	Armac HR
0	0.00	0.00	0.00
5	2.05	2.07	2.60
10	2.20	2.90	2.60
20	2.40	3.10	2.90
30	2.60	3.30	3.00
40	2.80	3.40	3.10
50	3.00	3.40	3.10
60	3.00	3.40	3.10

**Figure 3-2**

Time (mins)	Armac T	Armac C	Armac HR
0	4.19	1.99	3.86
5	3.97	1.89	3.65
10	3.65	1.85	3.26
20	3.10	1.80	2.58
30	2.90	1.79	2.16
40	2.89	1.78	1.68
50	2.89	1.77	1.59
60	2.87	1.76	1.55

**Figure 3-3**

Concentration (g/L)	Armac T (A°)	Armac C (A°)	Armac HR (A°)
1.23	64.4	57.1	54.7
0.62	62.0	53.0	53.6
0.37	58.6	52.0	53.9
0.00	26.0	26.0	26.0

**Figure 3-4**

Untreated pH	Untreated Zeta potential	Armac T pH	Armac T Zeta potential	Armac HR pH	Armac HR Zeta potential
3.1	11.39	3.0	-	3.0	-
4.0	12.20	4.0	-	4.0	-
5.0	12.80	5.0	-	5.0	-
5.5	10.71	5.8	46.49	5.3	46.35
6.0	5.10	6.0	-	6.0	-
6.5	-8.96	6.5	37.43	6.5	-
7.1	-12.58	7.0	33.48	7.0	-

**Figure 3-4 (cont.)**

Untreated pH	Untreated Zeta potential	Armac T pH	Armac T Zeta potential	Armac HR pH	Armac HR Zeta potential
7.5	-15.20	7.2	28.38	7.4	30.73
8.1	-21.17	7.4	25.15	7.6	28.00
8.5	-	7.8	22.36	8.2	26.66
9.0	-25.70	8.5	15.43	8.7	26.11
9.5	-27.80	9.5	-	8.9	22.72
10.2	-33.06	10.0	11.23	9.2	21.55

**Figure 3-6**

Time (mins)	Untreated (25°C)	Untreated (40°C)	Untreated (60°C)
0	0.003	0.009	0.022
60	0.005	0.015	0.048
120	0.006	0.020	0.078
180	0.007	0.023	0.105
240	0.007	0.024	0.156
300	0.008	0.036	0.230
360	0.008	0.044	0.339
420	0.009	0.065	0.441
480	0.010	0.094	0.653
540	0.011	0.125	0.896
600	0.012	0.150	1.166

**Figure 3-7**

Time (mins)	100 psi	200 psi	500 psi	1000 psi
0	0.015	0.015	0.044	0.022
60	0.031	0.025	0.071	0.048
120	0.060	0.060	0.104	0.078
180	0.089	0.107	0.142	0.105
240	0.128	0.141	0.195	0.156
300	0.172	0.198	0.240	0.230
360	0.222	0.262	0.313	0.339
420	0.269	0.331	0.426	0.441
480	0.334	0.410	0.620	0.653
540	0.403	0.504	0.843	0.896
600	0.470	0.619	1.032	1.166

**Figure 3-8**

Time (mins)	Untreated	Armac T	Armac C	Armac HR
0	0.015	0.008	0.000	0.013
60	0.025	0.010	0.009	0.016
120	0.060	0.011	0.021	0.019
180	0.107	0.013	0.043	0.022
240	0.141	0.015	0.069	0.027
300	0.198	0.020	0.079	0.034
360	0.262	0.029	0.102	0.041
420	0.331	0.036	0.119	0.056
480	0.410	0.051	0.151	0.076
540	0.504	0.070	0.170	0.087
600	0.619	0.081	0.188	0.113



**Figure 3-10**

Time (mins)	100 psi	200 psi	500 psi	1000 psi
0	0.008	0.008	0.003	0.010
60	0.008	0.010	0.005	0.019
120	0.009	0.011	0.012	0.048
180	0.009	0.013	0.017	0.100
240	0.010	0.015	0.031	0.129
300	0.012	0.020	0.052	0.185
360	0.015	0.029	0.071	0.252
420	0.023	0.036	0.112	0.300
480	0.030	0.051	0.158	0.390
540	0.040	0.070	0.200	0.510
600	0.040	0.081	0.289	0.613

**Figure 3-11**

Time (days)	Armac T (cum. % oxid.)	Armac C (Cum. % oxid.)	Armac HR (Cum. % oxid.)	Untreated (Cum. % oxid.)
0	0.000	0.000	0.000	0.000
7	0.003	0.001	0.004	0.032
12	0.010	0.003	0.010	0.064
17	0.019	0.009	0.020	0.088
24	0.033	0.024	0.036	0.126
29	0.044	0.036	0.050	0.151
34	0.052	0.048	0.062	0.176
40	0.060	0.059	0.075	0.213
47	0.072	0.071	0.090	0.252
51	0.077	0.076	0.101	0.281
56	0.083	0.082	0.113	0.306
63	0.090	0.085	0.125	0.342
70	0.099	0.088	0.130	0.380
75	0.100	0.091	0.140	0.410
81	0.110	0.099	0.150	0.450

## CHAPTER 4

Figure 4-1

Time (days)	Fe <sup>2+</sup> control (g/L)	Fe <sup>2+</sup> Culture (g/L)	MPN/mL
0	2.93	2.92	3.60 x 10 <sup>4</sup>
1	2.93	2.80	5.07 x 10 <sup>4</sup>
2	2.93	0.88	2.91 x 10 <sup>6</sup>
3	2.90	0.60	7.07 x 10 <sup>6</sup>
4	2.89	0.28	2.40 x 10 <sup>7</sup>
5	2.88	0.23	2.40 x 10 <sup>7</sup>
6	2.88	0.19	4.63 x 10 <sup>6</sup>
9	2.86	0.17	4.93 x 10 <sup>5</sup>

Figure 4-2

MPN/mL	Ferric (g/L)
3.60 x 10 <sup>4</sup>	0.01
5.07 x 10 <sup>4</sup>	0.13
2.91 x 10 <sup>6</sup>	2.05
7.07 x 10 <sup>6</sup>	2.30
2.40 x 10 <sup>7</sup>	2.61
2.40 x 10 <sup>7</sup>	2.65
4.63 x 10 <sup>6</sup>	2.69
4.93 x 10 <sup>5</sup>	2.69

**Figure 4-3**

Time (days)	MPN/mL	Turbidity (600 nm)
0	$3.60 \times 10^4$	0.0110
1	$5.07 \times 10^4$	0.0340
2	$2.91 \times 10^6$	0.1012
3	$7.07 \times 10^6$	0.1065
4	$2.40 \times 10^7$	0.1127
5	$2.40 \times 10^7$	0.1240
6	$4.63 \times 10^6$	0.1367
9	$4.93 \times 10^5$	0.2053

**Figure 4-4 & 4-5**

Time (days)	MPN/mL	Protein ( $\mu\text{g/mL}$ )
0	$3.60 \times 10^4$	0.412
1	$5.07 \times 10^4$	1.63
2	$2.91 \times 10^6$	8.39
3	$7.07 \times 10^6$	9.54
4	$2.40 \times 10^7$	10.1
5	$2.40 \times 10^7$	10.6
6	$4.63 \times 10^6$	12.3
9	$4.93 \times 10^5$	14.0

**Figure 4-6**

Time (days)	Protein ( $\mu\text{g/mL}$ )	Turbidity (600 nm)
0	0.412	0.0110
1	1.63	0.0340
2	8.39	0.1012
3	9.54	0.1065
4	10.1	0.1127
5	10.6	0.1240
6	12.3	0.1367
9	14.0	0.2053

**Figure 4-7**

Ferric (g/L)	13598 Protein ( $\mu\text{g/L}$ )	13661 Protein ( $\mu\text{g/L}$ )	14119 Protein ( $\mu\text{g/L}$ )
0.00	-	0.47	0.41
0.01	0.41	-	-
0.04	-	1.92	-
0.11	-	-	0.60
0.13	1.63	-	-
0.17	-	-	0.96
0.18	-	-	1.68
2.02	-	11.25	-
2.05	8.40	-	8.68
2.15	-	12.03	-
2.30	9.54	-	-
2.31	-	13.09	-
2.46	-	13.74	10.35
2.47	-	-	10.81
2.52	-	-	12.04
2.61	10.11	-	-
2.65	10.60	-	-

**Figure 4-7 (cont.)**

Ferric (g/L)	13598	13661	14119
	Protein (µg/L)	Protein (µg/L)	Protein (µg/L)
2.66	-	15.45	-
2.67	-	16.00	-
2.69	12.30	-	-
2.69	14.00	-	-

**Figure 4-8**

Time (days)	MPN/mL	pH
0	$3.60 \times 10^4$	1.66
1	$5.07 \times 10^4$	1.69
2	$2.91 \times 10^6$	1.91
3	$7.07 \times 10^6$	1.92
4	$2.40 \times 10^7$	1.93
5	$2.40 \times 10^7$	1.92
6	$4.63 \times 10^6$	1.91
9	$4.93 \times 10^5$	1.90

**Figure 4-9**

Time (days)	0.0 g/L Fe <sup>3+</sup> (MPN/mL)	1.0 g/L Fe <sup>3+</sup> (MPN/mL)	2.0 g/L Fe <sup>3+</sup> (MPN/mL)
0	$3.50 \times 10^4$	$3.80 \times 10^4$	$3.70 \times 10^4$
1	$4.30 \times 10^4$	$3.50 \times 10^4$	$4.30 \times 10^3$
2	$1.10 \times 10^6$	$4.30 \times 10^4$	$4.3 \times 10^3$
3	$8.00 \times 10^6$	$4.60 \times 10^5$	$4.30 \times 10^4$
4	$2.60 \times 10^7$	$2.30 \times 10^6$	$5.60 \times 10^4$
5	$2.60 \times 10^7$	$2.40 \times 10^6$	$4.50 \times 10^4$
6	$4.60 \times 10^6$	$2.30 \times 10^4$	$2.30 \times 10^3$
9	$4.63 \times 10^5$	$2.20 \times 10^3$	$1.10 \times 10^2$

**Figure 4-10**

Ferric (g/L)	Strain 13598 (MPN/mL)	Strain 13661 (MPN/mL)
0.00	$2.60 \times 10^7$	$2.60 \times 10^7$
1.00	$2.40 \times 10^6$	$3.20 \times 10^5$
2.00	$5.60 \times 10^4$	$3.00 \times 10^4$

**CHAPTER 5****Figure 5-1**

Time (days)	Strain 13598 (MPN/mL)	Strain 13661 (MPN/mL)	Strain 14119 (MPN/mL)
0	$3.60 \times 10^4$	$2.95 \times 10^4$	$2.40 \times 10^3$
1	$5.07 \times 10^4$	$2.95 \times 10^4$	$2.40 \times 10^3$
2	$2.91 \times 10^6$	$1.27 \times 10^7$	$2.40 \times 10^3$
3	$7.07 \times 10^6$	$1.93 \times 10^7$	$6.20 \times 10^3$
4	$2.40 \times 10^7$	$1.93 \times 10^7$	$3.40 \times 10^5$
5	$2.40 \times 10^7$	$1.63 \times 10^7$	$3.40 \times 10^5$
6	$4.63 \times 10^6$	$8.44 \times 10^6$	$2.40 \times 10^4$
9	$4.93 \times 10^5$	$1.11 \times 10^5$	$1.00 \times 10^4$

**Figure 5-2**

Time (min)	Fe (mg/L)	Time (min)	Fe (mg/L)	Time(min)	Fe (mg/L)
0.0	12.0	80.0	8.8	240.0	6.0
5.0	11.8	100.0	8.4	270.0	5.3
10.0	11.6	120.0	8.0	300.0	4.7
20.0	11.2	150.0	7.4	330.0	4.4
40.0	10.4	180.0	6.9	360.0	4.1
60.0	9.6	210.0	6.3		

**Figure 5-3**

Fe <sup>2+</sup> mg/L	1/Fe <sup>2+</sup>	Fe <sup>2+</sup> (10 µL)	Time (10 µL)	V <sup>-1</sup> (10 µL)	Fe <sup>2+</sup> (20 µL)	Time (20 µL)	V <sup>-1</sup> (20 µL)	Fe <sup>2+</sup> (50 µL)	Time (50 µL)	V <sup>-1</sup> (50 µL)
3.60	15.56	2.33	1.90	5.03	1.30	1.8	2.63	0.30	1.2	1.22
5.90	9.49	4.00	1.90	3.36	2.50	1.8	1.78	0.35	1.4	0.85
7.20	7.78	4.80	1.90	2.66	3.50	1.8	1.63	0.72	1.4	0.73
11.0	5.09	7.80	1.90	2.00	5.20	1.8	1.04	2.20	1.4	0.53
28.0	2.00	23.5	1.90	1.42	18.0	1.8	0.66	12.2	1.4	0.30

**Figure 5-4**

Fe <sup>2+</sup> mg/L	1/Fe <sup>2+</sup>	Fe <sup>2+</sup> (100 µL)	Time (100 µL)	V <sup>-1</sup> (100 µL)	Fe <sup>2+</sup> (200 µL)	Time (200 µL)	V <sup>-1</sup> (200 µL)
3.60	15.6	0.33	1.0	1.028	0.33	0.80	0.822
5.90	9.50	0.33	1.0	0.603	0.33	0.80	0.483
7.20	7.78	0.33	1.0	0.489	0.33	0.80	0.391
11.0	5.09	1.00	1.0	0.336	0.5	0.80	0.256
28.0	2.00	9.50	1.0	0.182	8.3	0.80	0.136

**Figure 5-5**

Fe <sup>2+</sup>	1/Fe <sup>2+</sup>	Fe <sup>2+</sup> (10 µL)	Time (10 µL)	V <sup>-1</sup> (10 µL)	Fe <sup>2+</sup> (20 µL)	Time (20 µL)	V <sup>-1</sup> (20 µL)	Fe <sup>2+</sup> (50 µL)	Time (50 µL)	V <sup>-1</sup> (50 µL)
72.0	0.778	55.30	1.8	0.362	49.00	1.5	0.219	15.30	1.4	0.083
144.0	0.389	127.0	1.8	0.356	121.0	1.5	0.219	50.50	1.4	0.050
720.0	0.078	710.0	1.0	0.336	695.0	1.5	0.202	346.0	1.4	0.013
3600	0.016	3590	1.0	0.336	3575	1.5	0.202	3230	1.4	0.013

**Figure 5-6 (cont.)**

Fe <sup>2+</sup>	1/Fe <sup>2+</sup>	Fe <sup>2+</sup> (100 μL)	Time (100 μL)	V <sup>-1</sup> (100 μL)	Fe <sup>2+</sup> (200 μL)	Time (200 μL)	V <sup>-1</sup> (200 μL)
72.0	0.778	6.30	1.0	0.051	3.00	0.8	0.039
144.0	0.389	4.33	1.0	0.0240	2.33	0.8	0.019
720.0	0.078	17.0	1.0	0.005	8.00	0.8	0.004
3600	0.016	30.0	1.0	0.001	27.0	0.8	0.001

**CHAPTER 6**

**Figure 6-1**

0 g/L Fe <sup>3+</sup> (Fe <sup>2+</sup> )	0 g/L 1/Fe <sup>2+</sup>	0 g/L Fe <sup>3+</sup> (Fe <sup>2+</sup> )	0 g/L Fe <sup>3+</sup> (Time)	0 g/L Fe <sup>3+</sup> (1/V)	0.5g/L Fe <sup>3+</sup> (Fe <sup>2+</sup> )	0.5 g/L 1/Fe <sup>2+</sup>	0.5 g/L Fe <sup>3+</sup> (Time)
9.00	6.222	0.10	1.0	0.3675	9.00	3.80	1.0
35.0	1.600	2.75	2.0	0.1584	34.50	17.25	1.0
88.0	0.6364	18.25	2.0	0.0963	83.00	37.50	2.0
176.0	0.3182	90.00	2.0	0.0881	164.00	105.00	2.0
950.0	0.0589	850.0	2.0	0.0772	900.00	800.00	2.0

**Figure 6-1 (cont.)**

0.5 g/L Fe <sup>3+</sup> (1/V)	1.0 g/L Fe <sup>3+</sup> (Fe <sup>2+</sup> )	1.0 g/L 1/Fe <sup>2+</sup>	1.0 g/L Fe <sup>3+</sup> (Time)	1.0 g/L Fe <sup>3+</sup> (1/V)
0.646	7.25	1.38	2.0	1.0718
0.1949	32.50	13.75	2.0	0.3584
0.1477	78.00	49.0	2.0	0.2017
0.1139	152.0	79.0	2.0	0.0921
0.0672	850.0	750.0	2.0	0.0672



**Figure 6-2**

Fe <sup>3+</sup> (Fe <sup>2+</sup> )	1/Fe <sup>2+</sup>	0 g/L Fe <sup>3+</sup> (Fe <sup>2+</sup> )	0 g/L Fe <sup>3+</sup> (Time)	0 g/L Fe <sup>3+</sup> (1/V)	0.5g/L Fe <sup>3+</sup> (Fe <sup>2+</sup> )	0.5 g/L 1/Fe <sup>2+</sup>
9.00	6.220	0.00	0.7	0.251	9.0	2.5
35.0	1.600	4.80	0.8	0.098	34.5	9.5
88.0	0.6364	9.20	1.0	0.073	83.0	30.0
176.0	0.3182	85.0	1.0	0.070	164.0	87.0
950.0	0.0589	880.0	1.0	0.048	900.0	780.0

**Figure 6-2 (cont.)**

0.5 g/L Fe <sup>3+</sup> (Time)	0.5 g/L Fe <sup>3+</sup> (1/V)	1.0 g/L Fe <sup>3+</sup> (Fe <sup>2+</sup> )	1.0 g/L 1/Fe <sup>2+</sup>	0 g/L Fe <sup>3+</sup> (Time)	1.0 g/L Fe <sup>3+</sup> (1/V)
1.0	0.4869	7.25	0.80	1.5	0.7814
1.0	0.1544	32.50	8.25	1.5	0.2078
1.0	0.0834	78.00	34.50	1.5	0.1159
1.0	0.0536	152.00	65.00	1.5	0.0579
1.0	0.0380	850.00	750.00	1.5	0.0504

**Figure 6-3**

Fe <sup>3+</sup> (Fe <sup>2+</sup> )	1/Fe <sup>2+</sup>	0 g/L Fe <sup>3+</sup> (Fe <sup>2+</sup> )	0 g/L Fe <sup>3+</sup> (Time)	0 g/L Fe <sup>3+</sup> (1/V)	0.5g/L Fe <sup>3+</sup> (Fe <sup>2+</sup> )	0.5 g/L 1/Fe <sup>2+</sup>
9.00	6.220	0.00	0.5	0.1867	9.0	0.80
35.0	1.600	2.80	0.8	0.0605	34.5	4.75
88.0	0.6364	5.00	1.0	0.0255	83.0	13.5
176.0	0.3182	25.0	1.0	0.0183	164.0	16.0
950.0	0.0589	700.0	1.0	0.0104	900.0	650.0

**Figure 6-3 (cont.)**

0.5 g/L Fe <sup>3+</sup> (Time)	0.5 g/L Fe <sup>3+</sup> (1/V)	1.0 g/L Fe <sup>3+</sup> (Fe <sup>2+</sup> )	1.0 g/L 1/Fe <sup>2+</sup>	0 g/L Fe <sup>3+</sup> (Time)	1.0 g/L Fe <sup>3+</sup> (1/V)
1.0	0.4098	7.25	0.00	1.5	0.6752
1.0	0.1129	32.50	3.50	1.5	0.1738
1.0	0.0483	78.00	23.00	1.5	0.0917
1.0	0.0227	152.00	50.00	1.5	0.0494
1.0	0.0134	850.00	650.00	1.5	0.0252

**Figure 6-4**

Ferric (mg/L)	Slope (4.3 x 10 <sup>5</sup> /mL)	Slope (2.3 x 10 <sup>6</sup> /mL)	Slope (9.3 x 10 <sup>7</sup> /mL)
0.00	0.0475	0.0335	0.0286
0.50	0.0917	0.0728	0.0648
1.00	0.1620	0.1202	0.1055

**Figure 6-5**

MPN ([C])	A = 1/[C]	A x 10 <sup>8</sup>	Slope
4.30 x 10 <sup>5</sup>	2.33 x 10 <sup>-6</sup>	232.56	0.1145
2.30 x 10 <sup>6</sup>	4.35 x 10 <sup>-7</sup>	43.48	0.0867
9.30 x 10 <sup>7</sup>	1.08 x 10 <sup>-8</sup>	1.08	0.0769

CHAPTER 7

Figure 7-3

Time (days)	Fe <sup>2+</sup> grown (Fe)	Fe <sup>2+</sup> grown (Fe/Log MPN)	FeS <sub>2</sub> grown (Fe)	FeS grown (Fe/Log MPN)
0	0.00	0.00	0.00	0.00
1	4.00	0.568	4.50	0.615
3	5.50	0.781	6.50	0.888
6	7.00	0.994	8.25	1.127
9	8.00	1.136	9.50	1.297
12	9.50	1.349	10.00	1.366
15	11.00	1.562	10.70	1.461
18	12.25	1.740	11.10	1.516
20	13.25	1.882	11.63	1.588

Figure 7-4

Time (days)	Total Fe (mg/L)	Fe <sup>2+</sup> (mg/L)	MPN/mL
0	0.5	0.5	2.40 x 10 <sup>7</sup>
2	17.5	0.6	1.10 x 10 <sup>7</sup>
4	38.8	1.0	4.70 x 10 <sup>6</sup>
6	63.5	1.5	2.50 x 10 <sup>6</sup>
8	85.6	2.0	3.30 x 10 <sup>6</sup>
10	135.6	3.5	4.00 x 10 <sup>6</sup>
12	201.0	5.5	4.30 x 10 <sup>6</sup>

**Figure 7-5**

Time (days)	Colonized FeS <sub>2</sub> Fe <sup>2+</sup> (mg/L)	FeS <sub>2</sub> -grown cells Fe <sup>2+</sup> (mg/L)	Fe <sup>2+</sup> -grown cells Fe <sup>2+</sup> (mg/L)
0	176	176	176
1	176	146	51
2	165	125	40
3	155	87	29
4	150	70	28
5	140	54	27
6	68	39	26
7	38	28	25
8	28	27	4

**Figure 7-6**

Time (days)	10% Col.	10% Fe/MPN	50% Col.	50% Fe/MPN	100% /1g Col.	100% /1g Fe/MPN	100% /2g Col.	100%/2g Fe/MPN
0	0.00	0.00	0.00	0.00	0.00	0.00	0.00	0.00
1	3.50	0.427	5.50	0.617	7.00	0.761	9.50	0.904
3	6.10	0.744	7.20	0.808	8.30	0.902	10.50	1.000
6	8.00	0.975	9.00	1.010	9.80	1.065	12.00	1.142
9	9.10	1.109	11.20	1.256	11.90	1.293	13.50	1.285
12	10.70	1.304	13.50	1.515	13.80	1.499	15.75	1.499
15	12.00	1.463	14.50	1.627	15.40	1.673	17.80	1.694
20	14.50	1.767	16.50	1.851	17.30	1.880	20.00	1.904

**Figure 7-7**

Time (days)	2.6 x 10 <sup>5</sup> /mL Fe (mg/L)	4.6 x 10 <sup>6</sup> /mL Fe (mg/L)	9.3 x 10 <sup>7</sup> /mL Fe (mg/L)	1.1 x 10 <sup>9</sup> /mL Fe (mg/L)
0	0.0	0.0	0.0	0.0
3	4.0	5.5	5.5	5.5
7	6.0	8.5	8.0	9.25
13	7.5	11.0	11.5	11.5
19	18.5	25.5	26.5	31.5
25	45.8	67.0	70.5	84.5
30	89.0	120.0	132.0	138.0
35	150.0	180.0	188.0	195.0
40	206.0	240.0	245.0	255.0

**Figure 7-8**

Time (days)	No cells Fe <sup>2+</sup> (mg/L)	4.3 x 10 <sup>3</sup> /mL Fe <sup>2+</sup> (mg/L)	1.5 x 10 <sup>5</sup> /mL Fe <sup>2+</sup> (mg/L)	7.5 x 10 <sup>7</sup> /mL Fe <sup>2+</sup> (mg/L)	4.6 x 10 <sup>9</sup> /mL Fe <sup>2+</sup> (mg/L)
0	578.0	568.0	590.0	598.0	592.0
1	570.0	532.0	500.0	318.0	152.0
2	565.0	92.0	90.0	84.0	79.0
3	570.0	28.0	28.0	27.0	26.0

**Figure 7-9**

Time (days)	Suspended (10mL) cells	Suspended (10mL) + FeS <sub>2</sub> cells (Fe <sup>2+</sup> )	Suspended cells (40 mL)	Flask attached cells (Fe <sup>2+</sup> )
0	195.0	210.0	200.0	200.0
1	134.0	154.0	60.0	180.0
2	78.0	85.0	7.0	156.0
3	27.0	38.0	6.0	124.0
4	11.0	12.0	6.0	85.0
5	9.0	9.0	6.0	25.0
6	-	-	-	15.0
7	-	-	-	6.0
8	-	-	-	6.0

**Figure 7-10**

Time (mins)	pH 1.0 Control (Fe <sup>2+</sup> )	pH 1.0 Cell (Fe <sup>2+</sup> )	pH 1.5 Control (Fe <sup>2+</sup> )	pH 1.5 Cell (Fe <sup>2+</sup> )	pH 2.0 Control (Fe <sup>2+</sup> )	pH 2.0 Cell (Fe <sup>2+</sup> )	pH 4.5 Control (Fe <sup>2+</sup> )	pH 4.5 Cell (Fe <sup>2+</sup> )
0	7.0	7.0	7.0	7.0	7.0	7.0	7.0	7.0
10	7.0	2.3	7.0	2.3	7.0	3.0	6.8	3.5
20	7.0	1.0	7.0	1.0	7.0	1.6	6.6	2.0
30	7.0	0.0	7.0	0.0	7.0	0.0	6.7	0.2
50	7.0	0.0	7.0	0.0	7.0	0.0	6.7	0.0

**Figure 7-11**

Time (days)	pH 1.5 (control) Fe (mg/L)	pH 1.5 (T.f) Fe (mg/L)	pH 4.5 (control) Fe (mg/L)	pH 4.5 (T.f) Fe (mg/L)
0	0.00	0.00	0.00	0.00
1	2.00	2.75	0.00	0.00
2	3.00	6.50	0.00	0.00
3	4.38	10.63	0.20	0.20
4	5.88	15.25	0.63	0.70
5	7.63	20.25	0.63	0.75
8	13.25	37.80	1.00	1.00
11	19.50	56.50	3.00	3.25

**Figure 7-12**

Time (days)	pH 4.5 (T.f) Initial Fe <sup>2+</sup> (mg/L)	pH 4.5 (T.f) Final Fe <sup>2+</sup> (mg/L)
0	7.0	0.0
1	6.5	0.0
2	6.0	0.0
3	5.5	0.0
4	5.25	0.0
5	5.4	0.0
8	5.5	0.0
11	5.0	0.0

**Figure 7-13**

Time (days)	pH 1.5 (control) $E_h$ (mV)	pH 1.5 (T.f) $E_h$ (mV)	pH 4.5 (control) $E_h$ (mV)	pH 4.5 (T.f) $E_h$ (mV)
0	279.2	279.8	86.0	85.7
1	283.6	286.5	102.7	115.6
2	283.3	286.8	112.6	124.2
3	286.7	290.0	117.2	135.4
4	288.3	291.4	121.3	141.5
5	290.4	292.4	131.1	148.4
8	291.6	293.7	151.5	166.5
11	289.7	293.0	166.0	186.5

**Figure 7-14**

Time (days)	pH 1.5 Control	pH 1.5 T. f	pH 4.5 Control	pH 4.5 T. f
0	1.73	1.73	4.70	4.70
1	1.60	1.58	4.60	4.45
2	1.60	1.58	4.50	4.25
3	1.60	1.56	4.40	4.10
4	1.58	1.52	4.35	3.90
5	1.54	1.51	4.32	3.82
8	1.53	1.48	4.00	3.50
11	1.51	1.48	3.72	3.30



**CHAPTER 8****Figure 8-1**

Time (days)	Control Fe (mg/L)	Strain 13598 Fe (mg/L)	Strain 13661 Fe (mg/L)	Strain 14119 Fe (mg/L)
0	2.5	1.00	0.50	1.50
8	10.0	20.50	28.50	30.00
15	19.0	38.00	36.00	33.00
20	28.5	58.00	52.00	42.00
23	35.0	79.50	76.00	52.00
30	49.0	172.00	153.00	118.00
35	59.0	191.00	193.00	149.00
40	79.0	230.00	215.00	201.00

**Figure 8-2**

Time (days)	Untreated Total Fe (mg/L)	Armac T Total Fe (mg/L)	Armac HR Total Fe (mg/L)
0	0.00	0.00	0.0
2	8.75	3.25	3.50
7	15.50	4.50	5.00
13	23.25	9.50	9.00
20	32.00	15.50	16.00
31	48.50	22.00	20.00
40	65.00	28.00	30.00

**Figure 8-3**

Time (days)	Untreated (Fe <sup>2+</sup> )	Armac T (Fe <sup>2+</sup> )	Armac HR (Fe <sup>2+</sup> )	Untreated % Fe <sup>2+</sup>	Armac T % Fe <sup>2+</sup>	Armac HR % Fe <sup>2+</sup>
0	0.00	0.00	0.00	-	-	-
2	7.75	2.25	3.00	88.57	87.69	85.71
7	13.50	4.25	4.00	87.10	94.44	80.00
13	19.75	8.75	8.50	84.95	92.11	94.44
20	30.00	14.00	15.00	93.75	90.32	93.75
31	48.00	20.00	19.50	100	90.91	97.50
40	57.00	23.00	28.50	87.69	82.14	95.00

**Figure 8-4**

Time (days)	Untreated Total Fe (mg/L)	Armac T Total Fe (mg/L)	Armac HR Total Fe (mg/L)
0	0.00	0.00	0.00
2	5.25	2.25	3.50
7	6.00	5.00	6.50
13	7.75	5.75	7.75
20	20.00	10.00	12.50
31	107.50	25.50	30.00
40	350.00	58.00	56.50

**Figure 8-5**

Time (days)	Untreated (Fe <sup>2+</sup> )	Armac T (Fe <sup>2+</sup> )	Armac HR (Fe <sup>2+</sup> )	Untreated % Fe <sup>2+</sup>	Armac T % Fe <sup>2+</sup>	Armac HR % Fe <sup>2+</sup>
0	0.00	0.00	0.00	-	-	-
2	0.20	0.10	0.10	3.81	4.44	2.86
7	0.20	0.20	0.20	3.33	4.00	3.08
13	0.20	0.20	0.20	2.58	3.48	2.58
20	0.50	0.20	0.20	2.50	2.00	1.60
31	0.50	0.20	0.30	0.47	0.78	1.00
40	6.50	3.75	4.00	1.86	6.47	7.08

**CHAPTER 9****Figure 9-1**

Time (days)	Control Total Fe (mg/L)	Control Fe <sup>2+</sup> (mg/L)	Strain 13661 Total Fe (mg/L)	Strain 13661 Fe <sup>2+</sup> (mg/L)
0	2.5	0.5	0.5	0.0
8	10.0	9.5	28.5	0.5
15	19.0	18.0	36.0	1.0
20	28.5	24.5	52.0	1.0
23	35.0	30.5	76.0	2.5
30	49.0	44.0	153.0	4.5
35	59.0	53.0	193.0	8.5
40	79.0	76.0	215.0	10.0

**Figure 9-2**

Time (days)	Untreated	Phosphate treated (40°C)	Phosphate treated (25°C)
	Total Fe (mg/L)	Total Fe (mg/L)	Total Fe (mg/L)
0	0.00	0.00	0.00
2	8.75	8.00	4.20
7	15.50	15.25	11.50
13	23.25	25.25	18.70
20	32.00	35.50	26.60
31	48.50	55.00	40.50
40	65.00	70.50	51.00

**Figure 9-3**

Time (days)	Untreated	Phosphate 40°C	Phosphate 25°C	Untreated	Phosphate 40°C	Phosphate 25°C
	(Fe <sup>2+</sup> )	(Fe <sup>2+</sup> )	(Fe <sup>2+</sup> )	% Fe <sup>2+</sup>	% Fe <sup>2+</sup>	% Fe <sup>2+</sup>
0	0.00	0.00	0.00	-	-	-
2	7.75	7.25	5.90	88.57	90.63	90.77
7	13.50	14.00	9.50	87.10	91.80	82.61
13	19.75	22.50	15.60	84.95	89.11	83.42
20	30.00	34.00	24.00	93.75	95.78	90.23
31	48.50	45.00	35.00	100	81.82	88.40
40	57.50	61.00	47.80	87.69	86.53	93.73

**Figure 9-4**

Time (days)	Untreated Total Fe (mg/L)	Phosphate treated	Phosphate treated
		(25°C) Total Fe (mg/L)	(40°C) Total Fe (mg/L)
0	0.00	0.00	0.00
2	5.25	4.25	5.25
7	6.00	5.0	6.25
13	7.75	6.5	8.75
20	20.00	13.0	21.0
31	107.5	65.5	131.5
40	350.0	231.0	340.0

**Figure 9-5**

Time (days)	Untreated (Fe <sup>2+</sup> )	Phosphate	Phosphate	Untreated % Fe <sup>2+</sup>	Phosphate	Phosphate
		25°C (Fe <sup>2+</sup> )	40°C (Fe <sup>2+</sup> )		25°C % Fe <sup>2+</sup>	40°C % Fe <sup>2+</sup>
0	0.00	0.00	0.00	-	-	-
2	0.10	0.10	0.10	1.905	1.905	1.905
7	0.20	0.10	0.10	3.333	1.818	1.600
13	0.20	0.20	0.30	2.581	2.857	3.429
20	0.50	0.50	0.50	2.500	3.571	2.381
31	0.50	0.50	0.50	0.465	0.763	0.380
40	6.5	4.25	8.25	1.857	1.840	2.427